

แอนไอออนเซ็นเซอร์เชิงเคมีไฟฟ้าและเชิงแสงที่มีพื้นฐานจาก  
คาลิกซ์[4]เอรีนควราวน์อีเทอร์

นางสาวเบญจมาศ ไชยลาภ

วิทยานิพนธ์นี้เป็นส่วนหนึ่งของการศึกษาตามหลักสูตรปริญญาวิทยาศาสตรดุษฎีบัณฑิต  
สาขาวิชาเคมี ภาควิชาเคมี  
คณะวิทยาศาสตร์ จุฬาลงกรณ์มหาวิทยาลัย  
ปีการศึกษา 2554  
ลิขสิทธิ์ของจุฬาลงกรณ์มหาวิทยาลัย

บทคัดย่อและแฟ้มข้อมูลฉบับเต็มของวิทยานิพนธ์ตั้งแต่ปีการศึกษา 2554 ที่ให้บริการในคลังปัญญาจุฬาฯ (CUIR)  
เป็นแฟ้มข้อมูลของนิสิตเจ้าของวิทยานิพนธ์ที่ส่งผ่านทางบัณฑิตวิทยาลัย

The abstract and full text of theses from the academic year 2011 in Chulalongkorn University Intellectual Repository (CUIR)  
are the thesis authors' files submitted through the Graduate School.

ELECTROCHEMICAL AND OPTICAL ANION SENSORS BASED ON CALIX[4]ARENE  
CROWN ETHER

Miss Benjamat Chailap

A Dissertation Submitted in Partial Fulfillment of the Requirements  
for the Degree of Doctor of Philosophy Program in Chemistry

Department of Chemistry

Faculty of Science

Chulalongkorn University

Academic Year 2011

Copyright of Chulalongkorn University

Thesis Title                    ELECTROCHEMICAL    AND    OPTICAL    ANION  
   SENSORS    BASED    ON    CALIX[4]ARENE    CROWN  
   ETHER  
By                                    Miss Benjamat Chailap  
Field of Study                    Chemistry  
Thesis Advisor                  Professor Thawatchai Tuntulani

---

Accepted by the Faculty of Science, Chulalongkorn University in Partial  
Fulfillment of the Requirements for the Doctoral Degree

.....Dean of the Faculty of Science  
(Professor Supot Hannongbua, Dr.rer.nat.)

THESIS COMMITTEE

.....Chairman  
(Assistant Professor Warinthorn Chavasiri, Ph.D.)

.....Thesis Advisor  
(Professor Thawatchai Tuntulani, Ph.D.)

.....Examiner  
(Associate Professor Orawon Chailapakul, Ph.D.)

.....Examiner  
(Assistant Professor Soamwadee Chaianansutcharit, Ph.D.)

.....External Examiner  
(Associate Professor Sujittra Youngme, Ph.D.)

เบญจมาศ ไชยลาภ : แอนไอออนเซ็นเซอร์เชิงเคมีไฟฟ้าและเชิงแสงที่มีพื้นฐานจาก  
คาลิกซ์[4]เอรีนควานอีเทอร์ (ELECTROCHEMICAL AND OPTICAL ANION  
SENSORS BASED ON CALIX[4]ARENE CROWN ETHER) อ. ที่ปรึกษา  
วิทยานิพนธ์หลัก: ศ.ดร.ธวัชชัย ต้นทุลานี, 165 หน้า.

ได้สังเคราะห์และศึกษาสมบัติของเฮเทอร์โรไดโตนิกรีเซปเตอร์ ที่มีโครงสร้างพื้นฐาน  
เป็นคาลิกซ์[4]เอรีนแบบ 1,3-แอลเทอร์เนต โดยมีหมู่เฟอร์โรซีนเป็นหน่วยให้สัญญาณ (สาร  
L1) โดยเปรียบเทียบกับสาร L1 กับสาร L2 ซึ่งเป็นรีเซปเตอร์ที่มีโครงสร้างคล้ายกันแต่อยู่ในคา  
ลิกซ์[4]เอรีน รูปแบบโคน จากการศึกษาโดยใช้เทคนิค<sup>1</sup>H NMR ไทเทรชัน พบว่าในกรณีที่มี  
แคทไอออนในระบบการทดลอง ความสามารถในการตอบสนองต่อแอนไอออนของสาร L1  
และสาร L2 จะแตกต่างกัน โดยสารประกอบ[L2•Na<sup>+</sup>] จะมีความเลือกจำเพาะต่อ AcO<sup>-</sup> และ  
Br<sup>-</sup> เพิ่มมากขึ้น ในขณะที่ [L1•Na<sup>+</sup>] สามารถตรวจวัดแอนไอออนหลายตัวด้วยค่าคงที่การจับ  
ที่สูงขึ้นใน 5% CD<sub>3</sub>CN/CDCl<sub>3</sub> นอกจากนี้เมื่อใช้เทคนิคทางเคมีไฟฟ้าพบว่า [L2•Na<sup>+</sup>]  
ตรวจวัด Cl<sup>-</sup> และ AcO<sup>-</sup> ได้ชัดเจนมากขึ้นใน 40% CH<sub>3</sub>CN/CH<sub>2</sub>Cl<sub>2</sub>

ได้สังเคราะห์ และศึกษาคุณสมบัติของเฮเทอร์โรไดโตนิกรีเซปเตอร์ที่สามารถให้  
สัญญาณได้ทั้งในเชิงแสง และเชิงเคมีไฟฟ้า โดยมีโครงสร้างพื้นฐานเป็นคาลิกซ์[4]เอรีนแบบ  
โคน และ 1,3-แอลเทอร์เนต (สาร L3 และ L4 ตามลำดับ) โดยมีหมู่แอนทราควิโนนเป็นหน่วย  
ให้สัญญาณ ในกรณีที่ไม่มี K<sup>+</sup>ในระบบการทดลองพบว่าสารทั้งสองตอบสนองต่อแอนไอออน  
คล้ายกัน นั่นคือสามารถตรวจวัด F<sup>-</sup> ได้โดยใช้เทคนิคฟลูออเรสเซนซ์ใน CH<sub>3</sub>CN และตรวจวัด  
H<sub>2</sub>PO<sub>4</sub><sup>-</sup> ใน 40% CH<sub>3</sub>CN/CH<sub>2</sub>Cl<sub>2</sub> ได้โดยใช้เทคนิคไซคลิกโวลแทมเมตรี ในกรณีที่มี K<sup>+</sup>ใน  
ระบบการทดลองพบว่าสาร L3 มีความไวต่อการตรวจวัด F<sup>-</sup> มากขึ้น และสามารถตรวจวัด F<sup>-</sup>  
และ AcO<sup>-</sup> โดยใช้เทคนิคทางเคมีไฟฟ้า ในขณะที่สาร L4 ไม่ได้แสดงสมบัตินี้ จากผล  
การศึกษาในครั้งนี้สามารถสรุปได้ว่า การตรวจวัดแอนไอออนสามารถควบคุมได้โดยใช้แรง  
ทางไฟฟ้าสเถิตจากแคทไอออนและรูปร่างของโมเลกุลตัวรับเป็นตัวกำหนด

ภาควิชา.....เคมี..... ลายมือชื่อนิติ.....  
สาขาวิชา.....เคมี..... ลายมือชื่อ อ.ที่ปรึกษาวิทยานิพนธ์หลัก.....

# # 4973825423 : MAJOR CHEMISTRY

KEYWORDS: CALIX[4]ARENE, DUAL SENSING, COOPERATIVE EFFECTS

BENJAMAT CHAILAP: ELECTROCHEMICAL AND OPTICAL ANION SENSORS BASED ON CALIX[4]ARENE CROWN ETHER

ADVISOR: PROF.THAWATCHAI TUNTULANI, Ph.D, 165 pp.

A new heteroditopic receptor derived from calix[4]arene crown ether in 1,3-alternate conformation with amidoferrocene as a signaling unit, receptor **L1**, was synthesized and its anion binding properties with the analogous receptor **L2** were compared. It was found that the presence of cations alter anion binding abilities. Complexation studies using  $^1\text{H}$  NMR titration found that the complex of  $[\text{L2}\cdot\text{Na}^+]$  gave more selectivity with  $\text{AcO}^-$  and  $\text{Br}^-$  ions, whereas  $[\text{L1}\cdot\text{Na}^+]$  showed higher binding constants with all anions in 5% v/v of  $\text{CD}_3\text{CN}$  in  $\text{CDCl}_3$ . In addition, only oxidized form of  $[\text{L2}\cdot\text{Na}^+]$  detected  $\text{Cl}^-$  and  $\text{AcO}^-$  in 40% v/v of  $\text{CH}_3\text{CN}$  in  $\text{CH}_2\text{Cl}_2$  to more cathodically shifts compared to its normal form.

Two heteroditopic dual sensors based on calix[4]arene crown ether containing amidoanthraquinone pendants in cone and 1,3-alternate conformations (receptors **L3** and **L4**, respectively) were synthesized. Both receptors exhibited dual sensing modes through photophysical and electrochemical properties. Receptors **L3** and **L4** can sense  $\text{F}^-$  photophysically in dried  $\text{CH}_3\text{CN}$  and  $\text{H}_2\text{PO}_4^-$  electrochemically in 40%  $\text{CH}_3\text{CN}/\text{CH}_2\text{Cl}_2$ . Interestingly, in the presence of  $\text{K}^+$ , receptor **L3** showed higher sensitivity with  $\text{F}^-$  via the higher fluorescence intensity at 520 nm and the higher binding constants, while this phenomenon was not observed in the case of receptor **L4**. In addition, only receptor **L3** gave remarkably potential shifts in its redox wave II upon adding  $\text{F}^-$  and  $\text{AcO}^-$  in the presence of  $\text{K}^+$ . According to these studies, the cooperative effects were controlled by not only the additional electrostatic forces but also the topology of the receptor molecules.

Department : CHEMISTRY Student's Signature .....

Field of Study : CHEMISTRY Advisor's Signature .....

Academic Year : 2011 .....

## ACKNOWLEDGEMENTS

First of all, I would like to thank my research advisor, Professor Dr. Thawatchai Tuntulani, for the opportunity to work in this great research unit and his invaluable assistance in all aspects of this research. He gave me a lot of great suggestions for doing this research. In addition, I would like to thank and pay my respect to Assistant Professor Dr. Warinthorn Chavasiri, Assoc. Professor Dr. Orawon Chailapakul, Assistance Professor Dr. Soamwadee Chaianansutcharit and Assoc. Professor Dr. Sujittra Youngme for their valuable advices and comments as thesis committee.

Furthermore, I would like to thank the Development and Promotion of Science and Technology Talents Project (DPST), The Thailand Research Fund (TRF), and Center of Excellence on Petrochemical and Materials Technology for financial support. I sincerely thank all members of the Supramolecular Chemistry Research Unit at the Department of Chemistry Chulalongkorn University for their supports. Special thanks should give to Ms. Nisachol Nerngchamnong and Ms. Duangrat Thongkum for being both my friends and my mentors. I have learnt many chemistry techniques from them.

Finally, I would like to thank all members of my family, especially my parents, for their love, kindness, suggestions, encouragement, and financial support throughout my life.

# CONTENT

	Page
<b>ABSTRACT IN THAI.....</b>	iv
<b>ABSTRACT IN ENGLISH.....</b>	v
<b>ACKNOWLEDGEMENTS.....</b>	vi
<b>CONTENTS.....</b>	vii
<b>LIST OF TABLES.....</b>	x
<b>LIST OF FIGURES.....</b>	xi
<b>LIST OF SCHEMES.....</b>	xvii
<b>LIST OF ABBREVIATIONS .....</b>	xviii
<b>CHAPTER I INTRODUCTION.....</b>	1
1.1 Heteroditopic receptors.....	1
1.1.1 Definitiion and their characteristics.....	1
1.1.2 The design of heteroditopic anion receptors.....	3
1.1.3 Heteroditopic receptors for anion sensing.....	4
1.1.4 Literature reviews regarding heteroditopic anion receptors.....	5
1.2 Multisignaling sensors.....	10
1.2.1 Multisignaling sensors for anions.....	11
1.2.2 Multisignaling sensors for cations.....	13
1.2.3 Multisignaling sensors for organic molecules.....	15
1.2.4 Multisignaling sensors for cobound ion pair.....	15
1.3 Concept of this study.....	16
<b>CHAPTER II EXPERIMENTAL .....</b>	18
2.1 Experimental section for chapter III.....	18
2.1.1 Synthesis of receptor <b>L1</b> .....	18
2.1.2 Complexation studies by <sup>1</sup> H NMR titration of <b>L1</b> and <b>L2</b> .....	24

2.1.3	Electrochemical studies of <b>L1</b> and <b>L2</b> .....	27
2.2	Experimental section for chapter IV.....	30
2.2.1	Synthesis of receptors, <b>L3</b> and <b>L4</b> .....	30
2.2.2	Complexation studies by <sup>1</sup> H NMR titration of <b>L3</b> and <b>L4</b> .....	36
2.2.3	Anion sensing abilities of <b>L3</b> and <b>L4</b> by UV-vis spectrophotometry.....	37
2.2.4	Anion sensing abilities of <b>L3</b> and <b>L4</b> by fluorescence spectrophotometry.....	39
2.2.5	Electrochemical studies of <b>L3</b> and <b>L4</b> .....	41

**CHAPTER III ELECTROCHEMICAL HETERODITOPIC RECEPTORS  
DERIVED FROM CROWN ETHER BASED CALIX[4]ARENE WITH  
AMIDO-FERROCENE PANDANTS ..... 43**

3.1	General information and literature reviews of heteroditopic receptors based ferrocene.....	43
3.1.1	Cation sensors derived form ferrocene.....	43
3.1.2	Anion sensors derived from ferrocene.....	44
3.1.3	Heteroditopic receptors derived from ferrocene.....	45
3.2	Objective and scope of the research.....	48
3.3	Results and discussion.....	49
3.3.1	Synthesis and characterization of receptor <b>L1</b> .....	49
3.3.2	Complexation studies of the receptor <b>L1</b> by <sup>1</sup> H NMR titration	52
3.3.3	Electrochemical studies of <b>L1</b> .....	68
3.4	Concluding remarks.....	82

**CHAPTER IV OPICAL ELECTROCHEMICAL HETERODITOPIC  
RECEPTORS DERIVED FROM CROWN ETHER BASED  
CALIX[4]ARENE WITH AMIDO-ANTHRAQUINONE PANDANTS..... 84**

4.1	General information and literature reviews of receptors based anthraquinone.....	84
-----	---	----



4.1.1	Cation sensors derived form anthraquinone.....	84
4.1.2	Anion sensors derived from anthraquinone.....	89
4.1.3	Ion sensors containing anthraquinone based on calix[4]arene scaffold.....	92
4.2	Objective and scope of the research.....	94
4.3	Results and discussion.....	95
4.3.1	Synthesis and characterization of receptor <b>L3</b> and <b>L4</b> .....	95
4.3.2	Complexation studies of the receptor <b>L3</b> and <b>L4</b> by <sup>1</sup> H NMR titration.....	98
4.3.3	Anion sensing abilities of receptors <b>L3</b> and <b>L4</b> using UV-visible spectrophotometry.....	106
4.3.4	Anion sensing abilities of receptors <b>L3</b> and <b>L4</b> using fluorescence spectrophotometry.....	113
4.3.5	Electrochemical studies of receptors <b>L3</b> and <b>L4</b> using cyclic voltammetry.....	122
4.4	Concluding remarks.....	137
<b>CHAPTER V CONCLUSION .....</b>		<b>139</b>
<b>REFERENCES.....</b>		<b>143</b>
<b>APPENDIX.....</b>		<b>155</b>
<b>VITAE.....</b>		<b>164</b>

## LIST OF TABLES

<b>Table</b>	<b>Page</b>
2.1 Volume and concentration of guest solutions used in $^1\text{H}$ NMR titration.....	26
2.2 Volume and Concentration of guest solutions used in CV titration of <b>L1</b> .....	29
2.3 Amounts of anions (0.1 M) added to 2 mL of <b>L3</b> and <b>L4</b> ( $5.0 \times 10^{-5}$ M) in UV-vis and fluorescence titration experiments.....	38
2.4 Amounts of fluoride ( $1 \times 10^{-4}$ M) and a ligand ( $1 \times 10^{-4}$ M) added in cuvette for Job's method.....	40
2.5 Volume and concentration of guest solution used in the CV titration of <b>L3</b> and <b>L4</b> .....	42
3.1 Binding constants for the $\text{Na}^+$ and $\text{K}^+$ cations complex with receptors <b>L1</b> and <b>L2</b> in 5% v/v $\text{CD}_3\text{CN}/\text{CDCl}_3$ .....	56
3.2 Binding constants (K) for receptors <b>L1</b> and <b>L2</b> with anionic guests.....	65
3.3 Electrochemical data ( $\text{Fc}/\text{Fc}^+$ redox couple) of receptor <b>L1</b> .....	69
3.4 Anodic shifts ( $\Delta E_{\text{pa}}$ ) of the ferrocene redox couples of receptors <b>L1</b> and <b>L2</b> on addition of 1.4 equivalents of $\text{Na}^+$ and $\text{K}^+$ .....	71
3.5 Electrochemical recognition data $^a\Delta E$ for receptor <b>L1</b> towards anions...	77
4.1 Binding constants of <b>L3</b> and <b>L4</b> with cations from $^1\text{H}$ NMR titration...	100
4.2 Association Constants for receptors <b>L3</b> and <b>L4</b> with $\text{F}^-$ in the presence and in the absence of cation.....	121
4.3 Half wave potentials of receptors <b>L3</b> and <b>L4</b> in 40% $\text{CH}_3\text{CN}$ v/v in $\text{CH}_2\text{Cl}_2$ .....	124
4.4 The changes in reduction potentials (mV) of receptors <b>L3</b> and <b>L4</b> after addition of various anions (10 equiv.).....	129

## LIST OF FIGURES

<b>Figure</b>	<b>Page</b>
1.1 Proposed binding mode of cobound ion pair complex of receptor <b>1.1</b> ...	7
1.2 Various geometries of ion-pair complexation of receptor <b>1.4</b> .....	8
1.3 Proposed binding mode of <b>1.8</b> •Cu <sup>I</sup> and <b>1.8</b> •Cu <sup>I</sup> A <sup>-</sup> .....	10
1.4 Chemical structure of <b>1.24</b> and calculated structure of cobound ion pair of <b>1.24</b> .....	16
3.1 Partial <sup>1</sup> H NMR titration spectra from 3-5 ppm between the receptor <b>L1</b> and KPF <sub>6</sub> (0-2 equivalents) in 5% v/v CD <sub>3</sub> CN in CDCl <sub>3</sub> .....	53
3.2 Partial <sup>1</sup> H NMR titration spectra from 6-8 ppm between the receptor <b>L1</b> and KPF <sub>6</sub> (0-2 equivalents) in 5% v/v CD <sub>3</sub> CN in CDCl <sub>3</sub> ...	54
3.3 <sup>1</sup> H NMR titration spectra of receptor <b>L1</b> +NaClO <sub>4</sub> •H <sub>2</sub> O and <b>L1</b> + KPF <sub>6</sub> (1.2 equivalents) in 5% v/v CD <sub>3</sub> CN in CDCl <sub>3</sub> .....	55
3.4 <sup>1</sup> H-NMR titration spectra of <b>L1</b> with TBAAcO (0-4 equivalents) in 5% v/v CD <sub>3</sub> CN in CDCl <sub>3</sub> .....	58
3.5 <sup>1</sup> H-NMR titration spectra of <b>L1</b> with TBABzO (0-4 equivalents) in 5% v/v CD <sub>3</sub> CN in CDCl <sub>3</sub> .....	59
3.6 Change in NH chemical shift (ΔNH) of receptor <b>L1</b> as function of increasing of anions (added as TBAsalts) in 5% v/v CD <sub>3</sub> CN in CDCl <sub>3</sub> ..	59
3.7 <sup>1</sup> H-NMR titration spectra of <b>L1</b> +K <sup>+</sup> (1.2 equivalents) with TBABzO (0-4 equivalents) in 5% v/v CD <sub>3</sub> CN in CDCl <sub>3</sub> .....	61
3.8 Change in NH chemical shift (ΔNH) of receptor <b>L3</b> as function of increasing of anions (added as TBAsalts) in 5% v/v CD <sub>3</sub> CN in CDCl <sub>3</sub> ..	62
3.9 Change in NH chemical shift (ΔNH) of receptor <b>L1</b> .....	63
3.10 <sup>1</sup> H-NMR titration spectra of <b>L1</b> +K <sup>+</sup> (1.2 equivalents) with TBAH <sub>2</sub> PO <sub>4</sub> (0-4 equivalents) in 5% v/v CD <sub>3</sub> CN in CDCl <sub>3</sub> .....	64

<b>Figure</b>	<b>Page</b>
3.11 Proposed binding mode of receptor <b>L1</b> and anions.....	66
3.12 Proposed binding modes of receptor <b>L1</b> and anions in the presence of cations.....	67
3.13 Cyclic voltammogram of receptor <b>L1</b> .....	69
3.14 Cyclic voltammogram titration of receptor <b>L1</b> (1 mM) upon gradual addition $\text{KPF}_6$ (0-1.4 equivalents).....	71
3.15 Square wave voltammogram titration of receptor <b>L1</b> (1 mM) before and after addition of $\text{KPF}_6$ 1.4 equivalents.....	72
3.16 Cyclic voltammogram titration of receptor <b>L1</b> (1 mM) upon gradual addition $\text{NaClO}_4 \cdot \text{H}_2\text{O}$ .....	72
3.17 Square wave voltammogram of receptor <b>L1</b> (1 mM) before and after addition of $\text{NaClO}_4 \cdot \text{H}_2\text{O}$ .....	73
3.18 Cyclic voltammograms of receptor <b>L1</b> with various anions.....	76
3.19 Square wave voltammograms of receptor <b>L1</b> (1 mM) with various anions.....	76
3.20 Cyclic voltammogram titration of receptor <b>L1</b> (1 mM) upon gradual addition $\text{TBACl}$ .....	78
3.21 Square wave voltammogram titration of receptor <b>L1</b> (1 mM) upon gradual addition $\text{TBACl}$ .....	79
3.22 Cyclic voltammogram titration of receptor <b>L1</b> (1 mM) upon gradual addition $\text{TBAAcO}$ .....	79
3.23 Square wave voltammogram titration of receptor <b>L1</b> (1 mM) upon gradual addition $\text{TBAAcO}$ .....	80
3.24 Cyclic voltammogram titration of receptor <b>L1</b> (1 mM) upon gradual addition $\text{TBABzO}$ .....	80
3.25 Square wave voltammogram titration of receptor <b>L1</b> (1 mM) upon gradual addition $\text{TBABzO}$ .....	81
3.26 Cyclic voltammogram titration of receptor <b>L1</b> (1 mM) upon gradual addition $\text{TBAH}_2\text{PO}_4$ .....	81

<b>Figure</b>	<b>Page</b>
3.27 Square wave voltammogram titration of receptor <b>L1</b> (1 mM) upon gradual addition TBAH <sub>2</sub> PO <sub>4</sub> .....	82
4.1 Structures of heteroditopic receptors, <b>L3</b> and <b>L4</b> .....	95
4.2 <sup>1</sup> H-NMR spectrum of receptor <b>L3</b> in CDCl <sub>3</sub> .....	97
4.3 <sup>1</sup> H-NMR spectrum of receptor <b>L4</b> in CDCl <sub>3</sub> .....	98
4.4 Partial <sup>1</sup> H NMR titration spectra between the receptor <b>L3</b> and potassium ions in 5% v/v CD <sub>3</sub> CN in CDCl <sub>3</sub> .....	99
4.5 Partial <sup>1</sup> H NMR titration spectra between the receptor <b>L4</b> and potassium ions in 5% v/v CD <sub>3</sub> CN in CDCl <sub>3</sub> .....	100
4.6 <sup>1</sup> H NMR titration spectra of <b>L3</b> on addition of TBAF.3H <sub>2</sub> O in 5% v/v CD <sub>3</sub> CN in CDCl <sub>3</sub> .....	102
4.7 <sup>1</sup> H NMR titration spectra of <b>L4</b> on addition of TBAF.3H <sub>2</sub> O in 5% v/v CD <sub>3</sub> CN in CDCl <sub>3</sub> .....	102
4.8 <sup>1</sup> H NMR titration spectra of [ <b>L3</b> •K <sup>+</sup> ] on addition of TBAAcO in 5% CD <sub>3</sub> CN/CDCl <sub>3</sub> .....	104
4.9 <sup>1</sup> H NMR titration spectra of [ <b>L3</b> •K <sup>+</sup> ] on addition of TBABzO in 5% v/v CD <sub>3</sub> CN in CDCl <sub>3</sub> .....	104
4.10 <sup>1</sup> H NMR titration spectra of [ <b>L3</b> •K <sup>+</sup> ] on addition of TBAF.3H <sub>2</sub> O 5% v/v CD <sub>3</sub> CN in CDCl <sub>3</sub> .....	105
4.11 <sup>1</sup> H NMR titration spectra of [ <b>L3</b> •K <sup>+</sup> ] on addition of TBAH <sub>2</sub> PO <sub>4</sub> 5% v/v CD <sub>3</sub> CN in CDCl <sub>3</sub> .....	105
4.12 <sup>1</sup> H NMR titration spectra of [ <b>L4</b> •K <sup>+</sup> ] on addition of TBAF.3H <sub>2</sub> O in 5% v/v CD <sub>3</sub> CN in CDCl <sub>3</sub> .....	106
4.13 UV-visible spectra of <b>L3</b> (50 μM) and various anions (100 equivalents) in CH <sub>3</sub> CN.....	107
4.14 UV-visible spectra of <b>L4</b> (50 μM) and various anions (100 equivalents) in CH <sub>3</sub> CN.....	107
4.15 UV-visible spectra of <b>L3</b> (50 μM) and KPF <sub>6</sub> in CH <sub>3</sub> CN.....	109

<b>Figure</b>	<b>Page</b>
4.16 UV-visible spectra of <b>L4</b> (50 $\mu\text{M}$ ) and $\text{KPF}_6$ in $\text{CH}_3\text{CN}$ .....	110
4.17 UV-visible spectra of [ <b>L3</b> • $\text{K}^+$ ] (50 $\mu\text{M}$ ) and various anions (100 equivalents) in $\text{CH}_3\text{CN}$ .....	110
4.18 UV- vis titration spectra of [ <b>L3</b> • $\text{K}^+$ ] (50 $\mu\text{M}$ ) upon addition of $\text{TBAF}\cdot 3\text{H}_2\text{O}$ (0-50 equivalents) in $\text{CH}_3\text{CN}$ .....	111
4.19 UV- vis spectra of <b>L3</b> (50 $\mu\text{M}$ ) and $\text{TBAF}\cdot 3\text{H}_2\text{O}$ (50 equiv.) in the absence and presence of $\text{KPF}_6$ (1.2 equiv.) in $\text{CH}_3\text{CN}$ .....	111
4.20 UV-vis spectra of <b>L3</b> (50 $\mu\text{M}$ )+ $\text{K}^+$ (1.2 eq) and $\text{F}^-$ (100 equiv.) (red line) in $\text{CH}_3\text{CN}$ upon addition various amount of $\text{EtOH}$ .....	112
4.21 UV-visible spectra of [ <b>L4</b> • $\text{K}^+$ ] (50 $\mu\text{M}$ ) and various anions (100 equivalents) in $\text{CH}_3\text{CN}$ .....	112
4.22 Normalized fluorescence emission spectra spectra of (a) <b>L3</b> (50 $\mu\text{M}$ ) in various solvents.....	113
4.23 Normalized fluorescence emission spectra spectra of <b>L4</b> (50 $\mu\text{M}$ ) in various solvents.....	114
4.24 Fluorescence spectra of <b>L3</b> (50 $\mu\text{M}$ ) in $\text{CH}_3\text{CN}$ in the presence of 100 equiv. of TBA salts of various anions.....	115
4.25 Fluorescence titration emission spectra of <b>L3</b> (50 $\mu\text{M}$ ) upon gradual addition of $\text{TBAF}\cdot 3\text{H}_2\text{O}$ in $\text{CH}_3\text{CN}$ .....	115
4.26 Fluorescence spectra of <b>L4</b> (50 $\mu\text{M}$ ) in $\text{CH}_3\text{CN}$ in the presence of 100 equiv. of TBA salts of various anions.....	116
4.27 Fluorescence titration emission spectra of <b>L4</b> (50 $\mu\text{M}$ ) upon gradual addition of $\text{TBAF}\cdot 3\text{H}_2\text{O}$ in $\text{CH}_3\text{CN}$ .....	116
4.28 Fluorescence titration emission spectra of <b>L4</b> (50 $\mu\text{M}$ ) upon gradual addition of $\text{KPF}_6$ in $\text{CH}_3\text{CN}$ from 0 to 100 equiv.....	117
4.29 Fluorescence titration emission spectra of <b>L4</b> (50 $\mu\text{M}$ ) upon gradual addition of $\text{KPF}_6$ in $\text{CH}_3\text{CN}$ from 0 to 100 equiv.....	118

<b>Figure</b>	<b>Page</b>
4.30 Fluorescence titration emission spectra of <b>L3</b> (50 $\mu$ M)+ $\text{KPF}_6$ (1.2 equiv.) upon gradual addition of $\text{TBAF}\cdot 3\text{H}_2\text{O}$ in $\text{CH}_3\text{CN}$ .....	119
4.31 Fluorescence emission spectra of <b>L3</b> (50 $\mu$ M) and $\text{TBAF}\cdot 3\text{H}_2\text{O}$ (100 equiv.) in the absence and presence of $\text{KPF}_6$ (1.2 equiv.) in $\text{CH}_3\text{CN}$ ...	119
4.32 Fluorescence emission spectra of <b>L4</b> (50 $\mu$ M) and $\text{TBAF}\cdot 3\text{H}_2\text{O}$ (100 equiv.) in the absence and presence of $\text{KPF}_6$ (1.2 equiv.) in $\text{CH}_3\text{CN}$ ...	120
4.33 Propose binding mode of <b>L3</b> in photophysical studies.....	121
4.34 Propose binding mode of <b>L4</b> in photophysical studies.....	122
4.35 Cyclic voltammograms of <b>L3</b> (1 mM) and <b>L4</b> (1 mM) in 40% $\text{CH}_3\text{CN}$ v/v in $\text{CH}_2\text{Cl}_2$ .....	124
4.36 Cyclic voltammogram of receptors (a) <b>L3</b> and (b) <b>L4</b> in 40% $\text{CH}_3\text{CN}$ v/v in $\text{CH}_2\text{Cl}_2$ .....	125
4.37 Graphs plotted between square root of various scanrates in cyclic voltammetry experiments and current of reduction waves of <b>L3</b> (a) $I_{\text{pcI}}$ and (b) $I_{\text{pcII}}$ .....	126
4.38 Graphs plotted between square root of various scanrates in cyclic voltammetry experiments and current of reduction waves of <b>L4</b> (a) $I_{\text{pcI}}$ and (b) $I_{\text{pcII}}$ . .....	127
4.39 Half wave potential differences of anthraquinone (AQ).....	129
4.40 Cyclic voltammograms of receptor (a) <b>L3</b> (1 mM) and $\text{H}_2\text{PO}_4^-$ in 40% $\text{CH}_3\text{CN}$ v/v in $\text{CH}_2\text{Cl}_2$ .....	130
4.41 Cyclic voltammograms of receptor <b>L4</b> (1 mM) and $\text{H}_2\text{PO}_4^-$ in 40% $\text{CH}_3\text{CN}$ v/v in $\text{CH}_2\text{Cl}_2$ .....	130
4.42 Cyclic voltammograms of receptor (a) <b>L3</b> (1 mM) and $\text{KPF}_6$ in 40% $\text{CH}_3\text{CN}$ v/v in $\text{CH}_2\text{Cl}_2$ .....	132
4.43 Cyclic voltammograms of receptor <b>L4</b> (1 mM) and $\text{KPF}_6$ in 40% $\text{CH}_3\text{CN}$ v/v in $\text{CH}_2\text{Cl}_2$ .....	132

<b>Figure</b>	<b>Page</b>
4.44 Cyclic voltammograms of <b>L4</b> (1 mM) in 40% CH <sub>3</sub> CN v/v in CH <sub>2</sub> Cl <sub>2</sub> with 0.1 M TBAPF <sub>6</sub> at various scan rates.....	133
4.45 Cyclic voltammograms of receptor <b>L3</b> (1 mM) + KPF <sub>6</sub> 3.0 equiv. after addition of various anions.....	134
4.46 Cyclic voltammograms of receptor <b>L3</b> (1 mM) + KPF <sub>6</sub> 3.0 equiv. after addition of (a) 10 equiv. F <sup>-</sup> in 40% CH <sub>3</sub> CN v/v in CH <sub>2</sub> Cl <sub>2</sub> .....	135
4.47 Cyclic voltammograms of receptor <b>L3</b> (1 mM) + KPF <sub>6</sub> 3.0 equiv. after addition of 10 and 20 equiv. AcO <sup>-</sup> .....	135
4.48 Cyclic voltammograms of receptor <b>L4</b> (1 mM) + KPF <sub>6</sub> 3.0 equiv. and 10.0 equivalents of F <sup>-</sup> in 40% CH <sub>3</sub> CN v/v in CH <sub>2</sub> Cl <sub>2</sub> .....	136
4.49 Cyclic voltammograms of receptor <b>L4</b> (1 mM) + KPF <sub>6</sub> 3.0 equiv. after gradual addition of 1.0, 4.0 and 10.0 equivalents of H <sub>2</sub> PO <sub>4</sub> <sup>-</sup> .....	137
4.50 Proposed structures of co-bound ion pairs of <b>L3</b> and <b>L4</b> .....	138



**LIST OF SCHEMES**

<b>Scheme</b>	<b>Page</b>
1.1 Monomeric allosteric protein: Activation of substrate binding or catalytic conversion by an allosteric effector [38].....	3
1.2 Three types of allosteric receptors [38].....	4
3.1 Synthetic pathway of receptor <b>L1</b> .....	50
3.2 Synthetic pathway of receptor <b>L2</b> .....	51
4.1 Chemodosimetric reaction mechanism upon addition of $\text{Cu}^{2+}$ ions.....	88
4.2 Synthetic pathway of receptor <b>L3</b> .....	96
4.3 Synthetic pathway of receptor <b>L4</b> .....	96

**LIST OF ABBREVIATIONS**

$^{13}\text{C-NMR}$	Carbon-13-Nuclear Magnetic Resonance
$\text{AcO}^-$	Acetate
K	Association Constant
$\text{Br}^-$	Bromide
$\text{BzO}^-$	Benzoate
$\delta$	Chemical Shift
J	Coupling Constant
d	Doublet
equiv. or eq.	Equivalent
m/z	Mass per Charge Ratio
mg	Milligram
m	Multiplet
mL	Milliliter
mmol	Millimol
mV	Millivolt
$\mu\text{L}$	Microliter
ppm	Part per million
$^1\text{H-NMR}$	Proton-Nuclear Magnetic Resonance
s	Singlet
$\text{NEt}_3$	Triethylamine
TBA	Tetrabutylammonium
UV-Vis	Ultraviolet-Visible

# CHAPTER I

## INTRODUCTION

Anions play important roles in many areas such as biological systems, medicine, and catalysis [1]. In biological system; for example, DNA, the majority of enzyme substrates and co-factors are anionic. However, pollutant anions could lead to eutrophication of river (from the over use of phosphate-containing fertilizers) and carcinogenesis (metabolites of nitrate). From this point of views, the design and synthesis of effective anion sensors have been interesting subjects [2-32].

The design of anions receptors is particularly challenging in molecular design because of many reasons. First, anions are larger than isoelectronic cations leading to a lower charge to radius ratio. Thus, electrostatic binding interactions from anions are weaker than they would be for the smaller cation. Second, anions may be sensitive to pH values such as the protonation at low pH resulting in losing their negative charge. Therefore, receptors must function within the pH window of their target anions. Anions have various geometries resulting in difficulty in the design of receptors that are complementary to their anionic guests [1].

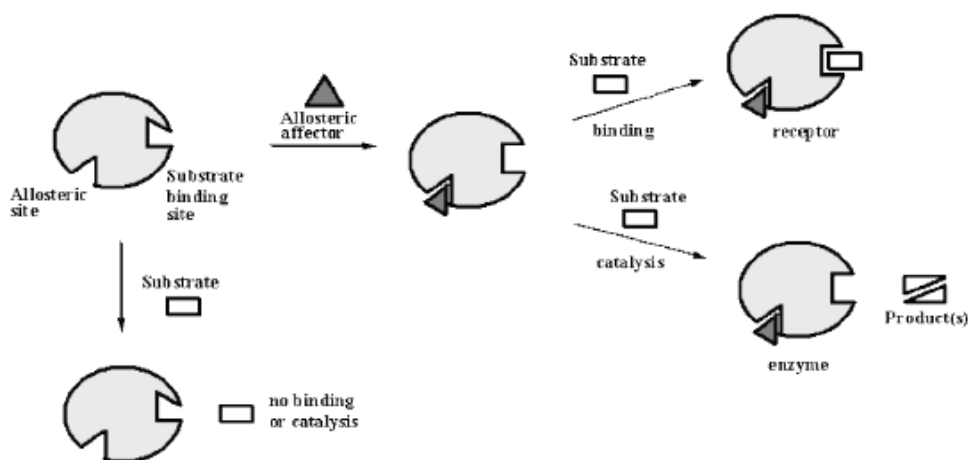
### 1.1 Heteroditopic receptors

#### 1.1.1 Definition and their characteristics

Heteroditopic receptors or ion-pair receptors have been increasingly interesting recently due to their great potential applications, such as in efficient extraction [33], as a carrier transportation reagent for environmentally important ion-pair species [11, 34] and as salt solubilization [1, 10, 23-26, 29, 32, 35-37]. The Heteroditopic receptors having two different ion binding sites are designed based on “biomimetic design principles” involving allosteric systems. The allosteric systems originally come from the concept of allosteric proteins exhibiting the controlling biological functions by external chemical input. The allosteric proteins consist of an allosteric site and a substrate binding site. The binding of a molecule or ion (the effector) to a specific allosteric site of the protein,

structurally distinct from the active site, leads to an alteration of the conformation of the protein that indirectly changes the properties of the biologically active site [38]. The effector can either enhance (positive allostery) or decrease (negative allostery) the binding or catalytic efficiency of the protein. The simplest mode of the allosteric steric system represented by a monomeric protein is shown in **Scheme 1.1**. If the binding of a molecule to the protein influences the interaction with a different or a same molecule, interactions are defined as “heterotropic” or “homotropic”, respectively.

Negative or positive heterotropic allostery can be useful in different purposes in molecular recognition systems. Negative heterotropic allostery is very important in dynamic molecular or ion recognition systems, for example, to release guests only in the presence of some certain threshold concentration of effectors, to regenerate guest-selective electrodes, to control the membrane transport rate of a specific guest by and effector. On the other hand, positive heterotropic allostery is very useful in term of the enhancement of target selectivity in the presence of the effector. In the most cases, the affinity of ion binding is significantly increased. This phenomenon can lead to an ON or OFF switching of the receptor properties by the allosteric effector. Therefore, the use of allosteric interactions enables chemists to control molecular function by external stimuli. It is very useful to amplify, integrate, and convert the weak chemical or physical signals into other signals so that we can detect their signals easily [39].

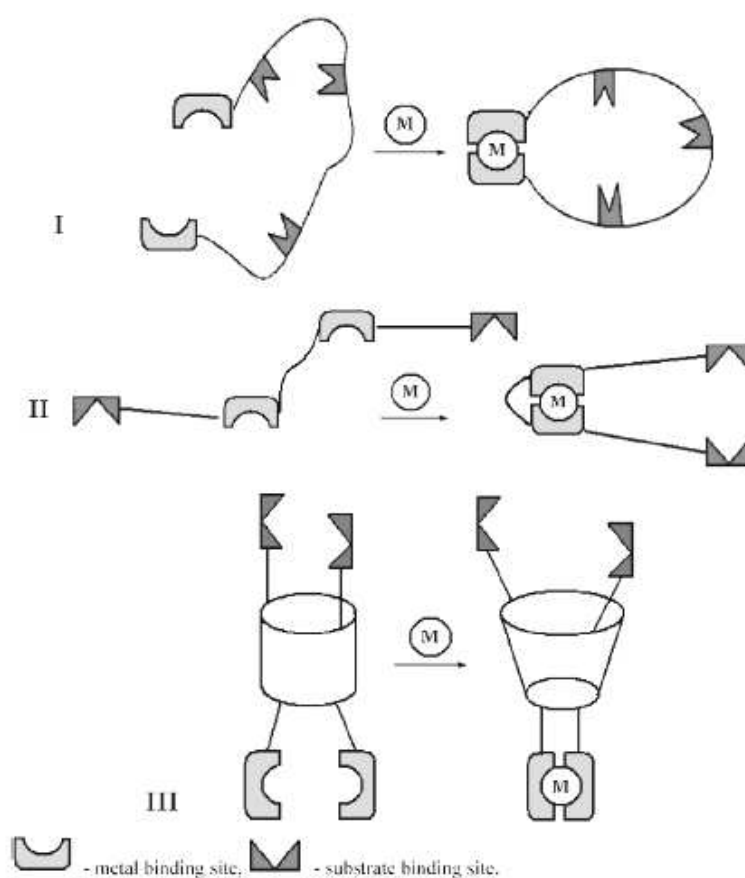


**Scheme 1.1** Monomeric allosteric protein: Activation of substrate binding or catalytic conversion by an allosteric effector [38].

### 1.1.2 The design of heteroditopic anion receptors

Generally, heteroditopic receptors are designed to have an allosteric sites and a receptor site. To design a negative heterotropic system, the first guest binding must induce a major conformational change so as to make the second guest binding less favorable. Conversely, the first guest binding must make the remote site more suitable for the second guest binding in a positive heterotropic system [40]. The effectors could be metal ions, simple anions or organic molecules. The synthesized heteroditopic receptors have been classified into three major groups which are (I) open-chain structures [25, 35, 41], (II) di- and tri-brachial (pincer-like systems) [13, 14, 24, 26, 30, 33, 42-44] and (III) calixarenes or pseudocalixarenes [1, 12, 15, 23, 32, 36-40, 45-53] as shown in **Scheme 1.2**. Allosteric effects are found to be more pronounced if the interaction area between the receptor and the guest is large (spheric > cyclic > two-point recognition) [38]. Mainly, open-chain and di- or tri-brachial structures of heteroditopic sensors are composed of crown ether (or pseudo crown ether) connected with anion binding sites such as amide, urea and thiourea groups [37]. In the past decade, heteroditopic anion sensors based on calixarenes [1, 36-40, 45-53] (or pseudocalixarenes) have been developed because the

coordination of the effector to the upper/lower rim can effects the shape and size of the hydrophobic cavity and/or the spatial organization of the functional groups that interact with the substrate [38]. Various kinds of calixarenes, calix[4]arene [36, 45-47], calix[5]arene [48], calix[6]arene [49], calix[4]pyrole [36, 50, 51] have been applied to heteroditopic receptors depending on the size of target molecules that can fit within the cavity of those calixarenes.



**Scheme 1.2** Three types of allosteric receptors [38]

### 1.1.3 Heteroditopic receptors for anion sensing

Typically, for heteroditopic anion sensors, the allosteric site and the receptor site are the cation and the anion binding site, respectively. Mostly, the effectors are cations including alkali metal ions as well as transition metal ions [40]. In the field of anion sensors, positive heterotropic allosterism systems have been interested. The reason is not

only the allosteric effect but also the additional electrostatic interactions from a cation are expected to be present in the ion-pair system. Thus, anion binding affinity in ion-pair systems is expected to be higher compared to simple monotopic anion receptors. Generally, the cation and the anion binding in ion-pair systems depends on the size of the ions, distance between the anion and cobound cation, the nature of the constituent recognition sites and solvents [36]. Therefore, the development of heteroditopic receptors is a challenging problem in molecular design because the two binding sites have to be suitably preorganized which can hold the two different ions in close proximity, but not so close that the two species can interact [43, 54].

Anion recognition in ion-pair system operates by the competition of the formation of three major components; a cobound ion-pair, a cobound cation-free anion and a salt ion-pair. Major species formed depend on the strength of the binding constant ( $K$ ) of such species. The cobound ion-pair results in positive binding or cooperative binding with an increasing of the binding constants of anions compared to the traditional anion receptor. The salt ion-pair formation causes the negative binding of the anions because anions can pull the metal ion trapped in the receptor out and forming stable salt ion-pairing in solution. As for cobound cation-free anion formation, which leads to the negative binding as well, the first equivalent of anion behaves like counter anion to balance the positive charge of cobound receptor until the net charge is zero.

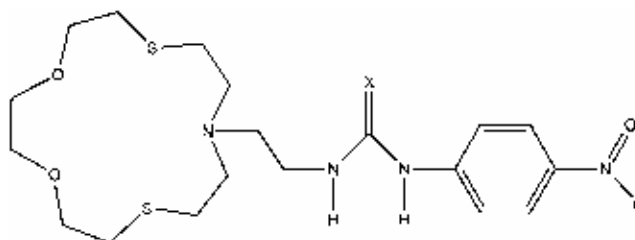
#### **1.1.4 Literature reviews regarding heteroditopic anion receptors**

Many efforts have been dedicated to the development of ion-pair receptors [1, 33-53, 55]. The outstanding characteristics of these receptors are allosteric and cooperative effects, where the binding of one ion converts the binding ability of the different charge of ion through electrostatic and conformational effects. One of the key factors making heteroditopic receptors very impressive to the chemists is the role of the allosteric effector. The effector influences not only the affinity for a specific substrate, but sometimes also the substrate selectivity pattern such as the improving or changing of selectivity of the substrates. Moreover, in some cases, variation of the metal effectors can

effect the selectivity of target ions [38]. These researches below show many examples of heteroditopic receptors and the factors that control the characteristic in each ion-pair system.

#### 1.1.4.1 Open-chain structures

Two derivatives of ditopic receptor bearing a 15-membered  $\text{NO}_2\text{S}_2$  crown connected to a nitrophenylurea/thiourea, **1.1** and **1.2** respectively have been synthesized [41]. The crown ligand due to the presence of the two thioetheral sulfur atoms can form complex with  $\text{Ag(I)}$ , a soft metal, which resulted in drastically increase the H-bond donor tendencies of a urea/thiourea subunit. The increase in H-bond donor tendencies led to the higher anion affinity. It can be said that the  $\text{Ag(I)}$  induced enhancement effect on anion affinity which is higher than that observed in the previously investigated systems containing alkali metal ions. However, in the presence of more basic anions, and in particular with the more acidic thiourea subunit, the  $\text{C=X-Ag(I)}$  interaction caused the deprotonation of the N-H fragments. The proposed binding modes of ion-pairs are shown below in **Fig 1.1**.



X = O: **1.1**

X = S: **1.2**



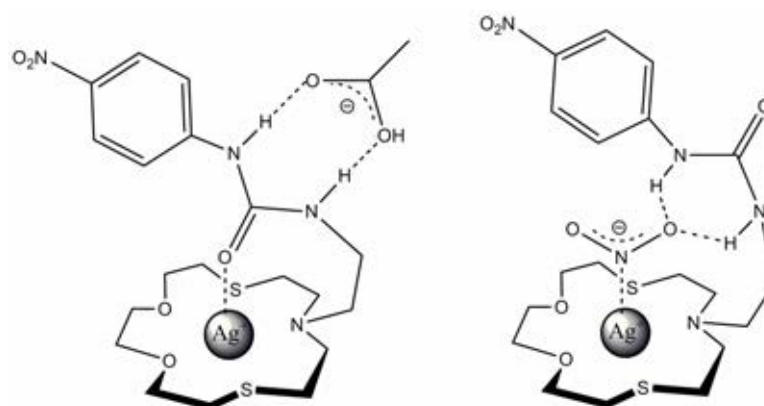
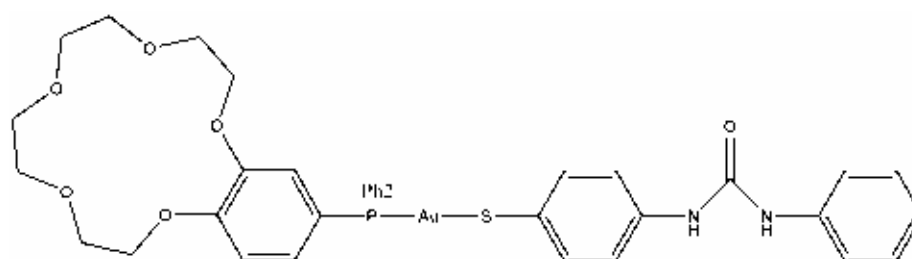


**Fig. 1.1** Proposed binding modes of cobound ion pair complex of receptor **1.1**

A novel ditopic receptor based on the gold(I) phosphine thiolate complex containing a urea-functionalized thiolate as an anion-binding site, and a benzo-15-crown-5 ether unit in the phosphine auxiliary ligand for cation binding, **1.3** has been synthesized [35]. Gold(I) was selected to be a platform because of its excellent photophysical properties as well as the good affinity of gold with a variety of ligands. The presence of  $\text{Na}^+$  showed a positive cooperative effect between **1.3** and  $\text{I}^-$  through the higher binding constants from  $^1\text{H}$  NMR titration techniques. Moreover, the ditopic receptor **1.3** showed a good ability to solubilize  $\text{NaCl}$  and  $\text{NaI}$  salts in organic chloroform solution.



**1.3**

### 1.1.4.2 Di-and tribrachial (pincer-like systems)

A new heteroditopic consisting of bis(*m*-phenylene)-32-crown-10, **1.4** was designed for binding the dicationic bipyridinium part of paraquat, an effective but highly toxic herbicide [42]. The binding constants of divalent salts of paraquat can be greatly improved by the influence of solvent polarity and the nature of the anion, the effector. The different cobound anions led to various geometries of ion-pair complexation motif which was confirmed by X-ray structure. Compound **1.4** preferred to be a pseudorotaxane in the presence of trifluoroacetate anions, while hexafluorophosphate and chloride anion contributed to a taco complex. This enables the researchers to control the host-guest complexation geometry by simply changing anions which could be useful in the future fabrication of molecular machines and storage materials.

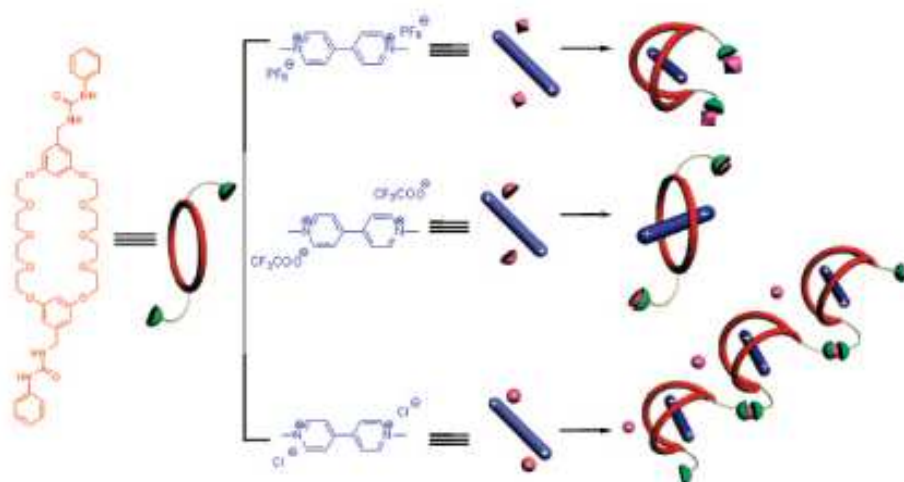
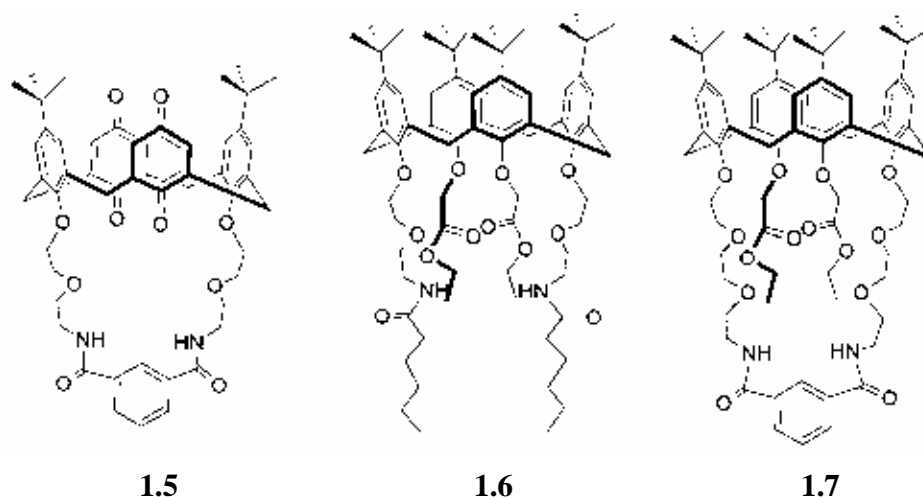


**Fig. 1.2** Various geometries of ion-pair complexation of receptor **1.4**.

### 1.1.4.3 Calixarenes or pseudocalixarenes

A new heteroditopic receptor which is calix[4]diquinone linked with isophthalamide, **1.5** was reported [52]. It was found that coordinating cations such as alkali metal ions and ammonium induced the chloride recognition. On the other hands, chloride bound with **1.5** can switch on sodium and ammonium cation recognition as well. However, this receptor was not particularly discriminatory between the ion-pairs of different cations.

Later, two new heteroditopic calix[4]arene bisester compounds, **1.6** and **1.7** demonstrated that the strength and selectivity of ion-pair recognition may be turned on by the appropriate design of cation and anion binding sites within their scaffolds [53]. Both of these ditopic receptors will bind ion pairs in a cooperative fashion when they are given the correct condition. Receptor **1.7** bearing isophthalamide linked with a single macrobicyclic of ester and amide groups is expected to have greater preorganization through macrocyclic effect. The results revealed that in the presence of  $\text{Na}^+$ , receptor **1.6** bound with  $\text{Cl}^-$  and  $\text{Br}^-$  moderately. Interestingly, receptor **1.7** showed unique ditopic properties in each specific system. In the presence of  $\text{Li}^+$  or  $\text{Na}^+$ , it bound with  $\text{Br}^-$  strongly. Conversely, in the presence of  $\text{Br}^-$ , it showed better interaction with  $\text{Li}^+$ , while the interaction with  $\text{Na}^+$  was lower probably due to the anticooperative effect. Therefore, receptor **1.7** provides an example of a system wherein the ion-pair cooperativity is highly selective for certain salts. This selectivity may be very useful in the design of molecular devices and suggests a use for ditopic receptors in the fine-tuning of ion-recognition processes. Moreover, the key factor that makes receptor **1.7** behaving as a superior binder for ion-pairs is a macrocyclic effect for ion-pair recognition. These works showed that the selectivity of ion-pair recognition critically depended on the structure of the receptors.



In 2009, a new calix[4]arene ditopic receptor containing naphthalene pendants, **1.8** was synthesized [46]. Compound **1.8** showed strong fluorescence enhancement upon titration with Cu(II) because metal ions help to lock the conformation of the fluorophores. During the complexation of **1.8** with Cu(II), the Cu(II) was reduced to Cu(I) by the free phenolic OH of **1.8**, whereas the phenol was oxidized by Cu(II), after which it assisted in the trapping of Cu(I). However, no significant changes in the absorption or fluorescence of **1.8** were observed when anions were added. Interestingly,  $\mathbf{1.8}\cdot\text{Cu}^{\text{I}}$  gave further enhancement of its UV-vis absorption and fluorescence intensity upon complexation with anions such as acetate or fluoride. The anion may be bound both through the hydrogen bonds of the acidic protons on the nitrogen atoms as well as through the electrostatic force between the ion pairs. The possible binding mode were shown in **Fig. 1.3**.



**Fig. 1.3** Possible binding mode of of  $\mathbf{1.8}\cdot\text{Cu}^{\text{I}}$  and  $\mathbf{1.8}\cdot\text{Cu}^{\text{I}}\text{A}^-$ .

## 1.2 Multisignaling sensors

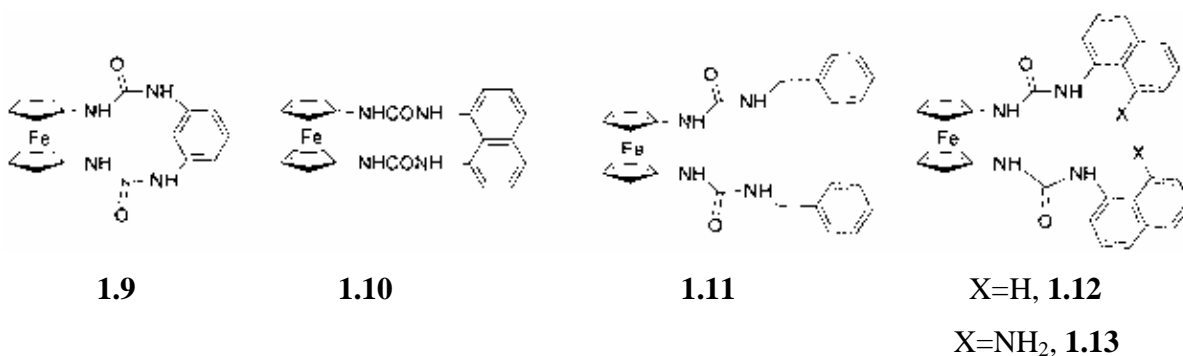
Recently, sensors exhibiting various signals have been attractive to the chemists because of their potential utilization in many applications [56-68]. Most of them were designed to have a fluorophore and a redox center within the same molecule for emitting both optical and electrochemical signals [56-66]. There have been diverse fluorophores selected for the development in molecular design of multisignaling sensors such as pyrene [62], anthracene [57], rhodamine [58, 59] and so on. Conversely, only few redox

centers have been used such as ferrocene [56, 58, 59, 61-68], iridium complex [60], and tetrathiafulvalene [57]. Even though many efforts have been focused on multisignaling sensors for cations or anions, ion-pair receptors exhibiting multiple channels were still rarely reported [54].

### 1.2.1 Multisignaling sensors for anions

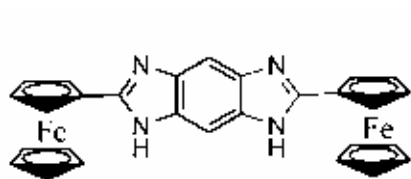
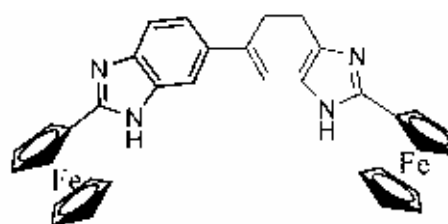
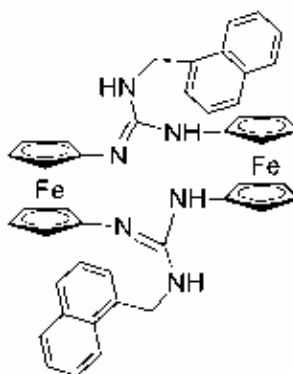
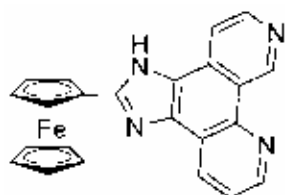
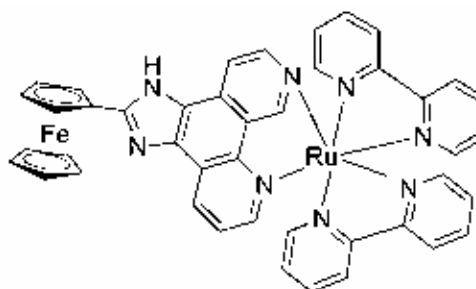
Molina et. al have reported ferrocene-based sensors for anions and cations detection which can exhibit multisignalling sensing through optical and electrochemical channels [54, 56, 61, 65, 68]. Most of these receptors sense ions optically through UV-vis absorption spectra, fluorescence emission spectra, and color changes. Electrochemical behaviors of these receptors can be observed through the shift of oxidation peaks. Additionally, spectral changes in  $^1\text{H}$  NMR titration also can be noticed upon ions complexation.

Homotopic receptors ferrocene-based ureas displaying spectral and electrochemical for anion sensing, **1.9-1.13**, have been synthesized [56]. All receptors displayed a selective downfield shift of the urea protons and a cathodic shift of the ferrocene/ferrocinium redox couple with hydrogen phosphate and fluoride anions. Specially, receptor **1.10** showed selective fluorescent responses to fluoride anion.

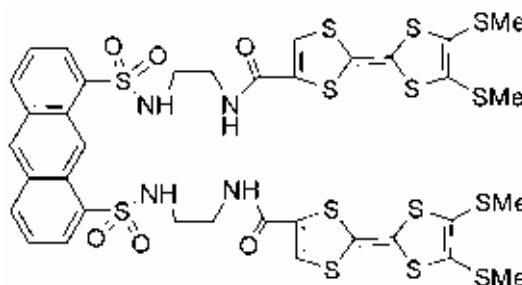


Various multisignaling sensors base on ferrocene connected to benzobisimidazole (**1.14** and **1.15**) [68], a bis-guanidine (**1.16**) [67], and imidazophenanthroline (**1.17** and **1.18**) [61] have been designed and developed. Each receptor showed highly selective with different anions ( $\text{AcO}^-$ ,  $\text{H}_2\text{PO}_4^-$ ,  $\text{HP}_2\text{O}_7^{3-}$ ,  $\text{Cl}^-$ ,  $\text{F}^-$ ,  $\text{NO}_3^-$ ). Receptors **1.14**, **1.15**, **1.17**

and **1.18** displayed chelation enhanced fluorescence effect (CHEF) after binding with specific anions and a progressive red-shift of the absorption bands (and/or appearance of a new low energy band). Moreover, anion complex of these receptors led to the shift of the oxidation peak cathodically. Additionally, the receptor **1.16** recognized either anions ( $\text{Cl}^-$ ,  $\text{F}^-$ ,  $\text{NO}_3^-$ ,  $\text{HSO}_4^-$  and  $\text{H}_2\text{PO}_4^-$ ) electrochemically or cations  $\text{Zn}^{2+}$ ,  $\text{Ni}^{2+}$  and  $\text{Cd}^{2+}$ ) optically. Interestingly, the receptor **1.17** also can detect the organic anions ADP and ATP.

**1.14****1.15****1.16****1.17****1.18**

An anthracene disulfonamide derivative incorporating two tetrathiafulvalene (TTF) units, **1.19**, has been reported [57]. The redox character of the TTF unit can induce quenching of the emission intensity of a signaling subunit, anthracene via a photoinduced electron transfer (PET) process. According to the Marcus theory, the electron transfer rate exponentially decreases with the donor-acceptor distance. It was expected that the distance between TTF units and fluorophore would be adjusted by the conformational changes of the receptors upon anion complexation. Fluorescence emission of **1.19** was completely quenched due to intramolecular PET mechanism. Upon addition of fluoride ions, the efficiency of the PET process was reduced due to rigidified receptor by bonded fluoride ions resulting in the enhancement of emission spectra. In addition, receptor **1.19** showed remarkable cathodic displacement of the first oxidation potential of the TTF unit upon addition of  $\text{H}_2\text{PO}_4^-$ . The negative charge from  $\text{H}_2\text{PO}_4^-$  complexation makes this receptor easier to be oxidized.



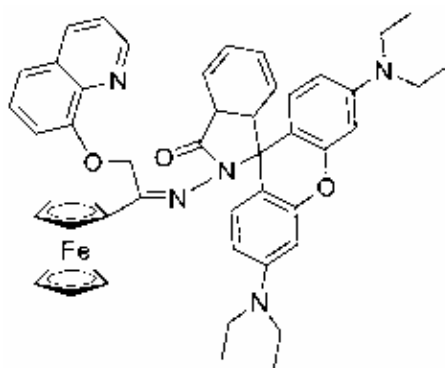
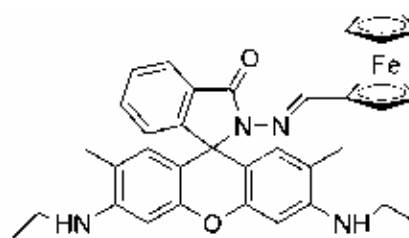
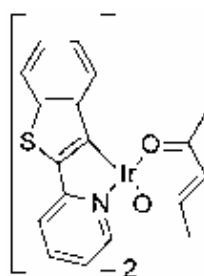
**1.19**

### 1.2.2 Multisignaling sensors for cations

Multisignaling sensors for a cation, especially  $\text{Hg}^{2+}$  have been synthesized. New multisignaling sensors based on rhodamine with ferrocene substituents, **1.20** [58] and **1.21** [59] exhibited highly selective detection of  $\text{Hg}^{2+}$  through UV/vis absorption, fluorescence emission, and electrochemical measurement. Interestingly, the receptor **1.20** can be used as a fluorescent probe for monitoring  $\text{Hg}^{2+}$  in living cells. Moreover, the receptor **1.21** can detect  $\text{Hg}^{2+}$  in natural water at very low detection limit, parts per billion

(ppb) for fluorescence measurement and parts per million (ppm) for electrochemical measurement.

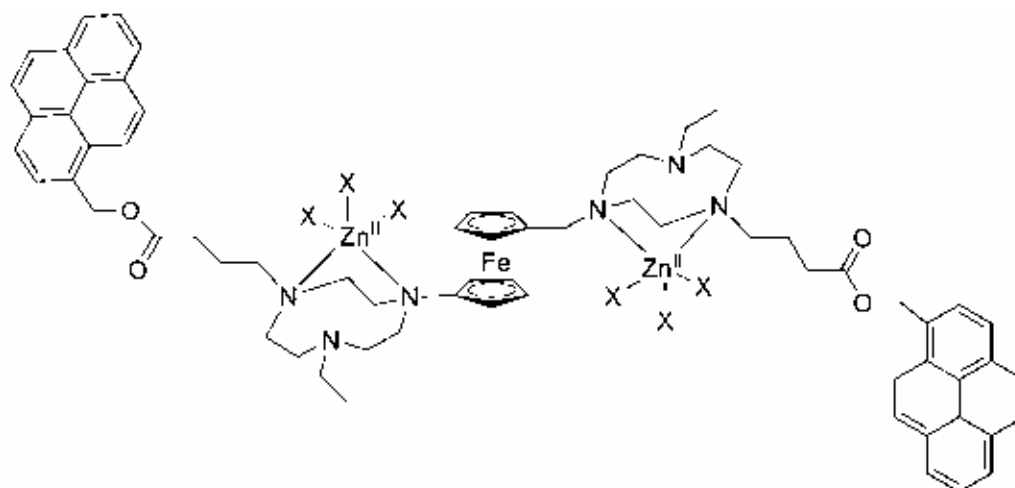
The first report of a chemosensor for transition- and heavy-metal ions based on phosphorescent iridium(III) complex, **1.22**, has been reported [60]. Multisignaling changes were observed through the new absorption and emission spectra at shorter wavelengths of **1.22** upon addition of  $\text{Hg}^{2+}$ . In addition,  $\text{Hg}^{2+}$  complex of receptor **1.22** showed remarkable anodic shift of cyclic voltammograms. The mechanism of **1.22** in sensing  $\text{Hg}^{2+}$  was also confirmed by density functional theory (DFT) calculation. It was the charge transfer from the iridium center to cyclometalated ligands that increased the electron density of cyclometalated ligands making easier coordination of sulfur and  $\text{Hg}^{2+}$ .

**1.20****1.21****1.22**



### 1.2.3 Multisignaling sensors for organic molecules

A receptor consisting of two pyrene-bearing  $\text{Zn}^{\text{II}}$ (TACN) complexes (TACN= 1,4,7-triazacyclononane) linked by ferrocene, **1.23** has been developed to show selectivity for biological polyphosphate anions [62]. Binding of a variety of polyphosphate anionic guests (pyrophosphate (PPi) anion and nucleotide di- and triphosphate) caused major disruption in the structure resulting in an enhancement in excimer emission from  $\pi$ - $\pi$  stacking of the two aromatic pyrenes and changes in electrochemical behaviour of the Fc/Fc<sup>+</sup> centre (0.1V).



**1.23**

### 1.2.4 Multisignaling sensors for cobound ion pair

In 2011, a redox and optical molecular sensor for ion pairs based on ferrocene-imidazopyrene, **1.24** exhibited an easily detectable signal change in the redox potential of the ferrocene/ferrocinium redox couple and in the emission spectrum [54].  $[\mathbf{1.24} \cdot \text{Zn}(\text{H}_2\text{PO}_4)_2]$  complex gave the oxidation peak which was intermediate between those found for the cationic  $[\mathbf{1.24} \cdot \text{Zn}]^{2+}$  and the anionic  $[\mathbf{1.24} \cdot \text{H}_2\text{PO}_4]^-$ . In addition, cobound ion pairs  $[\mathbf{1.24}_2 \cdot \text{M} \cdot (\text{H}_2\text{PO}_4)_2]$  (M: Zn, Hg, Pb) also caused a new band of the fluorescence emission spectrum at 422 nm which was remarkably different from the bands originated from its cationic (502 nm) or anionic (402 nm) complexes. Interestingly,

the new band stemmed from cobound ion pairs not only existed in a new position, but the intensity of this band was also much higher than a cationic or an anionic bands.

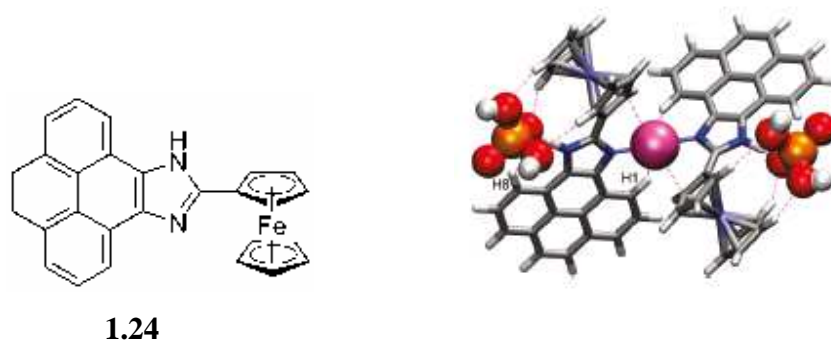


**Fig. 1.4** Chemical structure of **1.24** and calculated structure of cobound ion pair of **1.24**

### 1.3 Concept of this study

In this study, the design and synthesis of new heteroditopic receptors, containing two different signaling subunits, anthraquinone and ferrocene moieties have been interested. Diverse conformations of calix[4]arenes, cone and 1,3-alternate conformation, have been selected for building heteroditopic scaffolds. Crown ether and amide groups have been modified to be a cation and an anion binding sites, respectively. The combination of various signaling units attached to amide groups and calix-crown ether in different conformations of calix[4]arenes would be expected to get an optimized structure for the ion-pair system to enhance the anion affinity, recognition and sensing.

In the first part of this thesis, a novel heteroditopic receptor based on amidoferrocene-crown ether calix[4]arene in 1,3-alternate conformation, **L1**, has been synthesized and compared with an analogous receptor, **L2**, in which calix[4]arene was in cone conformation. Their complexation studies and electrochemical properties were investigated using  $^1\text{H}$  NMR titration technique and cyclic voltammetry, respectively. From this study, ditopic properties regarding to the distance between the two different binding sites and the metal effectors have been evaluated. Later, to improve the anion sensing abilities, two new heteroditopic ion receptors based on amidoanthraquinone-

crown ether calix[4]arene, **L3** and **L4**, have been designed and synthesized. These receptors showed interesting features of heteroditopic receptors exhibiting multisignaling, both optical and electrochemical signal, due to diverse properties of anthraquinone.

## CHAPTER II

### EXPERIMENTAL

#### 2.1. Experimental section for chapter III

##### 2.1.1 Synthesis of receptor L1, crown ether-based calix[4]arene with amido-ferrocene pendants

###### 2.1.1.1 General Procedure

###### 2.1.1.1.1 Analytical Measurements

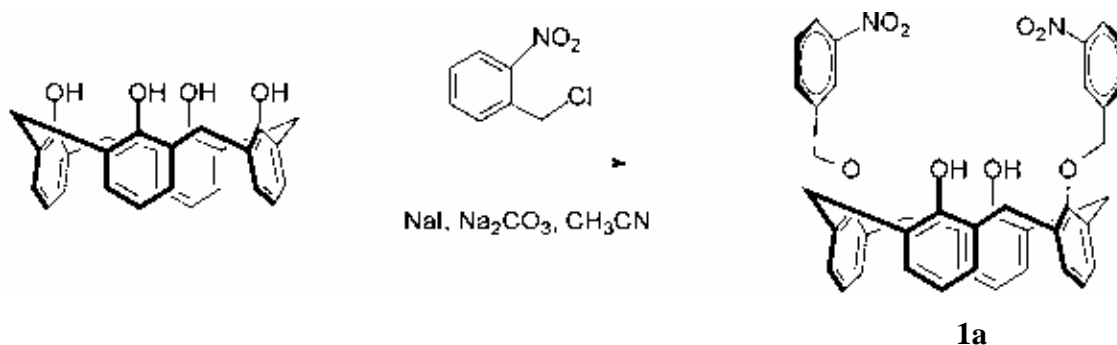
$^1\text{H}$  NMR spectra and  $^{13}\text{C}$  NMR spectra were recorded on a Varian Mercury 400 NMR spectrometer and a Bruker Avance 400 NMR spectrometer. All chemical shifts were reported in part per million (ppm) using the residual proton or carbon signal in deuterated  $\text{CDCl}_3$  as internal reference.

###### 2.1.1.1.2 Materials

Unless otherwise specified, the solvents and materials were reagent grades purchased from Fluka, BDH, Aldrich, Carlo erba, Merk or Lab scan and used without further purification. Commercial grade solvents such as acetone, dichloromethane, hexane, methanol and ethyl acetate were purified by distillation before used. Acetonitrile and dichloromethane for set up the reaction were dried over calcium hydride and freshly distilled under nitrogen prior to use. Column chromatography was carried out on silica gel (Kieselgel 60, 0.063-0.200 mm, Merck). Thin layer chromatography (TLC) was performed on silica gel plates (Kieselgel 60,  $F_{254}$ , 1 mm). *p-tert*-Butylcalix[4]arene was prepared according to published procedures [69].

## 2.1.1.2 Synthesis

### 2.1.1.2.1 Preparation of 1a



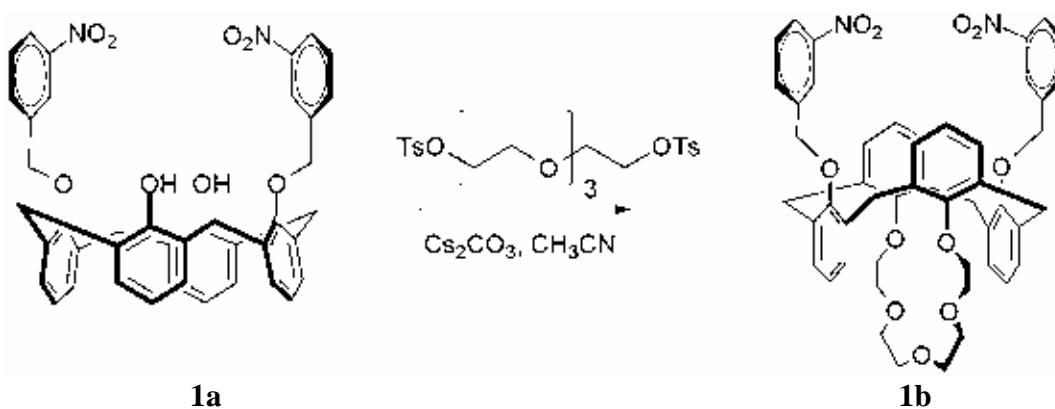
The mixture of calix[4]arene (0.5 g, 1.18 mmol) and  $\text{Na}_2\text{CO}_3$  (0.5 g, 3.53 mmol) and a catalytic amount of NaI in 50 mL of dried acetonitrile was stirred at room temperature under nitrogen atmosphere for 30 minutes. The solution of 3-nitrobenzyl chloride (0.5 g, 2.94 mmol) in 30 mL of dried acetonitrile was added dropwise and the mixture was reflux for 48 hours. Then,  $\text{Na}_2\text{CO}_3$  was removed by filtration. The filtrate was evaporated and the residue was dissolved in  $\text{CH}_2\text{Cl}_2$  (50 mL) and stirred with 3M HCl (15 mL) for 30 minutes. The aqueous solution was extracted with  $\text{CH}_2\text{Cl}_2$  and the organic layer was dried over anhydrous  $\text{MgSO}_4$ , filtered, and concentrated in vacuo. The crude product was purified by column chromatography ( $\text{SiO}_2$ , 30% hexane in  $\text{CH}_2\text{Cl}_2$ ) The pure product was obtained by recrystallization from  $\text{CH}_2\text{Cl}_2$ - $\text{CH}_3\text{OH}$  as white solid (0.32g, 40 % yield).

### Characterization data for 1a

$^1\text{H}$  NMR:  $\delta_{\text{H}}$  (400 MHz,  $\text{CDCl}_3$ , ppm) 3.47 and 4.18 (dd,  $J = 12.8$  Hz,  $\text{ArCH}_A\text{CH}_B\text{Ar}$ , AB system, 8H), 5.21 (s,  $\text{OCH}_2\text{Ar}$ , 4H), 6.62 (t,  $J = 7.6$  Hz,  $p\text{-ArHOH}$ , 2H), 6.83 (t,  $J = 7.6$  Hz,  $p\text{-ArHOCH}_2\text{ArNO}_2$ , 2H), 7.07 (d,  $J = 7.2$  Hz,  $m\text{-ArHOH}$ , 4H), 7.17 (d,  $J = 7.2$  Hz,  $m\text{-ArHOCH}_2\text{ArNO}_2$ , 4H), 7.48 (t,  $J = 8.0$  Hz,  $m\text{-ArHNO}_2$ , 2H), 8.05 (d,  $J = 7.6$  Hz,  $p\text{-ArHNO}_2$ , 2H), 8.13 (d,  $J = 8.0$  Hz,  $o\text{-ArHNO}_2$ , 2H), 8.20 (s,  $o\text{-ArHNO}_2$ , 2H), 8.75 (s,  $\text{ArOH}$ , 2H).

$^{13}\text{C}$  NMR:  $\delta_{\text{C}}$  (100 MHz,  $\text{CDCl}_3$ , ppm) 153.0, 151.7, 148.1, 139.5, 134.0, 133.9, 130.2, 129.6, 129.1, 127.8, 126.2, 123.2, 122.5, 119.7, 76.8, 31.1.

#### 2.1.1.2.2 Preparation of **1b**



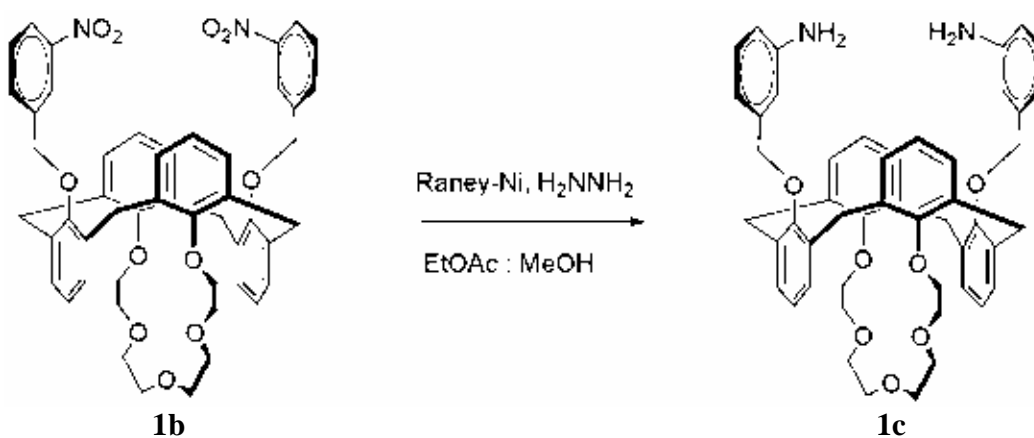
The mixture of **1a** (0.30 g, 0.43 mmol) and  $\text{Cs}_2\text{CO}_3$  (0.70 g, 2.15 mmol) in 85 mL of dried acetonitrile was stirred at room temperature under nitrogen atmosphere for 30 minutes. The solution of tetraethyleneglycol ditosylate (0.216 g, 0.43 mmol) (prepared from tetraethyleneglycol) in 30 mL of dried acetonitrile was added dropwise and the mixture was reflux for 24 hours. Then,  $\text{Cs}_2\text{CO}_3$  was removed by filtration. The filtrate was evaporated and the residue was dissolved in  $\text{CH}_2\text{Cl}_2$  (50 mL) and stirred with 3M HCl (50 mL) for 30 minutes. The aqueous solution was extracted with  $\text{CH}_2\text{Cl}_2$  and the organic layer was dried over anhydrous  $\text{MgSO}_4$ , filtered, and concentrated in vacuo. The crude product was purified by column chromatography ( $\text{SiO}_2$ , 20% ethylacetate in  $\text{CH}_2\text{Cl}_2$ ) (0.17g, 47% yield).

### Characterization data for **1b**

$^1\text{H}$  NMR:  $\delta_{\text{H}}$  (400 MHz,  $\text{CDCl}_3$ , ppm) 3.33-3.81 (m,  $\text{OCH}_2\text{CH}_2\text{O}$ , 16H), 3.60 (s,  $\text{ArCH}_2\text{Ar}$ , 8H), 4.80 (s,  $\text{NO}_2\text{ArCH}_2\text{O}$ , 4H), 6.38 (t,  $J = 7.6$  Hz,  $p\text{-ArH}$ , 2H), 6.69 (d,  $J = 7.2$  Hz,  $m\text{-ArH}$ , 4H), 6.96 (t,  $J = 7.6$  Hz,  $p\text{-ArH}$ , 2H), 7.18 (d,  $J = 7.2$  Hz,  $m\text{-ArH}$ , 4H), 7.20 (d,  $J = 7.6$  Hz,  $p\text{-ArHNO}_2$ , 2H), 7.37 (t,  $J = 8.0$  Hz,  $m\text{-ArHNO}_2$ , 2H), 7.85 (s,  $o\text{-ArHNO}_2$ , 2H), 8.11 (d,  $J = 8.0$  Hz,  $o\text{-ArHNO}_2$ , 2H).

$^{13}\text{C}$  NMR:  $\delta_{\text{C}}$  (100 MHz,  $\text{CDCl}_3$ , ppm) 155.9, 155.8, 147.8, 139.6, 134.2, 134.0, 133.9, 130.1, 130.0, 128.8, 123.3, 122.5, 122.35, 122.30, 72.2, 71.0, 70.5, 70.2, 69.1, 37.9.

#### 2.1.1.2.3 Preparation of **1c**



Raney nickel (0.154g, 2.66 mmole) was added to the solution of compound **1b** (0.23 g, 0.266 mmole) in 30 mL of ethylacetate and 22 mL of methanol under nitrogen atmosphere. Hydrazine (0.75 mL, 15.96 mmole) was added and then was refluxed for 2 hours. The suspension was filtered off and washed with methanol. The filtrate was then evaporated to dryness under reduced pressure. The residue was taken up with  $\text{CH}_2\text{Cl}_2$  (50 mL) and extracted with water. The organic layer was separated, dried with anhydrous magnesium sulfate, filtered, and concentrated in vacuo to give compound **1c** as white solid (0.19g, 90 % yield). Compound **1c** was used immediately for further reaction.

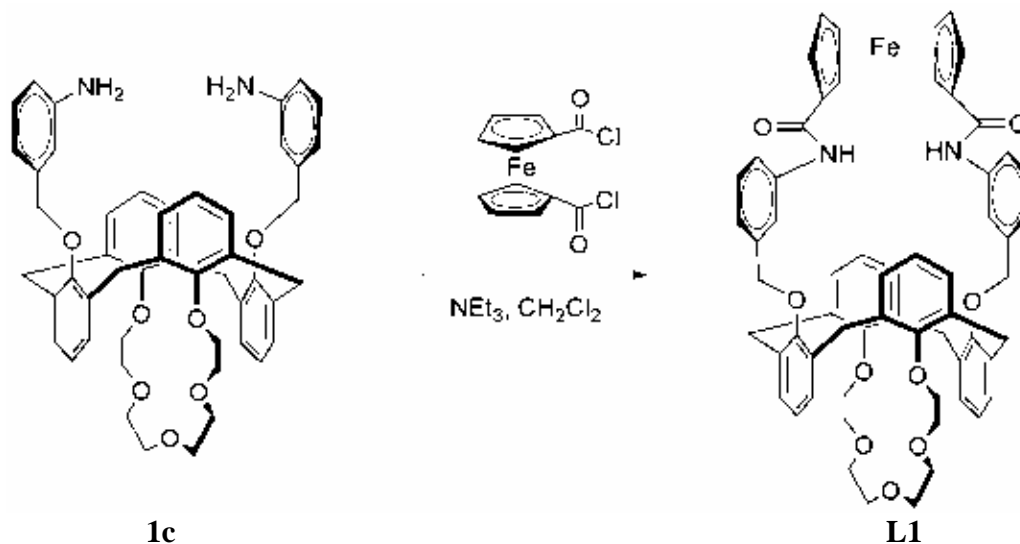
**Characterization data for 1c**

$^1\text{H}$  NMR:  $\delta_{\text{H}}$  (400 MHz,  $\text{CDCl}_3$ , ppm) 3.60 (s,  $\text{ArCH}_2\text{Ar}$ , 8H), 3.60-3.78 (m,  $\text{OCH}_2\text{CH}_2\text{O}$ , 16H), 4.64 (s,  $\text{CH}_2\text{OAr}$ , 4H), 6.61 (s, *o*- $\text{ArHNH}_2$ , 2H), 6.44 (d,  $J = 7.6$  Hz, *o*- $\text{ArHNH}_2$ , 2H), 6.50 (t,  $J = 7.6$  Hz, *p*- $\text{ArHNH}_2$ , 2H), 6.60 (d,  $J = 7.6$  Hz, *p*- $\text{ArHNH}_2$ , 2H), 6.75 (d,  $J = 7.6$  Hz, *m*- $\text{ArH}$ , 4H), 6.91 (t,  $J = 7.6$  Hz, *p*- $\text{ArH}$ , 2H), 7.09 (t,  $J = 7.6$  Hz, *p*- $\text{ArH}$ , 2H), 7.16 (d,  $J = 8.0$  Hz, *m*- $\text{ArH}$ , 4H).

$^{13}\text{C}$  NMR:  $\delta_{\text{C}}$  (100 MHz,  $\text{CDCl}_3$ , ppm) 156.8, 155.8, 146.0, 138.8, 134.5, 133.8, 130.5, 129.9, 128.6, 122.7, 122.2, 117.2, 114.7, 113.6, 72.4, 72.1, 70.4, 69.2, 37.9.



#### 2.1.1.2.4 Preparation of L1



Under nitrogen atmosphere, ferrocene diacid chloride (prepared from ferrocene dicarboxylic acid 0.073g, 0.266 mmole) in 20 mL of dry  $\text{CH}_2\text{Cl}_2$  was transferred via a cannula to a stirred solution of compound **1c** (0.19g, 0.24 mmole) and triethylamine (0.25 mL, 1.82 mmole) in 200 mL of  $\text{CH}_2\text{Cl}_2$ . The reaction was stirred for 3 hours at room temperature under nitrogen atmosphere. Water was then added, and the organic layer was separated and washed with water. The organic was dried with  $\text{MgSO}_4$  and filtrated. The solvent was evaporated off under reduced pressure. The crude product was purified by column chromatography ( $\text{SiO}_2$ , 8% methanol in  $\text{CH}_2\text{Cl}_2$ ). The pure product, **L1**, was obtained by recrystallization from  $\text{CH}_2\text{Cl}_2$ - $\text{CH}_3\text{OH}$  as yellow solid (0.096g, 40% yield).

#### Characterization data for L1

$^1\text{H}$  NMR:  $\delta_{\text{H}}$  (400 MHz,  $\text{CDCl}_3$ , ppm) 3.15-3.71 (*m*- $\text{OCH}_2\text{CH}_2\text{O}$ , 16H), 3.64 (s,  $\text{ArCH}_2\text{Ar}$ , 8H), 3.82 (s,  $\text{ArOCH}_2\text{Ar}$ , 4H), 4.67 (s,  $\text{C}_p\text{H}$ , 4H), 4.46 (s,  $\text{C}_p\text{H}$ , 4H), 6.68 (t,  $J = 6.8$  Hz, *p*- $\text{ArH}$ , 2H), 6.73 (d,  $J = 6.8$  Hz, *m*- $\text{ArH}$ , 4H), 6.82 (t,  $J = 7.2$  Hz, 2H), 6.93 (d,  $J = 7.6$  Hz, *p*- $\text{ArHNHCO}$ , 2H), 7.08 (d,  $J = 7.2$  Hz, *m*- $\text{ArH}$ , 4H), 7.22 (t,  $J = 7.2$  Hz, *m*- $\text{ArH}$ , 2H), 7.562 (s, *o*- $\text{ArH}$ , 4H), 8.967 (s,  $\text{NH}$ , 2H).

$^{13}\text{C}$  NMR:  $\delta_{\text{C}}$  (100 MHz,  $\text{CDCl}_3$ , ppm): 168.2, 156.2, 155.4, 139.3, 138.8, 134.7, 133.9, 129.6, 129.4, 127.9, 123.0, 122.7, 121.9, 120.3, 117.9, 79.5, 72.9, 72.4, 71.0, 70.8, 70.1, 68.7, 68.1, 40.2, 39.9, 39.7, 39.3, 39.1, 38.9, 37.3.

Elemental analysis :Anal. Calcd. For  $\text{C}_{62}\text{H}_{58}\text{O}_9\text{N}_2\text{Fe}$ : C, 72.23; H, 5.67; N, 2.72  
found: C, 71.44; H, 5.39; N, 2.87.

MALDI-TOF (m/z)  $[\text{M}]^+$ : calcd 1030.98, found  $[\text{L1}+\text{K}^+]$  1069.62 .

## 2.1.2 Complexation studies by $^1\text{H}$ NMR titrations of L1 and L2

### 2.1.2.1 General procedure

#### 2.1.2.1.1 Apparatus

$^1\text{H}$  NMR spectra and  $^{13}\text{C}$  NMR spectra were recorded on a Varian Mercury 400 NMR spectrometer and a Bruker Avance 400 NMR spectrometer.

#### 2.1.2.1.2 Chemical

All materials and solvents were standard analytical grade. Anions selected in this study are benzoate, acetate, dihydrogenphosphate, fluoride, chloride, bromide and iodide (as tetrabutylammonium salts). Cations used in this study are potassium hexafluorophosphate ( $\text{KPF}_6$ ) and sodium perchlorate monohydrate ( $\text{NaClO}_4 \cdot \text{H}_2\text{O}$ ).

### 2.1.2.2 Experimental Procedure

#### 2.1.2.2.1 Anion and cation binding studies of L1

Typically, a 0.005 M solution of a receptor **L1** ( $2.5 \times 10^{-6}$  mole) in 5%  $\text{CD}_3\text{CN}$  v/v in  $\text{CDCl}_3$  0.5 mL was prepared in a NMR tube. A 0.05 M stock solution of various anionic guests in 5% v/v  $\text{CD}_3\text{CN}$  in  $\text{CDCl}_3$  was prepared in a small vial. Similarly, cationic guests were prepared in  $\text{CD}_3\text{CN}$ . The solution of guest molecules was added into NMR tubes via a microsyringe (50  $\mu\text{L}$  portions) according to the ratio shown in **Table 2.1**.  $^1\text{H}$ -NMR spectra were recorded after each addition.

#### 2.1.2.2.2 Simultaneous cation and anion binding studies of L1

A mixture (0.5 mL) of 0.005 M solution of a receptor **L1** ( $2.5 \times 10^{-6}$  mole) and 1.2 equivalents of a cationic guest was prepared in 5% CD<sub>3</sub>CN v/v in CDCl<sub>3</sub> in a NMR tube. A 0.05 M stock solution of anionic guest molecules in 5% v/v CD<sub>3</sub>CN in CDCl<sub>3</sub> was prepared in a small vial. The solution of anionic guest molecules was added into NMR tubes via a microsyringe (50 μL portions) according to the ratio shown in **Table 2.1**. <sup>1</sup>H-NMR spectra were recorded after each addition.

**Table 2.1** Volume and concentration of guest solutions used in the  $^1\text{H}$  NMR titration.

Mole ratio Guest : Receptor	Added volume of 0.05 M of guest solution ( $\mu\text{L}$ )	Concentration of a guest molecule(M)	Concentration of a receptor (M)
<b>0.0 : 1.0</b>	0	0.00000	0.00500
<b>0.1 : 1.0</b>	5	0.00050	0.00495
<b>0.2 : 1.0</b>	5	0.00098	0.00490
<b>0.3 : 1.0</b>	5	0.00146	0.00485
<b>0.4 : 1.0</b>	5	0.00192	0.00481
<b>0.5 : 1.0</b>	5	0.00238	0.00476
<b>0.6 : 1.0</b>	5	0.00283	0.00472
<b>0.7 : 1.0</b>	5	0.00327	0.00467
<b>0.8 : 1.0</b>	5	0.00370	0.00463
<b>0.9 : 1.0</b>	5	0.00413	0.00459
<b>1.0 : 1.0</b>	5	0.00455	0.00455
<b>1.2 : 1.0</b>	10	0.00536	0.00446
<b>1.4 : 1.0</b>	10	0.00614	0.00439
<b>1.6 : 1.0</b>	10	0.00690	0.00431
<b>1.8 : 1.0</b>	10	0.00763	0.00424
<b>2.0 : 1.0</b>	10	0.00833	0.00417
<b>3.0 : 1.0</b>	50	0.01154	0.00385
<b>4.0 : 1.0</b>	50	0.01429	0.00357

## **2.1.3 Electrochemical studies of L1 and L2**

### **2.1.3.1 General procedure**

#### **2.1.3.1.1 Apparatus**

Cyclic Voltammetry (CV) was performed using a  $\mu$ -AUTOLAB TYPE III potentiostat. All electrochemical experiments carried out with three electrode cells comprising of a working electrode, a counter electrode and a reference electrode at room temperature. A platinum electrode with a diameter 3 mm was used as a working electrode. A Pt wire was used as a counter electrode. A silver wire immersed in silver nitrate solution was used as a reference electrode.

#### **2.1.3.1.2 Chemical**

All materials and solvents were standard analytical grade. Anions selected in this study are benzoate, acetate, dihydrogenphosphate, chloride, bromide and iodide (as tetrabutylammonium salts). Cations used in this study is sodium perchlorate monohydrate ( $\text{NaClO}_4 \cdot \text{H}_2\text{O}$ ), potassium hexafluorophosphate ( $\text{KPF}_6$ ). Tetrabutylammonium hexafluorophosphate ( $\text{TBAPF}_6$ ) was used to prepare a supporting electrolyte solution. Silver nitrate ( $\text{AgNO}_3$ ) was used to prepare the solution in reference electrode.

#### **2.1.3.2 Experimental procedure**

The supporting electrolyte is 0.1 M tetrabutylammonium hexafluorophosphate ( $\text{TBAPF}_6$ ) in 40%  $\text{CH}_3\text{CN}$  v/v in  $\text{CH}_2\text{Cl}_2$ . The surface of a working electrode was polished with slurries of 1.0  $\mu\text{m}$  followed with 0.3  $\mu\text{m}$  alumina powder, and then rinsed with water. Residual alumina particles were thoroughly removed by sonicating for 5 minutes in 0.05 M  $\text{H}_2\text{SO}_4$ . The electrode was then rinsed successively with water and acetone, and dried. The  $\text{Ag}/\text{AgNO}_3$  electrode, constructed by immersing a silver wire into a solution of 0.01 M  $\text{AgNO}_3$  in 0.1 M  $\text{TBAPF}_6$ , was used as a reference electrode. Oxygen in solution was purged with  $\text{N}_2$  gas for 5 minutes before performing the experiment. The experiments were run at room temperature. The appropriate scan rate was found to be 100 mV/s.

#### **2.1.3.2.1 Electrochemical studies of L1 and various anions**

Typically, a 0.001 M solution of a receptor in 5 mL of supporting electrolyte solution was prepared. A 0.1 M stock solution of anionic guests was also prepared in the supporting electrolyte solution. Upon titration, the solution of anionic guests was added into the solution of the receptor following the ratio shown in **Table 2.2**.

#### **2.1.3.2.2 Electrochemical studies of L1 and cations**

Typically, a 0.001 M solution of a receptor in 5 mL of supporting electrolyte was prepared. A 0.1 M stock solution of metal salts,  $\text{KPF}_6$  and  $\text{NaClO}_4 \cdot \text{H}_2\text{O}$  was prepared in the supporting electrolyte solution. Upon titration, the solution of a metal salt was added into the solution of the receptor following the ratio shown in **Table 2.2**.

#### **2.1.3.2.3 Simultaneous cation and anion binding studies of L1**

Typically, a mixture of a 0.001 M solution of a receptor and 3.0 equivalents of a cationic guest ( $\text{KPF}_6$ ) in 5 mL of supporting electrolyte was prepared. A 0.1 M stock solution of anionic guests in the supporting electrolyte solution was prepared. Upon titration, the solution of anionic guests was added into the solution of the receptor following the ratio shown in the **Table 2.2**.

**Table 2.2** Volume and concentration of guest solutions used in the CV titration of L1

Equivalents of Anions	Added volume of 0.05 M of guest solution ( $\mu\text{L}$ )	Concentration of a guest molecule(M)	Concentration of a receptor (M)
0	0	0	0.001
0.2	10	0.0002	0.000998
0.4	20	0.000398	0.000996
0.6	30	0.000596	0.000994
0.8	40	0.000794	0.0009921
1	50	0.00099	0.0009901
1.5	75	0.001478	0.0009852
2	100	0.001961	0.0009804
3	150	0.002913	0.0009709
4	200	0.003846	0.0009615

## 2.2 Experimental section for chapter IV

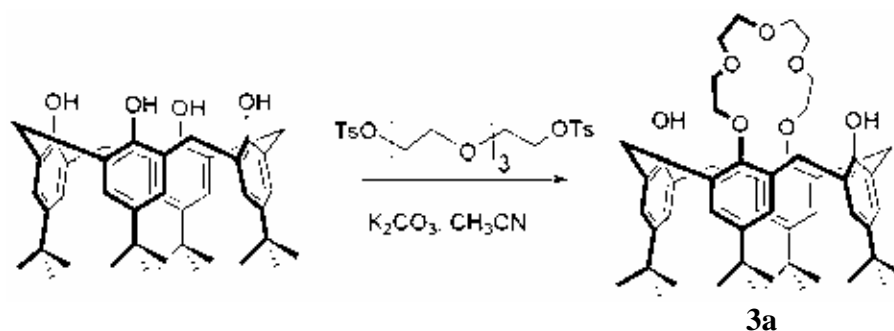
### 2.2.1 Synthesis of receptors, L3 and L4, crown ether-based calix[4]arene with amido- anthraquinone pendants

#### 2.2.1.1 General Procedure

(See section 2.1.1.1)

#### 2.2.1.2 Synthesis

##### 2.2.1.2.1 Preparation of 3a



The mixture of *p*-tert butylcalix[4]arene (2.00 g, 3.08 mmol) and  $K_2CO_3$  (0.51 g, 3.70 mmol) in 150 mL of dried acetonitrile was refluxed under nitrogen atmosphere for an hour. The solution of tetraethyleneglycol ditosylate, which was prepared from tetraethyleneglycol, (1.86 g, 3.70 mmol) in 50 mL of dried acetonitrile was added dropwise and the mixture was reflux for 48 hours. Then,  $K_2CO_3$  was removed by filtration. The filtrate was evaporated and the residue was dissolved in  $CH_2Cl_2$  (50 mL) and stirred with 3M HCl (50 mL) for 30 minutes. The aqueous solution was extracted with  $CH_2Cl_2$  and the organic layer was dried over anhydrous  $MgSO_4$ , filtered, and concentrated in vacuo. The crude product was purified by column chromatography ( $SiO_2$ , 20% ethylacetate in Hexane). Compound 1a was precipitated in  $CH_2Cl_2/MeOH$  as white solid (1.0 g, 40 % yield).



**Characterization data for 3a**

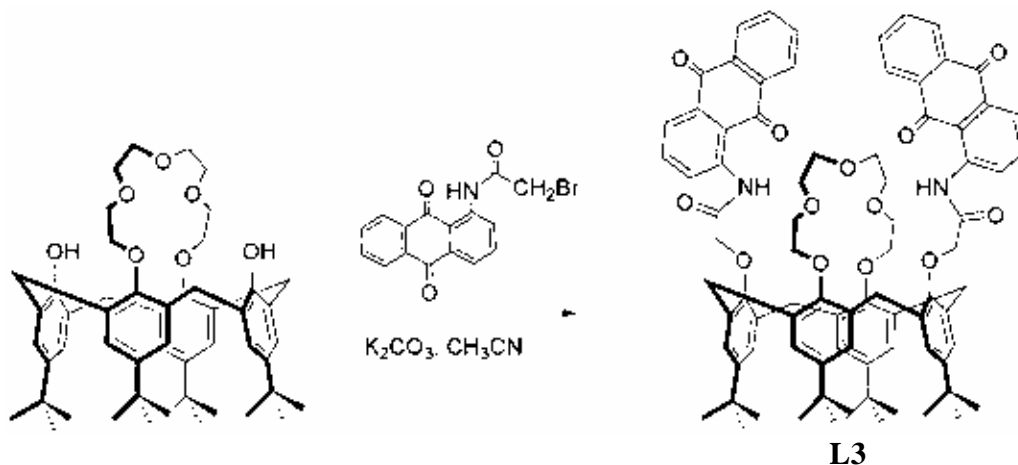
$^1\text{H}$  NMR:  $\delta_{\text{H}}$  (400 MHz,  $\text{CDCl}_3$ , ppm) 0.91 (s, 18H, tBu), 1.31 (s, 18H, tBu), 3.29 (d,  $J = 12.8$  Hz, 4H,  $\text{ArCH}_2$ ), 3.84 (t,  $J = 5.2$  Hz, 4H,  $\text{OCH}_2$ ), 3.96 (t,  $J = 5.2$  Hz, 4H,  $\text{OCH}_2$ ), 4.08 (s, 8H,  $\text{OCH}_2$ ), 4.37 (d,  $J = 12.8$  Hz, 4H,  $\text{ArCH}_2$ ), 6.75 (s, 4H,  $\text{ArH}$ ), 7.07 (s, 4H,  $\text{ArH}$ ), 7.20 (s, 2H, OH)

$^{13}\text{C}$  NMR:  $\delta_{\text{C}}$  (100 MHz,  $\text{CDCl}_3$ , ppm) 31.0, 31.4, 31.7, 33.8, 33.9, 70.3, 70.9, 71.0, 76.6, 125.0, 125.4, 127.8, 132.5, 141.2, 146.8, 149.8, 150.8.

Elemental analysis: calculated for  $\text{C}_{52}\text{H}_{70}\text{O}_7$ : C, 77.38; H, 8.74,  
found: C, 77.33; H, 8.73

MALDI-TOF (m/z) calcd **3a**: 807.12 found: [**3a**+ $\text{Na}^+$ ]: 829.90

### 2.2.1.2.2 Preparation of L3



The mixture of **3a** (0.50 g, 0.62 mmol) and  $K_2CO_3$  (0.085 g, 0.62 mmol) in 100 mL of dried acetonitrile was heated at reflux under nitrogen atmosphere for 30 minutes. Bromoacetyl amidoanthraquinone (0.216 g, 0.43 mmol) was added to the mixture and then the mixture was reflux for 24 hours. The filtrate was evaporated and the residue was dissolved in  $CH_2Cl_2$  (50 mL) and stirred with 3M HCl (50 mL) for 30 minutes. The aqueous solution was extracted with  $CH_2Cl_2$  and the organic layer was dried over anhydrous  $MgSO_4$ , filtered, and concentrated in vacuo. The crude product was purified by column chromatography ( $SiO_2$ , 20% methanol in dichloromethane). Compound **1** was precipitated in  $CH_2Cl_2/MeOH$  as yellow solid (74 mg, 9%).

### Characterization data for L3

$^1H$  NMR:  $\delta_H$  (400 MHz,  $CDCl_3$ , ppm) 0.96 (s, 18H, tBu), 1.182 (s, 18H, tBu), 3.27 (d,  $J = 12.8$  Hz, 4H,  $ArCH_2$ ), 3.30 (s, 4H,  $OCH_2$ ), 3.53 (s, 4H,  $OCH_2$ ), 4.21 (t,  $J = 6.8$  Hz, 4H,  $OCH_2$ ), 4.30 (t,  $J = 6.8$  Hz, 4H,  $OCH_2$ ), 4.73 (d,  $J = 12.8$  Hz, 4H,  $ArCH_2$ ), 5.01 (s, 4H,  $CH_2CO$ ), 6.68 (s, 4H,  $ArH$ ), 6.96 (s, 4H,  $ArH$ ), 7.71-7.78 (m, 6H,  $ArH$ ), 8.05 (d,  $J = 7.6$  Hz, 2H,  $ArH$ ), 8.28-8.25 (m, 4H,  $ArH$ ), 9.09 (d,  $J = 8.4$  Hz, 2H,  $ArH$ ), 12.41 ( $s_b$ , 2H).

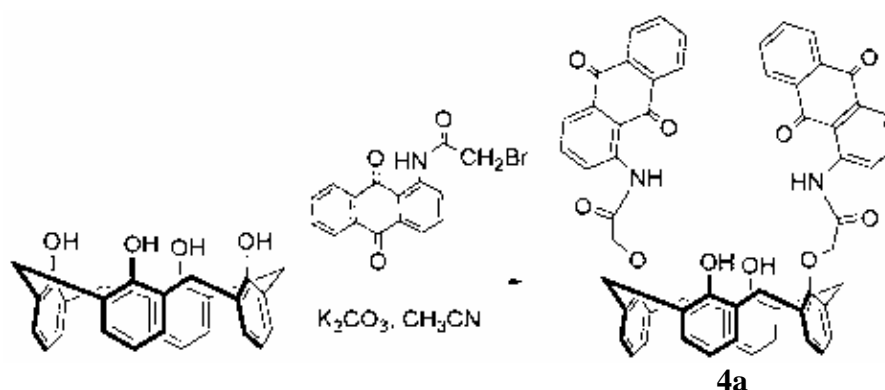
$^{13}\text{C}$  NMR:  $\delta_{\text{C}}$  (100 MHz,  $\text{CDCl}_3$ , ppm) 31.2, 31.5, 31.6, 33.7, 33.9, 70.4, 70.7, 71.2, 72.8, 75.1, 118.3, 122.5, 125.1, 125.4, 126.7, 126.9, 127.5, 132.7, 132.9, 134.0, 134.1, 134.2, 134.3, 134.4, 135.3, 141.6, 144.9, 152.0, 154.1, 169.3, 182.7, 186.7

Elemental analysis: calculated for  $\text{C}_{84}\text{H}_{88}\text{N}_2\text{O}_{13}$ : C, 75.65; H, 6.65; N, 2.10

found: C, 75.62; H, 6.60; N, 2.12.

MALDI-TOF (m/z): calcd: **L3**: 1333.62, found [**L3**+ $\text{Na}^+$ ]: 1356.48.

#### 2.2.1.2.3 Preparation of 4a



The mixture of calix[4]arene (0.5 g, 1.18 mmol) and  $\text{K}_2\text{CO}_3$  (0.48 g, 3.53 mmol) in 150 mL of dried acetonitrile was refluxed under nitrogen atmosphere for half an hour. The solution of bromoacetyl amidoanthraquinone (0.93 g, 2.71 mmol) was added, and the mixture was reflux for 24 hours. The filtrate was evaporated and the residue was dissolved in  $\text{CH}_2\text{Cl}_2$  (50 mL) and stirred with 3M HCl (50 mL) for 30 minutes. The aqueous solution was extracted with  $\text{CH}_2\text{Cl}_2$  and the organic layer was dried over anhydrous  $\text{MgSO}_4$ , filtered, and concentrated in vacuo. The crude product was purified by column chromatography ( $\text{SiO}_2$ , 5% ethylacetate in dichloromethane). Compound **4a** was precipitated in  $\text{CH}_2\text{Cl}_2/\text{MeOH}$  as yellow solid (0.35g, 32%).

**Characterization data for 4a**

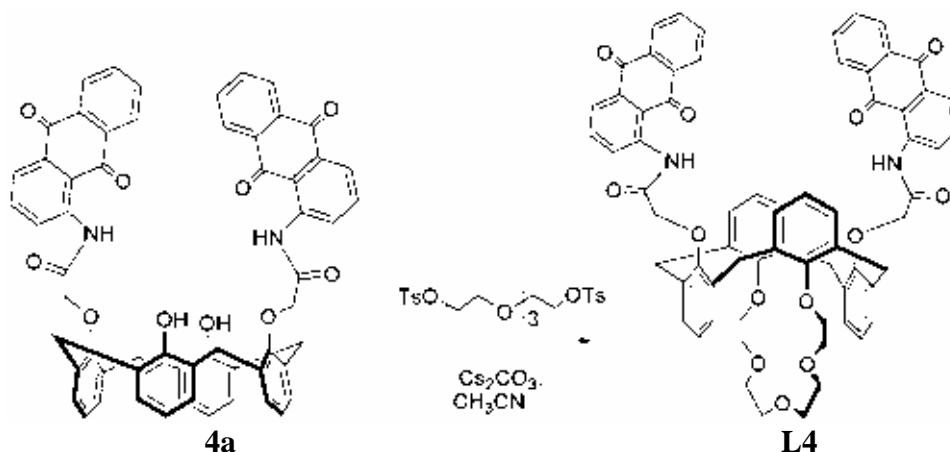
$^1\text{H}$  NMR:  $\delta_{\text{H}}$  (400 MHz,  $\text{CDCl}_3$ , ppm) 3.49 (d,  $J = 14$  Hz, 4H,  $\text{CH}_2\text{Ar}$ ), 4.44 (s, 4H,  $\text{CH}_2\text{CO}$ ), 4.53 (d,  $J = 14$  Hz, 4H,  $\text{ArCH}_2\text{Ar}$ ), 5.98 (s, 2H,  $\text{OH}$ ), 6.57 (s, 6H,  $\text{ArH}$ ), 6.77 (t,  $J = 7.2$  Hz, 2H,  $\text{ArH}$ ), 7.16 (d,  $J = 7.2$  Hz, 4H,  $\text{ArH}$ ), 7.42 (t,  $J = 8$  Hz, 2H,  $\text{ArH}$ ), 7.48 (t,  $J = 7.6$  Hz, 2H,  $\text{ArH}$ ), 7.55 (t,  $J = 7.2$  Hz, 2H,  $\text{ArH}$ ), 7.73 (t,  $J = 8$  Hz, 4H,  $\text{ArH}$ ), 8.17 (d,  $J = 7.2$  Hz, 2H,  $\text{ArH}$ ), 8.48 (d,  $J = 8$  Hz, 2H,  $\text{ArH}$ ), 13.172 ( $s_b$ , 2H,  $\text{NH}$ ).

$^{13}\text{C}$  NMR:  $\delta_{\text{C}}$  (100 MHz,  $\text{CDCl}_3$ , ppm) 30.6, 74.4, 117.7, 119.2, 123.0, 124.7, 125.7, 126.5, 127.6, 128.7, 129.0, 129.7, 131.9, 132.3, 133.1, 133.2, 133.7, 134.2, 135.5, 140.0, 152.7, 153.2, 167.7, 181.3, 186.2.

Elemental analysis: calculated for  $\text{C}_{60}\text{H}_{42}\text{O}_{10}\text{N}_2$ : C, 75.78; H, 4.45; N, 2.95  
found: C, 75.50; H, 4.47; N, 2.94;

MALDI-TOF (m/z): calcd: **4a** : 950.98, found [**4a**+ $\text{K}^+$ ] 990.22.

#### 2.2.1.2.4 Preparation of L4



The mixture of **4a** (0.2 g, 0.2 mmol) and  $\text{Cs}_2\text{CO}_3$  (0.64 g, 1.96 mmol) in 100 mL of dried acetonitrile was refluxed under nitrogen atmosphere for half an hour. The solution of tetraethyleneglycol ditosylate, which was prepared from tetraethylene glycol, (1.0 g, 1.98 mmol) in 20 mL of dried acetonitrile was added dropwise, and the mixture was reflux for 24 hours. Then,  $\text{Cs}_2\text{CO}_3$  was removed by filtration. The filtrate was evaporated and the residue was dissolved in  $\text{CH}_2\text{Cl}_2$  (50 mL) and stirred with 3M HCl (50 mL) for 30 minutes. The aqueous solution was extracted with  $\text{CH}_2\text{Cl}_2$  and the organic layer was dried over anhydrous  $\text{MgSO}_4$ , filtered, and concentrated in vacuo. The crude product was purified by column chromatography ( $\text{SiO}_2$ , 5% methanol in dichloromethane) (15 mg, 7 % yield).

#### Characterization data for L4

$^1\text{H}$  NMR:  $\delta_{\text{H}}$  (400 MHz,  $\text{CDCl}_3$ , ppm ) 3.20 (t,  $J = 6.8$  Hz, 4H,  $\text{CH}_2\text{O}$ ), 3.38 (s, 4H,  $\text{CH}_2\text{O}$ ), 3.66- 4.37 (m, 12H,  $\text{CH}_2\text{O}$ ), 3.90 (d,  $J = 16.4$  Hz, 4H,  $\text{ArCH}_2\text{Ar}$  ), 4.20 (d,  $J = 16.4$  Hz, 4H,  $\text{ArCH}_2\text{Ar}$ ), 6.71 (t,  $J = 7.2$  Hz, 2H,  $\text{ArH}$ ), 6.94 (t,  $J = 7.6$  Hz, 2H,  $\text{ArH}$ ), 7.03 (d,  $J = 7.6$  Hz, 4H,  $\text{ArH}$ ), 7.19 (d,  $J = 7.6$  Hz, 4H,  $\text{ArH}$ ), 7.61 (t,  $J = 8$  Hz, 2H,  $\text{ArH}$  ), 7.76-7.74 (m, 4H,  $\text{ArH}$ ), 8.04 (d,  $J = 7.6$  Hz, 2H,  $\text{ArH}$ ), 8.29-8.23 (m, 4H,  $\text{ArH}$ ), 8.95 (d,  $J = 8.4$  Hz, 2H,  $\text{ArH}$ ), 12.23 ( $s_b$ , 2H,  $\text{NH}$ )

$^{13}\text{C}$  NMR:  $\delta_{\text{C}}$  (100 MHz,  $\text{CDCl}_3$ , ppm) 38.2, 68.6, 69.5, 71.0, 71.3, 73.0, 118.7, 122.6, 123.2, 123.8, 126.8, 126.9, 127.4, 130.2, 130.3, 132.7, 134.1, 134.13, 134.2, 134.26, 134.3, 135.0, 135.2, 141.3, 154.9, 156.7, 169.5, 182.9, 186.2.

Elemental analysis calculated for  $\text{C}_{68}\text{H}_{56}\text{N}_2\text{O}_{13}$  : C, 73.61; H, 5.08; N, 2.52.

found: C, 73.48; H, 5.12; N, 2.61.

MALDI-TOF (m/z): calcd: **L4** :1109.20 Found [**L4**+ $\text{K}^+$ ] = 1148.81

## 2.2.2 Complexation studies by $^1\text{H}$ NMR titrations of **L3** and **L4**

### 2.2.2.1 General procedure

(See section 2.1.2.1)

### 2.2.2.2 Experimental Procedure

#### 2.2.2.2.1 Anion and cation binding studies of **L3** and **L4**

Typically, a 0.005 M solution of receptors, **L3** and **L4** ( $2.5 \times 10^{-6}$  mole) in 5%  $\text{CD}_3\text{CN}$  v/v in  $\text{CDCl}_3$  0.5 mL was prepared in a NMR tube. A 0.05 M stock solution of various anionic guests in 5% v/v  $\text{CD}_3\text{CN}$  in  $\text{CDCl}_3$  was prepared in a small vial. Similarly, cationic guests were prepared in  $\text{CD}_3\text{CN}$ . The solution of guest molecules was added into NMR tubes via a microsyringe (50  $\mu\text{L}$  portions) according to the ratio shown in **Table 2.1**.  $^1\text{H}$ -NMR spectra were recorded after each addition.

#### 2.2.2.2.2 Simultaneous cation and anion binding studies of **L3** and **L4**

A mixture (0.5 mL) of 0.005 M solution of a receptor ( $2.5 \times 10^{-6}$  mole) and 1.2 equivalents of a cationic guest was prepared in 5%  $\text{CD}_3\text{CN}$  v/v in  $\text{CDCl}_3$  in a NMR tube. A 0.05 M stock solution of anionic guest molecules in 5% v/v  $\text{CD}_3\text{CN}$  in  $\text{CDCl}_3$  was prepared in a small vial. The solution of anionic guest molecules was added into NMR tubes via a microsyringe (50  $\mu\text{L}$  portions) according to the ratio shown in **Table 2.1**.  $^1\text{H}$ -NMR spectra were recorded after each addition.

## **2.2.3 Anion sensing abilities of L3 and L4 by UV-vis spectrophotometry**

### **2.2.3.1 General procedure**

#### **2.2.3.1.1 Apparatus**

All UV-vis spectra were recorded with a Varian Cary 50 Probe UV-Visible spectrometer. The emission spectra were recorded in the range of 200-800 nm at room temperature.

#### **2.2.3.1.2 Chemical**

All materials and solvents were standard analytical grade. Anions selected in this study are benzoate, acetate, dihydrogenphosphate, fluoride, chloride, bromide and iodide (as tetrabutylammonium salts). A cation used in this study is potassium hexafluorophosphate ( $\text{KPF}_6$ ).

### **2.2.3.2 Experimental procedure**

#### **2.2.3.2.1 UV-vis titration with various anions**

Solutions of ligands **L3** and **L4** ( $5.0 \times 10^{-5}$  M) were prepared. The 2 mL of each ligand was pipetted into a 1 cm pathlength quartz cuvette. The solution of each anion (0.1 M) was prepared in 1 mL of a vial. The anion solution was transferred in portion to the cuvette and stirred for 3 minutes prior to measure. Amounts of added anions were listed in **Table 2.3**.

#### **2.2.3.2.2. UV-vis titration with various anions in the presence of a cation**

A mixture of 0.005 M solution of a receptor ( $2.5 \times 10^{-6}$  mole) and 1.2 equivalents of a cationic guest (potassium hexafluorophosphate,  $\text{KPF}_6$ ) was prepared in  $\text{CH}_3\text{CN}$ . The solution of each anion (0.1 M) was prepared in 1 mL of a vial. The anion solution was transferred in portion to the cuvette and stirred for 3 minutes prior to measure. Amounts of added anions were listed in **Table 2.3**.

**Table 2.3** Amounts of anions (0.1 M) added to 2 mL of **L3** and **L4** ( $5.0 \times 10^{-5}$  M) in UV-vis and fluorescence titration experiments

Equivalents of Anions	Added volume of 0.05 M of guest solution ( $\mu\text{L}$ )	Concentration of a guest molecule(M)	Concentration of a receptor (M)
0	0	0	0.00005
5	5	0.0002494	4.9875E-05
10	5	0.0004975	4.9751E-05
15	5	0.0007444	4.9628E-05
20	5	0.0009901	4.9505E-05
25	5	0.0012346	4.9383E-05
30	5	0.0014778	4.9261E-05
35	5	0.0017199	4.914E-05
40	5	0.0019608	4.902E-05
45	5	0.0022005	4.89E-05
50	5	0.002439	4.878E-05
60	10	0.0029126	4.8544E-05
70	10	0.0033816	4.8309E-05
80	10	0.0038462	4.8077E-05
90	10	0.0043062	4.7847E-05
100	10	0.0047619	4.7619E-05



## **2.2.4 Anion sensing abilities of L3 and L4 by fluorescence spectrophotometry**

### **2.2.4.1 General procedure**

#### **2.2.4.1.1 Apparatus**

All fluorescence emission spectra were recorded using varian Cary Eclipse Fluorescence spectrophotometer.

#### **2.2.4.1.2 Chemical**

All materials and solvents were standard analytical grade. Anions selected in this study are benzoate, acetate, dihydrogenphosphate, fluoride, chloride, bromide and iodide (as tetrabutylammonium salts). A cation used in this study is potassium hexafluorophosphate ( $\text{KPF}_6$ ).

### **2.2.4.2 Experimental procedure**

The conditions set in each fluorescence experiment are shown below.

Excitation wavelength: 450 nm.

Range of emission spectrum: 460-800 nm.

Width of excitation and emission slit: 10 nm.

Smoothing factor: 15

Scan rate: medium

PMT voltage: medium

#### **2.2.4.2.1 Fluorescence titrations of ligands L3 and L4 with various anions**

Solutions of ligands **L3** and **L4** ( $5.0 \times 10^{-5}$  M) were prepared. The 2 mL of each ligand was pipetted into a 1 cm pathlength quartz cuvette. The solution of each anion (0.1 M) was prepared in 1 mL of a vial. The anion solution was transferred in portion to the cuvette and stirred for 3 minutes prior to measure. Amounts of added anions were listed in **Table 2.3**.

#### 2.2.4.2.2 Fluorescence titrations of L3 and L4 with various anions in the presence of a cation

A mixture of 0.005 M solution of a receptor ( $2.5 \times 10^{-6}$  mole) and 1.2 equivalents of a cationic guest (potassium hexafluorophosphate,  $\text{KPF}_6$ ) was prepared in  $\text{CH}_3\text{CN}$ . The solution of each anion (0.1 M) was prepared in 1 mL of a vial. The anion solution was transferred in portion to the cuvette and stirred for 3 minutes prior to measure. Amounts of added anions were listed in **Table 2.3**

#### 2.2.4.2.3 Determination of the stoichiometry of L3 and L4 with $\text{F}^-$ by Job's method

Solutions of each receptor and fluoride ( $1 \times 10^{-4}$  M) in  $\text{CH}_3\text{CN}$  were prepared in 20 mL of a volumetric flask. A mixture of the receptor and fluoride was pipetted to a 1 cm quartz cuvette to provide the total volume 2 mL according to **Table 2.4**. Emission spectra of each addition were measured after stirred 3 min.

**Table 2.4** Amounts of fluoride ( $1 \times 10^{-4}$  M) and a ligand ( $1 \times 10^{-4}$  M) added in cuvette for Job's method

Point	Volume of $\text{F}^-$ (mL)	Volume of a receptor (mL)
1	0	2.00
2	0.20	1.80
3	0.40	1.60
4	0.60	1.40
5	0.80	1.20
6	1.00	1.00
7	1.20	0.80
8	1.40	0.60
9	1.60	0.40
10	1.80	0.20
11	2.00	0.00

## **2.2.5 Electrochemical studies of L3 and L4**

### **2.2.5.1 General procedure**

#### **2.2.5.1.1 Apparatus**

(See section 2.1.3.1.1). A carbon electrode with a diameter 3 mm embedded in Teflon was used as a working electrode instead of a platinum electrode in this study.

#### **2.2.5.1.2 Chemical**

(See section 2.1.3.1.2).

### **2.1.5.2 Experimental procedure**

The experimental procedure was similar to the section 2.1.3.2. However, the appropriate scan rate for this study was found to be 50 mV/s.

#### **2.2.5.2.1 Electrochemical studies of L3 and L4 with various anions**

Typically, a 0.001 M solution of a receptor in 5 mL of supporting electrolyte solution was prepared. A 0.1 M stock solution of anionic guests was also prepared in the supporting electrolyte solution. Upon titration, the solution of anionic guests was added into the solution of the receptor following the ratio shown in **Table 2.5**.

#### **2.2.5.2.2 Electrochemical studies of L3 and L4 with $\text{KPF}_6$**

Typically, a 0.001 M solution of a receptor in 5 mL of supporting electrolyte was prepared. A 0.1 M stock solution of a metal salt,  $\text{KPF}_6$ , was prepared in the supporting electrolyte solution. Upon titration, the solution of a metal salt was added into the solution of the receptor following the ratio shown in **Table 2.5**.

### 2.2.5.2.3 Simultaneous cation and anion binding studies of receptors

#### L3 and L4

Typically, a mixture of a 0.001 M solution of a receptor and 3.0 equivalents of a cationic guest ( $\text{KPF}_6$ ) in 5 mL of supporting electrolyte was prepared. A 0.1 M stock solution of anionic guests in the supporting electrolyte solution was prepared. Upon titration, the solution of anionic guests was added into the solution of the receptor following the ratio shown in the **Table 2.5**.

**Table 2.5** Volume and concentration of guest solution used in the CV titration of **L3** and **L4**

Equivalents of Anions or cations	Added volume of 0.05 M of guest solution ( $\mu\text{L}$ )	Concentration of a guest molecule(M)	Concentration of a receptor (M)
0	0	0	0.001
0.2	10	0.0002	0.000998
0.4	20	0.000398	0.000996
0.6	30	0.000596	0.000994
0.8	40	0.000794	0.0009921
1	50	0.00099	0.0009901
1.5	75	0.001478	0.0009852
2	100	0.001961	0.0009804
3	150	0.002913	0.0009709
4	200	0.003846	0.0009615
6	300	0.00566	0.0009434
8	400	0.007407	0.0009259
10	500	0.009091	0.0009091

# CHAPTER III

## ELECTROCHEMICAL HETERODITOPIC RECEPTORS DERIVED FROM CROWN ETHER BASED CALIX[4]ARENE WITH AMIDO-FERROCENE PENDANTS

### 3.1 General information and literature reviews of heteroditopic receptors based ferrocene

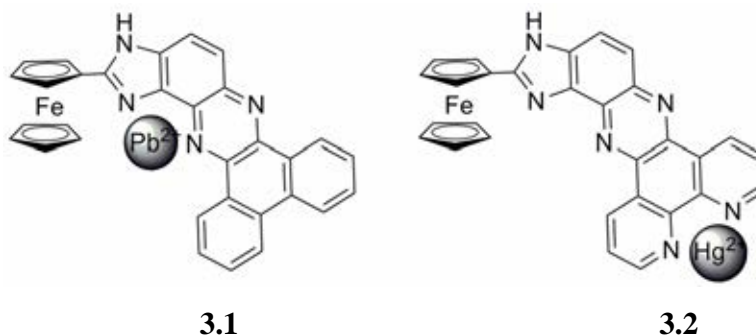
Ferrocene based redox responsive receptors can be exploited and most widely used as electrochemical sensor for both anions and cations [3, 4, 22, 27, 28, 54, 56, 60, 61, 65, 67, 68, 70-75]. In general, upon applying the potentials, ferrocene gives sharp reversible redox couple of ferrocene-ferrocenium ion ( $\text{Fc}/\text{Fc}^+$ ) through a fast one-electron transfer. Therefore, a cation or an anion binding site attaching ferrocene can give a perturbation of the ferrocene redox potential upon binding a cation or an anion. The oxidized form of ferrocene is stable in most organic solvents, but can decompose quickly in aqueous media, especially in basic condition.

#### 3.1.1 Cation sensors derived form ferrocene

Normally, anodic shifts are observed for cations sensing [18, 19, 28, 58-60, 70]. Once a metal ion is coordinated at the receptor binding site, the ferrocene itself becomes harder to be oxidized. Therefore, the  $\text{Fc}/\text{Fc}^+$  redox couple shifts to a higher potential.

Heteroditopic receptors based on ferrocene-imidazophenazine dyads, **3.1** and **3.2** were presented [70]. Both receptors contained a nitrogen-rich polycyclic system (transition metal binding site) linked to a ferrocene unit through an imidazole ring (anion binding site). Receptors **3.1** and **3.2** can sense different transition metals,  $\text{Pb}^{2+}$  and  $\text{Hg}^{2+}$  respectively, through a similar behavior. Upon binding with transition metals, the enhancement of their emission spectra, new low-energy absorption bands and anodic shifts of the oxidation waves were observed. Even though ditopic properties of these receptors could not successfully be studied due to the low solubility of the species formed

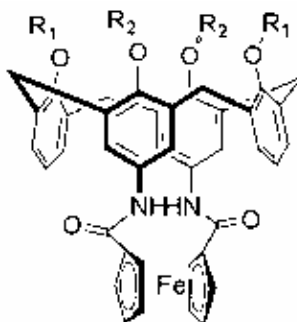
during the experiments, the simultaneous recognition of  $\text{H}_2\text{PO}_4^-$  and  $\text{Pb}^{2+}$  of the receptor **3.1** was observed via the electrospray mass spectrometry.



### 3.1.2 Anion sensors derived from ferrocene

In contrast, the cathodic shifts are observed for anions sensing, indicating that  $\text{Fc}^+$  is stabilized by the negative charge anions [16, 17, 22, 27, 28, 56, 61, 67, 68, 75]. For examples, three calix[4]arene derivatives, **3.3-3.5** have been synthesized [75]. Complexation studies by  $^1\text{H}$  NMR titration in  $\text{CD}_3\text{CN}$  revealed that all receptors were found to bind carboxylate anions,  $\text{BzO}^-$  and  $\text{AcO}^-$  selectively. However, they bind preferentially with acetate over benzoate because acetate is more basic than benzoate. Interestingly, **3.5** gave a higher affinity for anions compared to the others since **3.5** was rigidified by four bulky ethyl ester groups on the anion affinity of **3.5** which consists of ethyl ester groups as a cation binding site and as an inhibitor for phenyl ring rotation. Ditopic properties of **3.5** could not be investigated due to the abstraction of cations by anions. Electrochemical studies of these receptors found that upon addition benzoate anions to the solutions of receptors resulted in cathodic shifts of the oxidation waves of cyclic voltammograms. Moreover, gradual addition of carboxylate anions led to quasireversible voltammograms and became completely irreversible after adding 4 equivalents of anions. In square wave voltammograms, a new wave gradually appeared at less positive potential, while the initial wave decreased and disappeared completely. Presumably, the ferrocinium ( $\text{Fc}^+$ ) unit enhanced binding with anionic species through

electrostatic interactions. Anions, then, inhibited the electron-transfer back to ferrocene (Fc).



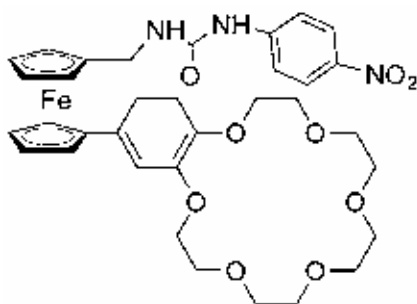
**3.3:**  $R_1=R_2=CH_3$

**3.4:**  $R_1=CH_3$ ,  $R_2=CH_2COOEt$

**3.5:**  $R_1=R_2=CH_2COOEt$

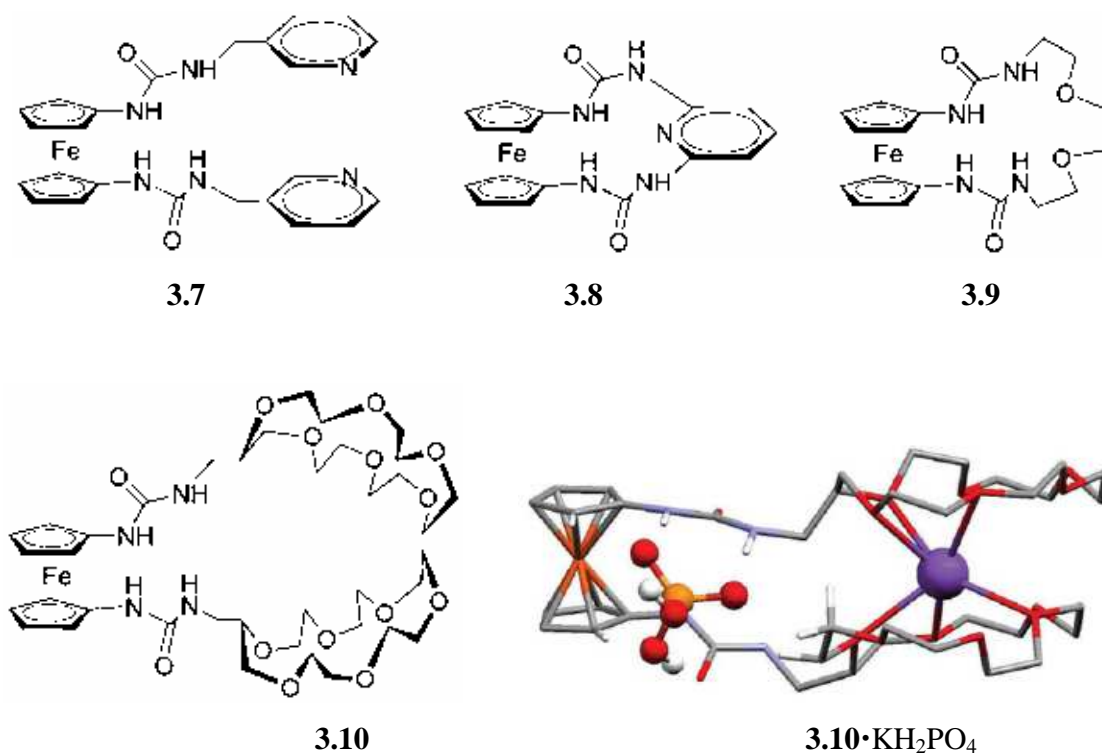
### 3.1.3 Heteroditopic receptors derived from ferrocene

A ditopic ferrocene receptor containing a nitrobenzene-linked urea moiety and benzocrown, **3.6**, has been synthesized [71]. It functioned as a chromogenic molecular switch. Addition of  $F^-$  led to yellow solution of the receptor **3.6**, while addition of  $K^+$  resulted in the original color of the receptor. Complexation studies from  $^1H$  NMR titration revealed that bound  $K^+$  interacted with the urea arm of the receptor in such a way that the hydrogen bonding interaction between **3.6** and  $F^-$  was weakened. Therefore, it was noticed that the presence of  $K^+$  in close proximity to the fluoride binding site of **3.6** caused the color quenching process.



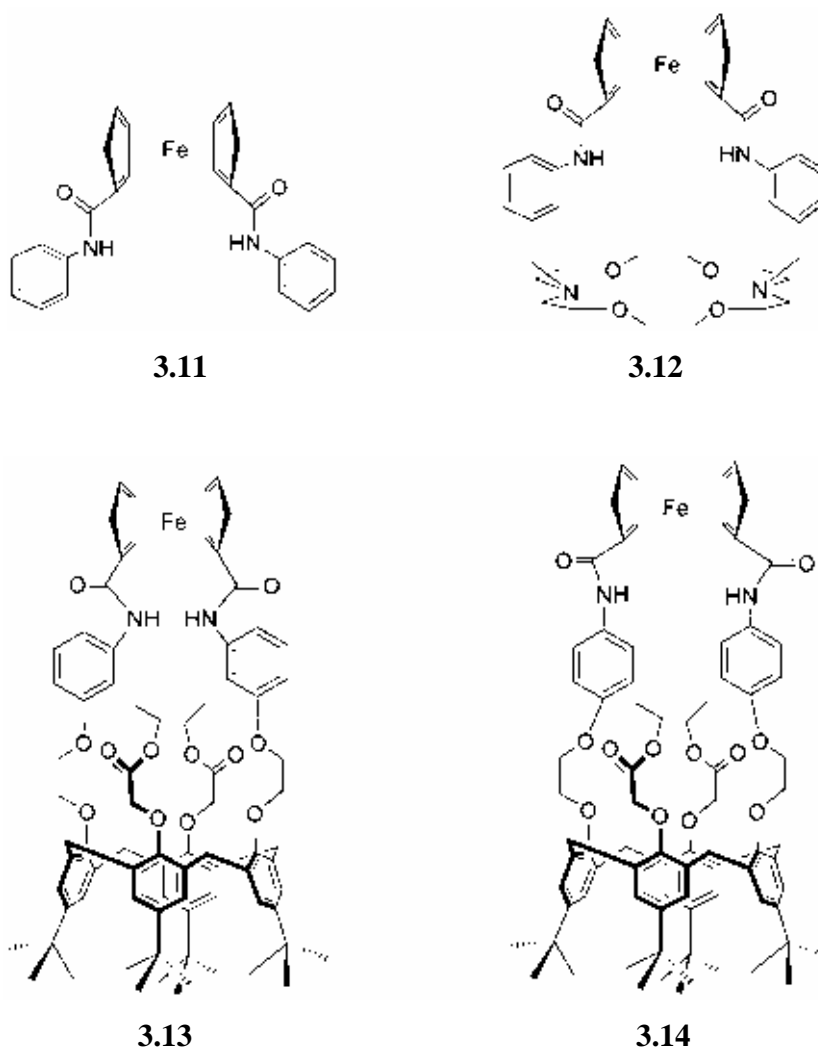
**3.6**

Simple and easy-to-make ferrocene based urea heteroditopic receptors having either an additional nitrogen donor atom belonging to a pyridine unit (a transition metal binding site) or multipoint binding sites belonging to crown ether subunits (as alkali metal binding sites), **3.7-3.10** have been synthesized [72]. Receptors **3.7**, **3.8** and **3.10** showed spectral and electrochemical anion-sensing for  $\text{H}_2\text{PO}_4^-$  and  $\text{F}^-$ . Interestingly, receptor **3.10** was able to sense  $\text{K}^+$  electrochemically in the presence of  $\text{H}_2\text{PO}_4^-$  which could be observed through less negative potential shift of differential pulse voltammetry of  $[\mathbf{3.10} \cdot \text{H}_2\text{PO}_4^-]$  complex. Addition of  $\text{K}^+$  to  $[\mathbf{3.10} \cdot \text{F}^-]$  solution had no effect as compared to the previous case. Calculated structure using B3LYP/3-21G\* for  $\mathbf{3.10} \cdot \text{KH}_2\text{PO}_4$  was shown below. In this case, **3.10** can bind  $\text{K}^+$  and  $\text{H}_2\text{PO}_4^-$  simultaneously as a contact ion pair.





In our research group, electrochemical heteroditopic receptors based on amidoferrocene linked to crown ether or pseudo crown ether have been in our efforts [47, 73]. In 2005, an ion-pair receptor derived from an azacrown ether unit linked with benzyl amidoferrocene moieties as a cation binding site and an anion binding site respectively, receptor **3.12**, has been synthesized [47, 73]. Receptor **3.11** was also synthesized as a control compound. It was found that both receptors themselves preferred to bind with Y-shaped anions,  $\text{AcO}^-$  and  $\text{BzO}^-$ , over other anions [73]. Thus, it implied that amidoferrocene receptors provided suitable cavity size for Y-shaped anion binding. Surprisingly, receptor **3.12** was able to bind  $\text{Br}^-$  selectively with high stability in the presence of  $\text{Na}^+$ . Moreover, electrochemically oxidized form of cobound cation receptor **3.12** was found to bind  $\text{Cl}^-$  with higher efficiency. From this study, it can be concluded that additional electrostatic interaction from a cation influenced the binding affinity of anions. As expected from heteroditopic receptors, the electrostatic force from a cation can improve anion affinity. However, the other factors that control cooperative effect such as the distance between a cation and an anion binding site have not been clear understood yet. Therefore, two isomers of bis-thyl ester-calix[4]arene-capped amidoferrocene **3.13** (*meta*) and **3.14** (*para*) have been synthesized [47]. Both receptors preferred to bind  $\text{Br}^-$  and  $\text{I}^-$  selectively in the presence of  $\text{Na}^+$ . The electrochemically oxidized ferrocenium form of *para*-isomer **3.14** in the free form recognized  $\text{AcO}^-$  selectively, but showed a negative recognition in the presence of  $\text{Na}^+$ . In contrast, *meta*-isomer **3.13** was enhanced sensing abilities of  $\text{AcO}^-$  and  $\text{Cl}^-$  electrochemically in the presence of  $\text{Na}^+$ . Therefore, this study indicated that the topology of the ligands and the presence of metal ions affected anion binding abilities of the ion-pair receptors **3.13** and **3.14**.



### 3.2 Objective and scope of the research

In this study, further investigation of the topology of the heteroditopic receptors that affect the cooperative binding effect has been concentrated. The unique properties of calix[4]arene, the molecular building block, such as its ease of functionalization and a variety of conformations have been utilized. Accordingly, crown ether-calix[4]arene-capped amidoferrocene, receptor **L1**, has been designed to have in 1,3-alternate conformation. Then, the synthesized receptor **L1** has been compared with receptor **L2**, an

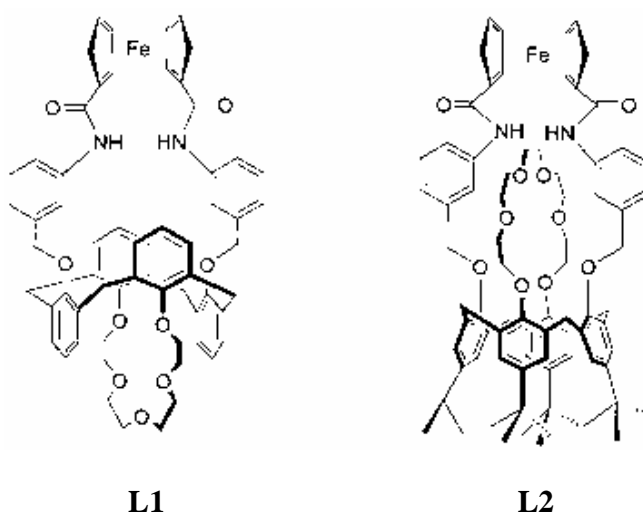
analogous ion-pair receptor synthesized by Suksai in which the calix[4]arene unit was in cone conformation [74].

Therefore, the objectives of this study are....

1. To synthesize a new heteroditopic receptor consisting of crown ether-calix[4]arene-capped amidoferrocene in 1,3-alternate conformation, receptor **L1**.

2. To study the influence of additional electrostatic interaction from a cation to the anion binding abilities of those receptors via  $^1\text{H}$  NMR titration and electrochemical properties.

3. To study the effect of the topology of ligands to cooperative effect of the heteroditopic receptors.



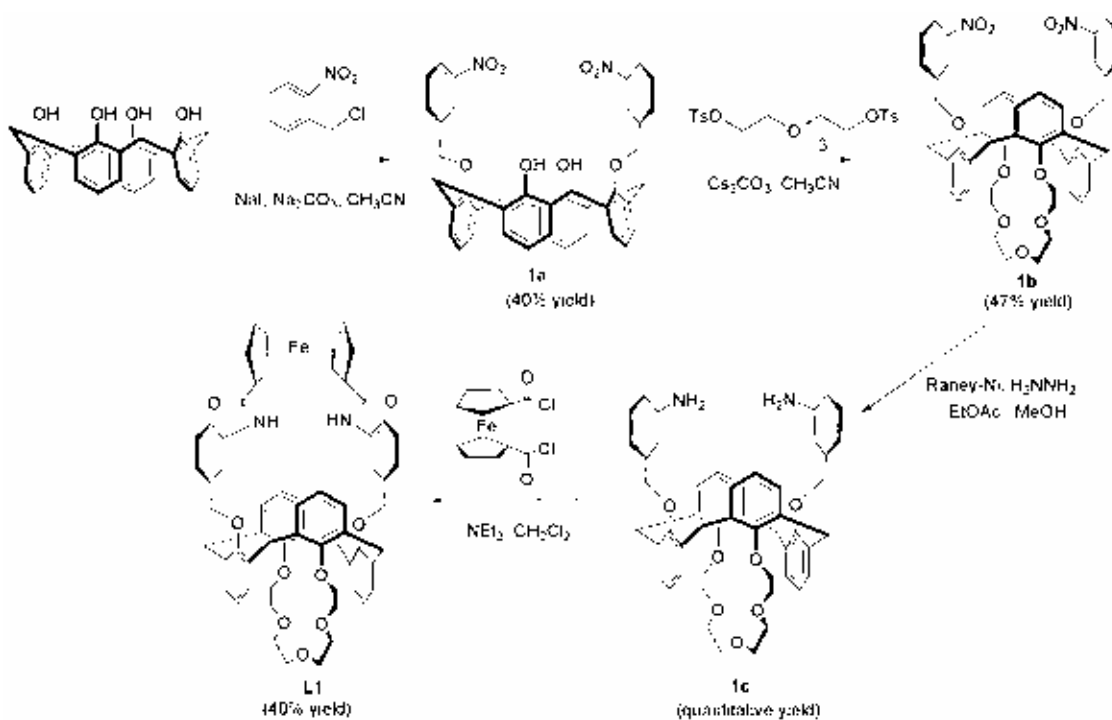
### 3.3 Results and discussion

#### 3.3.1 Synthesis and characterization of receptor L1 and L2

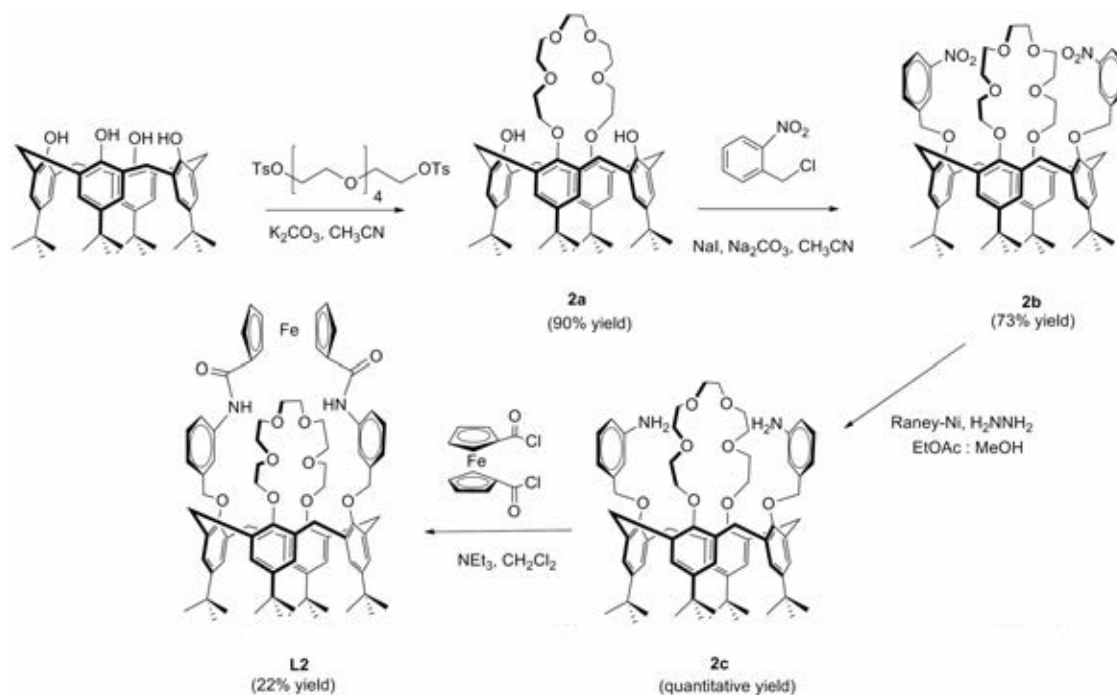
Synthesis of compound **L1** is shown in **Scheme 3.1**. Substitution reaction of calix[4]arene with 3-nitrobenzyl chloride using  $\text{Na}_2\text{CO}_3$  as base and catalytic amount of NaI in  $\text{CH}_3\text{CN}$  gave **1a** in 40% yield. Then, substitution reaction of **1a** with tetraethyleneglycol ditosylate (prepared from tetraethylene glycol) using  $\text{Cs}_2\text{CO}_3$  as base in  $\text{CH}_3\text{CN}$  gave **1b** in 47% yield. Reduction of **1b** by hydrazine and Raney Nickel in

ethyl acetate and methanol yielded diamine, **1c** quantitatively, which was immediately subjected to the reaction with ferrocene acid chloride (prepared from ferrocene in 3 steps) in  $\text{CH}_2\text{Cl}_2$  under nitrogen atmosphere to give **L1** which was purified by column chromatography. The pure product was obtained as yellow solid in 40% yield.

The 1,3-alternate conformation of the final product was confirmed by  $^1\text{H}$  NMR and  $^{13}\text{C}$  NMR spectroscopy. The methylene bridge ( $\text{ArCH}_2\text{Ar}$ ) appeared as a singlet peak at 3.64 in  $^1\text{H}$ -NMR spectrum and 38.20 ppm in  $^{13}\text{C}$  NMR spectrum indicating 1,3-alternate conformation of calix[4]arene. The signals of cyclopentadiene protons in ferrocene were appeared at 4.67 and 4.46 ppm. In addition, the NH amide protons were found at 8.96 ppm. The MALDI-TOF mass spectrum confirmed the structure of compound **L1** observed by an intense peak at 1069 m/z [**L1**+ $\text{Na}^+$ ].



**Scheme 3.1** Synthetic pathway of **L1**



**Scheme 3.2** Synthetic pathway of **L2** [74]

Synthetic pathway of **L2** reported previously by Suksai is shown in **Scheme 3.2** [74]. Generally, the methods of the synthesis of **L2** were similar to those of **L1**. However, **L2** was firstly synthesized by substitution reaction of *p-tert* butyl calix[4]arene with pentaethylene glycol ditosylate to get compound **2a** with high percent yield. Secondly, compound **2a** was substituted using 3-nitrobenzyl chloride to obtain compound **2b** with relatively high percent yield as well. Then compound **2b** was reduced using Raney-Ni and hydrazine and reacted with ferrocene diacid chloride immediately to get **L2** with 22% yield. The detail of **L2** characterizations was also reported thoroughly by Suksai [74]. The <sup>1</sup>H NMR spectrum of **L2** showed a cone conformation according to the ArCH<sub>2</sub>Ar signals, which appears as a pair of doublets (AB system) at 4.37 and 3.31 ppm.

### 3.3.2 Complexation studies of the receptor L1 by $^1\text{H}$ NMR titration

#### 3.3.2.1 Binding properties of the receptor L1 towards alkali metal cations by $^1\text{H}$ NMR studies

Ideally, the metal cation must be bound strongly so as to minimize ion-pairing outside the receptor. Therefore, complexation studies using  $^1\text{H}$  NMR titration were investigated to find the cation that can fit within the cavity of receptors. The  $^1\text{H}$  NMR titration experiments were performed in 5% v/v  $\text{CD}_3\text{CN}$  in  $\text{CDCl}_3$ . Two alkali metals,  $\text{Na}^+$  (added as  $\text{NaClO}_4 \cdot \text{H}_2\text{O}$ ) and  $\text{K}^+$  (added as  $\text{KPF}_6$ ) were tested in this experiment.

Upon addition of  $\text{NaClO}_4 \cdot \text{H}_2\text{O}$  and  $\text{KPF}_6$  into the solution of receptor, two sets of resonances were observed for all the proton signals in aromatic and aliphatic regions of the  $^1\text{H}$ -NMR spectra of the receptor **L1**, resulting from strong binding interactions with a slow complexation/decomplexation kinetics. The slow complexation behavior between receptor **L1** and  $\text{K}^+$  was shown in **Fig. 3.1 and 3.2**. In aliphatic region, the group of crown ether protons of receptor **L1** was gradually downfield shifted obviously upon complexation with  $\text{K}^+$ . This indicated that crown ether was involved in cation complexation. Ion-dipole interactions between oxygen atoms of crown ether and  $\text{K}^+$  led to less electron density of crown ether protons resulting in the downfield shift. In addition, the protons of  $\text{CH}_2\text{OAr}$  also downfield shifted significantly which were close to the proton signals of ferrocene as shown in **Fig. 3.1**. In aromatic region, the aromatic protons of benzyl and phenolic rings were changed dramatically. Cation complexation contributed to well splitted  $^1\text{H}$  NMR peaks as shown in **Fig 3.1 and 3.2**. Thus, this phenomenon implied that  $\text{K}^+$  ion not only located in crown ether but also moved to aromatic rings of calix[4]arene owing to the molecular tube properties of 1,3- alternate conformation of calix[4]arene. This hypothesis was strongly supported by the remarkably downfield shift of  $\text{CH}_2\text{OAr}$  (g) proton. Receptor **L1** also presented the downfield shift of amide NH protons  $\text{K}^+$  complexations. Presumably, metal ions binding with crown-ether like units force two amide groups to be close to each other and increase the strength of the hydrogen bonding possessing the rigid structure of complex cation. Complexation between receptor **L1** and  $\text{Na}^+$  gave the similar results as shown in **Fig. 3.3**. Therefore we

can conclude that the encapsulation of metal ions can effect the strength of intramolecular hydrogen bonding between two amide groups as well as the ability of the preorganization of the receptor structure

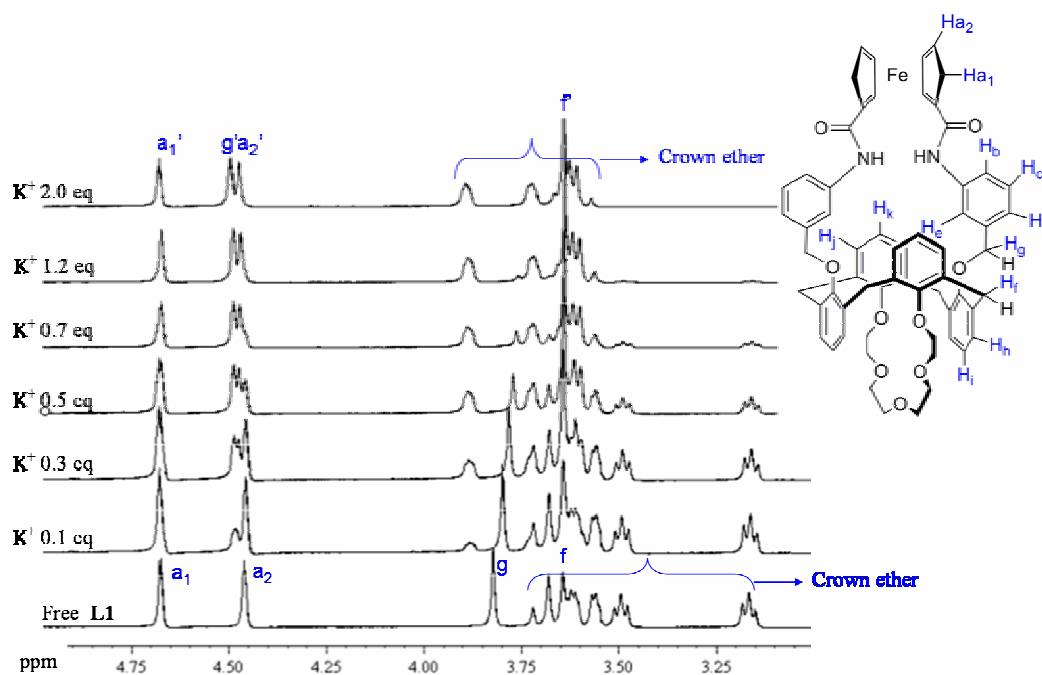


**Fig. 3.1** Partial  $^1\text{H}$  NMR titration spectra from 3-5 ppm between the receptor **L1** and  $\text{KPF}_6$  (0-2 equivalents) in 5% v/v  $\text{CD}_3\text{CN}$  in  $\text{CDCl}_3$ . x and x' represent protons of decomplexes and complexes with  $\text{K}^+$ , respectively.

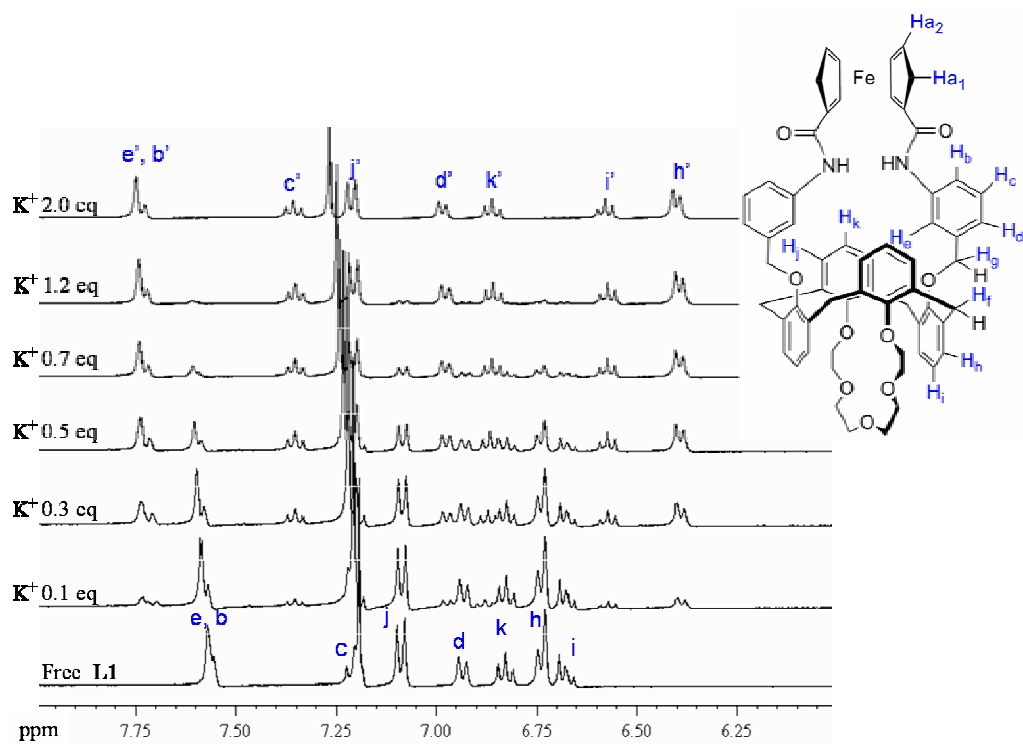


**Fig. 3.2** Partial  $^1\text{H}$  NMR titration spectra from 6-8 ppm between the receptor **L1** and  $\text{KPF}_6$  (0-2 equivalents) in 5% v/v  $\text{CD}_3\text{CN}$  in  $\text{CDCl}_3$ . x and x' represent protons of decomplexes and complexes with  $\text{K}^+$ , respectively.



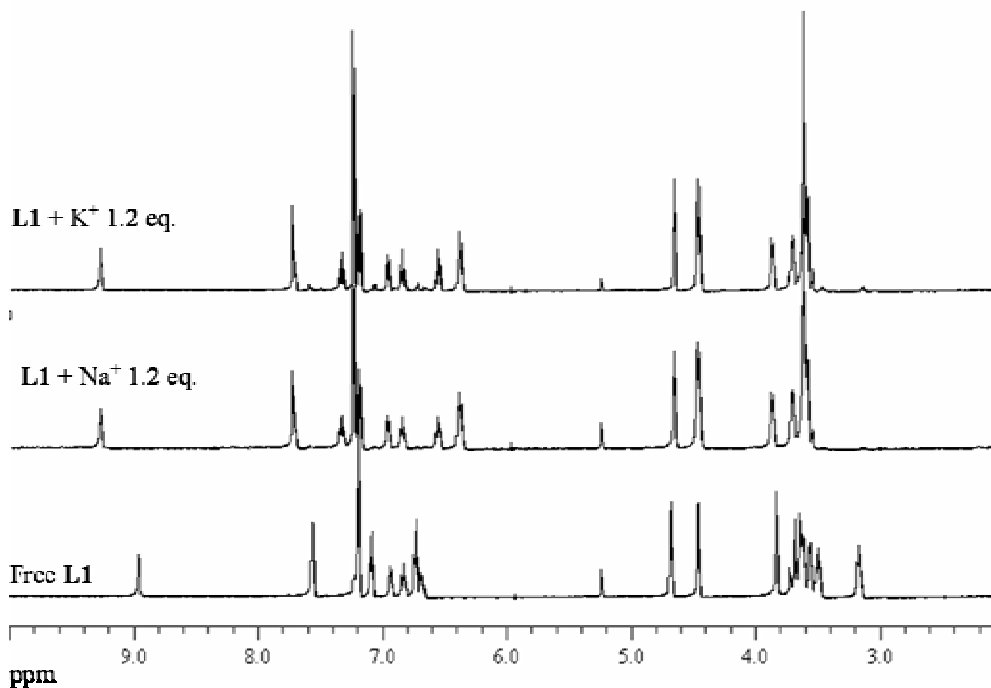


**Fig. 3.3** <sup>1</sup>H NMR titration spectra of receptor **L1** +NaClO<sub>4</sub>•H<sub>2</sub>O and **L1**+ KPF<sub>6</sub> (1.2 equivalents) in 5% v/v CD<sub>3</sub>CN in CDCl<sub>3</sub>.

The receptor/cation complexes formed completely upon addition of 1 equivalent of cations, which were consistent with a 1:1 binding mode. Binding constants were determined by direct integration of signals from free receptors and complexes in <sup>1</sup>H-NMR spectra which were described by Macober [76]. The stability constants could be determined from the variation of the intergration ratio between the complex and the free receptor at various amount of the cationic guest. When a complex formation between receptor and each cationic guest takes place, the stability constant (K) for the equilibrium is expressed as:

$$K = \frac{[C]}{([H]_0 - [C])([G]_0 - [C])}$$

$$K = \frac{n_c / [H]_0}{(1 - n_c)(R - n_c)}$$

Where  $[H]_0$  represents the initial concentration of the host

$[G]_0$  represents the initial concentration of the guest

$[C]$  represents the concentration of the complex

$$[C] = n_c[H]_0$$

$$R = [G]_0/[H]_0$$

$$n_c = \frac{I_c}{I_c + I_h}$$

Where  $I_c$  represents the integration of the complex

$I_h$  represents the integration of the host

**Table 3.1** Binding constants for the Na<sup>+</sup> and K<sup>+</sup> cation complexes with receptors **L1** and **L2** in 5% v/v CD<sub>3</sub>CN/CDCl<sub>3</sub>

Receptor	Binding Constant, K <sup>a</sup> (M <sup>-1</sup> )	
	Na <sup>+(a)</sup>	K <sup>+(b)</sup>
<b>L1</b>	254 <sup>c</sup>	2600 <sup>c</sup>
<b>L2</b>	522 <sup>c</sup>	222 <sup>c</sup>

<sup>a</sup> Na<sup>+</sup> and <sup>b</sup> K<sup>+</sup> cations were added as sodium perchlorate monohydrate and potassium hexafluorophosphate, respectively. <sup>c</sup> Maximum error estimated to be less than ±10%.

From **Table 3.1**, the binding constant of receptor **L1** with K<sup>+</sup> was much higher than that with Na<sup>+</sup>. The cause of the difference in values originated from the complexation ability of K<sup>+</sup> with the apolar 1,3-alternate conformation that interacted not only with the crown ether moiety but also with the two rotated benzene rings via cation-π

interactions. This was not possible in the case of  $\text{Na}^+$ . Regarding the  $\pi$ -metal preference,  $\text{K}^+$  seemed to be more tightly coordinated to the crown-5-ring than  $\text{Na}^+$  due to the extra cation- $\pi$  interactions between the  $\text{K}^+$  and meta-carbons of the upper benzene rings. These results were consistent with the previous study that reported the polyether ring of calix[4]crown-5 was more suitable for the complexation of  $\text{K}^+$ [77]. Binding constants of receptor **L2** with alkali metal cations were calculated using the same method. It was found that receptor **L2** preferred binding with  $\text{Na}^+$  over  $\text{K}^+$ . It should be noted that, the more steric interactions between pseudo-crown ether and amidoferrocene in calix[4]arene **L2** limited the binding of  $\text{Na}^+$  in the pseudo-crown cavity resulting in the low stability constants. Moreover, larger size of  $\text{K}^+$  facing to steric effect caused the lower in the binding constant compared to that observed in  $\text{Na}^+$ . According to these binding constants, co-bound cation complexes of  $\text{K}^+$  and  $\text{Na}^+$  were chosen to study the cooperative binding of receptor **L1** and **L2** with anions, respectively.

### 3.3.2.2 Binding properties of receptor **L1** towards anions by $^1\text{H}$ NMR titration in the absence and presence of cations

The ability of receptor **L1** to bind various anions such as  $\text{Cl}^-$ ,  $\text{Br}^-$ ,  $\text{I}^-$ ,  $\text{AcO}^-$ ,  $\text{BzO}^-$ ,  $\text{H}_2\text{PO}_4^-$  (added as their tetrabutylammonium salt) was tested in 5% v/v  $\text{CD}_3\text{CN}$  in  $\text{CDCl}_3$ . The binding constants between **L1** and anions were determined by analysis of the titration data with EQNMR program [78].

Upon addition of anions to the solution of receptor **L1**, the slightly downfield shifts of NH amide protons were observed for all anions, while no change of other  $^1\text{H}$  NMR peaks was observed. This indicated hydrogen bonding formation between amide groups and anions [47, 72]. This behavior can be observed in the examples,  $^1\text{H}$  NMR titration spectra of **L1** with TBAAcO (**Fig. 3.4**) and TBABzO (**Fig. 3.5**). However,  $\text{AcO}^-$  and  $\text{BzO}^-$  gave larger shifts of NH amide protons than other anions as shown in titration curves in **Fig.3.6**. The receptor **L2** also gave similar results upon titration with anions. The data from these experiments was fit using EQNMR program to get the binding constants between both receptors **L1** and **L2** with anions. The binding constants from

**Table 3.2** showed that even though all anions gave relatively low binding constant values with both receptors,  $\text{AcO}^-$  and  $\text{BzO}^-$  ions gave higher values than the others. Therefore, it implied that these receptors preferred binding with Y-shaped anions probably due to the matching between the cavity of the anion binding sites and the geometry of the anions.

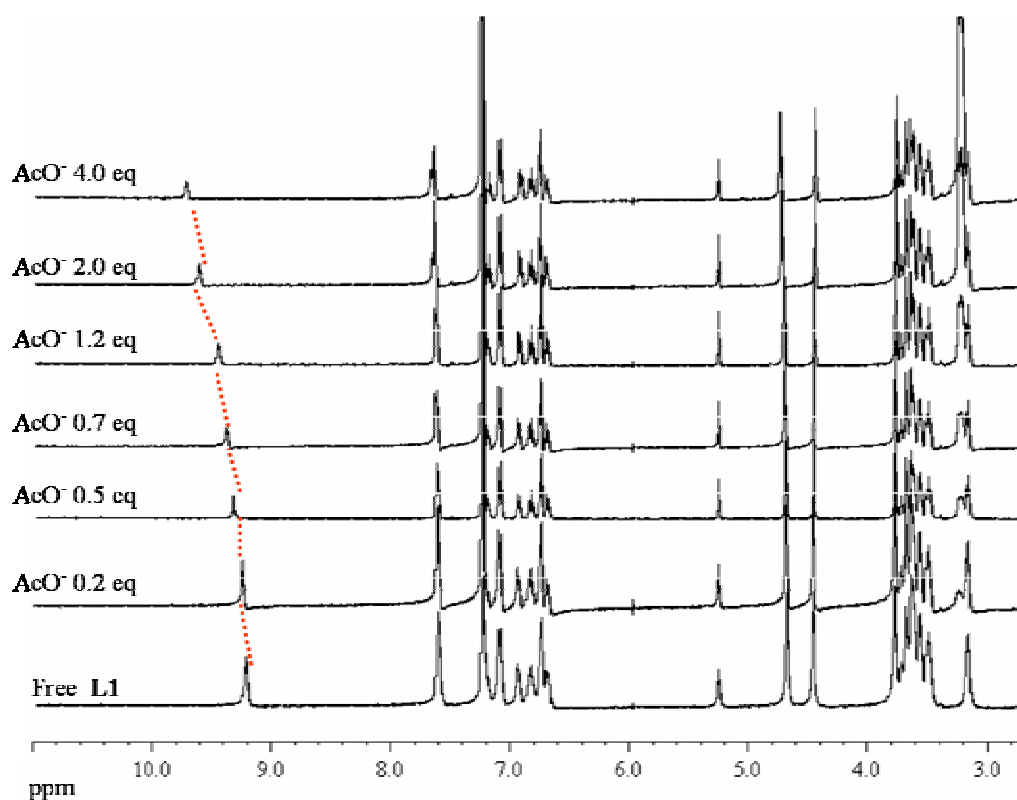


**Fig.3.4**  $^1\text{H}$ -NMR titration spectra of **L1** with TBAACO (0-4 equivalents) in 5% v/v  $\text{CD}_3\text{CN}$  in  $\text{CDCl}_3$ . Dash lines represent the shift direction of NH amide protons.

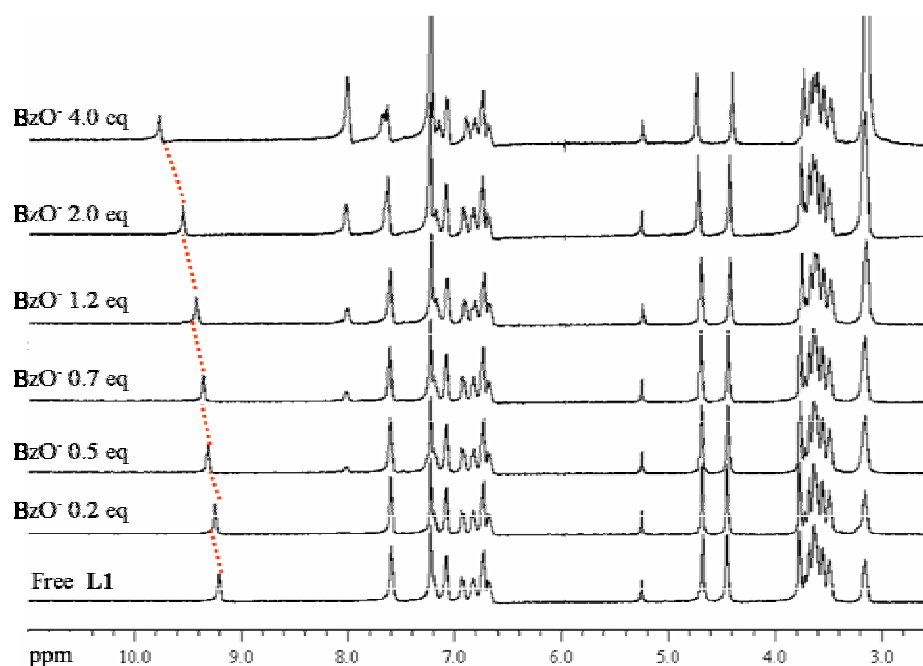


**Fig. 3.5**  $^1\text{H}$ -NMR titration spectra of **L1** with TBABzO (0-4 equivalents) in 5% v/v  $\text{CD}_3\text{CN}$  in  $\text{CDCl}_3$ . Dash lines represent the shift direction of NH amide protons.

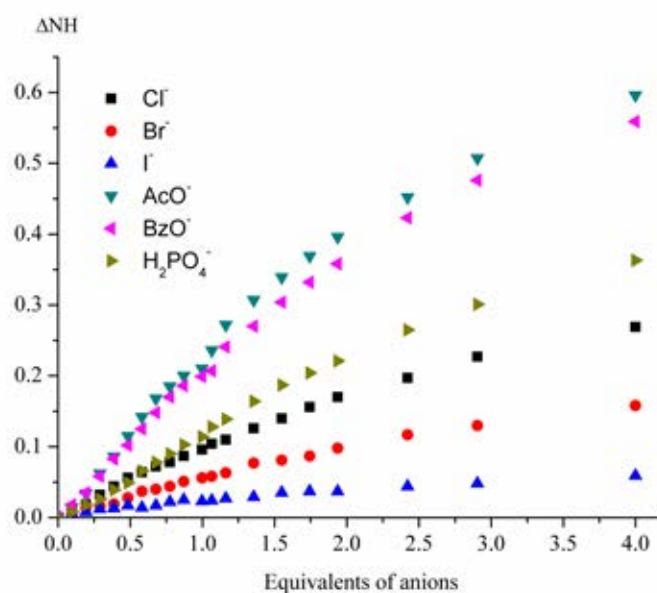


**Fig. 3.6** Change in NH chemical shift ( $\Delta\text{NH}$ ) of receptor **L1** as function of increasing of anions (added as TBAsalts) in 5% v/v  $\text{CD}_3\text{CN}$  in  $\text{CDCl}_3$ .

To study the effect of additional electrostatic interaction to anion binding abilities of receptor **L1**, 1.2 equivalents of cations were added to the solution of receptor **L1** before the addition of anions. The change in  $^1\text{H}$  NMR spectra of cation complex was noticed upon gradual addition of anions into the solution. For example, upon gradual addition of  $\text{AcO}^-$  to the solution of  $[\text{L1}\cdot\text{K}^+]$ , the NH amide protons of the complex shifted remarkably to downfield region. Especially at the beginning of the titration (0-1 equivalent of  $\text{AcO}^-$ ), NH amide proton shifts can be seen obviously as shown in **Fig. 3.7**. The change of other  $^1\text{H}$  NMR peaks was not observed. Addition of other anions ( $\text{Cl}^-$ ,  $\text{Br}^-$ ,  $\text{I}^-$ ,  $\text{BzO}^-$ ) to the solution of receptor  $[\text{L1}\cdot\text{K}^+]$  also resulted in the downfield shift of NH protons; however, the trends of NH shift were different for each anion as shown in  $^1\text{H}$  NMR titration curves, **Fig. 3.8**. In addition, the set of free receptor **L1** spectra was not presented during the titration experiment. This implied no abstraction of  $\text{K}^+$  by anions. Furthermore, it was found that in the presence of  $\text{K}^+$ , addition of anions to the solution of receptor **L1** led to a larger downfield shift of NH amide protons compared to that in the absence of  $\text{K}^+$  as shown in **Fig. 3.9**. As a result, these results implied that additional electrostatic interaction from  $\text{K}^+$  supported the hydrogen bonding interaction between the amide groups and anions as a stable cobound ion pair.

Binding constants can be calculated by EQNMR program as shown in **Table 3.2**. As expected, in the presence of  $\text{K}^+$ , all anions gave higher binding constants with receptor **L1** in the order,  $\text{AcO}^- > \text{BzO}^- > \text{Cl}^- > \text{Br}^- > \text{I}^-$ . It should be noted that even though electrostatic interactions from  $\text{K}^+$  can enhance anion binding ability of this receptor, receptor **L1** still preferred to bind with Y-shaped anions over other anions. Therefore, the additional electrostatic interactions can support the anion binding ability of receptor **L1** but it did not influence to the order of preference of the anion binding. However, during gradual addition  $\text{H}_2\text{PO}_4^-$  to the solution of receptor  $[\text{L1}\cdot\text{K}^+]$ , the set of  $^1\text{H}$  NMR peaks of free receptor **L1** was gradually appeared as shown in **Fig. 3.10**. This indicated the abstraction of  $\text{K}^+$  by  $\text{H}_2\text{PO}_4^-$  ion. Thus,  $\text{H}_2\text{PO}_4^-$  cannot form stable cobound ion pair with  $[\text{L1}\cdot\text{K}^+]$ .

Unfortunately, all anions caused the abstraction of the cation in  $[\mathbf{L1}\cdot\text{Na}^+]$  system which can be clearly seen from the reversion of the set of  $^1\text{H}$ -NMR peaks of free receptor  $\mathbf{L1}$ . It indicated that  $\text{Na}^+$  ion cannot form the stable cobound ion pairs with any anion within the molecule of receptor  $\mathbf{L1}$ . This was consistent with the low binding constant value of receptor  $\mathbf{L1}$  and  $\text{Na}^+$  ion. Thus, it was not surprise that it was easier for added anions to abstract  $\text{Na}^+$  from bound receptor  $\mathbf{L1}$ .

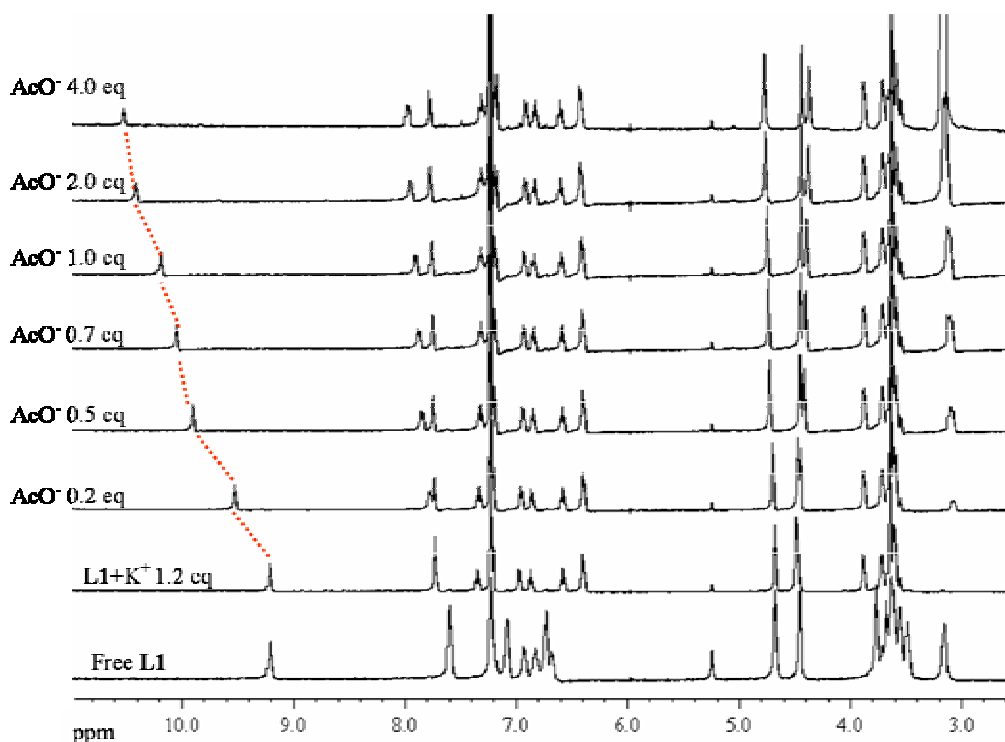


**Fig. 3.7**  $^1\text{H}$ -NMR titration spectra of  $\mathbf{L1}+\text{K}^+$  (1.2 equivalents) with TBABzO (0-4 equivalents) in 5% v/v  $\text{CD}_3\text{CN}$  in  $\text{CDCl}_3$ . Dash lines represent the shift direction of NH amide protons.

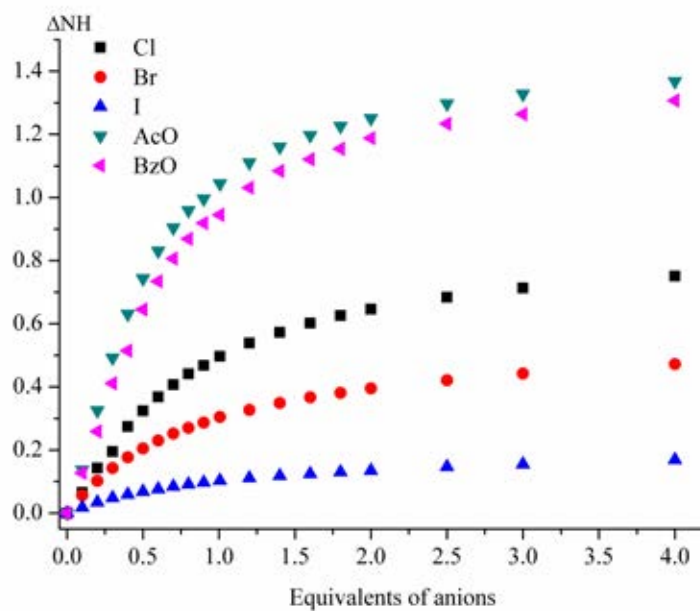


**Fig. 3.8** Change in NH chemical shift ( $\Delta\text{NH}$ ) of receptor **L1** as function of increasing of anions (added as TBAsalts) in 5% v/v  $\text{CD}_3\text{CN}$  in  $\text{CDCl}_3$ .



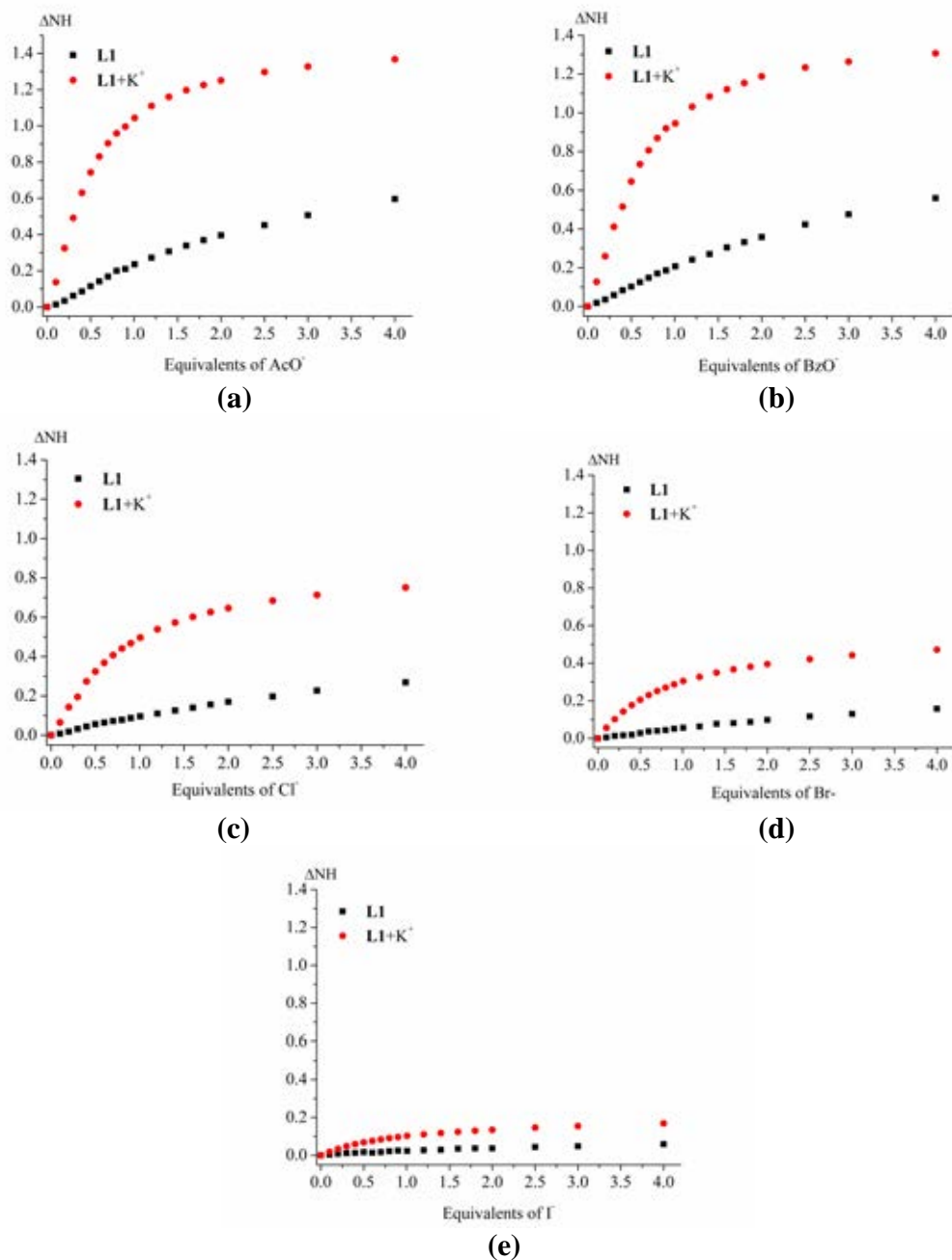


**Fig. 3.9** Change in NH chemical shift ( $\Delta\text{NH}$ ) of receptor **L1** in the presence ( $\bullet$ ) or absence ( $\blacksquare$ ) of  $\text{K}^+$  1.2 equivalents in 5% v/v  $\text{CD}_3\text{CN}$  in  $\text{CDCl}_3$  upon addition of (a) acetate, (b) benzoate, (c)  $\text{Cl}^-$ , (d)  $\text{Br}^-$ , and (e)  $\text{I}^-$  ions.

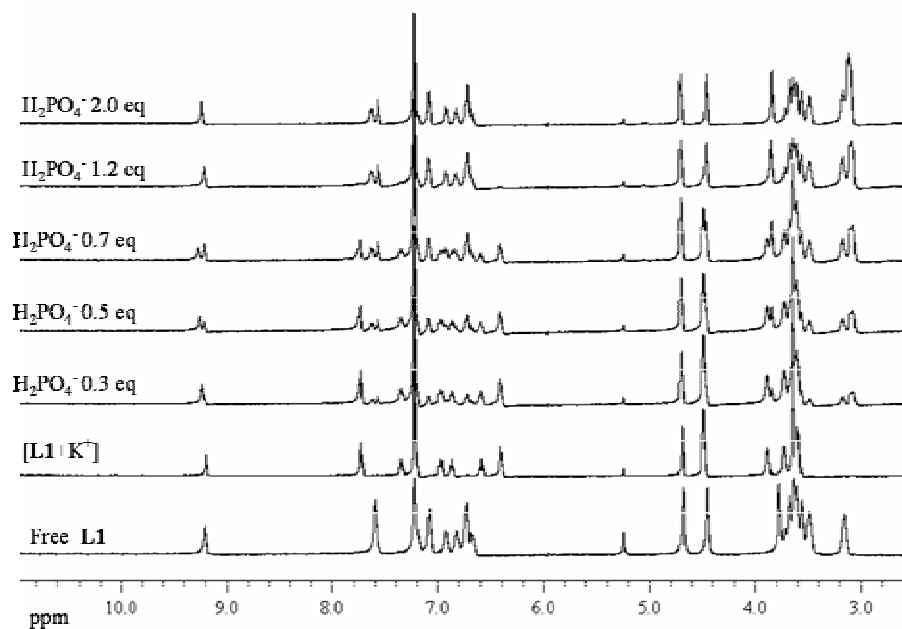


**Fig. 3.10**  $^1\text{H-NMR}$  titration spectra of **L1**+ $\text{K}^+$  (1.2 equivalents) with  $\text{TBAH}_2\text{PO}_4$  (0-4 equivalents) in 5% v/v  $\text{CD}_3\text{CN}$  in  $\text{CDCl}_3$ .

**Table 3.2** Binding constants ( $K$ ) for receptors **L1** and **L2** with anionic guests (as tetrabutylammonium salts) in 5% v/v CD<sub>3</sub>CN in CDCl<sub>3</sub>

Receptors	Binding Constants, $K^a$ (M <sup>-1</sup> )					
	Cl <sup>-</sup>	Br <sup>-</sup>	I <sup>-</sup>	AcO <sup>-</sup>	BzO <sup>-</sup>	H <sub>2</sub> PO <sub>4</sub> <sup>-</sup>
<b>L1</b>	21	<sub>-</sub> <sup>b</sup>	<sub>-</sub> <sup>b</sup>	42	26	<sub>-</sub> <sup>b</sup>
[ <b>L1</b> ·Na <sup>+</sup> ] <sup>c</sup>	<sub>-</sub> <sup>d</sup>	<sub>-</sub> <sup>d</sup>	<sub>-</sub> <sup>d</sup>	<sub>-</sub> <sup>d</sup>	<sub>-</sub> <sup>d</sup>	<sub>-</sub> <sup>d</sup>
[ <b>L1</b> ·K <sup>+</sup> ] <sup>c</sup>	768	514	32	1,810	1,616	<sub>-</sub> <sup>d</sup>
<b>L2</b>	40	<sub>-</sub> <sup>b</sup>	<sub>-</sub> <sup>b</sup>	92	77	<sub>-</sub> <sup>e</sup>
[ <b>L2</b> ·Na <sup>+</sup> ] <sup>c</sup>	<sub>-</sub> <sup>d</sup>	1,110	<sub>-</sub> <sup>d</sup>	1,046	<sub>-</sub> <sup>d</sup>	<sub>-</sub> <sup>e</sup>
[ <b>L2</b> ·K <sup>+</sup> ] <sup>c</sup>	<sub>-</sub> <sup>d</sup>	<sub>-</sub> <sup>d</sup>	<sub>-</sub> <sup>d</sup>	<sub>-</sub> <sup>d</sup>	<sub>-</sub> <sup>d</sup>	<sub>-</sub> <sup>e</sup>

<sup>a</sup> Maximum error estimated to be  $\pm 10\%$ . <sup>b</sup> Values are very small and errors are more than 10%. <sup>c</sup> The alkali metal cations were added at 1.2 equivalent as their perchlorate or hexafluorophosphate salts. <sup>d</sup> Cannot be calculated due to ion-pair formation between bound metal cations and added anions. <sup>e</sup> The experiment was not tested.

Therefore, complexation studies by <sup>1</sup>H NMR titration can be concluded using simple proposed binding modes. In the absence of cations, receptor **L1** bound with anions through hydrogen bonding from amide groups and anions as shown in **Fig. 3.11**. In addition, it was found that receptor **L1** preferred binding small Y-shape anions, especially acetate probably because the size of this anion matched with the binding cavity of the receptor **L1**. The presence of cations can influence to anion binding abilities either positive or negative binding as shown in **Fig. 3.12 (a) and (b)**, respectively. Positive binding can be found in the systems of [**L1**·K<sup>+</sup>]/Cl<sup>-</sup>, [**L1**·K<sup>+</sup>]/Br<sup>-</sup>, [**L1**·K<sup>+</sup>]/I<sup>-</sup>, [**L1**·K<sup>+</sup>]/AcO<sup>-</sup> and [**L1**·K<sup>+</sup>]/BzO<sup>-</sup>. In this case, K<sup>+</sup> bound in crown ether moiety of receptor **L1** enhanced anion binding abilities via additional electrostatic interaction from its positive charge. Therefore, both ion-ion interaction between different charges of a cation and an anion and hydrogen bonding interaction between anions and amide groups supported anion binding ability of receptor **L1**. Negative binding can be found in the

systems of  $[\mathbf{L1}\cdot\text{K}^+]/\text{H}_2\text{PO}_4^-$  and  $[\mathbf{L1}\cdot\text{Na}^+]/\text{anions}$ . In this case, added cations can be abstracted upon addition of anions. The reason may be from the weak ion-dipole interaction between receptor  $\mathbf{L1}$  and  $\text{Na}^+$  causing the preference of abstraction by anions instead of cooperative binding. For  $[\mathbf{L1}\cdot\text{K}^+]/\text{H}_2\text{PO}_4^-$  system, the cation abstraction was rationalized from the weak hydrogen bonding interaction between amide groups and  $\text{H}_2\text{PO}_4^-$  ion probably due to the unmatched shape of this anion with the cavity of receptor  $\mathbf{L1}$ . Thus, in the presence of  $\text{K}^+$ ,  $\text{H}_2\text{PO}_4^-$  ion preferred to bind with  $\text{K}^+$  ion instead of amide groups.

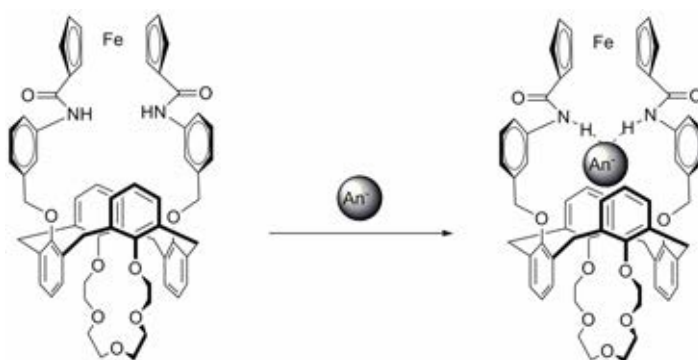


**Fig. 3.11** Proposed binding mode of receptor  $\mathbf{L1}$  and anions.

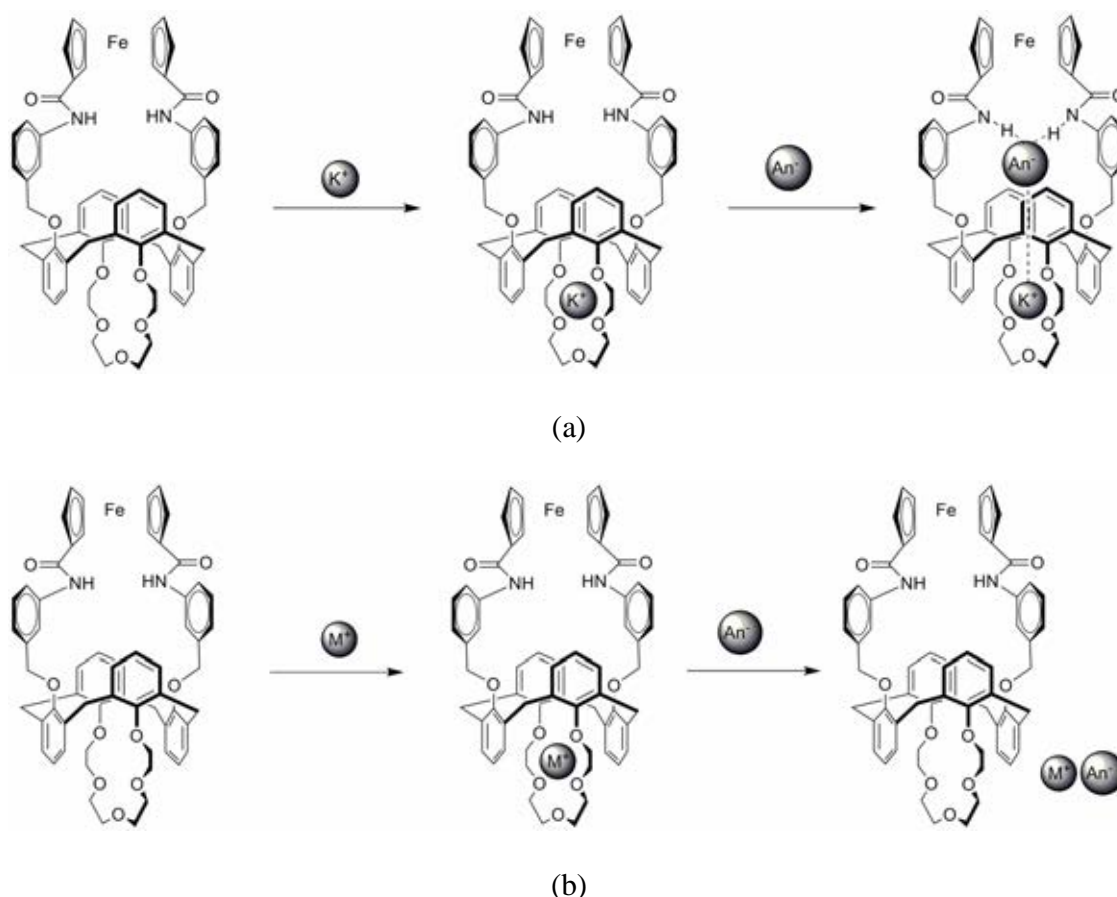


**Fig. 3.12** Proposed binding modes of receptor **L1** and anions in the presence of cations (a) positive binding and (b) negative binding.

The study of ditopic properties of cobound cation complexes of receptor **L2** and various anions was examined using similar method to this study. Binding constants were also calculated using EQNMR program. In the presence of  $\text{Na}^+$ , receptor **L2** showed higher binding constant values with  $\text{AcO}^-$  and  $\text{Br}^-$ . Accordingly, the cobound complexes of calix[4]arene in cone conformation **L2** provided higher selectivity with anions than cobound complex of 1,3-alternate calix[4]arene **L1** effecting from the rigidity of receptor **L2** as well as the conformation different of calix[4]arene. In addition, it indicated that the spherical anions preferred to bind strongly with cone conformation cobound receptors. Other systems, such as  $[\mathbf{L2}\cdot\text{K}^+]/\text{Anions}$ ,  $[\mathbf{L2}\cdot\text{Na}^+]/\text{Cl}^-$ ,  $[\mathbf{L2}\cdot\text{Na}^+]/\text{I}^-$ ,  $[\mathbf{L2}\cdot\text{Na}^+]/\text{BzO}^-$ ,

contributed to negative binding. This implied that cone conformation of receptor **L2** restricted more specific system for cooperative binding. In other words, the specificity and the selectivity of cooperative binding in anion sensing can be improved by controlling the conformation of calix[4]arene.

### 3.3.3 Electrochemical studies of **L1**

The synthetic receptor **L1** consisting of ferrocene as a sensory unit was expected to exhibit diverse electrochemical behaviors depending on anion or cation binding. In addition, ditopic property of receptor **L1** can be tested by the addition of both anions and cations together. The cyclic and square wave voltammetries were examined using the following conditions. A Pt working electrode, a Ag/Ag<sup>+</sup> reference electrode and a Pt coil counter electrode were immersed in a solution of receptor **L1** (1 mM) in 40% CH<sub>3</sub>CN v/v in CH<sub>2</sub>Cl<sub>2</sub> with 0.1 M TBAPF<sub>6</sub> as supporting electrolyte. The solution was purged with N<sub>2</sub> before measurements. The potential was scanned in the range of 0.1 to 0.8 V at a scan rate of 100 mV/s. Various guests were added to the solution of receptor **L1** and stirred before each scan. The cyclic voltammogram of receptor **L1** gave reversible redox couples (**Fig. 3.13**). Its electrochemical data was presented in **Table 3.3**. Using the same condition, receptor **L2** also showed reversible cyclic voltammogram with electrochemical data as shown in **Table 4.3**. It can be observed that receptor **L2** provided higher E<sub>pa</sub> (0.520 V) than that of receptor **L1** (0.456 V) indicating that the receptor **L2** is harder to be oxidized. The reason was probable due to the steric of calix-crown ether presented in receptor **L2** leading to the difficulty in oxidizing.

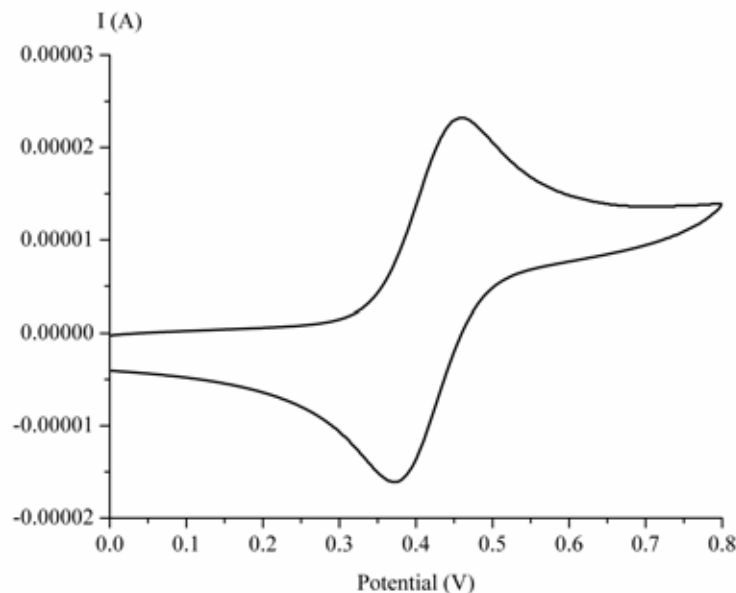


**Fig. 3.13** Cyclic voltammogram of receptor **L1** (1 mM) in 40% CH<sub>3</sub>CN v/v in CH<sub>2</sub>Cl<sub>2</sub> with 0.1 M TBAPF<sub>6</sub> at a scan rate of 100 mV/s.

**Table 3.3** Electrochemical data (Fc/Fc<sup>+</sup> redox couple) of receptor **L1** in 40% CH<sub>3</sub>CN in CH<sub>2</sub>Cl<sub>2</sub> with 0.1M TBAPF<sub>6</sub> at scan rate 100 mV/s.

Receptor	E <sub>pa</sub> (V)	E <sub>pc</sub> (V)
<b>L1</b>	0.456	0.366
<b>L2</b>	0.520	0.437

### 3.3.3.1 Electrochemical studies of the receptor **L1** towards alkali metal cations

Electrochemical sensing of receptor **L1** towards alkali metal cations was observed after gradual addition Na<sup>+</sup> or K<sup>+</sup> to the solution of receptor **L1** in 40% CH<sub>3</sub>CN v/v in CH<sub>2</sub>Cl<sub>2</sub> with 0.1 M TBAPF<sub>6</sub> at a scan rate of 100 mV/s. The solution was stirred for 3 minutes before each run. It was found that alkali ion sensing of receptor **L1** led to the anodic shift of the oxidation wave and the electrochemical response still remained

reversible as shown in **Fig. 3.14** and **Fig. 3.16**. This means the harder oxidation of the ferrocene to ferrocinium ion (the  $\text{Fc}/\text{Fc}^+$  redox couple). It was possibly that during the oxidation process the electrostatic repulsion between the bound-cation and the  $\text{Fc}^+$  ion was generated. Therefore, the  $\text{Fc}^+$  was destabilized by repulsive electrostatic interactions with the bound-cation. However, as considered the cathodic shifts of  $\text{Na}^+$  and  $\text{K}^+$ , it was found that the values of  $\Delta E_{\text{pa}}$  were not significantly different. They were 17 mV for  $\text{Na}^+$  and 22 mV for  $\text{K}^+$ . These results did not correspond to the binding constants from  $^1\text{H}$ -NMR titration shown in **Table 3.1** informing that receptor **L1** preferred to bind with  $\text{K}^+$  ion. Thus, it was supposed that  $\text{K}^+$  ion would show the larger anodic shifts than  $\text{Na}^+$  ion. This phenomenon could be explained in terms of the distance between the binding site of the cation and the signaling unit. Since receptor **L1** is in 1,3-alternate conformation of calix[4]arene providing relatively long distance between the binding site of the cation and the signaling unit, it cannot differentiate the strength of ion-dipole forces of different cations through electrochemical signals. In addition, both alkali metal ions also showed low anodic shifts values probably due to the low electropositive repulsion between the cation and the  $\text{Fc}^+$  resulting from the distance issue as well. Accordingly, the relatively long distance between the binding site of the cation and the signaling unit of receptor **L1** caused low anodic shifts and no remarkable difference in  $\Delta E_{\text{pa}}$  values of difference cations. Square wave voltammograms of receptor **L1** and alkali metal ions also displayed anodic shifts as well (**Fig. 3.15** and **Fig. 3.17**) which were consistent with the results from cyclic voltammetric experiments.

Cation sensing of receptor **L2** also showed anodic shifts of the oxidation wave; however, in this case cation sensing can differentiate using cyclic voltammetry. The difference of  $\Delta E_{\text{pa}}$  of **L2** with  $\text{Na}^+$  (40 mV) is much higher than  $\text{K}^+$  (25 mV) resulting from the increasing charge-to-size ratios of those cations. The large  $\text{K}^+$  might not be allowed to stay in the small crown ether-like cavity of the bis-ester side arms on the lower rim calix[4]arene. This result agrees with the NMR titration data. Accordingly, the electrochemical responses led us to conclusion that the strength of the electropositive repulsion between  $\text{Fc}^+$  and a co-bound cation not only depends on the charge to size



ratios of metal ions but also the inter-cationic distance between those two cations participating in electrochemical cation sensing.

**Table 3.4** Anodic shifts ( $\Delta E_{pa}$ ) of the ferrocene redox couples of receptors **L1** and **L2** on addition of 1.4 equivalents of  $\text{Na}^+$  and  $\text{K}^+$ .

Receptor	$\Delta E_{pa}$ (mV)	
	$\text{Na}^+$	$\text{K}^+$
<b>L1</b>	17	22
<b>L2</b>	40	25

<sup>a</sup>  $\Delta E$  is defined as  $E_{pa}(\text{complex}) - E_{pa}(\text{free receptor})$ .  $\text{Na}^+$  was added as  $\text{NaClO}_4 \cdot \text{H}_2\text{O}$ .  $\text{K}^+$  was added as  $\text{KPF}_6$ .

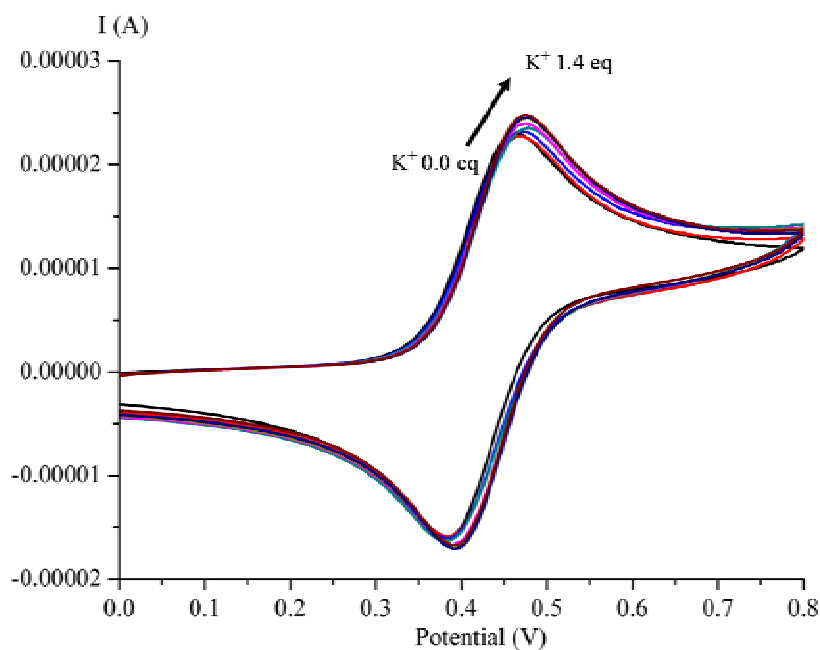


**Fig. 3.14** Cyclic voltammogram titration of receptor **L1** (1 mM) upon gradual addition  $\text{KPF}_6$  (0-1.4 equivalents) in 40%  $\text{CH}_3\text{CN}$  v/v in  $\text{CH}_2\text{Cl}_2$  with 0.1 M  $\text{TBAPF}_6$  at a scan rate of 100 mV/s.

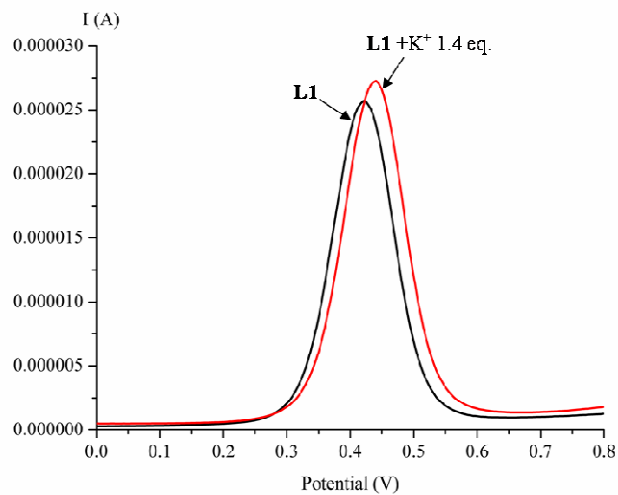


**Fig. 3.15** Square wave voltammogram titration of receptor **L1** (1 mM) before and after addition of  $\text{KPF}_6$  1.4 equivalents in 40%  $\text{CH}_3\text{CN}$  v/v in  $\text{CH}_2\text{Cl}_2$  with 0.1 M  $\text{TBAPF}_6$  at a scan rate of 100 mV/s.

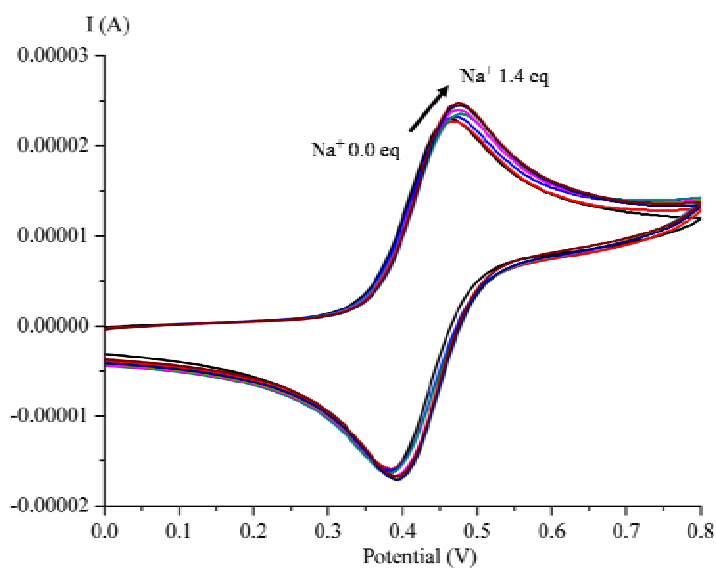


**Fig. 3.16** Cyclic voltammogram titration of receptor **L1** (1 mM) upon gradual addition  $\text{NaClO}_4 \cdot \text{H}_2\text{O}$  (0-1.4 equivalents) in 40%  $\text{CH}_3\text{CN}$  v/v in  $\text{CH}_2\text{Cl}_2$  with 0.1 M  $\text{TBAPF}_6$  at a scan rate of 100 mV/s.

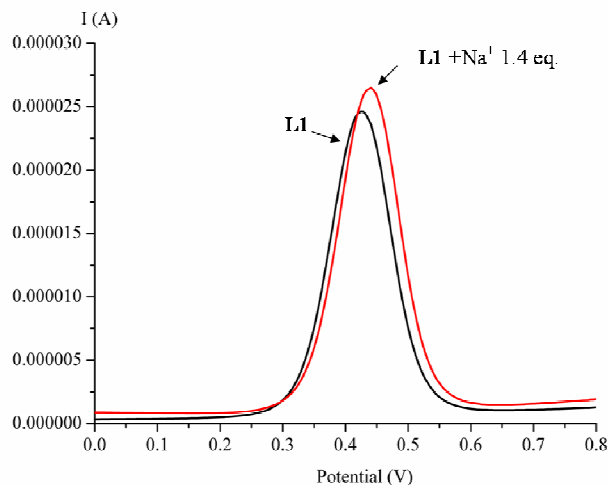


**Fig. 3.17** Square wave voltammogram of receptor **L1** (1 mM) before and after addition of  $\text{NaClO}_4 \cdot \text{H}_2\text{O}$  1.4 equivalents in 40%  $\text{CH}_3\text{CN}$  v/v in  $\text{CH}_2\text{Cl}_2$  with 0.1 M  $\text{TBAPF}_6$  at a scan rate of 100 mV/s.

### 3.3.3.2 Electrochemical studies of the receptor **L1** towards anions in the absence and presence of alkali metal ions.

The anion sensing properties receptor **L1** both in the absence and in the presence of alkali metal cations were investigated by cyclic voltammetry and square wave voltammetry in 30%  $\text{CH}_3\text{CN}$  in  $\text{CH}_2\text{Cl}_2$  with 0.1 M  $\text{TBAPF}_6$  as the supporting electrolyte. Cyclic and square wave voltammograms of receptor **L1** and various anions ( $\text{Cl}^-$ ,  $\text{AcO}^-$ ,  $\text{BzO}^-$  and  $\text{H}_2\text{PO}_4^-$ ) were presented in **Fig. 3.18** and **Fig. 3.19**. Cyclic and square wave voltammograms of receptor **L1** with these anions showed cathodic shift of the oxidation waves. The difference of values of the oxidation potential ( $E_{\text{pa}}$ ) between the anion complexes and the free receptor **L1** were considered as a parameter for indicating the effectiveness of electrochemical sensing in this electrochemical study. The electrochemical data was summarized in **Table 3.5**. It was found that after 4 equivalents of anions added, the order of changes in the  $\text{Fc}/\text{Fc}^+$  redox couples was  $\text{H}_2\text{PO}_4^- > \text{BzO}^- > \text{AcO}^- > \text{Cl}^-$ . This cathodic shift could be attributed to hydrogen bonding interactions between the NH protons of the amide groups and negative charge of anions which

facilitated the oxidation of Fc to  $\text{Fc}^+$ . It can thus be assumed that the oxidized ferrocene in the vicinity of amide groups increased the acidity of the amide protons due to the stronger cation- $\pi$  interaction acting as an electron withdrawing group. This led to the stronger hydrogen bonding formation between **L1** and anions. In other words, ferrocenium ion in **L1** can be stabilized by hydrogen bonds of NH amide proton and anions. Therefore, compared to complexation study by  $^1\text{H-NMR}$  titration, oxidized amidoferrocene binding subunit of receptor **L1** can bind anions more effectively than its normal form due to electrostatic interactions between the ferrocenium group and the bound anions. Cyclic voltammetric titration and square wave voltammetric titration of receptor **L1** with these anions displayed two types of voltammograms observed upon adding anions to the electrolytic solution of receptor **L1**: one-wave and two-wave voltammograms [79-81]. The former corresponded to a gradual potential shift of the voltammetric curve as observed in the **L1**/ $\text{Cl}^-$  system in **Fig 3.20 and 3.21**. The latter demonstrated the emergence of a new voltammetric curve which developed at the expense of the original one following progressive addition of anionic guests as shown in **L1**/ $\text{BzO}^-$ , **L1**/ $\text{AcO}^-$  and **L1**/ $\text{H}_2\text{PO}_4^-$  (**Fig. 3.22-Fig. 3.27**). In addition, in all anion sensing studies, the cyclic voltammograms became quasi-reversible and completely irreversible after gradual adding aliquots of anions. This indicated an electrochemical-chemical (EC) mechanism which resulted in a complex formation leading to an irreversible redox process. Remarkably, the difference in the diffusion coefficients of the reduced forms of the free receptors and their anion adducts caused the differences in the current intensity observed in the voltammograms. Unfortunately, bromide and iodide ions did not interact with receptor **L1** which were obviously seen through the progressive increase of their oxidation waves upon gradual addition of these ions and the unchangeable cyclic voltammogram of receptor **L1**.

To study the ditopic property of **L1** through its electrochemical property, we measured cyclic voltammetry and square wave voltammetry of the cobound cationic receptors upon adding various anions. It was found that upon adding 0-1 equivalent of anions ( $\text{Cl}^-$ ,  $\text{BzO}^-$ ,  $\text{AcO}^-$  and  $\text{H}_2\text{PO}_4^-$ ), only insignificant changes of the oxidation waves

of cobound cationic receptor **L1** in cyclic voltammograms and square wave voltammograms were observed. Then addition of anions more than 1 equivalent led to cathodic shifts of the oxidation waves of cobound cationic receptor **L1**. Thus, at the beginning of the titration, added anions probably acted as counter ions for bound cation in receptor **L1** resulting in insignificant changes in the voltammograms. Afterwards, excess anions bound at the anion binding sites leading to the cathodic shifts of cobound cationic receptor **L1**. However, the cathodic shifts values at 4 equivalents of anion were not as high as that observed in free receptor **L1** and anions. Addition of  $\text{Br}^-$  and  $\text{I}^-$  to the solution of cobound cationic receptor **L1** did not result in any change in the oxidation waves of cobound cationic receptor **L1**, obviously seen in square wave voltammograms especially. Therefore, the the cobound  $[\text{L1}\cdot\text{K}^+]$  complex failed to recognize all anions electrochemically, which was attributed to the long distance between  $\text{Fc}^+$  and  $\text{K}^+$  cation compared with the others. Therefore the electrostatic attractions between the doubly positive charged of  $[\text{L1}^+\cdot\text{K}^+]$  and anions were decreased. This available data strongly supported that even in presence of the doubly positive cation in the receptor; however, the sensing ability of anions could not be increased if the inter-cationic distance between two cations is not suitable.

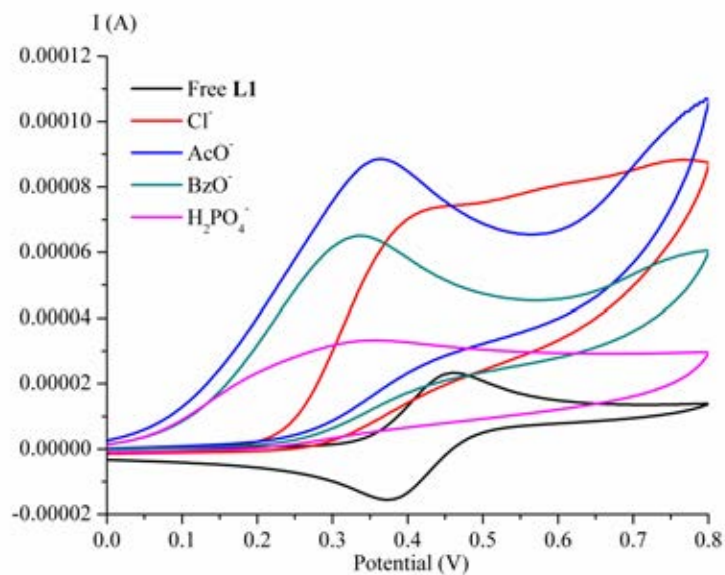


**Fig. 3.18** Cyclic voltammograms of receptor **L1** (1 mM) with various anions (4 equivalents) in 40% CH<sub>3</sub>CN v/v in CH<sub>2</sub>Cl<sub>2</sub> with 0.1 M TBAPF<sub>6</sub> at a scan rate of 100 mV/s

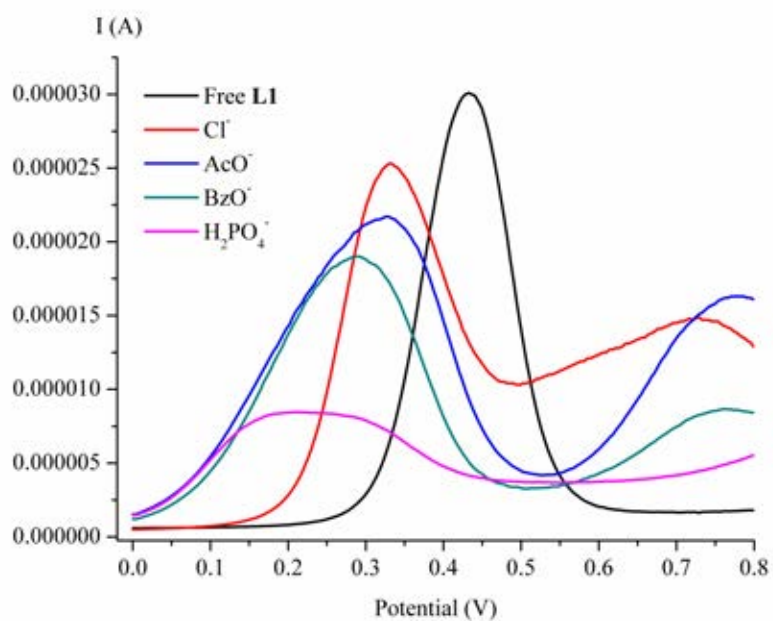


**Fig. 3.19** Square wave voltammograms of receptor **L1** (1 mM) with various anions (4 equivalents) in 40% CH<sub>3</sub>CN v/v in CH<sub>2</sub>Cl<sub>2</sub> with 0.1 M TBAPF<sub>6</sub> at a scan rate of 100 mV/s

**Table 3.5** Electrochemical recognition data  $^a\Delta E$  for receptor **L1** towards anions in 40% CH<sub>3</sub>CN:CH<sub>2</sub>Cl<sub>2</sub> with 0.1 M TBAPF<sub>6</sub> at scan rate 100 mV/s.

Receptor	$^a\Delta E(\text{mV})$					
	Cl <sup>-</sup>	Br <sup>-</sup>	I <sup>-</sup>	AcO <sup>-</sup>	BzO <sup>-</sup>	H <sub>2</sub> PO <sub>4</sub> <sup>-</sup>
<b>L1</b>	-94	<sub>-</sub> <sup>b</sup>	<sub>-</sub> <sup>b</sup>	-103	-140	-206
[ <b>L1</b> •K <sup>+</sup> ] <sup>d</sup>	<sub>-</sub> <sup>c</sup>	<sub>-</sub> <sup>b</sup>	<sub>-</sub> <sup>b</sup>	<sub>-</sub> <sup>c</sup>	<sub>-</sub> <sup>c</sup>	<sub>-</sub> <sup>c</sup>
[ <b>L1</b> •Na <sup>+</sup> ] <sup>e</sup>	<sub>-</sub> <sup>c</sup>	<sub>-</sub> <sup>b</sup>	<sub>-</sub> <sup>b</sup>	<sub>-</sub> <sup>c</sup>	<sub>-</sub> <sup>c</sup>	<sub>-</sub> <sup>c</sup>
<b>L2</b>	-82	<sub>-</sub> <sup>c</sup>	<sub>-</sub> <sup>b</sup>	-90	-70	<sub>-</sub> <sup>f</sup>
[ <b>L2</b> •K <sup>+</sup> ] <sup>d</sup>	-138	<sub>-</sub> <sup>c</sup>	<sub>-</sub> <sup>b</sup>	<sub>-</sub> <sup>c</sup>	<sub>-</sub> <sup>c</sup>	<sub>-</sub> <sup>f</sup>
[ <b>L2</b> •Na <sup>+</sup> ] <sup>e</sup>	-110	<sub>-</sub> <sup>c</sup>	<sub>-</sub> <sup>b</sup>	-250	<sub>-</sub> <sup>c</sup>	<sub>-</sub> <sup>f</sup>

<sup>a</sup> $\Delta E$  is defined as  $E_{\text{pa}}(\text{complex}) - E_{\text{pa}}(\text{free receptor})$ . <sup>b</sup> no interaction occur between receptor and anions. <sup>c</sup> ion pair formation between K<sup>+</sup> and anions. <sup>d</sup> Added as KPF<sub>6</sub>. <sup>e</sup> Added as NaClO<sub>4</sub>•H<sub>2</sub>O. <sup>f</sup> Data was not reported.

Electrochemical studies of receptor **L2** and its cobound cations with anions were briefly summarized in **Table 3.5**. Receptor **L2** sensed Cl<sup>-</sup>, AcO<sup>-</sup> and BzO<sup>-</sup> electrochemically through cathodic shifts of the oxidation waves. Interestingly, cobound cations of receptor **L2** detected Cl<sup>-</sup> more strongly compared to normal form of free receptor **L2** as shown in the higher values of  $\Delta E$ . Furthermore, AcO<sup>-</sup> sensing of [**L2**•Na<sup>+</sup>] gave the highest  $\Delta E$  (250 mV). These results can be assigned to the extra strong interaction between the oxidized fc<sup>+</sup> and those anions. Moreover, the inter-cationic distance between of Fc<sup>+</sup> and Na<sup>+</sup> in [**L2**<sup>+</sup>•Na<sup>+</sup>] could be more suitable to effectively sense acetate electrochemically than chloride. Therefore, ditopic properties of receptor **L2** studied by electrochemical techniques can be concluded that the suitable ionic distance between additional electrostatic interaction from Na<sup>+</sup> and fc<sup>+</sup> played a key role in anion sensing. The topology of receptor **L2** controlled the inter-cationic distance between the two positive ions Fc<sup>+</sup> and bound cation M<sup>+</sup> participated to the electrostatic attraction of

anions led to a greater shift in the oxidation potential of the Fc/Fc<sup>+</sup> redox couples. Cone conformation of calix[4]arene of receptor **L2** provided more suitable inter-ionic distance for cobound ion pair formation than 1,3-alternate conformation of receptor **L1**.

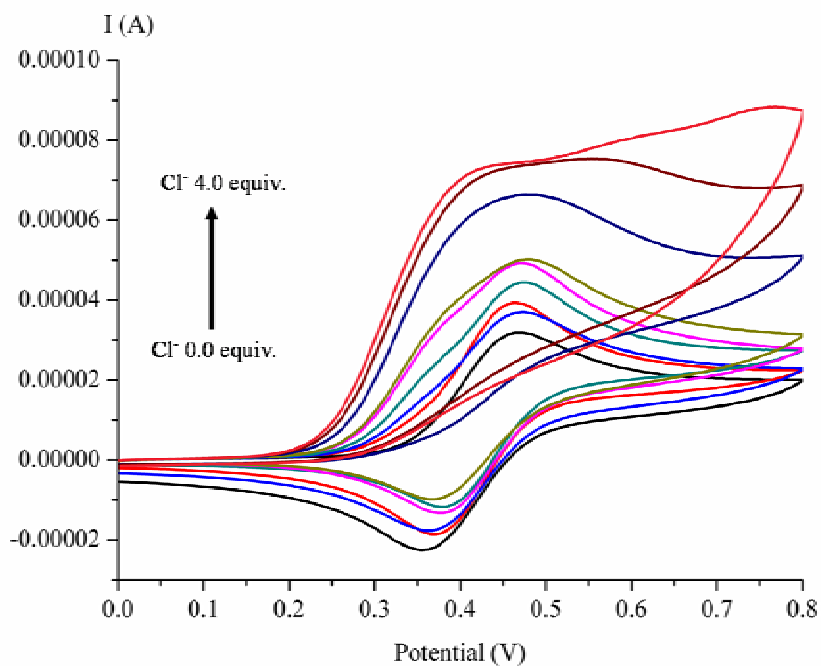


**Fig. 3.20** Cyclic voltammogram titration of receptor **L1** (1 mM) upon gradual addition TBACl (0-4 equivalents) in 40% CH<sub>3</sub>CN v/v in CH<sub>2</sub>Cl<sub>2</sub> with 0.1 M TBAPF<sub>6</sub> at a scan rate of 100 mV/s.



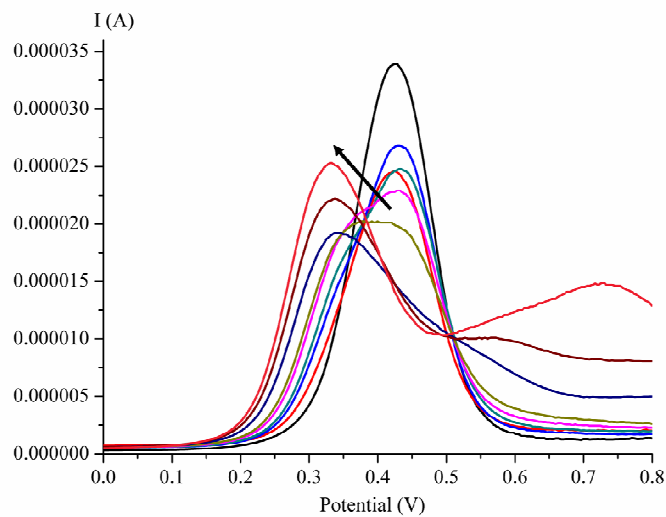


**Fig. 3.21** Square wave voltammogram titration of receptor **L1** (1 mM) upon gradual addition TBACl (0-4 equivalents) in 40%  $\text{CH}_3\text{CN}$  v/v in  $\text{CH}_2\text{Cl}_2$  with 0.1 M  $\text{TBAPF}_6$  at a scan rate of 100 mV/s.

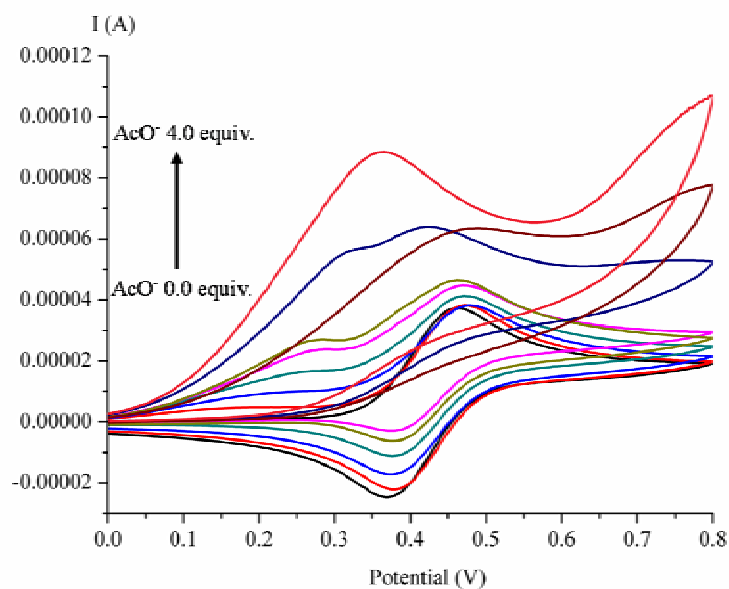


**Fig. 3.22** Cyclic voltammogram titration of receptor **L1** (1 mM) upon gradual addition TBAAcO (0-4 equivalents) in 40%  $\text{CH}_3\text{CN}$  v/v in  $\text{CH}_2\text{Cl}_2$  with 0.1 M  $\text{TBAPF}_6$  at a scan rate of 100 mV/s.

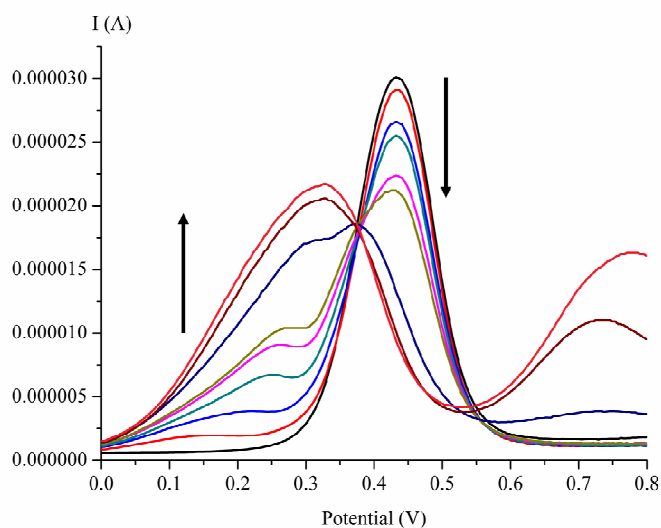


**Fig. 3.23** Square wave voltammogram titration of receptor **L1** (1 mM) upon gradual addition TBAAcO (0-4 equivalents) in 40% CH<sub>3</sub>CN v/v in CH<sub>2</sub>Cl<sub>2</sub> with 0.1 M TBAPF<sub>6</sub> at a scan rate of 100 mV/s.

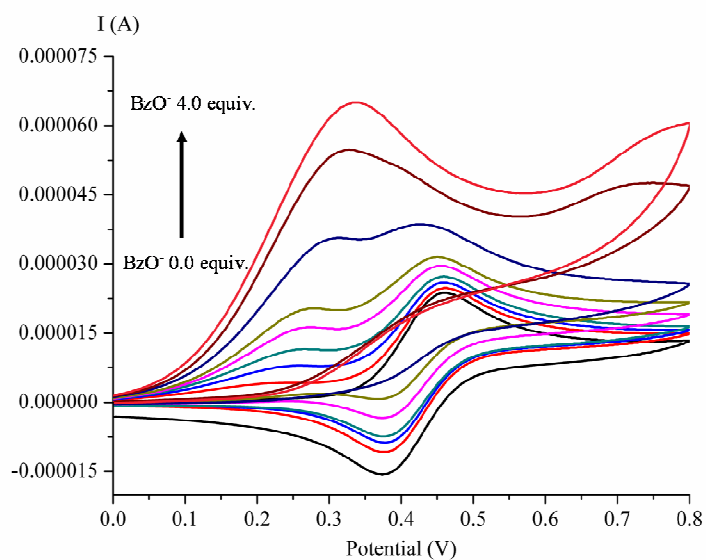


**Fig. 3.24** Cyclic voltammogram titration of receptor **L1** (1 mM) upon gradual addition TBABzO (0-4 equivalents) in 40% CH<sub>3</sub>CN v/v in CH<sub>2</sub>Cl<sub>2</sub> with 0.1 M TBAPF<sub>6</sub> at a scan rate of 100 mV/s.

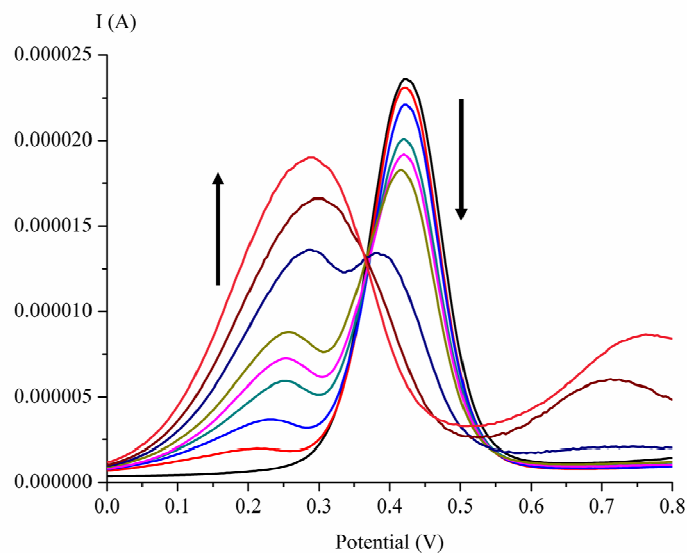


**Fig. 3.25** Square wave voltammogram titration of receptor **L1** (1 mM) upon gradual addition TBABzO (0-4 equivalents) in 40%  $\text{CH}_3\text{CN}$  v/v in  $\text{CH}_2\text{Cl}_2$  with 0.1 M  $\text{TBAPF}_6$  at a scan rate of 100 mV/s

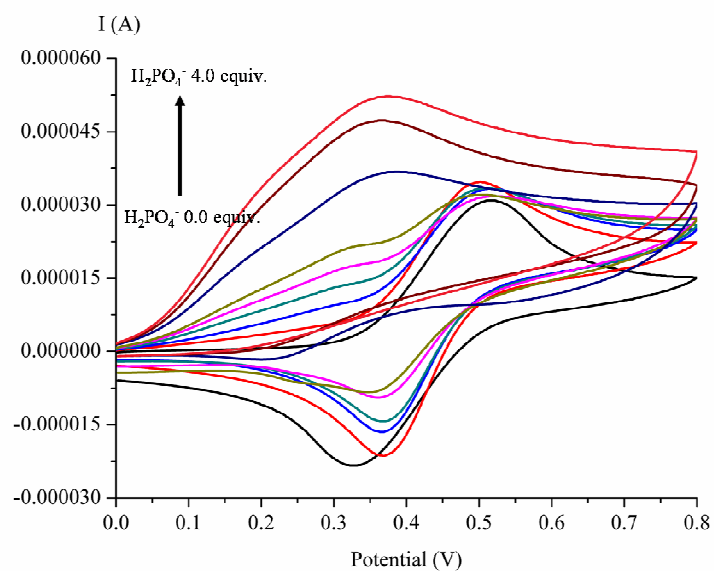


**Fig. 3.26** Cyclic voltammogram titration of receptor **L1** (1 mM) upon gradual addition  $\text{TBABH}_2\text{PO}_4$  (0-4 equivalents) in 40%  $\text{CH}_3\text{CN}$  v/v in  $\text{CH}_2\text{Cl}_2$  with 0.1 M  $\text{TBAPF}_6$  at a scan rate of 100 mV/s.

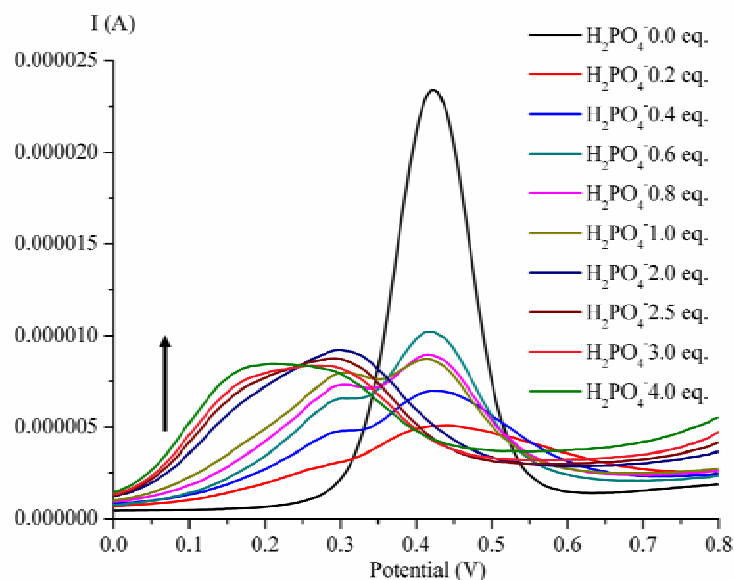


**Fig. 3.27** Square wave voltammogram titration of receptor **L1** (1 mM) upon gradual addition TBAH<sub>2</sub>PO<sub>4</sub> (0-4 equivalents) in 40% CH<sub>3</sub>CN v/v in CH<sub>2</sub>Cl<sub>2</sub> with 0.1 M TBAPF<sub>6</sub> at a scan rate of 100 mV/s.

### 3.4 Concluding remarks

A new heteroditopic receptor based on amidoferrocene calix-crown ether existed in 1,3-alternate conformation, **L1** was synthesized and compared to analogous ion-pair receptor, **L2**, which was in cone conformation. Complexation studies by <sup>1</sup>H NMR titration showed that without electrostatic interactions from cations, both receptors preferred binding AcO<sup>-</sup> and BzO<sup>-</sup> implying the preference of binding Y-shaped anions. In the presence of metal ions, receptor **L1** showed higher affinity with all anions, while receptor **L2** gave more specificity and selectivity with AcO<sup>-</sup> and Br<sup>-</sup> ions. Electrochemical studies of these receptors were investigated using cyclic and square wave voltammetries. Both receptors can sense AcO<sup>-</sup>, BzO<sup>-</sup> and Cl<sup>-</sup> through cathodic shifts of their oxidation waves. Interestingly, receptor **L1** also detected H<sub>2</sub>PO<sub>4</sub><sup>-</sup> remarkably. In the presence of cobound cations, receptor **L1** failed to recognize all anions

electrochemically. In contrast, cobound cations of receptor **L2** recognized  $\text{Cl}^-$  more strongly. Moreover,  $[\mathbf{L2}\cdot\text{Na}^+]$  gave the highest  $\Delta E$  (250 mV) upon adding  $\text{AcO}^-$ . Therefore, from these studies, additional electrostatic interactions from cations can improve anion binding abilities of the heteroditopic receptors. However, the ionic distance between the positive charge and the negative charge also played key role in cooperative effect as well as the selectivity of ion pair formation. Even though, double positive charge were presented in the molecule, anion binding abilities could not be improved if the ionic distance was not suitable. Cone conformation of receptor **L2** provided more suitable ionic distance for specific ion pair formation than 1,3-alternate conformation of receptor **L1**.

To improve the electrochemical sensing properties of compound **L1** and **L2**, the sensory unit has been changed from ferrocene to anthraquinone. This sensory unit is expected to provide a more sensitivity toward anionic analytes. The synthesis, characterization as well as the studies of the properties of compounds **L3** and **L4** containing amido-anthraquinone are described in Chapter IV.

## CHAPTER IV

# OPTICAL AND ELECTROCHEMICAL HETERODITOPIC RECEPTORS DERIVED FROM CROWN ETHER-BASED CALIX[4]ARENE WITH AMIDO-ANTHRAQUINONE PANDANTS

### 4.1 General information and literature reviews of receptors based anthraquinone

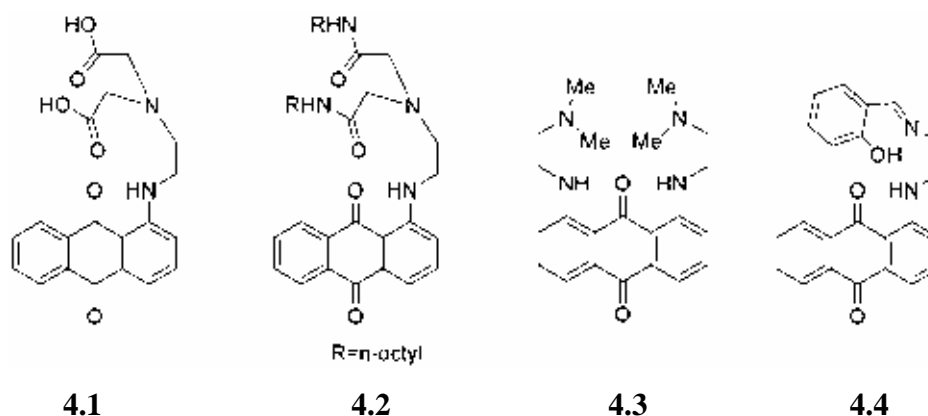
In the past decade, anthraquinone, a well-known important dye, was applied as a sensory unit in chemical sensors [82-101]. Chemical stimuli lead to different chemical changes of anthraquinone. For example, excited state intramolecular proton transfer (ESIPT) [95], chelation-enhanced fluorescence (CHEF) [86] and colour change can be exhibited from the interaction between anthraquinone derivative receptors and ions.

#### 4.1.1 Cation sensors derived from anthraquinone

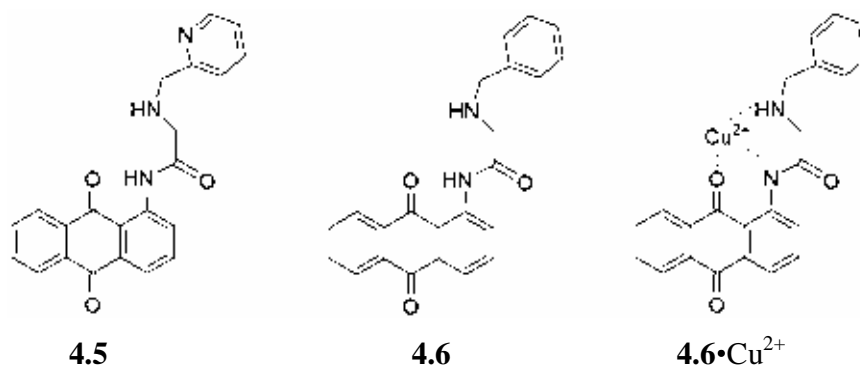
A number of anthraquinone derivatives showed optical signals upon interacting with metal ions such as  $\text{Cu}^{2+}$  [83-91],  $\text{Ni}^{2+}$  [90],  $\text{Al}^{3+}$  [92],  $\text{In}^{3+}$  [93], and  $\text{Hg}^{2+}$  [94], through their coordination or deprotonation at the binding sites.

Copper ion sensors based on anthraquinone, **4.1-4.4**, have been synthesized. A diamide-diamine based sensor **4.1** and **4.2** showed selectivity to copper ion [83]. The selective deprotonation of an aryl amine NH by  $\text{Cu}^{2+}$  caused a bathochromic shift and significant colour changes. However, **4.1** showed lower selectivity for  $\text{Cu}^{2+}$  than that observed for **4.2**. Different amounts of  $\text{Cu}^{2+}$  led to different colours of **4.3** solution which were fully reversible to the original colour and spectrum when EDTA was added [84]. UV-vis spectra of **4.3** upon titration with  $\text{Cu}^{2+}$  showed that at the low concentration of  $\text{Cu}^{2+}$ , the second band at 800 nm was not observed. These results pointed to the presence of more than one stoichiometric species between **4.3** and  $\text{Cu}^{2+}$ . Then this assumption was proved by a series of pH and UV-vis titrations. The results showed that the receptor **4.3** underwent mono- and di-deprotonation at aryl amine NH, respectively, which was responsible for these remarkable colour changes. Receptor **4.4** presented the different

optical responses towards  $\text{Cu}^{2+}$  and  $\text{Ni}^{2+}$  [90]. Deprotonation still played important role in the recognition of this receptor with those cations.

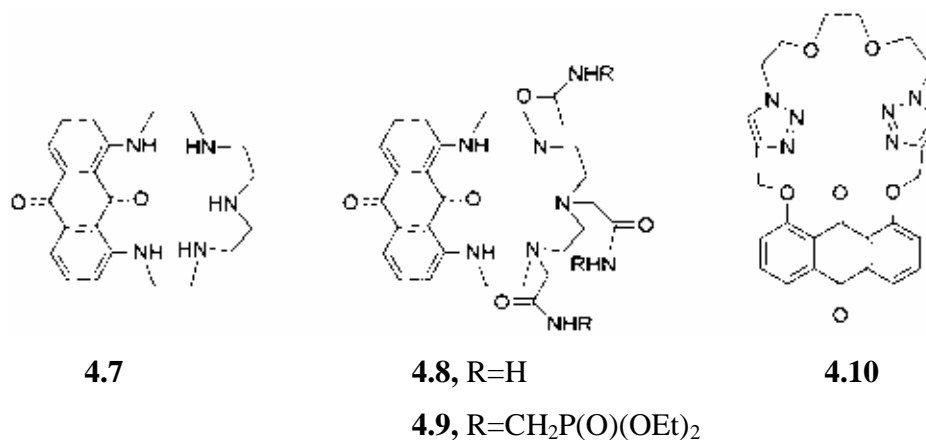


Two novel transition metal chemosensors consisting of a benzene and a pyridine ring linked to amido-antraquinone moiety, **4.5** and **4.6** have been synthesized.  $\text{Cu}^{2+}$  induced deprotonation of an amide proton contributed to the color changes of chemosensors, **4.5** and **4.6** [86]. A binding model of **4.5**- $\text{Cu}^{2+}$  was shown above. Interestingly, **4.6** showed dissimilar selectivity toward  $\text{Cu}^{2+}$ ,  $\text{Co}^{2+}$  and  $\text{Ni}^{2+}$  through different color changes. Both chemosensors detected  $\text{Cu}^{2+}$  through a fluorescence quenching process which arose from an energy or charge transfer mechanism. On the contrary,  $\text{Co}^{2+}$  enhanced fluorescence intensity of **4.6** via CHEF (chelation-enhanced fluorescence). Fluorescence studies revealed that **4.6** bound cations in order  $\text{Cu}^{2+} > \text{Ni}^{2+} > \text{Co}^{2+}$ . This finding was consistent with the Irving-Williams series, in which  $\text{Cu}^{2+}$  has the highest formation constant with ligands among the first row transition metal ions.



Three 1,8-diaminoanthraquinone-based polyazamacrocycles, **4.7-4.9** were synthesized [87]. Although **4.7** and **4.8** can sense some metal ions such as Cu<sup>2+</sup>, Al<sup>3+</sup> and Pb<sup>2+</sup>, low solubility of these receptors in water limited interest of these compounds. The introduction of pendent arms possessing additional metal binding sites to **4.9** was done to improve the Pb<sup>2+</sup> affinity and solubility in aqueous media. It was found that (diethoxyphosphoryl) methyl groups crucially change the solubility of the sensor. Compound **4.9** was perfectly soluble in most of organic solvents and in water. Moreover, it exhibited efficient binding for Pb<sup>2+</sup> in water and allowed naked-eye detection. The hypsochromic shift of the absorption maximum observed in the spectrum of Pb complex suggested conformational changes of the macrocyclic backbone and a decrease of  $\pi$ -delocalization of the nitrogen atom lone pair electron from metal complexation. A chemosensor bearing a 1,2,3-triazole ring spacer, **4.10** was synthesized [92]. This sensor can detect Al<sup>3+</sup> through both optical and electrochemical changing. From the absorption bands of **4.10** upon metal binding showed a red shift due to ICT (intramolecular charge transfer). Enhancement of the fluorescence intensity of **4.10** upon addition of Al<sup>3+</sup> was probably due to the coordination of a metal to triazole rings, followed by PET suppression, denoted as CHEF (chelation enhanced fluorescence). In addition, electrochemical behaviors of **4.10** showed significant changes upon addition of Al<sup>3+</sup>.





An optical selective and electrochemical active chemosensor for Cu<sup>2+</sup>, **4.11** was designed using a sugar moiety attached into an anthraquinone scaffold because of its conformational flexibility, high biocompatibility, low toxicity and abundance in nature [88]. In addition, carbohydrates are one of the most desired classes of molecular systems to sense metal cations in biological systems. The anthraquinone oxygen and triazole ring served as cation binding site. Electrochemistry behaviors of this compound were also observed by differential pulse voltammetry measurement.

Recently, an anthraquinone containing chemodosimeter, **4.12** and its mesoporous silica-immobilized anthraquinone change, have been synthesized to apply as a organic-inorganic hybrid materials [85]. The original intramolecular charge transfer band (ICT band) of **4.12** went to the blue-shift after addition of Cu<sup>2+</sup> which was attributed to a strong thiophilic affinity between thiourea and Cu<sup>2+</sup>, followed by desulfurization to give **4.13**, causing a visual color change from red to pale yellow. Chemodosimetric reaction mechanism upon Cu<sup>2+</sup> ion addition was shown in **Scheme 4.1**.

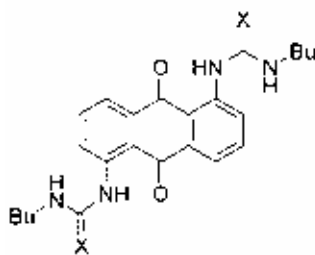
Yang et al. synthesized receptors **4.14-4.16** for cation binding [94]. The results showed that only **4.15** can sense Hg<sup>2+</sup> through UV-visible studies. The presence of Hg<sup>2+</sup> influenced the charge transfer band between the electron-rich urea moiety and the electron-deficient anthraquinone moiety. Computational studies revealed that both the



### 4.1.2 Anion sensors derived from anthraquinone

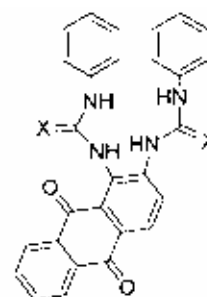
Various anion sensors based on anthraquinone exhibited high selectivities towards fluoride and acetate ions [95-101]. Most of the reported anthraquinone derivatives for detecting fluoride ions employed various signal transductions such as charge transfer bands in UV/vis spectra, color changes and emission spectra from excited-state intramolecular proton transfer (ESIPT) [95-101]. Mechanisms of the signal transductions were mainly due to the deprotonation [95-97] or hydrogen bonding interactions [98-101] between fluoride ion and the functional groups such as urea, thiourea as well as imidazolium salts.

Diego et al. and D.Amilan et al. synthesized receptors **4.17-4.20** having urea groups and thiourea groups as binding sites for anions [98, 99]. Receptors **4.18**, **4.19** and **4.20** were found to bind fluoride ions selectively through hydrogen bonding interaction. New absorption bands at longer wavelength were presented after addition of fluoride ions to the solution of these receptors which ascribed to the charge-transfer interaction between the electron-rich urea/thiourea-bound F<sup>-</sup> and the electron-deficient anthraquinone moieties. Also, the formation of these hydrogen bonds most likely affects the electronic properties of the chromophore, resulting in colour change.



X=O, **4.17**

X=S, **4.18**



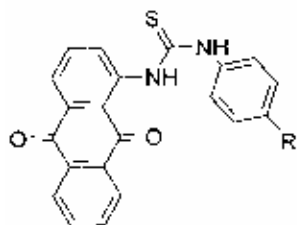
X=O, **4.19**

X=S, **4.20**

The recognition-structure relationship of compounds **4.21-4.25** was studied by introducing the electron-donating or electron-withdrawing groups. Fang-ying Wu and co-workers synthesized receptors **4.21** and **4.22** containing nitrobenzene and benzene

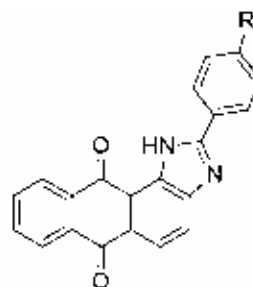
connected with a thiourea group respectively [100]. It was found that the NH protons connected with benzene rings of these receptors interacted with fluoride ions via hydrogen bonding. In addition, the nitro group of receptor **4.22** enhanced the binding ability of receptor to anions and facilitated the process of charge transfer in the ground state bringing a vivid color change.

Peng et al. synthesized receptors derived anthraquinone consisting imidazole moieties linked with benzene rings, **4.23-4.25** [95]. An absorption spectrum of **4.23** exhibited the charge transfer band at longer wavelength after addition of fluoride ions. The interaction between receptor **4.23** and fluoride ions was shown to be stepwise changes. Low concentration of fluoride ions caused authentic hydrogen bonding interaction with the NH proton of imidazole ring of **4.23**. Then, addition excess of fluoride ions led to deprotonation of the NH proton. The push-pull properties of the substituents on the phenyl para position of these sensors distinctly effected to the anion binding abilities of these receptors. The introduction of the electron-donating group of **4.24** enhanced the electron density of the imidazole ring and therefore increased the basicity of the hydrogen-bond donors, so the deprotonation became more difficult. In this case, a very large amount of fluoride ions contributed to the similar changes found in the absorption spectra of **4.23**. Conversely, only little amount of fluoride ions added to the solution of **4.25** resulted in the similar absorption spectra found in **4.23**. This result implied the strong electron-withdrawing *p*-NO<sub>2</sub> substituent made the charge delocalization more easily upon interaction with fluoride. However, fluoride, acetate and dihydrogenphosphate ions induced similar spectral changes in **4.25**. As a result, sensor **4.23** showed the best selectivity which was attributed to the fitness in the acidity of its NH-group. Moreover, in the presence of anions, these receptors presented longer wavelength emission spectra which stemmed from excited-state intramolecular proton transfer (ESIPT).



R=NO<sub>2</sub>, **4.21**

R=H, **4.22**



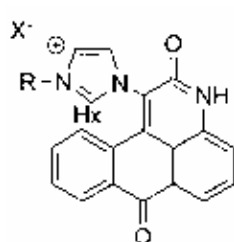
R=H, **4.23**

R=OCH<sub>3</sub>, **4.24**

R=NO<sub>2</sub>, **4.25**

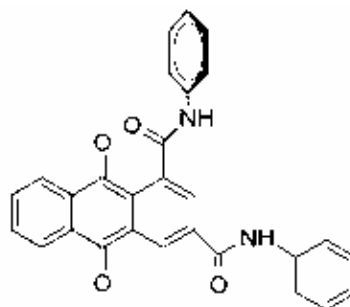
New *N*-aryl imidazolium based receptors **4.26** and **4.27**, which enable naked eye and dual channel (absorption and fluorescence) detection of F<sup>-</sup> and AcO<sup>-</sup> ions respectively were synthesized [96]. Imidazolium salts based anion probes were attractive to researchers because they remain unaffected by the pH of the medium and so can find applicability under physiological conditions.

Besides signals from optical spectroscopy, anthraquinone derivatives displayed electrochemical signals as well. The quinone group gave two successive 1 electron reduction steps, Q<sup>1-</sup> and Q<sup>2-</sup>, leading to two reversible redox waves in the cyclic voltammogram [102-105]. The electrochemistry of 1,3-diphenylcarboxamidoanthraquinone, **4.28** was studied [106]. In the absence of F<sup>-</sup> ion, the electrochemistry behavior of this receptor showed only one reduction peak instead of two one-electron quasireversible peaks which were the normally peaks found in electrochemistry of anthraquinone. The reason may be from the intra- or intermolecular hydrogen bonding interactions formed with oxygen atom of anthraquinone stabilized both the semiquinone and dianion species. However, addition of F<sup>-</sup> into the solution of this receptor led to the competition of hydrogen bonding formations between F<sup>-</sup> and oxygen atom of quinone. The results presented that the hydrogen-bond donor groups bound to F<sup>-</sup> rather than the quinone oxygen atom resulting in the return of the two one-electron quasireversible electrochemical processes.



R=Benzyl, X=Cl, **4.26**

R=dodecyl, X=Br, **4.27**

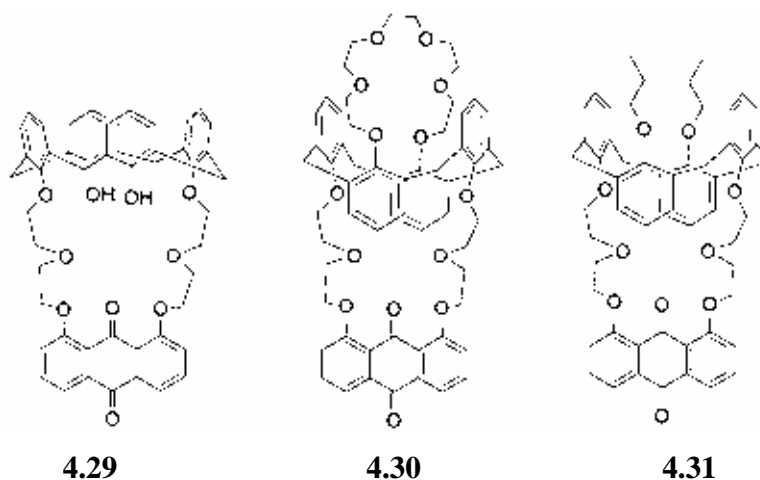


**4.28**

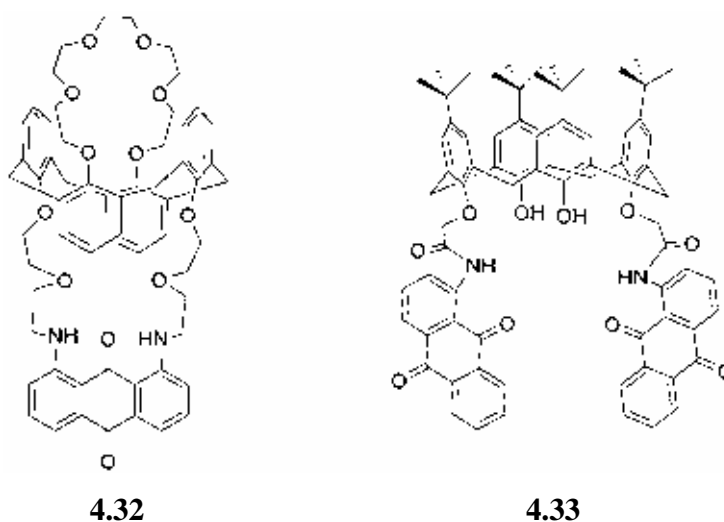
#### 4.1.3 Ion sensors containing anthraquinone based on calix[4]arene scaffold

Calix[4]arene is one of the most suitable synthetic macrocycles for the design of ion receptors since: (1) various functional groups can be modified to its wide and narrow rim and (2) calix[4]arene derivatives can stay in many conformations [4-6, 33-35, 40-48].

A series of calix[4]arene-base chromogenic sensors bearing the 9, 10-anthraquinone moiety, **4.29-4.31**, were synthesized [91]. Receptor **4.29** showed the best selectivity to  $\text{Cu}^{2+}$  ions through the Internal Charge Transfer (ICT) band at 450 nm, whereas **4.30** and **4.31** did not show any UV and color changes. It was believed that the  $\text{Cu}^{2+}$  ion interacts strongly with the lone pair electrons of the carbonyl oxygen atoms with the aid of the two proximal OHs of the calix[4]arene, then the charge transfer from the 1,8 oxygen atoms to the electron-deficient carbonyl group became stronger. The lack of two proximal OHs of **4.30** and **4.31** led to the low recognition of any ions.



1,8-anthraquinonylcalix[4]monocrown-6, **4.32**, was synthesized [93]. The addition of  $\text{In}^{3+}$  to the solution of this sensor resulted in a gradual decrease of the peak at 625 nm and a progressive increase of a new peak around 535 nm. These changes might be attributed to that the intramolecular H-bonds were blocked by the coordination with  $\text{In}^{3+}$  which therefore led to the inhibition of the ESIPT feature. In the same manner, addition  $\text{F}^-$  ion, to the solution of **4.33** caused a gradual decrease of the ESIPT peak at 560 nm concomitant with an increase of the normal peak at 527 nm. The ESIPT process of **4.33** is inhibited by the fluoride-induced H-bonding followed by deprotonation of NH of the 1-aminoanthraquinone [91].



## 4.2 Objective and scope of research

Compared to simple anion receptors, heteroditopic or ion-pair receptors generally display significantly enhanced affinities towards anions stemming from cooperative or allosteric effects which attributes to the electrostatic interactions from different charged ions bound to the receptors [1-6, 33-48]. Recently, dual redox and fluorescent sensors have become an interesting subject due to their multichannel for sensing ions. They can sense ions through not only the fluorescence changing but also the shift of redox potentials, anodically or cathodically [55-68]. From this point of view, anthraquinone is one of the interesting dual mode sensory units for sensing ions because of its diverse optical and electrochemical properties. In addition, sensors bearing anthraquinone moieties that display the dual ion-sensing mode were still rarely reported.

Therefore, in this study, two heteroditopic ion receptors based on amidoanthraquinone-crown ether calix[4]arene in cone conformation and 1,3-alternate conformation, **L3** and **L4**, respectively have been synthesized (**Fig. 4.1**). Due to various conformations of calix[4]arene and its ease to modify the functional groups, calix[4]arene was chosen to be the building block. The combination of amidoanthraquinone and calix-crown ether in different conformations would be expected to result in an optimized structure for the ion-pair system to enhance the anion affinity, recognition and sensing. Furthermore, dual sensing modes of the quinone moiety, both optical and electrochemical responses, would be anticipated to be useful for monitoring specific ions.

Briefly, the objectives of this work are...

1. To synthesize two new heteroditopic ion receptors based on amidoanthraquinone-crown ether calix[4]arene in cone conformation and 1,3-alternate conformation, **L3** and **L4**.
2. To study the influence of additional electrostatic interaction from a cation to the anion binding abilities of those receptors via their photophysical and electrochemical properties.



3. To study the effect of the topology of ligands to cooperative effect of the heteroditopic receptors.

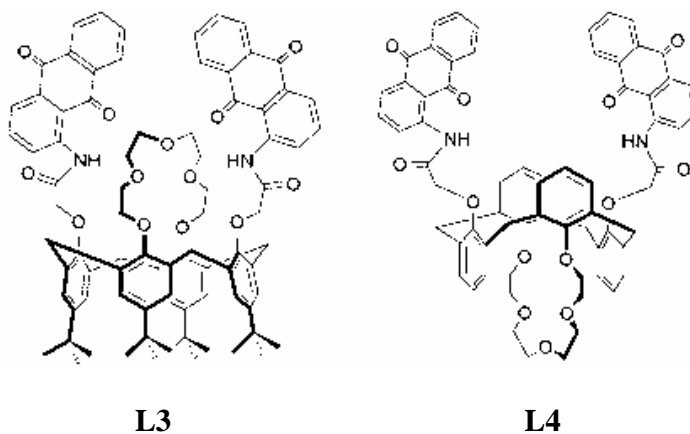
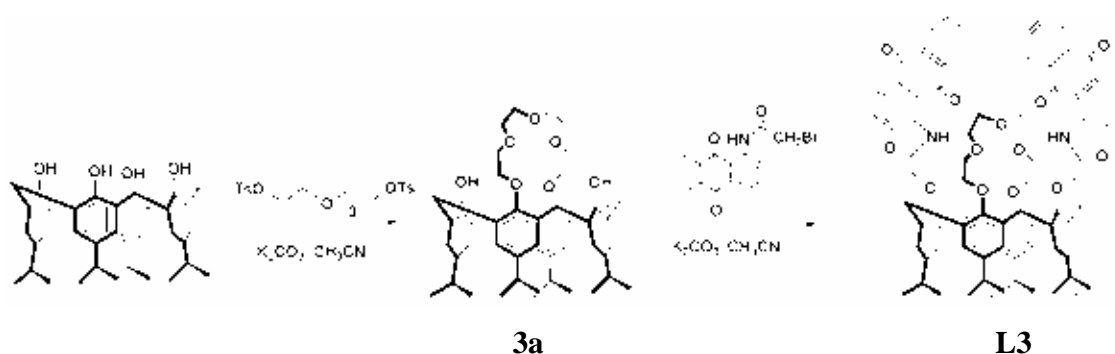


**Fig. 4.1** Structures of heteroditopic receptors, **L3** and **L4**

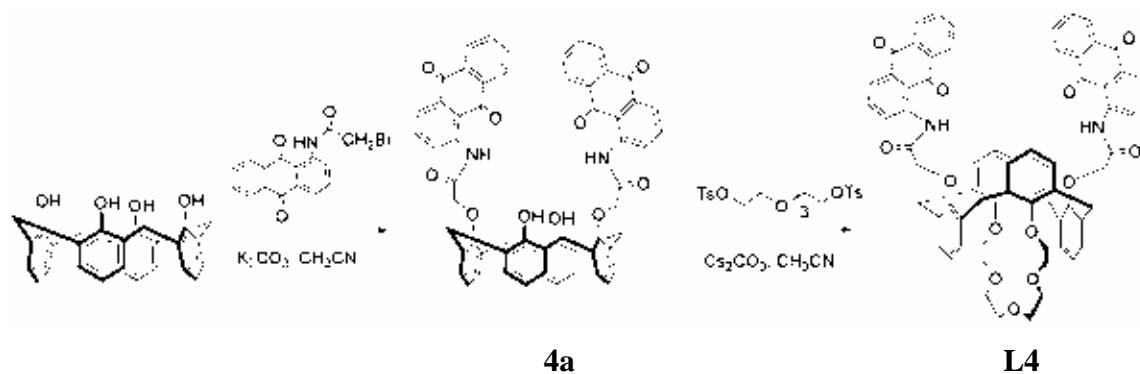
### 4.3 Results and discussion

#### 4.3.1 Synthesis and Characterization of Receptors L3 and L4

Substitution reaction of *p*-*tert*-butylcalix[4]arene with tetraethyleneglycol ditosylate (prepared from tetraethylene glycol) using  $K_2CO_3$  as base in  $CH_3CN$  gave **3a** in 40% yield. Compound **3a** was then reacted with bromoacetyl amidoanthraquinone in the presence of  $K_2CO_3$  in acetonitrile at reflux to give **L3** in 9% yield. Similarly, substitution reaction of calix[4]arene with bromoacetyl amidoanthraquinone using  $K_2CO_3$  as base in  $CH_3CN$  at reflux gave **4a** in 32% yield. Compound **4a** was then reacted with tetraethyleneglycol ditosylate in the presence of  $Cs_2CO_3$  in acetonitrile at reflux to give **L4** in 7% yield.



**Scheme 4.2** synthetic pathway of receptor **L3**



**Scheme 4.3** synthetic pathway of receptor **L4**

Both compounds **L3** and **L4** were characterized by NMR spectroscopy, mass spectrometry and elemental analysis. The  $^1\text{H-NMR}$  spectrum of **L3** suggested that the calix[4]arene unit was in a cone conformation according to the characteristic of cone conformation, the  $\text{ArCH}_2\text{Ar}$  signals, which appear as a pair of doublets (AB system) at 4.73 and 3.27 ppm ( $J = 12.8$  Hz). The  $^{13}\text{C}$  NMR spectrum of **L3** showed a signal of *syn*  $\text{Ar}_2\text{CH}_2$  around 31 ppm [107]. For receptor **L4**, the conformation of calix[4]arene was assigned as 1,3-alternate. Even though a pair of doublet  $\text{ArCH}_2\text{Ar}$  signals appeared at 3.90 and 4.20 ppm ( $J = 16.4$  Hz), the characteristic *anti*  $\text{Ar}_2\text{CH}_2$  appeared at around 38 ppm in the  $^{13}\text{C-NMR}$  spectrum supported the 1,3-alternate conformation of the calix[4]arene framework in compound **L4** [107]. In addition, the chemical shift of the NH amide proton of receptors **L3** and **L4** appeared in the downfield region at 12.40 and 12.23

ppm, respectively, suggesting intramolecular hydrogen bonding. This indicated that intramolecular hydrogen bonding interactions of the amide groups and the oxygen of anthraquinone could occur. Interestingly, the amide protons of **L3** shifted to a more downfield region than those of **L4**, implying that intramolecular hydrogen bonding interactions in **L3** were stronger than those in **L4**. This was probably due to the crown ether group in **L3** involved in H-bonding interactions.

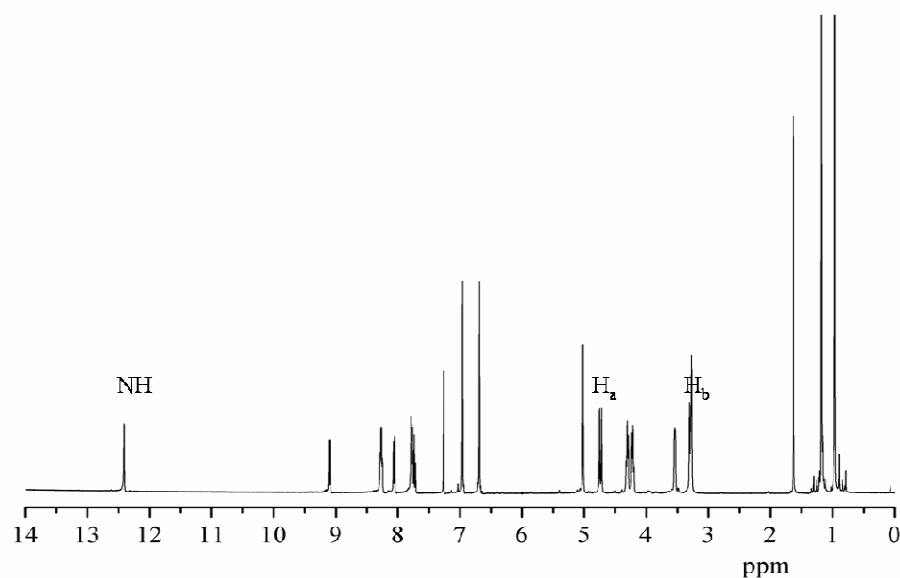


**Fig. 4.2**  $^1\text{H-NMR}$  spectrum of receptor **L3** in  $\text{CDCl}_3$

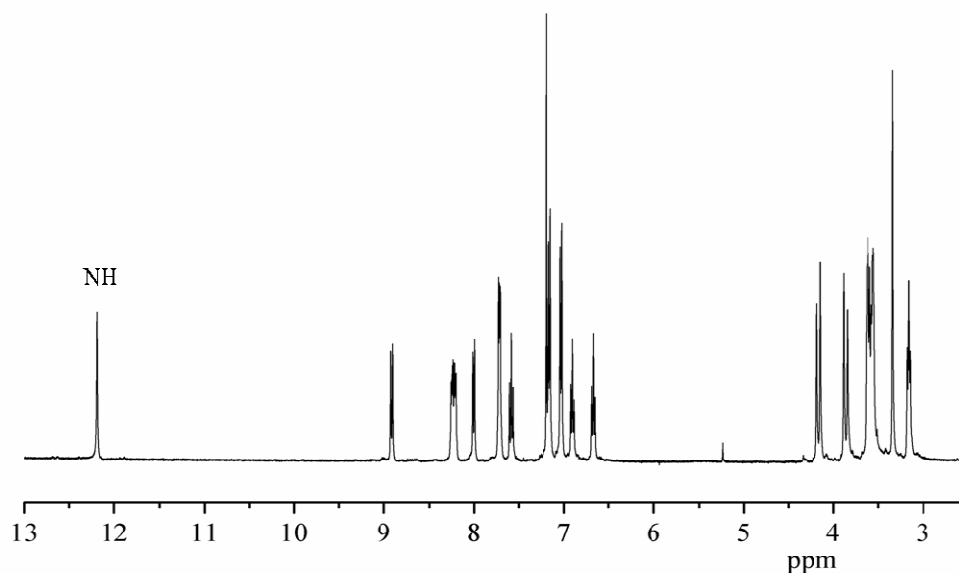


**Fig. 4.3**  $^1\text{H}$ -NMR spectrum of receptor **L4** in  $\text{CDCl}_3$

### 4.3.2 Complexation studies of receptors **L3** and **L4** by $^1\text{H}$ NMR titration

#### 4.3.2.1 Binding properties of receptors **L3** and **L4** towards alkali metal cation by NMR studies

Ideally the metal cation must be bound strongly so as to minimize ion-pairing outside the receptor. Therefore, complexation studies using  $^1\text{H}$  NMR titration were investigated to find the cation that can fit within the cavity of receptors. The  $^1\text{H}$  NMR titration experiments were performed in 5% v/v  $\text{CD}_3\text{CN}$  in  $\text{CDCl}_3$ . Two alkali metals,  $\text{Na}^+$  (added as  $\text{NaClO}_4 \cdot \text{H}_2\text{O}$ ) and  $\text{K}^+$  (added as  $\text{KPF}_6$ ) were tested in this experiment.

Upon addition  $\text{NaClO}_4 \cdot \text{H}_2\text{O}$  and  $\text{KPF}_6$  into the solution of receptor, two sets of resonances were observed for all the proton signals in the  $^1\text{H}$  NMR spectra of **L3** and **L4** resulting from strong binding interactions with a slow complexation behavior as shown in **Fig. 4.4** and **4.5**. The AB signals of methylene protons r' and s' of compound **L3** upon

complexing  $K^+$  shifted more upfield and downfield, respectively as compared to the AB signals of 1,3-alternate compound **L4**. This indicates a large cone angle change in the cone conformation of compound **L3** upon binding  $K^+$ . The receptor/cation complexes formed completely upon addition of 1 equivalent of cations, which were consistent with a 1:1 binding mode. Binding constants were determined by direct integration of signals from free receptors and complexes in  $^1H$ -NMR spectra which were described by Macober [71]. The stability constants could be determined from the variation of the integration ratio between the complex and the free receptor at various amount of the cationic guest.

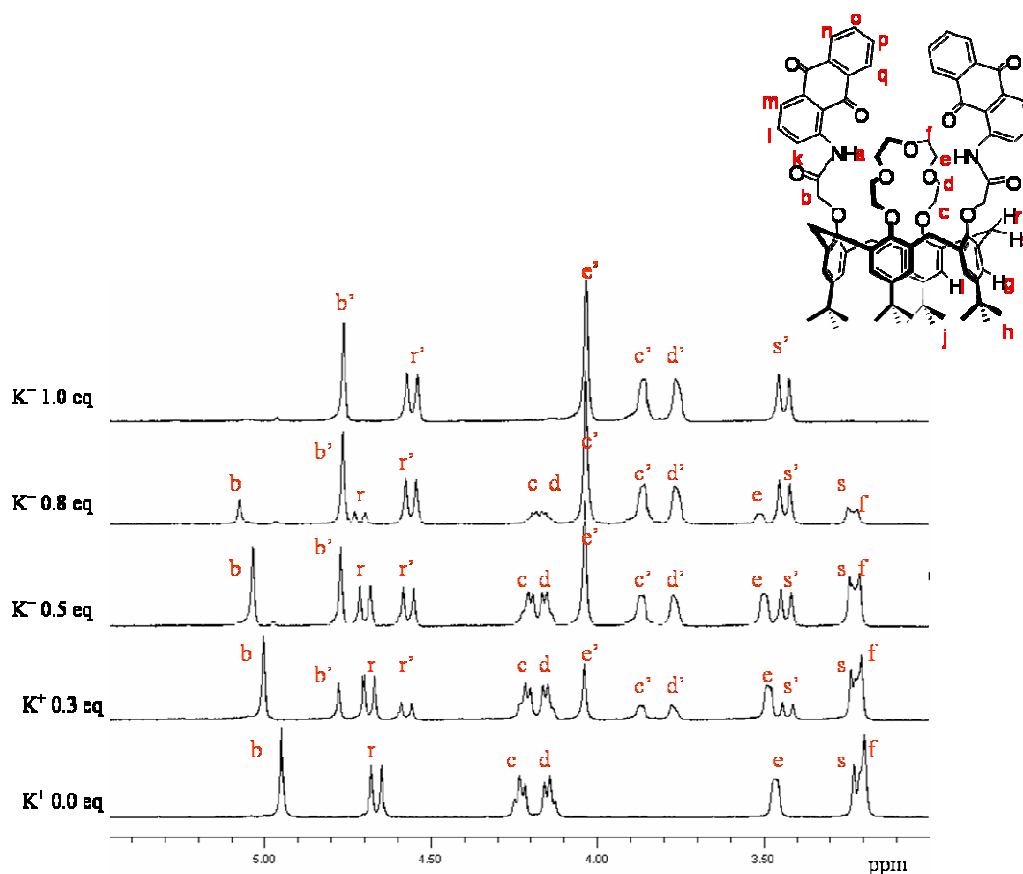


**Fig. 4.4** Partial  $^1H$  NMR titration spectra between the receptor **L3** and potassium ions in 5% v/v  $CD_3CN$  in  $CDCl_3$  showed slow complexation/decomplexation process. x and x' represented protons of decomplexes and complexes with  $K^+$ , respectively.

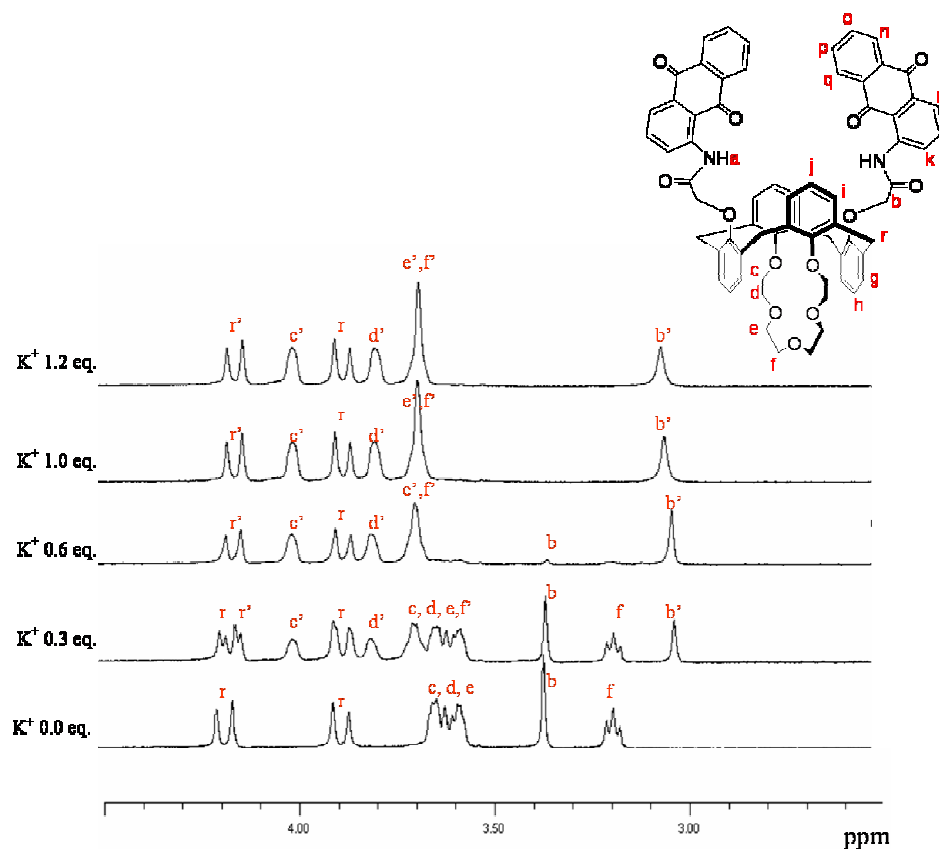


**Fig. 4.5** Partial  $^1\text{H}$  NMR titration spectra between the receptor **L4** and potassium ions in 5% v/v  $\text{CD}_3\text{CN}$  in  $\text{CDCl}_3$  showed slow complexation/decomplexation process. x and x' represented protons of decomplexes and complexes with  $\text{K}^+$ , respectively.

**Table 4.1** Binding constants of **L3** and **L4** with cations from  $^1\text{H}$  NMR titration

Receptor	Binding Constant, $K$ ( $\text{M}^{-1}$ )	
	$\text{Na}^+$ cation	$\text{K}^+$ cation
<b>L3</b>	333	2700
<b>L4</b>	250	2650

<sup>a</sup> Maximum error estimated to be less than  $\pm 10\%$ .

From **Table 4.1**, the binding constants of both receptors **L3** and **L4** with  $K^+$  were much higher than that with  $Na^+$ . These results were consistent with the previous study that reported the polyether ring of calix[4]crown-5 is more suitable for the complexation of  $K^+$  [77]. According to these binding constants, co-bound  $K^+$  complexes were chosen to study the cooperative binding of receptors **L3** and **L4** with anions.

#### **4.3.2.2 Binding properties of compounds L3 and L4 towards anions in the absence of $K^+$ by $^1H$ -NMR titration**

The ability of receptors **L3** and **L4** to bind anions (added as their tetrabutylammonium salt) was tested in 5% v/v  $CD_3CN$  in  $CDCl_3$ . In the absence of  $K^+$ , the amide-NH protons of receptor **L3** and **L4** were shifted slightly downfield and disappeared after addition of 1 equivalent of fluoride ions as shown in **Fig. 4.6 and 4.7**. These results indicated the formation of hydrogen-bond complex between those receptors and  $F^-$  [99, 100]. Furthermore, even though after the excess of fluoride ions (4 equiv.) were added, no new 1:2:1 triplet signal around 16 ppm. which was ascribed to the  $FHF^-$  dimer [95]. This result supported the formation of hydrogen bonding more than deprotonation. No changes in  $^1H$  NMR spectra were detectable for other anions. Thus, it implied that these two free ligands preferred to bind with  $F^-$ .

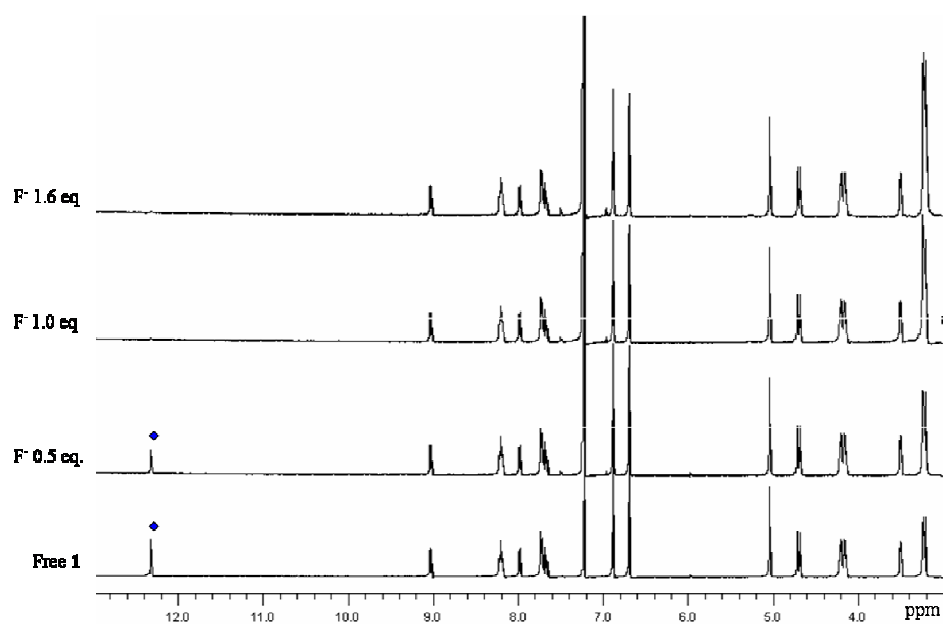


**Fig. 4.6**  $^1\text{H}$  NMR titration spectra of **L3** on addition of TBAF.3H<sub>2</sub>O in 5% v/v CD<sub>3</sub>CN in CDCl<sub>3</sub>. ♦ represents the NH amide protons.

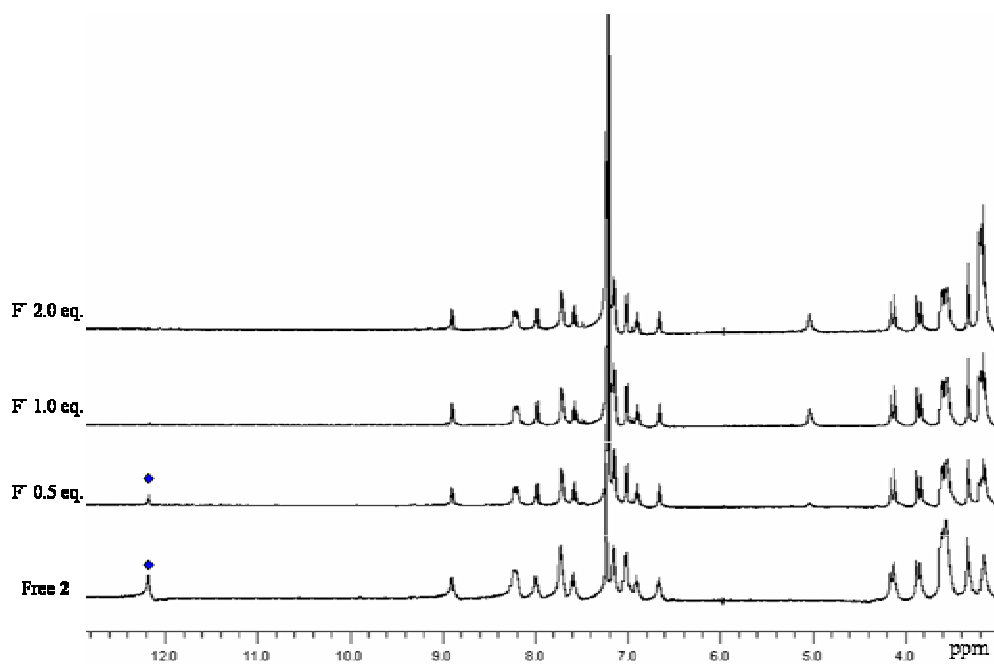


**Fig. 4.7**  $^1\text{H}$  NMR titration spectra of **L4** on addition of TBAF.3H<sub>2</sub>O in 5% v/v CD<sub>3</sub>CN in CDCl<sub>3</sub>. ♦ represents the NH amide protons.



#### 4.3.2.3 Binding properties of compounds **L3** and **L4** towards anions in the presence of $K^+$ by $^1H$ -NMR titration

The anion binding studies of receptors **L3** and **L4** in the presence of  $K^+$  were carried out in 5% v/v  $CD_3CN$  in  $CDCl_3$ . Interestingly, for receptor **L3**, in the case of acetate ions, the NH proton of  $[L3 \cdot K^+]$  complex went downfield and disappeared gradually after addition 1 equivalent of acetate ions as shown in **Fig. 4.8**. This result implies that co-bound ion pairs between acetate and a potassium ion form within the molecule **L3**. Benzoate ion also gave the similar result as in the case of the acetate ion, however; the equivalents of benzoate added (4 equiv.) were more than those in the acetate case as shown in **Fig. 4.9**. Addition of fluoride ions to the solution of  $[L3 \cdot K^+]$  complex led to a different behaviour. At low concentration of fluoride ions ( $< 0.5$  equivalents), NH protons of  $[L3 \cdot K^+]$  complex went slightly downfield and disappeared indicating the cobound ion pair formation. However, at higher concentration of fluoride ions ( $> 0.5$  equivalents), caused the formation of cobound ion pairs concomitant with the abstraction of  $K^+$  by fluoride ions which could be observed through the disappearance of the NH proton of  $[L3 \cdot K^+]$  complex together with the gradual inversion of the spectrum of free ligand as shown in **Fig. 4.10**. This was probably because the concentration of fluoride ion was so high that supported the formation of KF salt. Addition of  $H_2PO_4^-$  ions to the solution of  $[L3 \cdot K^+]$  complex resulted in the abstraction of  $K^+$  by  $F^-$  which was obviously presented by the complete inversion of free **L3** spectrum after added of 2 equivalents of fluoride ions as shown in **Fig. 4.11**. Other anions ( $Cl^-$ ,  $Br^-$  and  $I^-$ ) did not cause any change in  $[L3 \cdot K^+]$  spectrum.

Addition of low concentration of fluoride ions (0-1 equivalent) to  $[L4 \cdot K^+]$  solution did not lead to any change in the peaks of  $^1H$  NMR spectra of  $[L4 \cdot K^+]$  implying that the added fluoride ions acted as a counter ion for  $K^+$ . Then, after more equivalents of fluoride ion were added ( $> 2$  equivalents), abstraction of  $K^+$  by  $F^-$  occurred as shown in **Fig. 4.12**. However, addition other anions to  $[L4 \cdot K^+]$  solution did not cause any change in  $[L4 \cdot K^+]$  spectra.

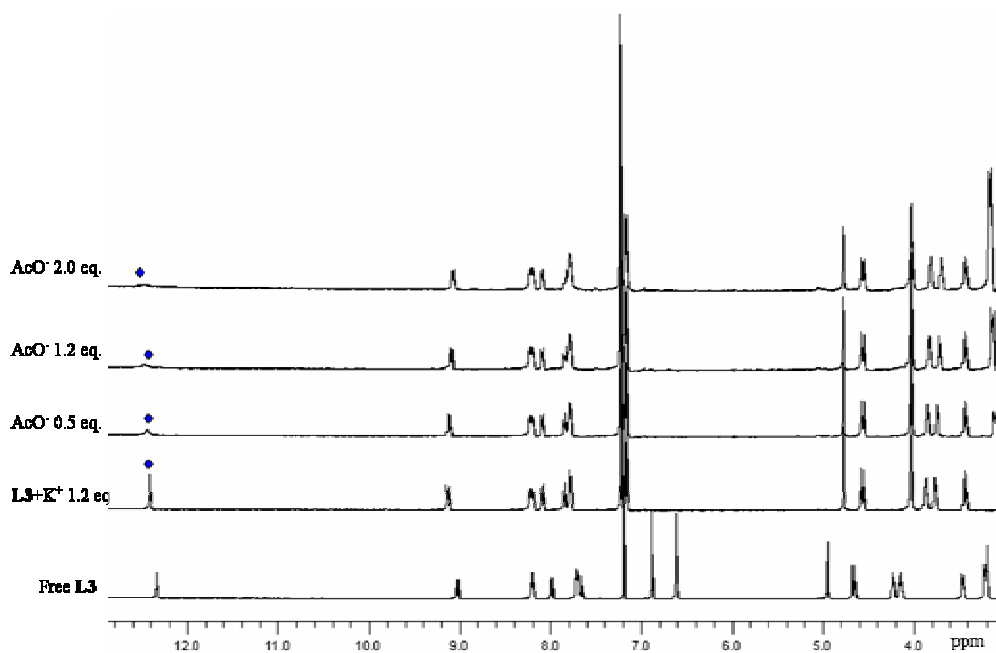


**Fig. 4.8**  $^1\text{H}$  NMR titration spectra of  $[\text{L3}\cdot\text{K}^+]$  on addition of TBAAcO in 5%  $\text{CH}_3\text{CN}/\text{CH}_2\text{Cl}_2$ . ♦ represents the NH amide protons.

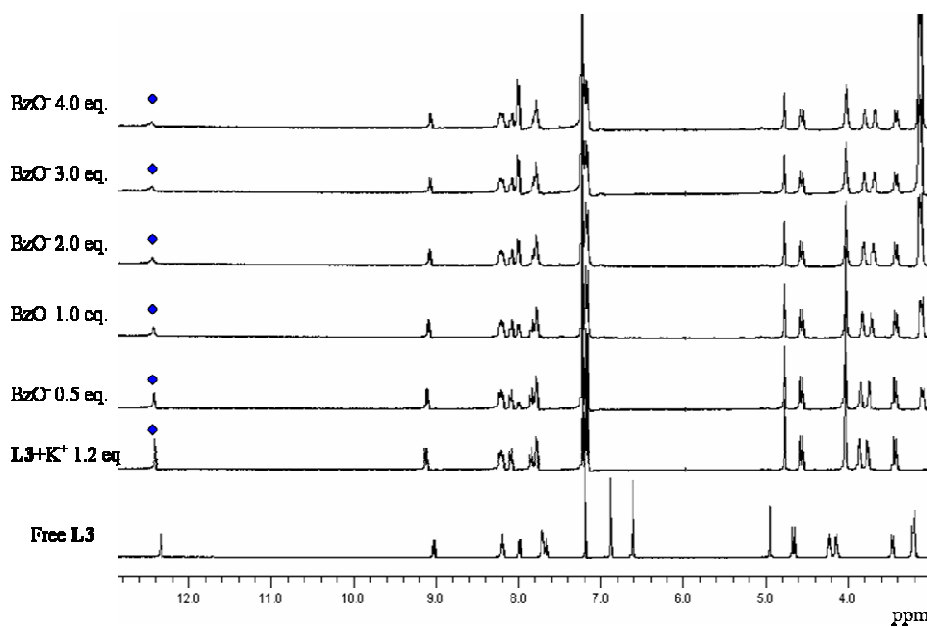


**Fig. 4.9**  $^1\text{H}$  NMR titration spectra of  $[\text{L3}\cdot\text{K}^+]$  on addition of TBABzO in 5% v/v  $\text{CD}_3\text{CN}$  in  $\text{CDCl}_3$ . ♦ represents the NH amide protons.

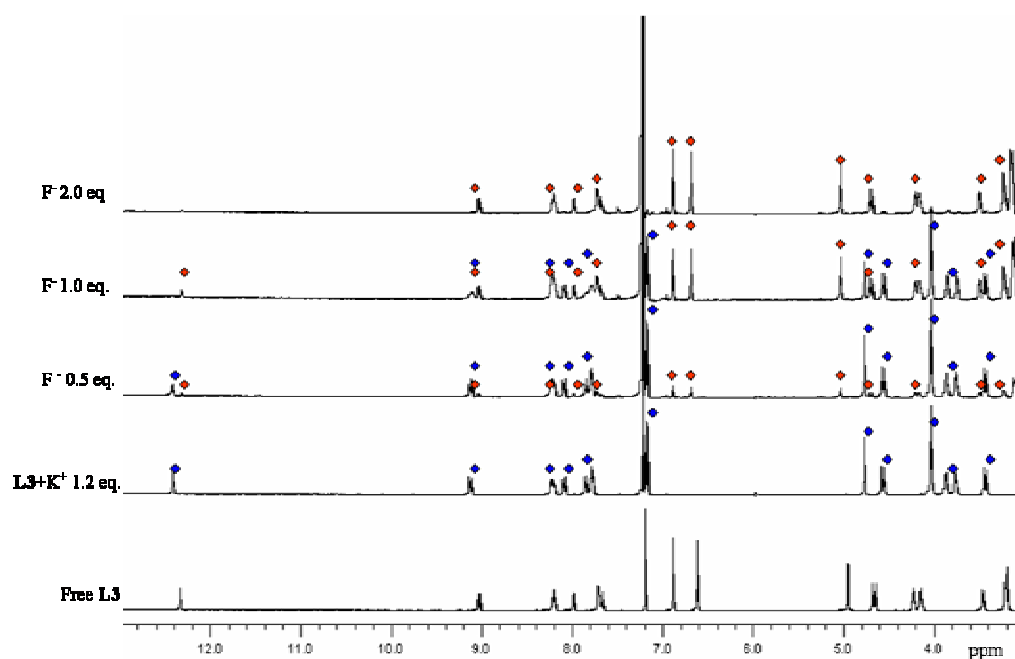


**Fig. 4.10**  $^1\text{H}$  NMR titration spectra of  $[\text{L3}\cdot\text{K}^+]$  on addition of  $\text{TBAF}\cdot 3\text{H}_2\text{O}$  5% v/v  $\text{CD}_3\text{CN}$  in  $\text{CDCl}_3$ . ♦ and ♦ represent cation complex and decomplex respectively.

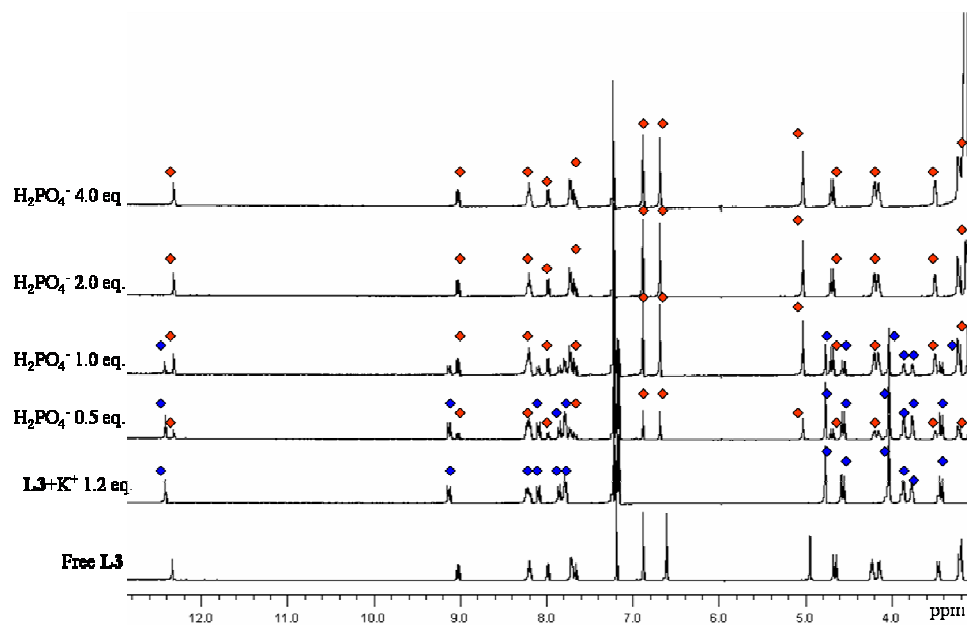


**Fig. 4.11**  $^1\text{H}$  NMR titration spectra of  $[\text{L3}\cdot\text{K}^+]$  on addition of  $\text{TBAH}_2\text{PO}_4$  5% v/v  $\text{CD}_3\text{CN}$  in  $\text{CDCl}_3$ . ♦ and ♦ represent cation complex and decomplex respectively.

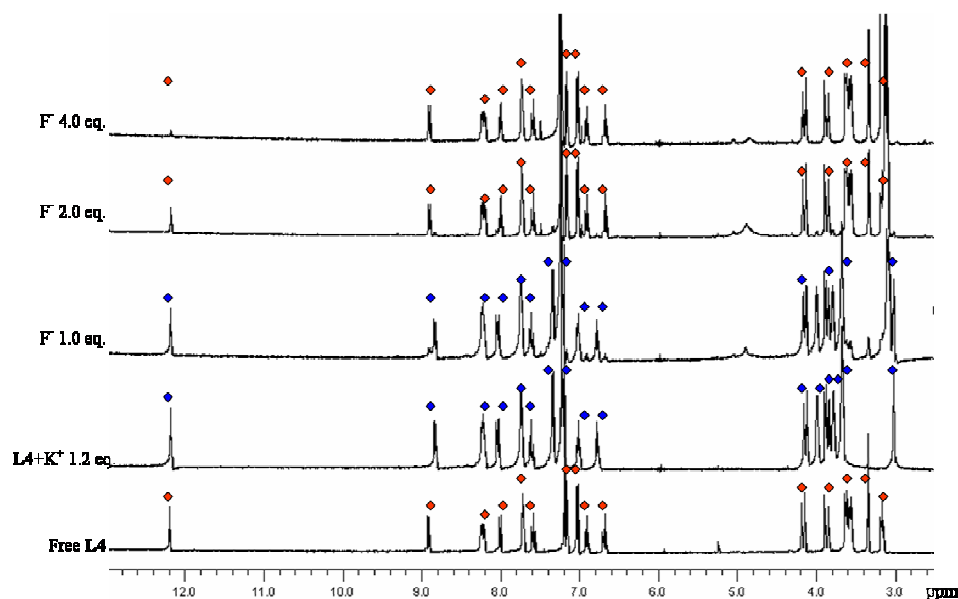


**Fig. 4.12**  $^1\text{H}$  NMR titration spectra of  $[\text{L4}\cdot\text{K}^+]$  on addition of  $\text{TBAF}\cdot 3\text{H}_2\text{O}$  in 5% v/v  $\text{CD}_3\text{CN}$  in  $\text{CDCl}_3$ . ◆ and ♦ represent cation complex and decomplex respectively.

### 4.3.3 Anion sensing abilities of receptors L3 and L4 using UV-visible spectrophotometry

#### 4.3.3.1 Anion sensing abilities of L3 and L4 in the absence of a cation

The anion sensing abilities of receptors **L3** and **L4** toward tetrabutylammonium anion salts ( $\text{F}^-$ ,  $\text{Cl}^-$ ,  $\text{Br}^-$ ,  $\text{I}^-$ ,  $\text{AcO}^-$ ,  $\text{BzO}^-$ ,  $\text{H}_2\text{PO}_4^-$ ) were investigated in  $\text{CH}_3\text{CN}$  solution using UV-vis spectrophotometry. Anion sensing abilities of these receptors were scanned by the addition of 100 equivalents of anions. Both receptors originally showed an absorption band at 400 nm which was ascribed to the  $\pi$ - $\pi^*$  transition of the chromophore [95]. The addition of fluoride ion produced a new absorption band at 500 nm (**Fig. 4.13 and 4.14**) and resulted in color change from pale yellow to pale orange after adding fluoride ion up to 100 equivalents, while other anions showed only insignificant decrease in an absorption band at 400 nm and did not cause any changes in color. The new absorption band corresponded to the charge transfer (CT) band between

the electron-rich amide-bound F<sup>-</sup> and the electron-deficient anthraquinone moieties [95, 96, 98, 100, 101]. It was obvious that these two receptors showed similar results.

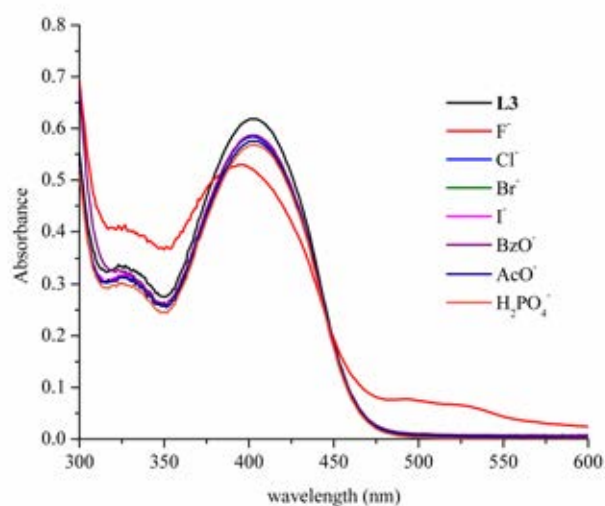


**Fig. 4.13** UV-visible spectra of L3 (50 μM) and various anions (100 equivalents) in CH<sub>3</sub>CN

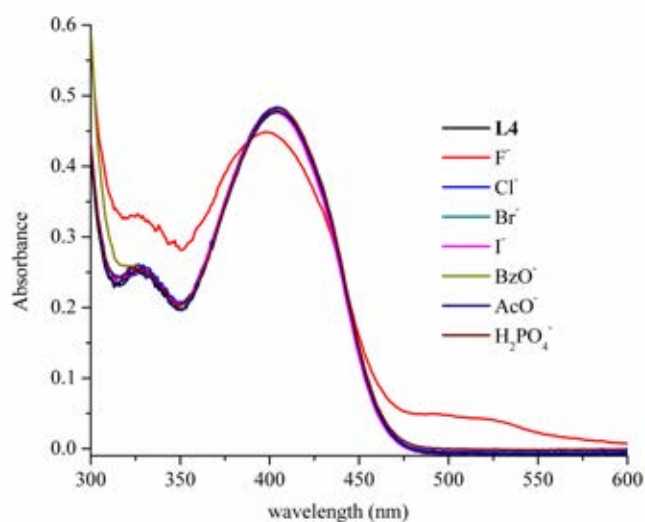


**Fig. 4.14** UV-visible spectra of L4 (50 μM) and various anions (100 equivalents) in CH<sub>3</sub>CN

#### 4.3.3.2 Anion sensing abilities of L3 and L4 in the presence of a cation

The UV-vis spectra of **L3** and **L4** with potassium ions displayed a slight hypsochromic shift of the absorption maximum (from 400 nm to 392 and 394 nm for **L3** and **L4** respectively) as shown in **Fig. 4.15** and **4.16**. This probably due to the preorganisation of the crown ether resulting in the decreasing in  $\pi$ -delocalization of nitrogen atom. Anion sensing abilities of receptors **L3** and **L4** in the presence of  $K^+$  were carried out by adding 1.2 equivalents of  $K^+$  (added as potassium hexafluorophosphate) to the solution of receptors.

Anion sensing abilities of **L3** and **L4** in the presence of  $K^+$  were also studied. Addition excess of anions (100 equivalents) to  $[L3 \cdot K^+]$  and  $[L4 \cdot K^+]$  solution was performed to access their anion sensing abilities in the presence of the electrostatic effect. Interestingly, after addition 100 equivalents of anions to  $[L3 \cdot K^+]$  solution, fluoride ion still gave the new charge transfer band at 500 nm as shown in **Fig. 4.17**. However, the intensity of the charge transfer band at 500 nm was distinctively increasing upon addition of fluoride ion into the solution of  $[L3 \cdot K^+]$  as shown in **Fig. 4.18**. In this case, at equal concentration of fluoride ion (same equivalents), the intensity of the charge transfer band was much higher than that of the free **L3** and fluoride ion as shown in **Fig 4.19**. Moreover, addition of only 10 equivalents of fluoride ion to the solution of  $[L3 \cdot K^+]$  solution caused a color change from pale yellow to orange as shown in **Fig. 4.18**, while the addition of the same equivalents of fluoride ion to the free receptor **L3** solution did not cause any changes in color. The result may stem from  $K^+$  residing in the crown ether cavity causing electrostatic interactions with  $F^-$  as well as cooperative hydrogen bonding interactions between  $F^-$  and the amide groups. Other anions caused no remarkable difference to  $\pi$ - $\pi^*$  transition or charge transfer bands in  $[L3 \cdot K^+]$  spectra.

The kind of interaction between  $[L3 \cdot K^+]$  and  $F^-$  was investigated. The addition of hydrogen-bond solvents such as ethanol into the solution of  $[L3 \cdot K^+]$  and  $F^-$  contributed to the recovery of the absorption band of  $[L3 \cdot K^+]$  as shown in **Fig. 4.20** [45]. This implied the competition between the proton solvent molecule and  $F^-$  for hydrogen-bond in **L3** [100]. Thus the interaction between  $[L3 \cdot K^+]$  and  $F^-$  tended to be the hydrogen bonding.

UV-visible studies of receptor **L4** showed similar results as the receptor **L3**. Addition of fluoride ion to  $[\mathbf{L4}\cdot\mathbf{K}^+]$  solution led to the increasing in the intensity of the charge transfer band at 500 nm compared to that of free receptor **L4**. However,  $\mathbf{K}^+$  did not lead to a remarkable increase in the band at 500 nm of  $[\mathbf{L4}\cdot\mathbf{K}^+]$  as much as the band found in the case of  $[\mathbf{L3}\cdot\mathbf{K}^+]$  as shown in **Fig. 4.21**.

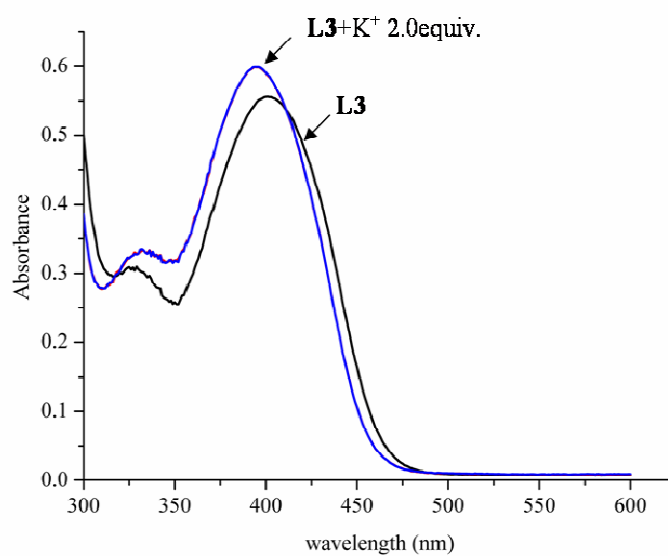


**Fig. 4.15** UV-visible spectra of **L3** (50  $\mu\text{M}$ ) and  $\text{KPF}_6$  in  $\text{CH}_3\text{CN}$

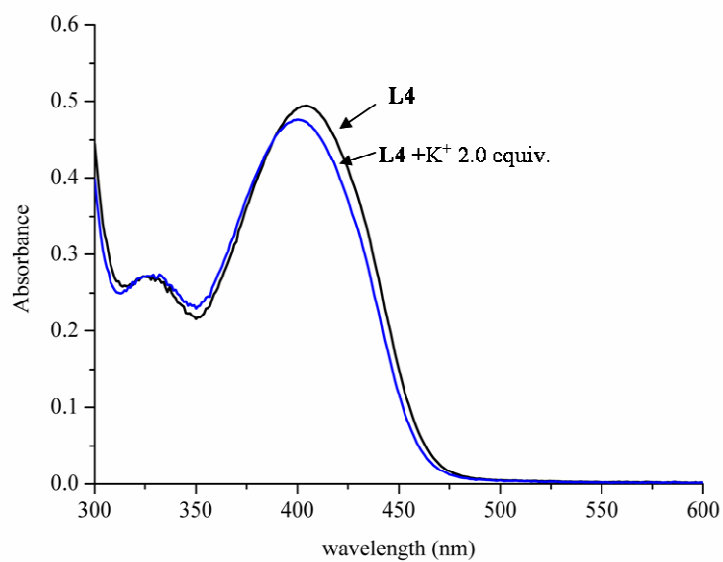


**Fig. 4.16** UV-visible spectra of **L4** (50  $\mu\text{M}$ ) and  $\text{KPF}_6$  in  $\text{CH}_3\text{CN}$

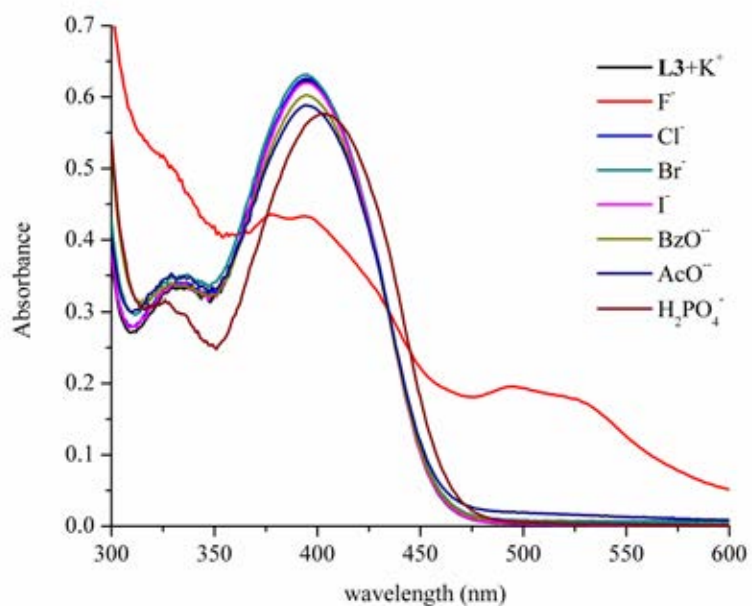


**Fig. 4.17** UV-visible spectra of  $[\text{L3}\cdot\text{K}^+]$  (50  $\mu\text{M}$ ) and various anions (100 equivalents) in  $\text{CH}_3\text{CN}$ .



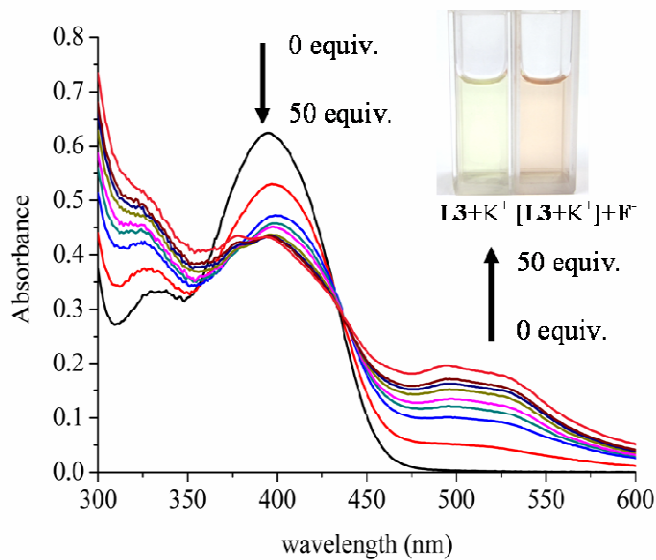


**Fig. 4.18** UV- vis titration spectra of  $[L3 \cdot K^+]$  ( $50 \mu\text{M}$ ) upon addition of  $\text{TBAF} \cdot 3\text{H}_2\text{O}$  (0-50 equivalents) in  $\text{CH}_3\text{CN}$ .

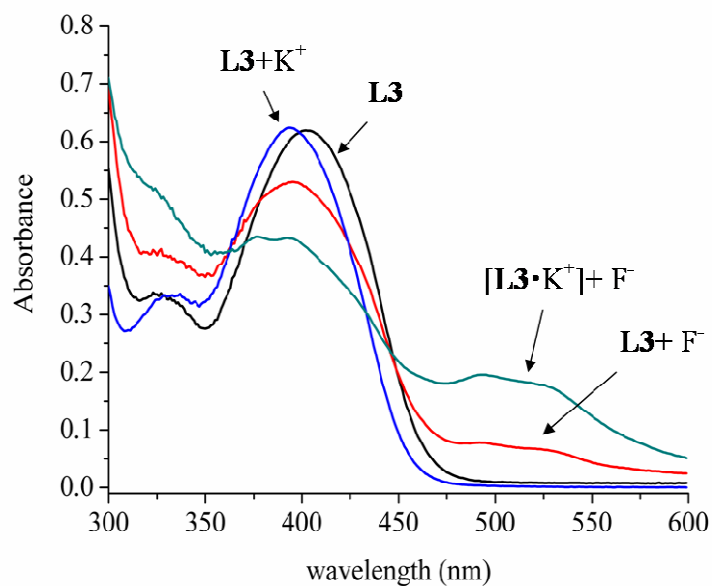


**Fig. 4.19** UV- vis spectra of  $L3$  ( $50 \mu\text{M}$ ) and  $\text{TBAF} \cdot 3\text{H}_2\text{O}$  (50 equiv.) in the absence (red spectrum) and presence (green spectrum) of  $\text{KPF}_6$  (1.2 equiv.) in  $\text{CH}_3\text{CN}$ .

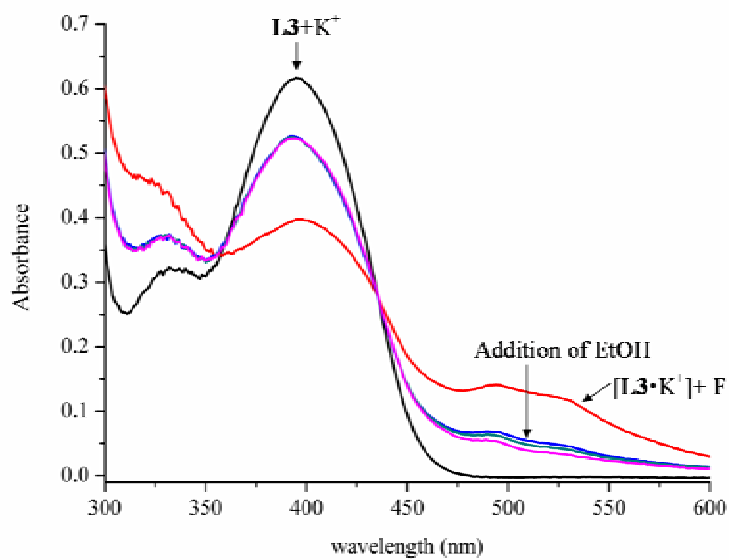


**Fig. 4.20** UV-vis spectra of  $L3$  ( $50 \mu M$ )+ $K^+$  (1.2 eq) and  $F^-$  (100 equiv.) (red line) in  $CH_3CN$  upon addition various amount of EtOH (blue-pink line).

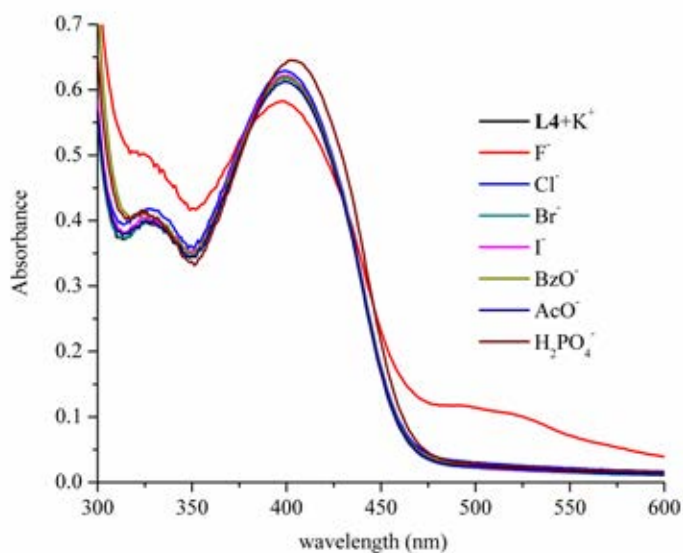


**Fig. 4.21** UV-visible spectra of  $[L4 \cdot K^+]$  ( $50 \mu M$ ) and various anions (100 equivalents) in  $CH_3CN$ .

#### 4.3.4 Anion sensing abilities of receptors **L3** and **L4** using fluorescence spectrophotometry

Since previous studies of anthraquinone derivatives revealed that anthraquinone can show excited-state intramolecular proton transfer (ESIPT) as dual fluorescence emission: short-wavelength emission (SWE) band around 520 nm for the normal structure and long wavelength emission (LWE) around 560 nm for the tautomer structure [95, 101]. The properties of receptors **L3** and **L4** to show ESIPT can be tested by changing the solvent polarity or donicity (DMSO, CH<sub>3</sub>CN, CHCl<sub>3</sub>, toluene and ethanol) in fluorescence experiments. If the solvents can form hydrogen bond with hydrogen donor of anthraquinone, ESIPT process will be inhibited [101]. It was found that both receptors displayed only the SWE band around 520 nm in all solvents indicating no ESIPT proceeded in free receptors.

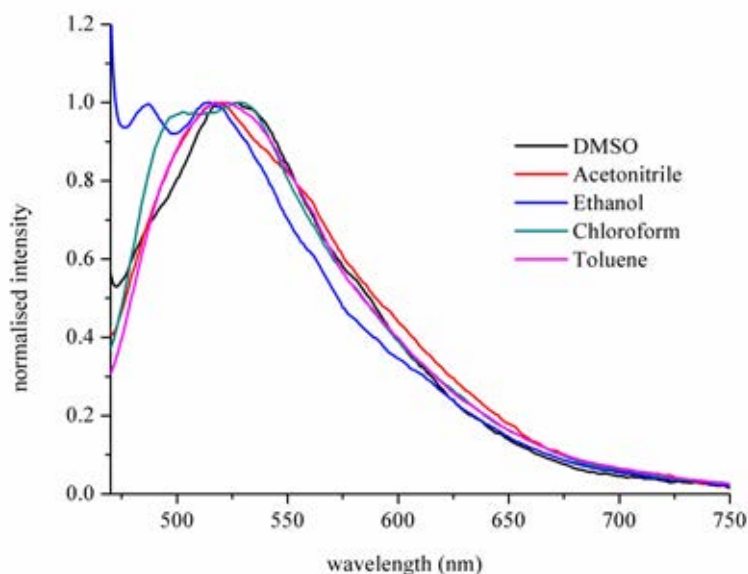


**Fig. 4.22** Normalized fluorescence emission spectra spectra of (a) **L3** (50 μM) in various solvents.

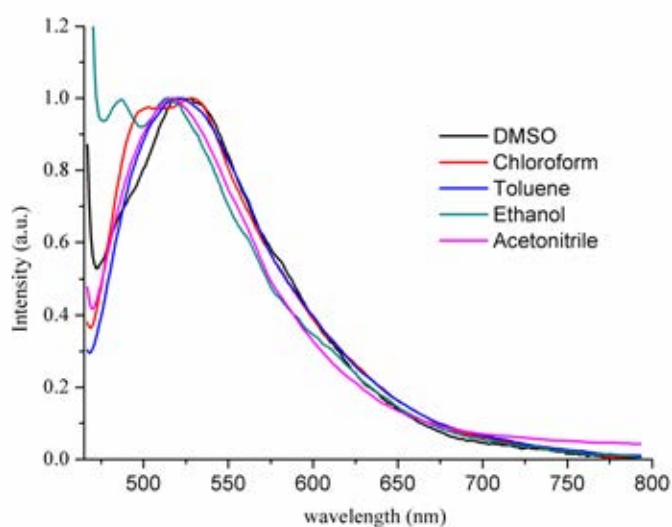


**Fig. 4.23** Normalized fluorescence emission spectra spectra of **L4** (50  $\mu\text{M}$ ) in various solvents.

#### 4.3.4.1 Anion sensing abilities of **L3** and **L4** in the absence of cation

Anion sensing abilities of receptors **L3** and **L4** were studied in  $\text{CH}_3\text{CN}$  using fluorescence spectrophotometry. Excess of various anions ( $\text{F}^-$ ,  $\text{Cl}^-$ ,  $\text{Br}^-$ ,  $\text{I}^-$ ,  $\text{AcO}^-$ ,  $\text{BzO}^-$ ,  $\text{H}_2\text{PO}_4^-$ ) was added to the solution of the receptors. Receptor **L3** and **L4** showed a weak emission maximum at 520 nm. It was found that receptor **L3** showed high selectivity with fluoride ion. Addition of other anions to the solution of receptor **L3** led to only insignificant increase in the intensities of the emission spectra as shown in **Fig. 4.24**. Upon gradual addition of fluoride ion, the intensity of fluorescence titration emission spectra were gradually increased. Moreover, the emission maxima were shifted to 542 nm as shown in **Fig. 4.25**. Similarly, receptor **L4** showed the highest sensitivity with fluoride ions as shown in **Fig. 4.26** Gradual addition of fluoride ion gave higher intensities of emission spectra at 528 nm with a shoulder at 560 nm as shown in **Fig. 4.27**. The high selectivity of **L3** and **L4** with  $\text{F}^-$  is probably due to the formation of intramolecular hydrogen-bonds between NH and F which promoted the delocalization of  $\pi$ -electrons through the 1-aminoantraquinone [46].

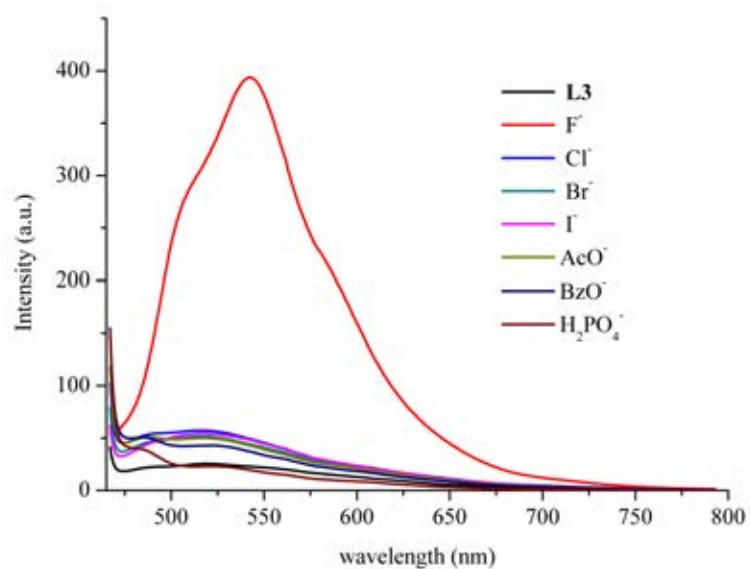


**Fig. 4.24** Fluorescence spectra of **L3** (50  $\mu$ M) in CH<sub>3</sub>CN in the presence of 100 equiv. of TBA salts of various anions (F<sup>-</sup>, Cl<sup>-</sup>, Br<sup>-</sup>, I<sup>-</sup>, AcO<sup>-</sup>, BzO<sup>-</sup>, H<sub>2</sub>PO<sub>4</sub><sup>-</sup>).

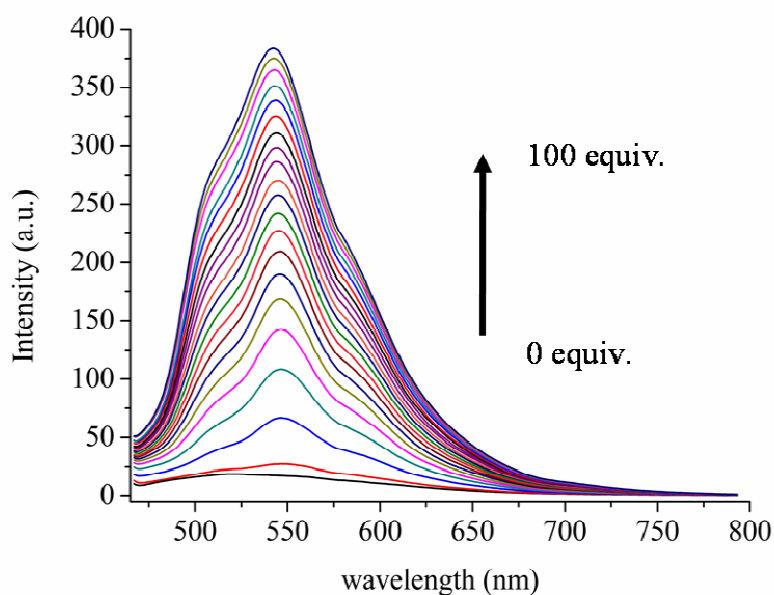


**Fig. 4.25** Fluorescence titration emission spectra of **L3** (50  $\mu$ M) upon gradual addition of TBAF·3H<sub>2</sub>O in CH<sub>3</sub>CN from 0 to 100 equiv.

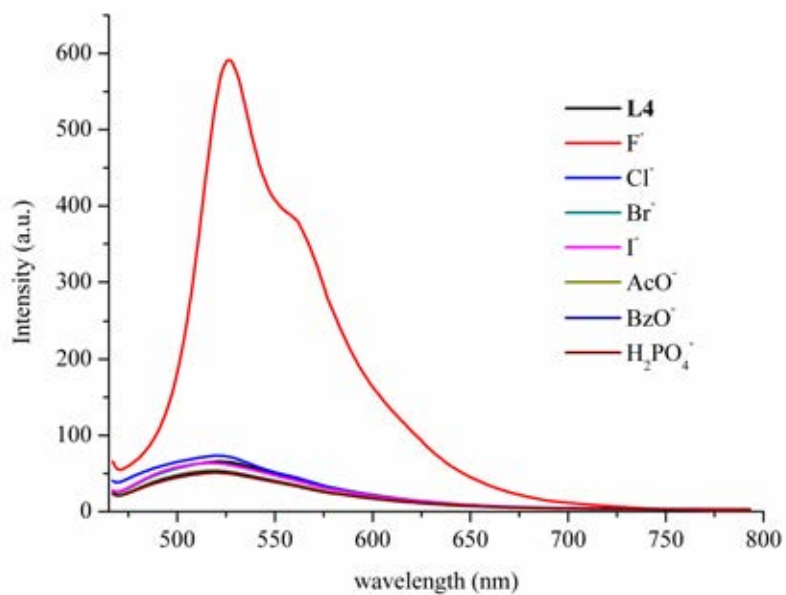


**Fig. 4.26** Fluorescence spectra of **L4** (50 μM) in CH<sub>3</sub>CN in the presence of 100 equiv. of TBA salts of various anions (F<sup>-</sup>, Cl<sup>-</sup>, Br<sup>-</sup>, I<sup>-</sup>, AcO<sup>-</sup>, BzO<sup>-</sup>, H<sub>2</sub>PO<sub>4</sub><sup>-</sup>).

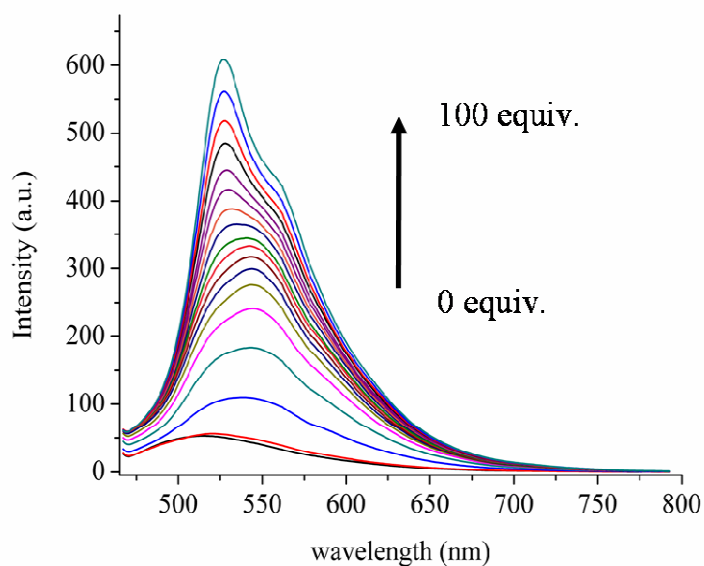


**Fig. 4.27** Fluorescence titration emission spectra of **L4** (50 μM) upon gradual addition of TBAF·3H<sub>2</sub>O in CH<sub>3</sub>CN from 0 to 100 equiv.  $\lambda_{\text{ex}}$  at 450 nm.

#### 4.3.4.2 Cation sensing abilities of L3 and L4

Cation sensing abilities of **L3** and **L4** were examined in  $\text{CH}_3\text{CN}$ . The enhancement of the intensities of fluorescence emission spectra at 520 nm was observed upon gradual addition of  $\text{KPF}_6$  to the solution of the receptors **L3** and **L4** as shown in **Fig. 4.28** and **4.29**. Addition of the  $\text{KPF}_6$  1.2 equivalents led to the saturation of emission spectra for both receptors.

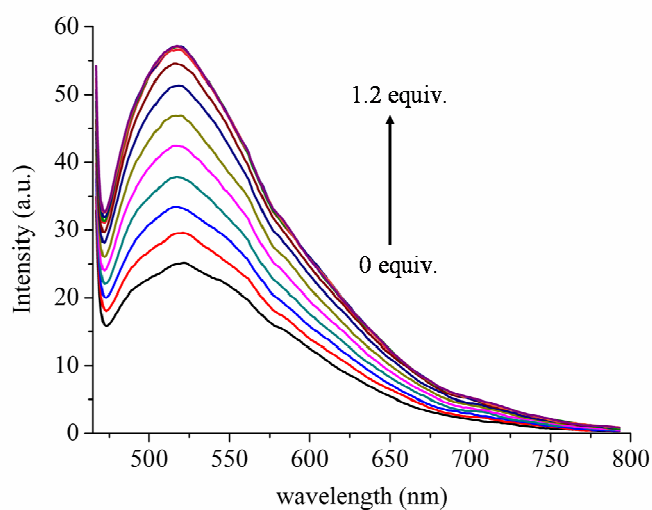


**Fig. 4.28** Fluorescence titration emission spectra of **L4** (50  $\mu\text{M}$ ) upon gradual addition of  $\text{KPF}_6$  in  $\text{CH}_3\text{CN}$  from 0 to 100 equiv.

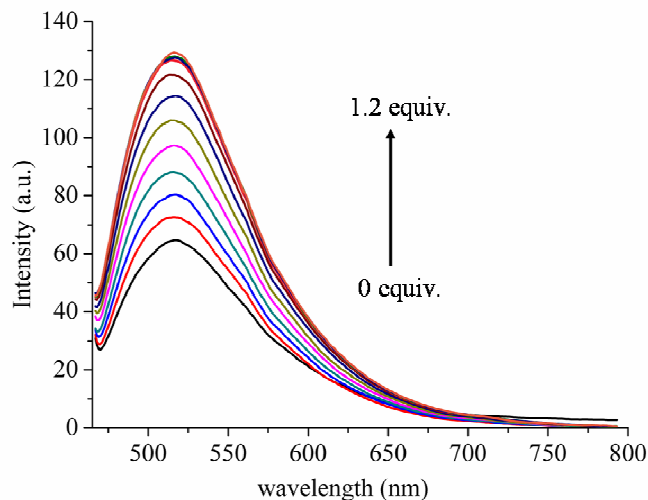


**Fig. 4.29** Fluorescence titration emission spectra of **L4** (50  $\mu\text{M}$ ) upon gradual addition of  $\text{KPF}_6$  in  $\text{CH}_3\text{CN}$  from 0 to 100 equiv.  $\lambda_{\text{ex}}$  at 450 nm.

#### 4.3.4.3 Anion sensing abilities of **L3** and **L4** in the presence of a cation

To study the influence of electrostatic effect from a cation to the photophysical properties of the receptors, 1.2 equivalents of  $\text{KPF}_6$  were added to the solution of the receptors before their anion sensing abilities were tested. Interestingly, addition of excess anions to the solution of cation complex of the receptor **L3** and **L4** led to dissimilar results. In the presence of 1.2 equivalents of  $\text{K}^+$ ,  $[\text{L3}\cdot\text{K}^+]$  still showed high selectivity with  $\text{F}^-$  over other anions. Gradual addition of fluoride ion gave higher intensities of emission spectra at 542 nm as shown in **Fig. 4.30**. However, compared to the spectrum of **L3**, the  $[\text{L3}\cdot\text{K}^+]$  spectrum showed around two-fold higher intensity in the presence of equal equivalents of added fluoride ion as shown in **Fig. 4.31**. This phenomenon was similar to the previous study reported by Senthivelan et al. A ditopic calix[4] arene receptor with naphthalene pendants showed further enhancement of its fluorescence intensity upon complexation with acetate or fluoride ions in the presence of  $\text{Cu(I)}$  [46]. In contrast, receptor **L4** showed lower sensitivity towards  $\text{F}^-$  in the presence of  $\text{K}^+$  as shown in **Fig 4.32**. However, receptor **L4** still displayed the highest selectivity with fluoride ion.



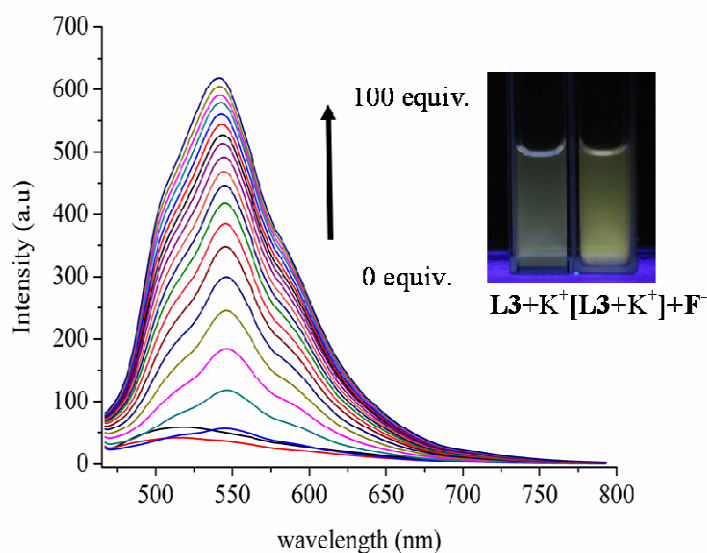


**Fig. 4.30** Fluorescence titration emission spectra of **L3** (50  $\mu\text{M}$ ) +  $\text{KPF}_6$  (1.2 equiv.) upon gradual addition of  $\text{TBAF}\cdot 3\text{H}_2\text{O}$  in  $\text{CH}_3\text{CN}$  from 0 to 100 equiv.  $\lambda_{\text{ex}}$  at 450 nm.

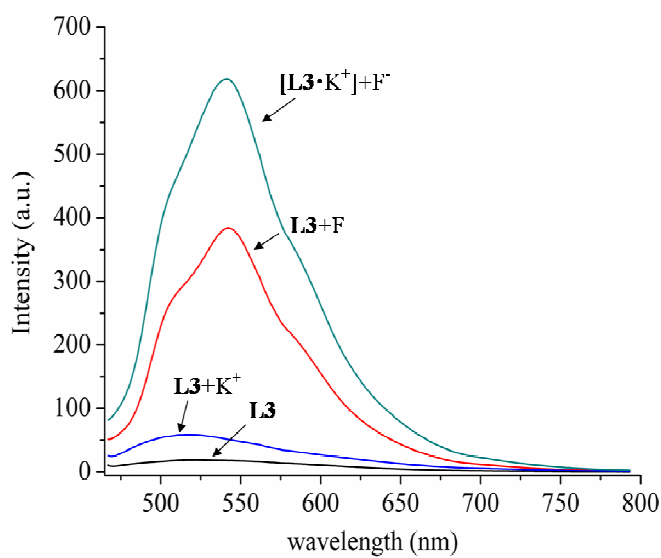


**Fig. 4.31** Fluorescence emission spectra of **L3** (50  $\mu\text{M}$ ) and  $\text{TBAF}\cdot 3\text{H}_2\text{O}$  (100 equiv.) in the absence (red spectrum) and presence (green spectrum) of  $\text{KPF}_6$  (1.2 equiv.) in  $\text{CH}_3\text{CN}$ .

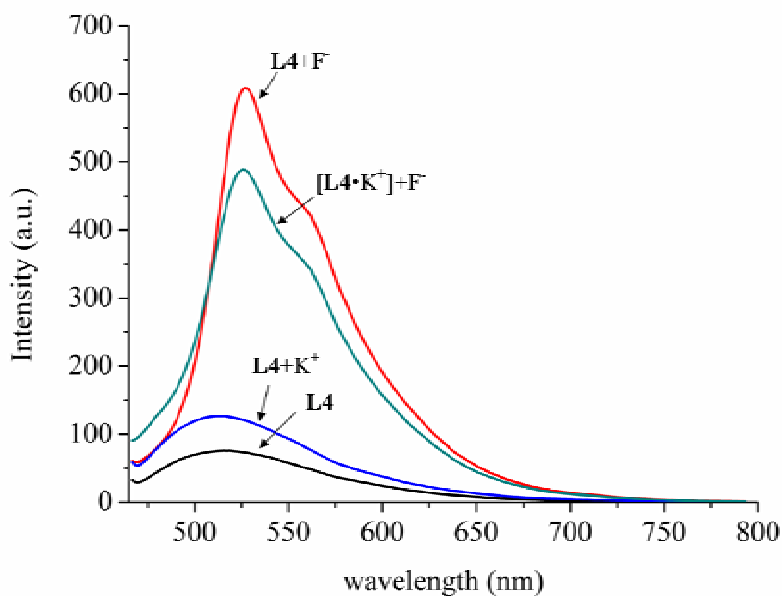


**Fig. 4.32** Fluorescence emission spectra of **L4** (50  $\mu\text{M}$ ) and TBAF $\cdot$ 3H $_2$ O (100 equiv.) in the absence (red spectrum) and presence (green spectrum) of KPF $_6$  (1.2 equiv.) in CH $_3$ CN.

The binding constants between receptors **L3** and **L4** with fluoride ion in the presence and in the absence of potassium ion were calculated using SPECFIT32 software and listed in **Table 4.2**. It was found that the association constant value for [**L3** $\cdot$ K $^+$ ] and F $^-$  was higher than that of free **1** and F $^-$ . Data fitting and refining suggested that receptor **L3** and [**L3** $\cdot$ K $^+$ ] bind F $^-$  in two stepwise fashions, a 1:1 following by a 1:2 fashion, while receptor **L4** forms a 1:1 complex with F $^-$ . Unfortunately, the association constant between [**L4** $\cdot$ K $^+$ ] and F $^-$  can not be calculated possibly due to the abstraction of K $^+$  by F $^-$  leading to the fluctuation of emission spectra and the lower in their intensities.

Therefore, the binding constants were considered to confirm that K $^+$  played a key role in the sensitivity of **L3** with F $^-$ . The results implied that K $^+$  residing in the crown ether of **L3** supported the formation of intermolecular H-bonds between the amide protons and F $^-$  ions resulting in promoting the delocalization  $\pi$ -electrons through the anthraquinone moiety and causing changes in  $\pi$ - $\pi^*$  transition with a fluorescence color

change from pale yellow to bright yellow as shown in **Fig. 4.30**. On the other hand,  $K^+$  bound in 1,3-alternate conformation of **L4** can not facilitate the cooperative effect with  $F^-$ . This is probably due to the topology of the ligand producing a long distance between crown ether and amide group, and reducing electrostatic interactions between  $K^+$  and  $F^-$ . The proposed binding modes in photophysical studies of **L3** and **L4** were shown in **Fig. 4.33** and **4.34**.

**Table 4.2** Association Constants for receptors **L3** and **L4** with  $F^-$  in the presence and in the absence of cation.

Receptor + anion	Binding constants	
	$\log K_1$	$\log K_2$
<b>L3</b> + $F^-$	$2.94 \pm 0.04$	$4.50 \pm 0.03$
<b>[L3·K<sup>+</sup>]</b> + $F^-$	$3.39 \pm 0.12$	$6.25 \pm 0.05$
<b>L4</b> + $F^-$	$3.77 \pm 0.14$	-
<b>[L4·K<sup>+</sup>]</b> + $F^-$	a	a

<sup>a</sup> cannot be calculated due to the abstraction of  $K^+$  by  $F^-$ .

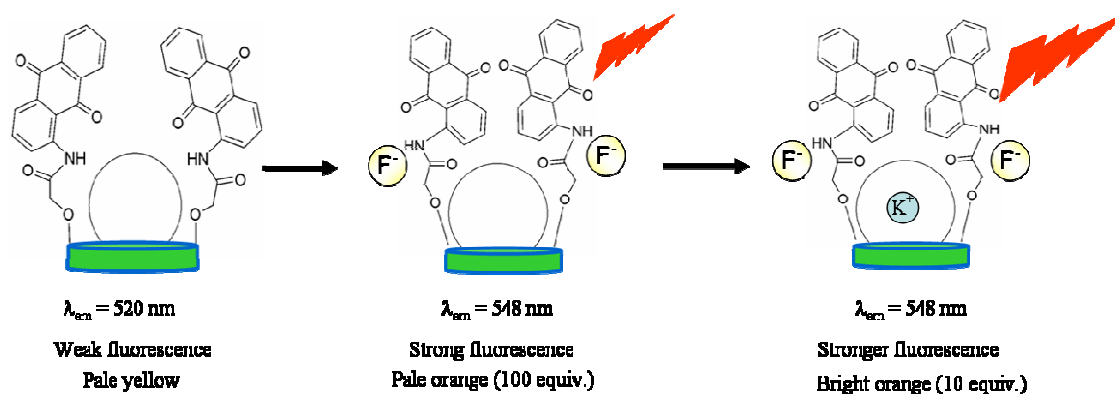


**Fig. 4.33** Propose binding mode of **L3** in photophysical studies.

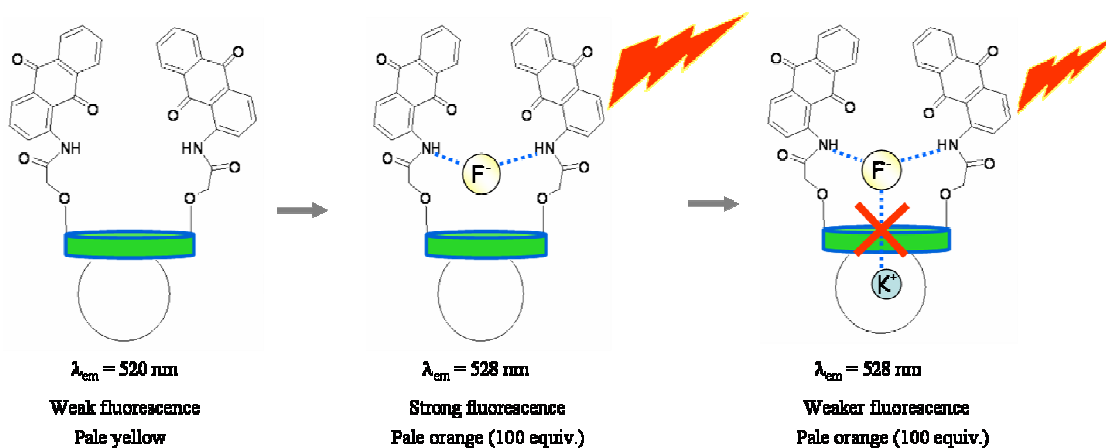


Fig. 4.34 Propose binding mode of L4 in photophysical studies.

### 4.3.5 Electrochemical studies of L3 and L4 with anions using cyclic voltammetry

#### 4.3.5.1 Electrochemical properties of receptors L3 and L4

Since anthraquinone moieties of receptors **L3** and **L4** can be reduced to give mono- and dianion by two steps of reduction. The binding abilities of these receptors can be investigated by electrochemical method. We have investigated the electrochemical response of the synthetic heteroditopic receptors **L3** and **L4** towards anions in the absence and presence of alkali metal cations by cyclic voltammetry (CV). Perturbation of the charge in a redox-active host can result in increased or decreased binding affinity and lead to different half-wave potentials.

The cyclic voltammetry was performed in solutions of **L3** and **L4** ( $1 \times 10^{-3} \text{ M}$ ) in 40%  $\text{CH}_3\text{CN}$  v/v in  $\text{CH}_2\text{Cl}_2$  with 0.1 M  $\text{TBAPF}_6$  as a supporting electrolyte. The system contained three electrodes which are a Carbon working electrode, a  $\text{Ag}/\text{Ag}^+$  reference electrode and a Pt coil counter electrode. All solutions were purged with  $\text{N}_2$  before measurements. The potential was scanned in the range of 0 to -2 V at a scan rate of 50 mV/s. From Fig. 4.35, receptors **L3** and **L4** showed two consecutive one-electron reversible waves in 40%  $\text{CH}_3\text{CN}$  v/v in  $\text{CH}_2\text{Cl}_2$ , corresponding to two single-electron reductions to give mono- (wave I) and dianions (wave II) respectively [104, 105]. The

electrochemical data of receptors **L3** and **L4** was presented in **Table 4.3**. Concerning the half-wave potentials for receptors **L3**, it was observed that the reduction redox potentials for waves I and II of receptor **L3** shifted towards less negative potentials. This means the energy required to reduce the neutral quinones of receptor **L3** was less than receptor **L4** [105]. This result may stem from the more stabilization of the radical anions through the intramolecular hydrogen bonding between the NH amide proton and the crown ether of receptor **L3**.

Cyclic voltammograms of receptor **L3** and **L4** at various scan rates with 0.1 M TBAPF<sub>6</sub> in 40% CH<sub>3</sub>CN v/v in CH<sub>2</sub>Cl<sub>2</sub> were presented in **Fig. 4.36**. Upon increasing the scan rates, the half wave potentials of both receptors ( $E_{1/2I}$  and  $E_{1/2II}$ ) shifted to more negative potentials. That meant more energies were required to reduced anthraquinone [104, 105]. Thus, the redox process of these receptors depended on the scan rate. However, these cyclic voltammograms still exhibited both reduction and oxidation waves which implied that no self-protonation reaction (keto-enol process) intervened their redox reactions [104, 105]. In addition, the correlation between current ( $I_p$ ) and square root of scan rate ( $v^{1/2}$ ) of receptors **L3** and **L4** were shown in **Fig. 4.37** and **4.38**, respectively. It was found that the proportion of  $I_p$  and  $v^{1/2}$  displayed the non-diffusion system due to the linear lines did not pass through the origin.

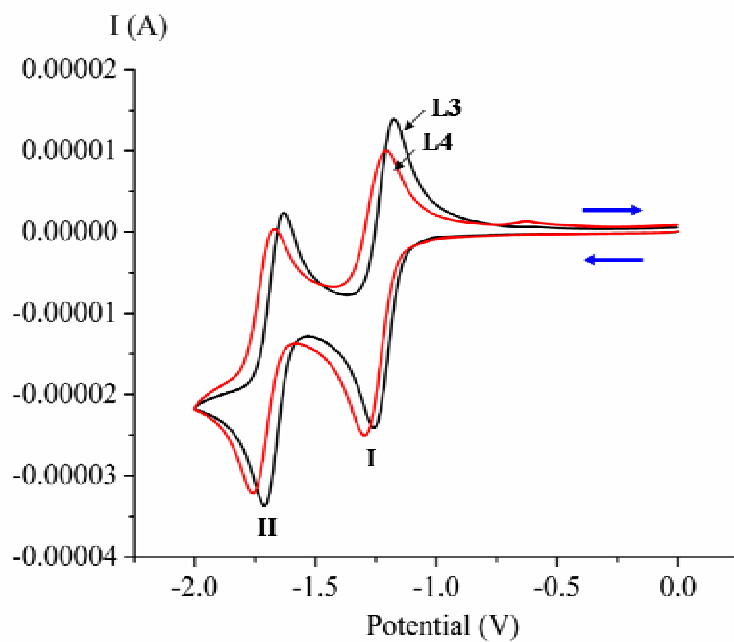
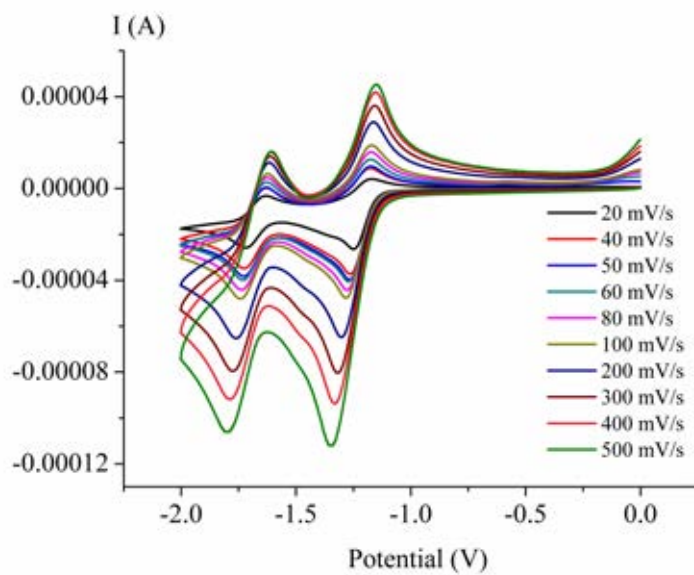


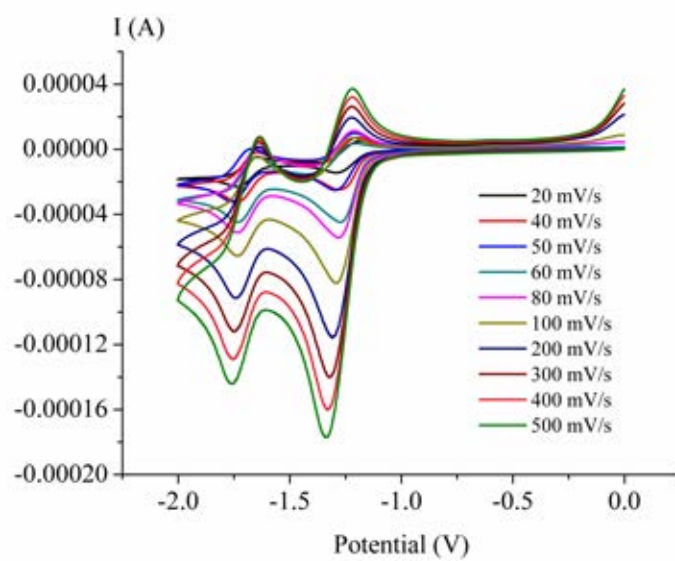
**Fig. 4.35** Cyclic voltammograms of **L3** (1 mM) and **L4** (1 mM) in 40% CH<sub>3</sub>CN v/v in CH<sub>2</sub>Cl<sub>2</sub> with 0.1 M TBAPF<sub>6</sub> at scan rate 50 mV/s. Horizontal arrows represent the scan direction.

**Table 4.3** Half wave potentials of receptors **L3** and **L4** in 40% CH<sub>3</sub>CN v/v in CH<sub>2</sub>Cl<sub>2</sub> with 0.1 M TBAPF<sub>6</sub> at scan rate 50 mV/s.

Receptors	E <sub>1/2</sub> I	E <sub>1/2</sub> II
<b>L3</b>	-1.21	-1.25
<b>L4</b>	-1.66	-1.71

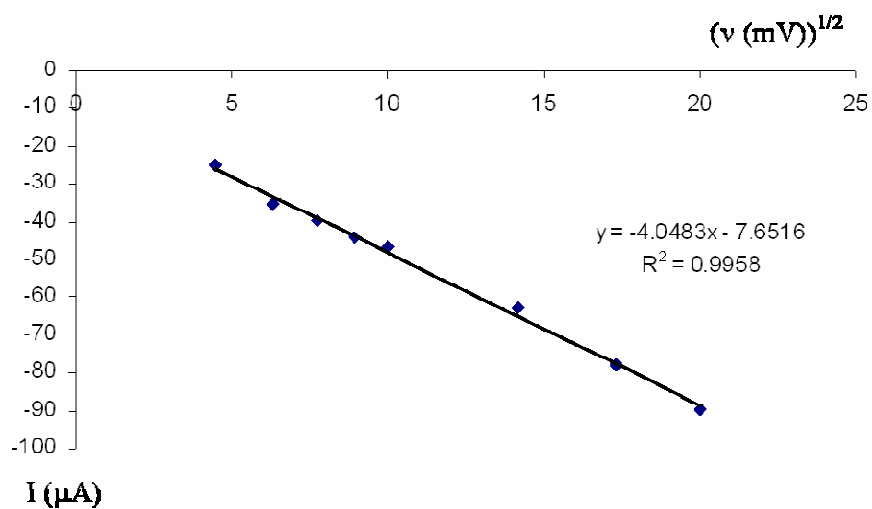


(a)

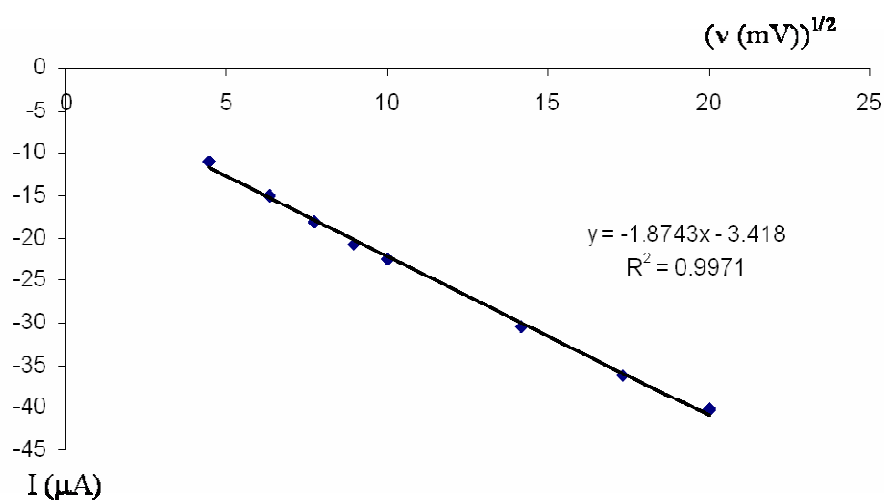


(b)

**Fig. 4.36** Cyclic voltammograms of receptors (a) **L3** and (b) **L4** in 40%  $\text{CH}_3\text{CN}$  v/v in  $\text{CH}_2\text{Cl}_2$  with 0.1 M  $\text{TBAPF}_6$  at various scan rates.



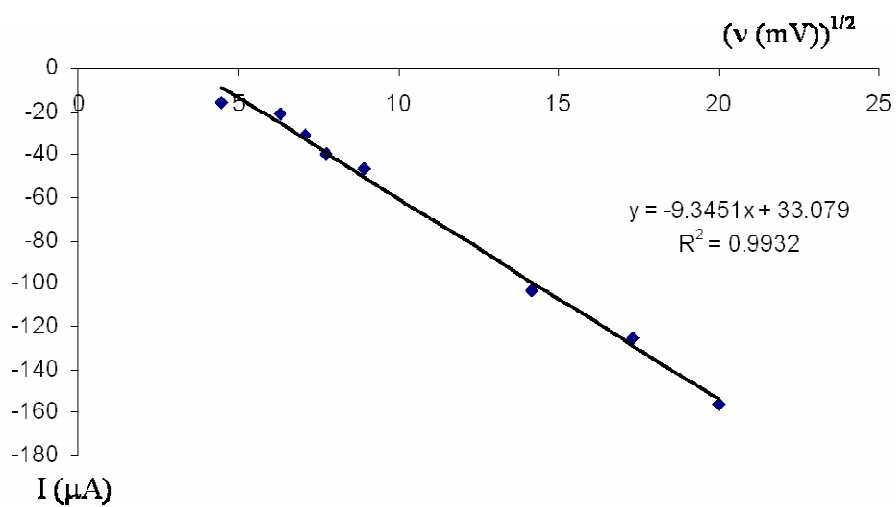
(a)



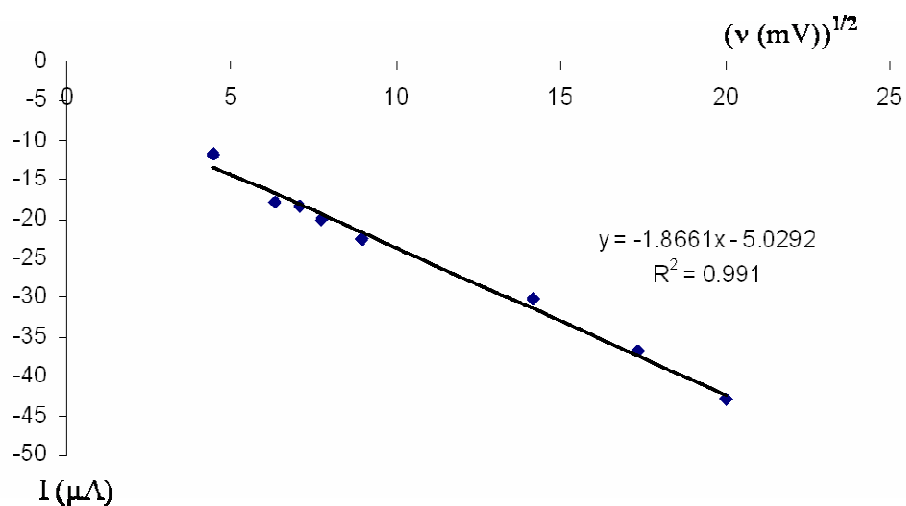
(b)

**Fig. 4.37** Graphs plotted between square root of various scanrates in cyclic voltammetry experiments and current of reduction waves of **L3** (a)  $I_{pcI}$  and (b)  $I_{pcII}$ .





(a)



(b)

**Fig. 4.38** Graphs plotted between square root of various scan rates in cyclic voltammetry experiments and current of reduction waves of **L4** (a)  $I_{pcI}$  and (b)  $I_{pcII}$ .

#### 4.3.5.2 Electrochemical studies of receptors **L3** and **L4** towards anions

Electrochemical studies of receptors **L3** and **L4** and anions were investigated in 40% CH<sub>3</sub>CN v/v in CH<sub>2</sub>Cl<sub>2</sub> with 0.1 M TBAPF<sub>6</sub> at scan rate 50 mV by addition various anions 0-10 equivalents (F<sup>-</sup>, Cl<sup>-</sup>, Br<sup>-</sup>, I<sup>-</sup>, AcO<sup>-</sup>, BzO<sup>-</sup>, H<sub>2</sub>PO<sub>4</sub><sup>-</sup>) into the solution of the receptors before each scan. Half wave potential difference between an anion complex and a receptor was used as a parameter for detecting the alteration during the redox process. If the half wave potential different is a positive value, that means the complex is easier to reduce indicating the stabilization of reduced anthraquinone. On the contrary, if the half wave potential different is a negative value, that means the complex is harder to reduce indicating the destabilization of reduced anthraquinone as simply presented in **Fig. 4.39**. Electrochemical data of this study was presented in **Table 4.4**. The results showed that all anions contributed to positive values of half wave potential difference for receptors **L3** and **L4**. Anion complexes caused both reduction waves shifted to the less negative potentials. Interestingly, upon addition of 10 equiv. of H<sub>2</sub>PO<sub>4</sub><sup>-</sup> into the solution of the receptors, wave II of both two receptors was shifted remarkably toward less negative potentials as shown in **Table 4.4** and **Fig. 4.40-4.41**. Conversely, addition of other anions to the solution of receptors resulted in only insignificant change in reduction potentials of wave I and II. As has been previously proposed, the larger negative potential shift of wave II was rationalized from the stabilization of dianions of anthraquinone formed during reduction process by the effect of the intermolecular hydrogen bonding interactions between hosts and guests [104, 105]. Thus, it implied that H<sub>2</sub>PO<sub>4</sub><sup>-</sup> can form strong hydrogen bonding with amide protons of both receptors **L3** and **L4** leading to the stabilization of dianion anthraquinone. On the other hand, small perturbation in reduction potentials of other anions was probably from the weak intermolecular hydrogen bonding between the receptors and these anions. It should be noted that in the absence of a cation, both receptors **L3** and **L4** showed very similar electrochemical behaviors towards anions.

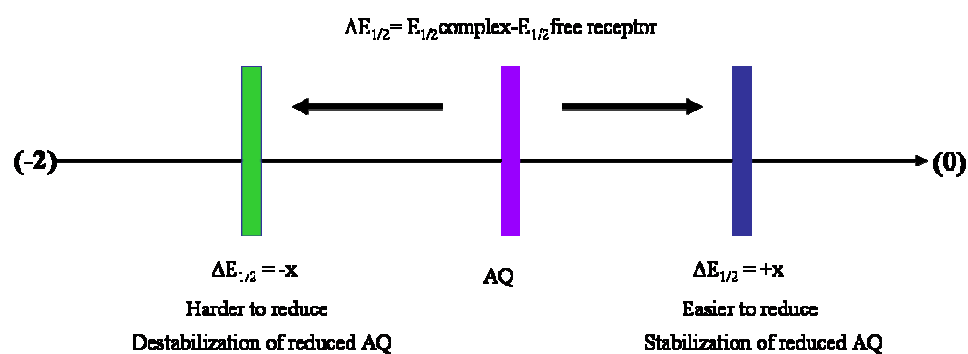


**Fig. 4.39** Half wave potential differences of anthraquinone (AQ).

**Table 4.4** The changes in reduction potentials (mV) of receptors **L3** and **L4** at 50 mV/s after addition of various anions (10 equiv.).

Anions	Receptors			
	<b>L3</b>		<b>L4</b>	
	$\Delta E_{1/2}$ (I)	$\Delta E_{1/2}$ (II)	$\Delta E_{1/2}$ (I)	$\Delta E_{1/2}$ (II)
F <sup>-</sup>	15	25	50	35
Cl <sup>-</sup>	20	15	25	30
Br <sup>-</sup>	0	20	30	5
I <sup>-</sup>	15	10	40	30
AcO <sup>-</sup>	15	10	40	30
BzO <sup>-</sup>	25	5	40	45
H <sub>2</sub> PO <sub>4</sub> <sup>-</sup>	5	195	20	215

$$\Delta E_{1/2} = E_{1/2}^{\text{anion cpx}} - E_{1/2}^{\text{free receptor}}$$

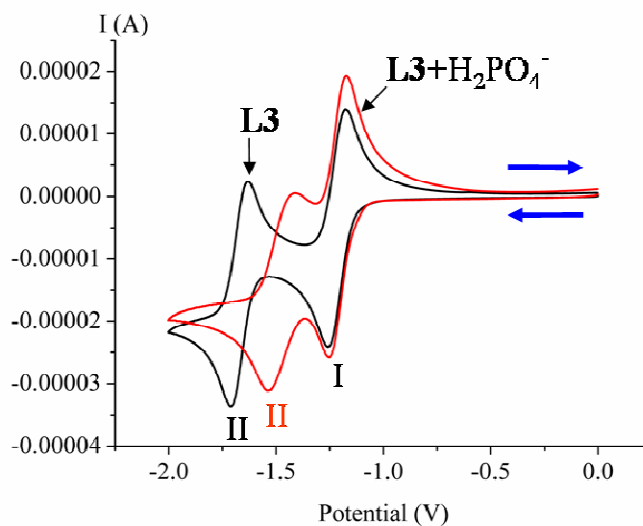


**Fig. 4.40** Cyclic voltammograms of receptor (a) **L3** (1 mM) and  $\text{H}_2\text{PO}_4^-$  in 40%  $\text{CH}_3\text{CN}$  v/v in  $\text{CH}_2\text{Cl}_2$  with 0.1 M  $\text{TBAPF}_6$  at scan rate 50 mV/s. Blue arrows represent scanned direction.

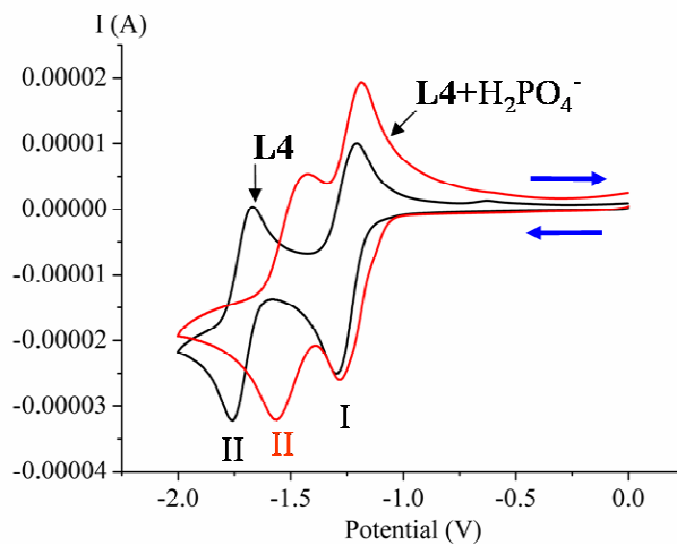


**Fig. 4.41** Cyclic voltammograms of receptor **L4** (1 mM) and  $\text{H}_2\text{PO}_4^-$  in 40%  $\text{CH}_3\text{CN}$  v/v in  $\text{CH}_2\text{Cl}_2$  with 0.1 M  $\text{TBAPF}_6$  at scan rate 50 mV/s. Blue arrows represent scanned direction.

#### 4.3.5.3 Electrochemical studies of receptors **L3** and **L4** towards a cation

Electrochemical study of receptors **L3** and **L4** and a cation,  $K^+$  was investigated in 40%  $CH_3CN$  v/v in  $CH_2Cl_2$  with 0.1 M  $TBAPF_6$  at scan rate 50 mV by addition of  $KPF_6$  (0-3 equivalents) into the solution of the receptors before each scan. Half wave potential difference between a cation complex and a receptor was used as a parameter for detecting the alteration during the redox process. Addition of  $K^+$  to the solution of the receptors **L3** and **L4** leads to the positive shift of the reduction potentials of both wave I and wave II in cyclic wave voltammogram as shown in **Fig. 4.42 and 4.43**. Electrochemical data of this study was presented in **Table 4.5**. The positive values of half wave potential difference indicated less energies provided in reduction process of anthraquinone resulting from the stabilization of the reduced quinone species by the presence of metal ions [108]. Surprisingly, the shift found in receptor **L4** was remarkably larger. This could be rationalized through the molecular tube characteristic of the 1,3-alternate conformation of calix[4]arene in receptor **L4** which can facilitate the  $K^+$  ion to move close to the sensory unit rather than staying only in the crown ether cavity [31, 109]. Furthermore, the oxidation peak of the redox wave II in the receptor **L4** showed the unique characteristic peak which was very sharp after adding 3 equivalents of  $K^+$  as shown in **Fig. 4.43**. This indicated that the wave II oxidation of anthraquinone in **L4** interacted strongly with  $K^+$ . However, after varying the scan rates, the ratio between the intensity of the current of the reduction and the oxidation peak of the redox wave II decreases (close to 1) at higher scan rates as shown in **Fig. 4.44**.

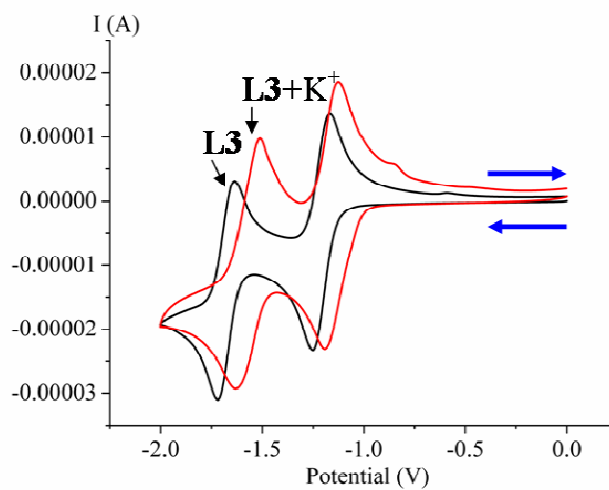


**Fig. 4.42** Cyclic voltammograms of receptor (a) **L3** (1 mM) and  $\text{KPF}_6$  in 40%  $\text{CH}_3\text{CN}$  v/v in  $\text{CH}_2\text{Cl}_2$  with 0.1 M  $\text{TBAPF}_6$  at scan rate 50 mV/s. Blue arrows represent scanned direction.

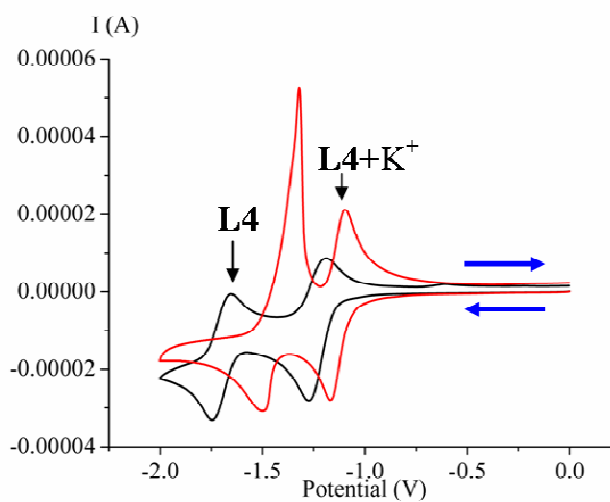


**Fig. 4.43** Cyclic voltammograms of receptor **L4** (1 mM) and  $\text{KPF}_6$  in 40%  $\text{CH}_3\text{CN}$  v/v in  $\text{CH}_2\text{Cl}_2$  with 0.1 M  $\text{TBAPF}_6$  at scan rate 50 mV/s. Blue arrows represent scanned direction.

**Table 4.5** Changes in reduction potentials (mV) at 50 mV/s of receptors **L3** and **L4** after addition of 3 equiv. of  $K^+$

Receptors	$K^+$ (3 equiv.)	
	$\Delta E_{1/2}$ (I) (mV)	$\Delta E_{1/2}$ (II) (mV)
<b>L3</b>	60	95
<b>L4</b>	120	305

$$\Delta E_{1/2} = E_{1/2 \text{ cation cpx}} - E_{1/2 \text{ free receptor}}$$

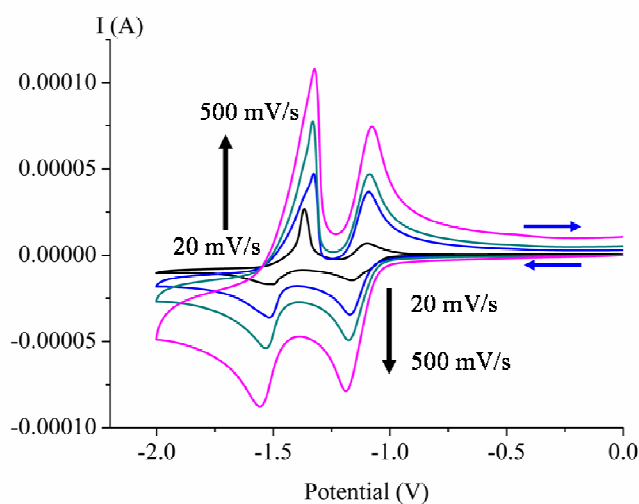


**Fig. 4.44** Cyclic voltammograms of **L4** (1 mM) in 40%  $CH_3CN$  v/v in  $CH_2Cl_2$  with 0.1 M  $TBAPF_6$  at various scan rates (20 mV/s (black line), 100 mV/s (blue line), 200 mV/s (green line) and 500 mV/s (pink line)). Arrows represent the scan direction.

#### 4.3.5.4 Electrochemical studies of receptors **L3** and **L4** towards anions in the presence of a cation

To study the electrochemical behaviour of the ion-pair binding ability of these receptors, 3.0 equivalents of  $K^+$  ions were added to the solution of the receptors **L3** and **L4** before addition of anions. The experiments were performed using the same condition as the previous study, 40%  $CH_3CN$  v/v in  $CH_2Cl_2$  with 0.1 M  $TBAPF_6$  at scan rate 50

mV. For receptor  $[\mathbf{L3}\cdot\mathbf{K}^+]$  system, it was found that addition of various anions ( $\text{Cl}^-$ ,  $\text{Br}^-$ ,  $\text{I}^-$ ,  $\text{BzO}^-$ ,  $\text{H}_2\text{PO}_4^-$ ) into  $[\mathbf{L3}\cdot\mathbf{K}^+]$  solution caused only slightly shifts of wave I and wave II as shown in **Fig. 4.45**. It implies that  $\text{K}^+$  and these anions could not form stable enough cobound ion pairs in the CV experiments. However,  $\text{F}^-$  and  $\text{AcO}^-$  gave the interesting results. Upon addition of  $\text{F}^-$  ion to  $[\mathbf{L3}\cdot\mathbf{K}^+]$  solution, the wave II of the cation complex  $[\mathbf{L3}\cdot\mathbf{K}^+]$  shifted to the less negative potentials as shown in **Fig 4.46**. Remarkably, addition of 10 equiv. of  $\text{AcO}^-$  to  $[\mathbf{L3}\cdot\mathbf{K}^+]$  solution resulted in an appearance of a new reversible wave III at -1.35 V. It should be noted that the current intensity of wave II also decreased. Interestingly, further increasing the amount of  $\text{AcO}^-$  to 20 equiv. resulted in the disappearance of wave II and the completion of the redox wave III as presented in **Fig. 4.47**. In both  $\text{F}^-$  and  $\text{AcO}^-$  cases, the results pointed to the formation of a stable cobound ion pair in this complex which can stabilize dianion of anthraquinone.

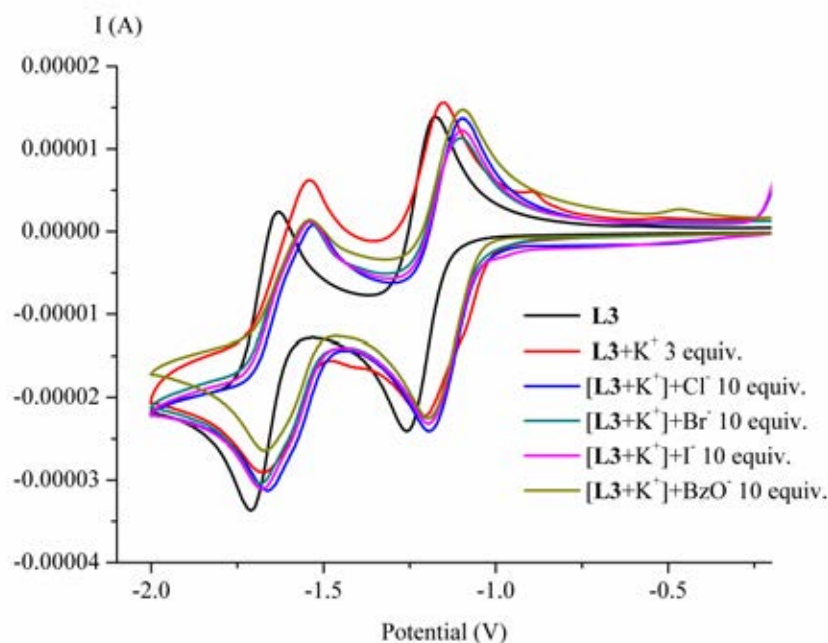


**Fig. 4.45.** Cyclic voltammograms of receptor **L3** (1 mM) +  $\text{KPF}_6$  3.0 equiv. after addition of various anions ( $\text{Cl}^-$ ,  $\text{Br}^-$ ,  $\text{I}^-$ ,  $\text{BzO}^-$ ) 10 equivalents in 40%  $\text{CH}_3\text{CN}$  v/v in  $\text{CH}_2\text{Cl}_2$  with 0.1 M  $\text{TBAPF}_6$  at a scan rate of 50 mV/s.



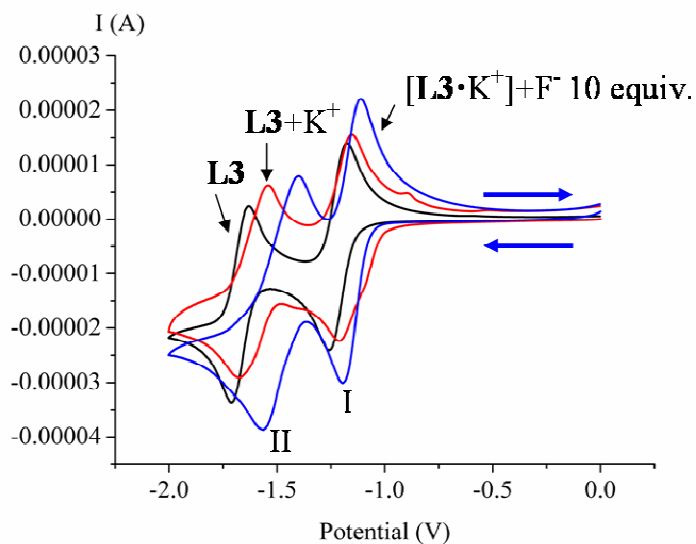


**Fig. 4.46.** Cyclic voltammograms of receptor **L3** (1 mM) +  $\text{KPF}_6$  3.0 equiv. after addition of (a) 10 equiv.  $\text{F}^-$  in 40%  $\text{CH}_3\text{CN}$  v/v in  $\text{CH}_2\text{Cl}_2$  with 0.1 M  $\text{TBAPF}_6$  at a scan rate of 50 mV/s.

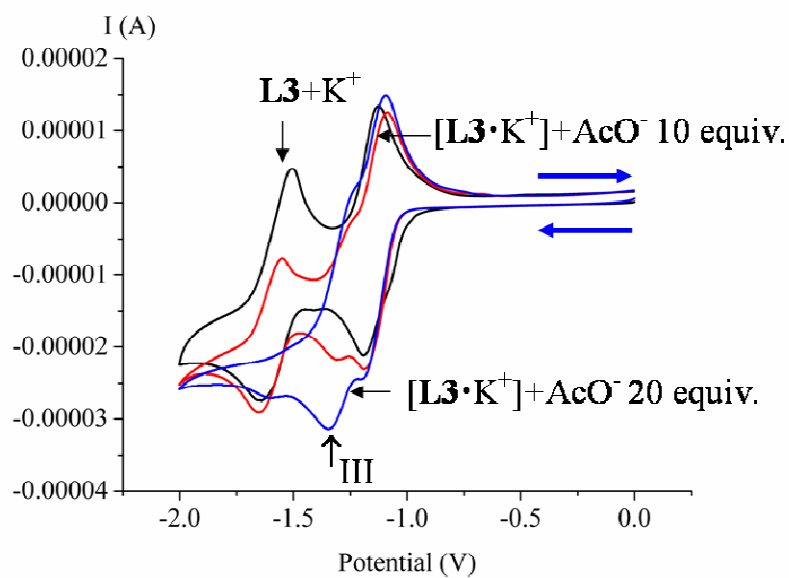


**Fig. 4.47.** Cyclic voltammograms of receptor **L3** (1 mM) +  $\text{KPF}_6$  3.0 equiv. after addition of 10 and 20 equiv.  $\text{AcO}^-$  in 40%  $\text{CH}_3\text{CN}$  v/v in  $\text{CH}_2\text{Cl}_2$  with 0.1 M  $\text{TBAPF}_6$  at a scan rate of 50 mV/s.

The ditopic properties of  $[\mathbf{L4}\cdot\mathbf{K}^+]$  system with various anions ( $\text{F}^-$ ,  $\text{Cl}^-$ ,  $\text{Br}^-$ ,  $\text{AcO}^-$ ,  $\text{BzO}^-$  and  $\text{H}_2\text{PO}_4^-$ ) were also explored. Upon addition anions into  $[\mathbf{L4}\cdot\mathbf{K}^+]$  solution, the reversing of the redox waves of  $[\mathbf{L4}\cdot\mathbf{K}^+]$  to the original voltammograms of receptor  $\mathbf{L4}$  can be seen obviously. This indicated the abstraction of  $\text{K}^+$  by anions. This result emphasized that the molecular tube behavior of receptor  $\mathbf{L4}$  did not facilitate the cooperative effect of these complexes. In this case,  $\text{K}^+$  was removed by negative charges from anions and the reduced anthraquinone probably through the movement in the tube-like 1,3-alternate conformation of calix[4]arene. The examples of the  $\text{K}^+$  abstraction by anions were shown in Fig. 4.48 and 4.49.

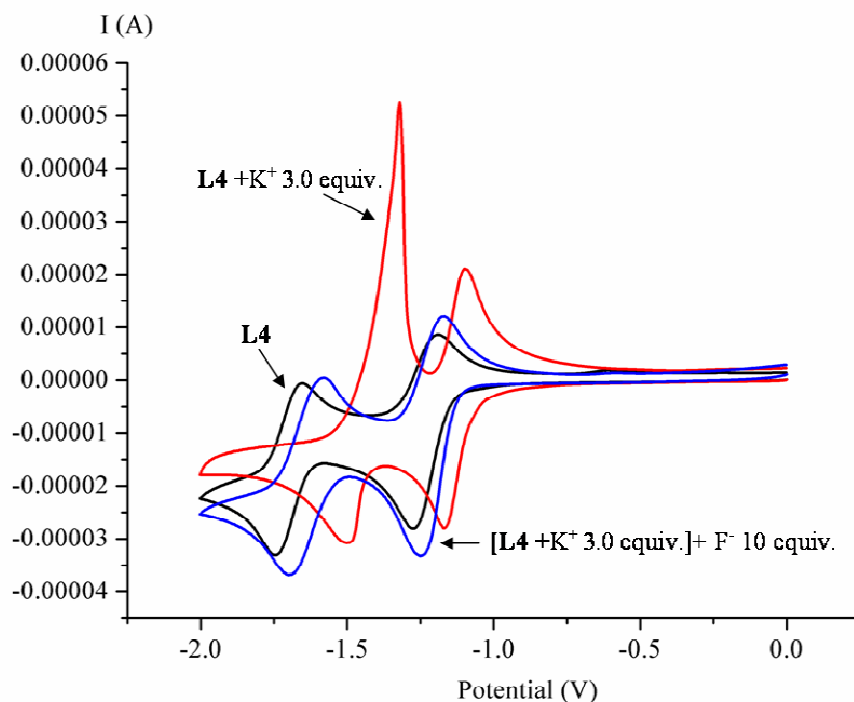


**Fig. 4.48.** Cyclic voltammograms of receptor  $\mathbf{L4}$  (1 mM) +  $\text{KPF}_6$  3.0 equiv. and 10.0 equivalents of  $\text{F}^-$  in 40%  $\text{CH}_3\text{CN}$  v/v in  $\text{CH}_2\text{Cl}_2$  with 0.1 M  $\text{TBAPF}_6$  at a scan rate of 50 mV/s.

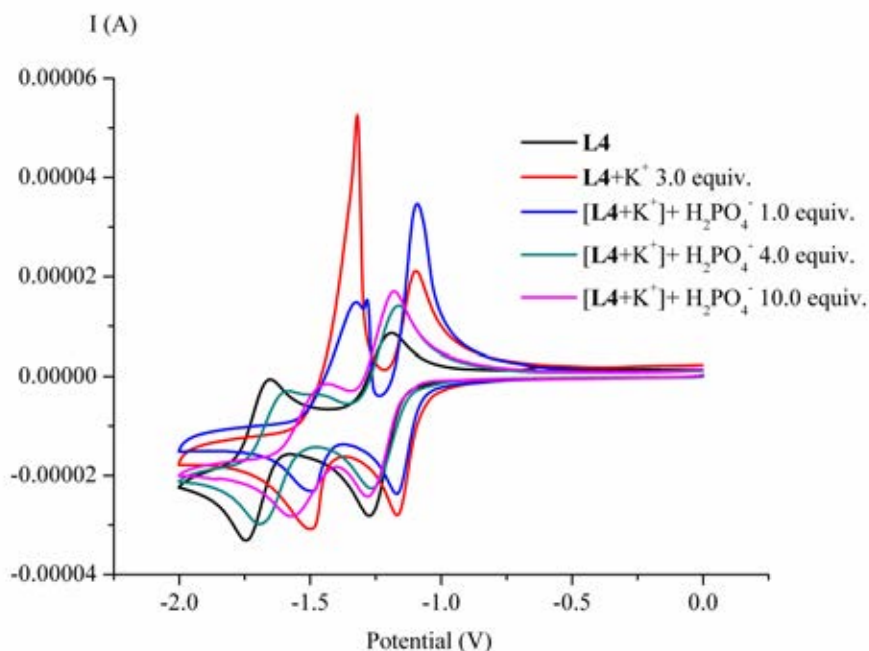


**Fig. 4.49.** Cyclic voltammograms of receptor **L4** (1 mM) + KPF<sub>6</sub> 3.0 equiv. after gradual addition of 1.0, 4.0 and 10.0 equivalents of H<sub>2</sub>PO<sub>4</sub><sup>-</sup> in 40% CH<sub>3</sub>CN v/v in CH<sub>2</sub>Cl<sub>2</sub> with 0.1 M TBAPF<sub>6</sub> at a scan rate of 50 mV/s.

#### 4.4 Concluding remarks

From both photophysical and electrochemical studies, the results brought us to the conclusion of properties of the receptors **L3** and **L4** based on the electrostatic effect from the cation and the different conformation of the calix[4]arene scaffold.

In the absence of K<sup>+</sup>, both receptors **L3** and **L4** showed similar anion binding abilities. They showed high selectivity for fluoride sensing through their optical properties. In addition, they can sense H<sub>2</sub>PO<sub>4</sub><sup>-</sup> electrochemically. Interestingly, it was found that the electrostatic effect from K<sup>+</sup> led to dissimilar anion binding properties of receptors **L3** and **L4**. In the presence of K<sup>+</sup>, receptor **L3** gave stronger fluorescence emission, while receptor **L4** gave weaker. For electrochemical studies, receptor **L3** can sense F<sup>-</sup> and AcO<sup>-</sup> electrochemically, whereas receptor **L4** failed to sense all anions. Thus, the electrostatic interaction from K<sup>+</sup> played a key role in the sensitivity of anions in

their optical properties. Moreover, the additional electrostatic interaction influenced on the selectivity of anions in their electrochemical properties.

As reported previously by Nerngchamnonng et al., the topology of the heteroditopic receptors and the presence of metal ions were able to differentiate the anion binding abilities [47]. The effect of the topology of ligands on their anion binding properties can be observed through the different conformation of calix[4]arene of receptors **L2** and **L4**. Apparently, cone conformation of receptor **L3** supported the formation of cobound ion pair more than 1,3-alternate conformation of receptor **L4**. The crown ether unit in the cone conformation of receptor **L3** intersected between the anion binding sites of the receptor. The closer distance between anion and cation binding sites in **L3** supported the cooperative binding abilities of **L3** towards  $K^+$  and  $F^-$  through both electrostatic and hydrogen bonding interactions. On the other hand, the 1,3-alternate conformation of receptor **L4** possessing a longer distance between cation and anion binding sites did not promote the cooperative binding abilities of **L4** towards  $K^+$  and various anions, but probably facilitated the abstraction of  $K^+$  as found in  $^1H$  NMR titration, photophysical as well as electrochemical studies. Proposed structures of the two receptors with  $F^-$  were, therefore, presented in **Fig. 4.50**.

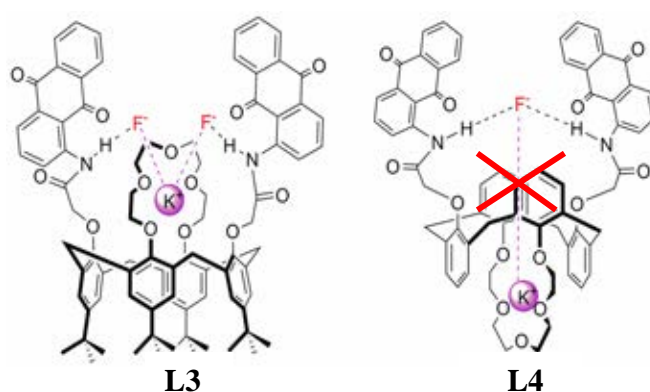


**Fig. 4.50.** Proposed structures of co-bound ion pairs. Dash lines represent electrostatic interactions (which are unlikely in the case of receptor **L4**)

## CHAPTER V

### CONCLUSION

New heteroditopic receptors containing cone and 1,3-alternate conformations of calix[4]arene as building blocks, **L1-L4**, have been reported. These receptors have two different signaling units, ferrocene moieties (receptors **L1** and **L2**) and anthraquinone pendants (receptors **L3** and **L4**). According to complexation studies using  $^1\text{H}$  NMR spectroscopy and electrochemical studies by cyclic voltammetry of these compounds, their ditopic properties were found to depend on two main factors, additional electrostatic effects from cations and the topology of ligands. In addition, photophysical studies of receptors **L3** and **L4** also supported the results from  $^1\text{H}$  NMR spectroscopy and electrochemical studies.

#### 5.1 The electrostatic effects from cations

In the absence of cations, these receptors showed similar anion binding abilities. Complexation studies by  $^1\text{H}$  NMR titration revealed that receptors **L1** and **L2** preferred binding Y-shaped anions with relatively low binding constants. In addition, receptors **L1** and **L2** can sense  $\text{AcO}^-$ ,  $\text{BzO}^-$  and  $\text{Cl}^-$  by giving cathodic shifts of their oxidation waves. Nevertheless, receptors **L3** and **L4** can sense  $\text{F}^-$  photophysically and  $\text{H}_2\text{PO}_4^-$  electrochemically.

The presence of cations led to diverse anion binding properties of these ligands. Cobound cation of receptor **L1**,  $[\text{L1}\cdot\text{K}^+]$ , presented higher binding constants with all anions especially Y-shaped anions, while  $[\text{L2}\cdot\text{Na}^+]$  complex gave more specificity and selectivity only with  $\text{AcO}^-$  and  $\text{Br}^-$  ions. Thus, in this case, the presence of cations effected the preference of anion binding. However,  $[\text{L1}\cdot\text{K}^+]$  failed to recognize all anions electrochemically due to salt ion pair formation. In contrast, oxidized cobound cations of receptor **L2** detected  $\text{Cl}^-$  and  $\text{AcO}^-$  to more catodically shifts compared to its normal form. Receptor **L3** displayed the enhancement of emission spectra with  $\text{F}^-$ , while receptor **L4** sensed  $\text{F}^-$  with lower intensities of the emission spectra in the presence of  $\text{K}^+$ .

Furthermore, cobound  $[\mathbf{L3}\cdot\mathbf{K}^+]$  could detect  $\text{AcO}^-$  electrochemically, whereas cobound cation of receptor **L4** failed to sense all anions due to the abstraction of cations by added anions.

## 5.2 The topology of the ligands

According to this study, the topology of ligands implying that the inter-ionic distance played a key role to the ditopic properties of the reported heteroditopic receptors. Cone conformation of calix[4]arene of receptors **L2** and **L3** supported cobound ion pair formation more than 1,3-alternate conformation of receptors **L1** and **L4**. The crown ether unit in the cone conformation of receptors **L2** and **L3** intersected between the anion binding sites of the receptors leading to the closer distance between anion and cation binding sites. The closer inter-ionic distance of specific cobound ion pairs promoted the cooperative or positive binding. On the other hand, the 1,3-alternate conformation of receptor **L1** and **L4** possessing a longer distance between cation and anion binding sites did not promote the effective cooperative binding abilities. Eventhough  $[\mathbf{L1}\cdot\mathbf{K}^+]$  complexes still showed higher binding constants with all anions, their oxidized forms failed to sense all anions electrochemically. This emphasized that although positive charge were presented in the molecule, anion binding abilities could not be improved if the distance between the two different charges was not suitable. In the case of receptor **L4**,  $\mathbf{K}^+$  was not even helpful in improving anion binding properties, but it also abstracted the bound anion as found in  $^1\text{H}$  NMR titration, photophysical as well as electrochemical studies.

## 5.3 Dual sensing properties

Obviously, receptor **L3** and **L4** showed dual anion sensing through optical and electrochemical signals. Interestingly, **L3** and **L4** presented different anion sensing properties involving sensitivity as well as selectivity using either photophysical or electrochemical measurement. Therefore, receptors exhibiting dual sensing properties

could fulfill the requirement of the sensor field in terms of the molecular device responding to different chemical stimuli using diverse techniques.

#### **5.4 Future outlook**

Considering the limitations of our synthesized receptors, **L1-L4**, which were the relatively low sensitivity of the sensors, the low yield of product due to the humidity as well as the insoluble receptors in aqueous solution, the design of anion sensors need to be further improved. In future study, other sensory units giving higher quantum yield should be considered for higher anion sensitivity. The synthesis pathway of the receptor should be as short as possible to obtain the higher yield of the product. The constituents of the sensors should facilitate the solubility in water which could support the applying of sensors in real samples. In addition, mixed organic solvent with water should be tested for possible systems in real sample. However, this study is valuable in terms of the novel knowledge of heteroditopic receptors regarding the topology of ligands which was rarely discussed in previous reports.

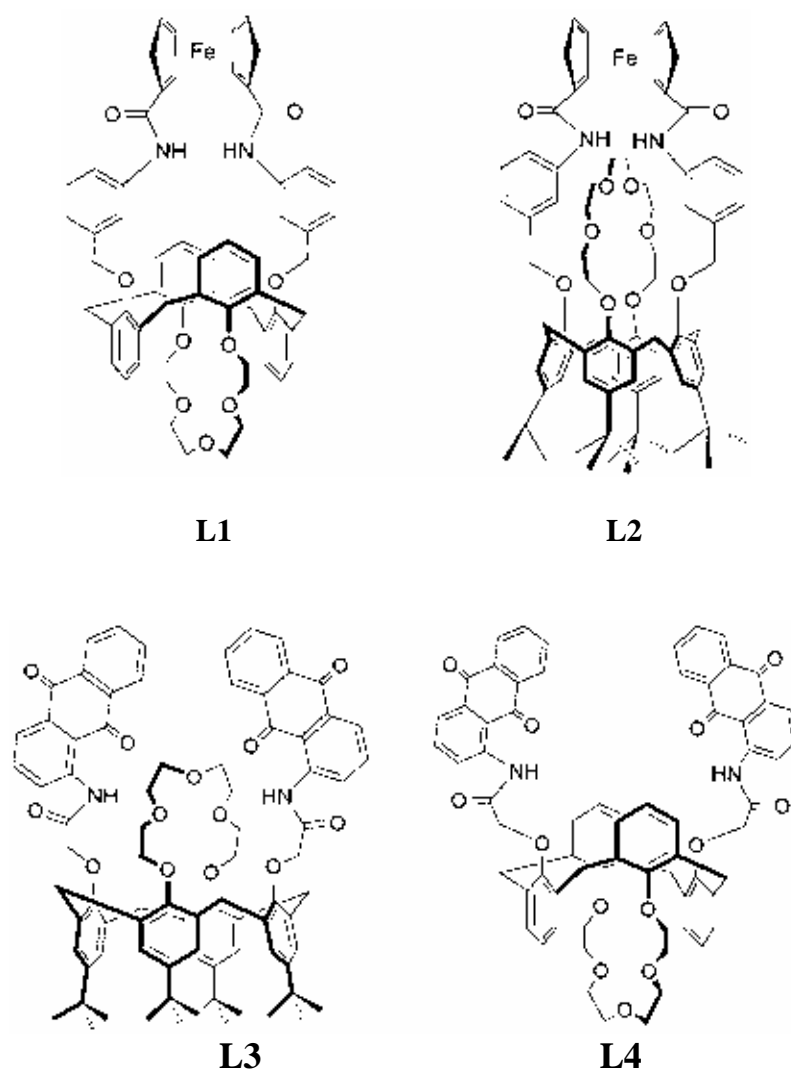


**Fig. 5.1** Chemical structure of receptors L1-L4.



## References

- [1] Beer, P.D., and Gale, P.A. Anion recognition and sensing: the state of the art and future perspectives. *Angew. Chem. Int. Ed.* 40(2001): 486-516.
- [2] Gunnlaugsson, T., Glynn, M., Tocci (née Hussey), G.M., Kruger, P.E. and Pfeffer, F.M. Anion recognition and sensing in organic and aqueous media using luminescent and colorimetric sensors. *Coordin. Chem. Rev.* 250(2006): 3094-3117.
- [3] Beer, P.D. and Hayes, E.J. Transition metal and organometallic anion complexation agents. *Coordin. Chem. Rev.* 240(2003): 167-189.
- [4] Beer, P.D. and Cadman, J. Electrochemical and optical sensing of anions by transition metal based receptors. *Coordin. Chem. Rev.* 205(2000): 131-155.
- [5] Gale, P.A. Anion corrodination and anion-directed assembly: highlights from 1997 and 1998. *Coordin. Chem. Rev.* 199(2000): 181-233.
- [6] Martínez-Mañez, R. and Sancenón, F. Fluorogenic and chromogenic chemosensors and reagents for anions. *Chem.Rev.* 103(2003): 4419-4476.
- [7] Gale, P.A., Garcá-Garrico, S.E., and Garric, J. Anion receptors based on organic frameworks: highlights from 2005 and 2006. *Chem. Soc. Rev.* 37(2008): 151-190.
- [8] Brooks, S.J., Gale, P.A., and Light, M.E. Anion-binding modes in a macrocyclic amidourea. *Chem. Commun.* (2006): 4344-4346.
- [9] Arduini, A., Giorgi, G., Pochini, A, Secchi, A., and Ugozzoli, F. Anion allosteric effect in the recognition of tetramethylammonium salts by calix[4]arene cone conformers. *J. Org. Chem.* 66(2001): 8302-8308.
- [10] Tumcharern, G., Tuntulani, T., Coles, S. J., Hursthouse, M.B., and Kilburn, J. D. A novel ditopic receptor and reversal of anion binding selectivity in the presence and absence of bound cation. *Org. Lett.* 5(2003): 4971-4974.

- [11] Mahoney, J. M., Nawaratna, G. U., Beatty, A. M., Duggan, P. J., and Smith, B. D. Transport of alkali halides through a liquid organic membrane containing a ditopic salt-binding receptor. *Inorg. Chem.* 43(2004): 5902-5907.
- [12] Geide, I. V., Soldatov, D. V., Kramarenko, O. A., Matern, A. I., and Morzherin, Y. Y. Novel ditopic receptor based on tetrakisaminosulfonyl-calix[4]arene. *J. Struct. Chem.* 46(2005): S28-S32.
- [13] Mahoney, J. M., Beatty, A. M., and Smith, B. D. Selective recognition of an alkali halide contact ion-pair. *J. Am. Chem. Soc.* 123(2001): 5847-5848.
- [14] Deetz, M. J., Shang, M., and Smith, B. D. A macrocyclic receptor with versatile recognition properties: simultaneous binding of an ion pair and selective complexation of dimethylsulfoxide. *J. Am. Chem. Soc.* 122(2000): 6201-6207.
- [15] Arduini, A., Brindani, E., Giorgi, G., Pochini, A., and Secchi, A. Recognition of guests bearing donor and acceptor hydrogen bonding groups by heteroditopic calix[4]arene receptors. *Tetrahedron* 59(2003): 7587-7594.
- [16] Evans, A. J., Matthews, S. U., Cowley, A. R., and Beer, P. D. Anion binding by calix[4]arene ferrocene ureas. *Dalton Trans.* (2003): 4644-4650.
- [17] Szymańska, I., Radecka, H., Radecki, J., Gale, P. A., and Warriner, C. N. Ferrocene-substituted calix[4]pyrrole modified carbon paste electrodes for anion detection in water. *J. Electroanal. Chem.* 591(2006), 223-228.
- [18] Hall, C. D., Djedovic, N., Asfari, Z., Pulpoka, B., and Vicens, J. Novel redox-active calixarenes. *J. Organomet. Chem.* 571(1998): 103-108.
- [19] Plenio, H., and Diodone, R. Complexation of Na<sup>+</sup> in redox-active ferrocene crown ether, a structural investigation, and an unexpected case of Li<sup>+</sup> selectivity. *Inorg. Chem.* 34(1995): 3964-3972.
- [20] Schazmann, B., Alhashimy, N., and Diamond, D. Chloride selective calix[4]arene optical sensor combining urea functionality with pyrene excimer transduction. *J. Am. Chem. Soc.* 128(2006): 8607-8614.

- [21] Kim, S. K., Bok, J. H., Bartsch, R. A., Lee, J. Y., and Kim, J. S. A Fluoride-selective PCT Chemosensor based on formation of a static pyrene excimer. *Org. Lett.* 7(2005): 4839-4842.
- [22] Beeren, S. R., and Sanders, J. K. M. Discovery of linear receptors for multiple dihydrogen phosphate ions using dynamic combinatorial chemistry. *J. Am. Chem. Soc.* 133(2011): 3804-3807.
- [23] Kim, S. K. and others. Controlling cesium cation recognition via cation metathesis within an ion pair receptor. *J. Am. Chem. Soc.* 134(2012): 1782-1792.
- [24] Kitamura, M., Nishimoto, H., Aoki, K., Tsukamoto, M., and Aoki, S. Molecular recognition of inositol 1,4,5-trisphosphate and model compounds in aqueous solution by ditopic  $Zn^{2+}$  complexes containing chiral linkers. *Inorg. Chem.* 49(2010): 5316-5327.
- [25] Amendola, V., Boiocchi, M., Colasson, B., and Fabbrizzi, L. Metal-controlled assembly and selectivity of a urea-based anion receptor. *Inorg. Chem.* 45(2006): 6138-6147.
- [26] Korendovych, I. V., Cho, M., Butler, P. L., Staples, R. J., and Rybak-Akimova, E. V. Anion binding to monotopic and ditopic macrocyclic amides. *Org. Lett.* 8(2006): 3171-3174.
- [27] Kebroy, P., Banerjee, M., Prasad, M., Moulik, S. P., and Roy, S. Binding of amino acids into a novel multiresponsive ferrocene receptor having an ene backbone. *Org. Lett.* 7(2005): 403-406.
- [28] Alfonso, M., Tárraga, A., and Molina, P. A bisferrocene-benzobisimidazole triad as a multichannel ditopic receptor for selective sensing of hydrogen sulfate and mercury ions. *Org. Lett.* 13(2011): 6432-6435.
- [29] Kuate, A. C. T., Iovkova, L., Hiller, W., Schürmann, M., and Jurkchat, K. Organotin-substituted [13]-crown-4 ethers: ditopic receptors for lithium and cesium halides. *Organometallics* 29(2010): 5456-5471.

- [30] Amato, M. E., Ballistreri, F. P., Gentile, S., Pappalardo, A., Tomaselli, G. A., and Toscano, R. M. Recognition of achiral and chiral ammonium salts by neutral ditopic receptors based on chiral salen-UO<sub>2</sub> macrocycles. *J. Org. Chem.* 75(2010): 1437-1443.
- [31] Baklouti, L., Harrowfield, J., Pulpoka, B., and Vicens, J. 1,3-Alternate, the smart conformation of calix[4]arenes. *Mini-Rev. Org. Chem.* 3(2006): 355-384.
- [32] Lascaux, A.; Gac, S. L.; Wouters, J.; Luhmer, M.; Jabin, I. An allosteric heteroditopic receptor for neutral guests and contact ion pairs with a remarkable selectivity for ammonium fluoride salts. *Org. Biomol. Chem.* 8(2010): 4607-4616.
- [33] Mahoney, J.M., and others. Molecular recognition of trigonal oxyanions using a ditopic salt receptor: evidence for anisotropic shielding surface around nitrate anion. *J. Am. Chem. Soc.* 127(2005): 2922-2928.
- [34] Rudkevich, D.M., Mercer-Chalmers, J.D., Verboom, W., Ungaro, R., Jong, F.D., and Reinhoudt, D.N. Bifunctional recognition: simultaneous transport of cations and anions through a supported liquid membrane. *J. Am. Chem. Soc.* 117(1995): 6124-6125.
- [35] He, X., Yam, and V.W.-W. Design, synthesis, photophysics, and ion-binding studies of a ditopic receptor based on gold(I) phosphine thiolate complex functionalized with crown ether and urea binding units. *Inorg. Chem.* 49 (2010): 2273-2279.
- [36] Kim, S.K., and others. A calix[4]arene strapped calix[4]pyrrole: an ion-pair receptor displaying three different cesium cation recognition modes. *J. Am. Chem. Soc.* 132(2010): 5827-5836.
- [37] Gale, P.A. Anion and ion-pair receptor chemistry: highlights from 2000 and 2001. *Coordin. Chem. Rev.* 240(2003): 191-221.
- [38] Kovbasyuk, L., and Krämer, R. Allosteric supramolecular receptors and catalysts. *Chem. Rev.* 104(2004): 3161-3187.

- [39] Shinkai, S., Ikeda, M., Sugasaki, A., and Takeuchi, M. Positive allosteric systems designed on dynamic supramolecular scaffolds: toward switching and amplification of guest affinity and selectivity. *Acc. Chem. Res.* 34(2001): 494-503.
- [40] Takeuchi, M., Ikeda, M., Sugasaki, A., and Shinkai, S. Molecular design of artificial molecular and ion recognition systems with allosteric guest responses. *Acc. Chem. Res.* 34(2001): 865-873.
- [41] Amendola, V., Esteban-Gómez, D., Fabbrizzi, L., Licchelli, M., Monzani, E., and Sancenón, F. Metal-enhanced H-bond donor tendencies of urea and thiourea toward anions: ditopic receptors for silver(I) salts. *Inorg. Chem.* 44(2005): 8690-8698.
- [42] Zhu, K., Li, S., Wang, F., and Huang, F. Anion-controlled ion-pair recognition of paraquat by a bis(*m*-phenylene)-32-crown-10 derivative heteroditopic host. *J. Org. Chem.* 74(2009): 1322-1328.
- [43] Deetz, M.J., Shang, M., and Smith, B.D. A macrobicyclic receptor with versatile recognition properties: simultaneous binding of an ion pair and selective complexation of dimethylsulfoxide. *J. Am. Chem. Soc.* 122(2000): 6201-6207.
- [44] Kumar, A. and Menon, S.K. Cooperative anion recognition by a novel heteroditopic receptor based on dibenzo[18]crown-6 fuller bis(pyrrolidine). *Supramolecular Chemistry* 22(2010): 46-56.
- [45] Arduini, A., Brindani, E., Giorgi, G., Pochini, A., and Secchi, A. Recognition of guests bearing donor and acceptor hydrogen bonding groups by heteroditopic calix[4]arene receptors. *Tetrahedron Lett.* 53(2003): 7587-7594.
- [46] Senthilvelan, A., Ho, I.-T., Chang, K.-C., Lee, G.-H., Liu, Y.-H., and Chung, W.-S. Cooperative Recognition of a Copper Cation and Anion by a Calix[4]arene Substituted at the Lower Rim by a  $\beta$ -Amino- $\alpha$ ,  $\beta$ -Unsaturated Ketone. *Chem. Eur. J.* 15(2009): 6152-6160.

- [47] Nerngchamng, N., Chailap, B., Leeladee, P., Chailapakul, O., Suksai, C., Tuntulani, T. Topological and metal ion effects on the anion binding abilities of new heteroditopic receptors derived from p-tert-butylcalix[4]arene. *Tetrahedron Lett.* 52(2011): 2914-2917.
- [48] Gargiulli, C., and others. Calix[5]arene-based heteroditopic receptor for 2-phenylethylamine hydrochloride. *J.Org. Chem.* 74(2009): 4350-4353.
- [49] Hamon, M., Ménand, M., Gac, S.L., Luhmer, M., Dalla, V., and Jabin, I. Calix[6]tris(thio)ureas: heteroditopic receptors for the cooperative binding of organic ion pairs. *J.Org. Chem.* 73(2008): 7067-7071.
- [50] Sessler, J.L., Kim, S.K., Gross, D.E., Lee, C.-H., Kim, J.S., and Lynch, V.M. Crown-6-calix[4]arene-capped calix[4]pyrrole: an ion-pair receptor for solvent-separated CsF ions. *J. Am. Chem. Soc.* 130(2008): 13162-13166.
- [51] Panda, P.K., and Lee, C.-H. Calix[4]pyrrole-capped metalloporphyrins as ditopic receptor models for anions. *Org. Lett.* 6(2004): 671-674.
- [52] Lankshear, M.D., Cowley, A.R., and Beer, P.D. Cooperative and receptor for ion-pairs. *Chem. Commun.* (2006): 612-614.
- [53] Lankshear, M.D., Dudley, I.M., Chan, K.-M., and Beer, P.D. Tuning the strength and selectivity of ion-pair recognition using heteroditopic calix[4]arene-based receptors. *New J. Chem.* 31(2007): 684-690.
- [54] Alfonso, M., Espinosa, A., Tárraga, A., and Molina, P. A Simple but effective dual redox and fluorescent ion pair receptor based on a ferrocene-imidazopyrene dyad. *Org. Lett.* 13(2011); 2078-2081.
- [55] Kirkovits, G., Shriver, J.A., Gale, P.A., and Sessler, J. Synthetic ditopic receptors. *J. Incl. Phenom. Macro.* 41(2001): 69-75.
- [56] Otón, F., Tárraga, A., Espinosa, A., Velasco, M.D., and Molina, P. Ferrocene-based ureas as multisignaling receptors for anions. *J. Org. Chem.* 71(2006): 4590-4598.

- [57] Lu, H., Xu, W., Zhang, D., Chen, C., and Zhu, D. A novel multisignaling optical-electrochemical chemosensor for anions based on tetrathiafulvalene. *Org. Lett.* 7(2005): 4629-4632.
- [58] Yang, H., and others. Multisignaling optical-electrochemical sensor for  $\text{Hg}^{2+}$  based on a rhodamine derivative with a ferrocene unit. *Org. Lett.* 9(2007): 4729-4732.
- [59] Wu, D., and others. Highly sensitive multiresponsive chemosensor for selective detection of  $\text{Hg}^{2+}$  in natural water and different monitoring environments. *Inorg. Chem.* 47(2008): 7190-7201.
- [60] Zhao, Q., and others. A highly selective and multisignaling optical-electrochemical sensor for  $\text{Hg}^{2+}$  based on a phosphorescent iridium(III) complex. *Organometallics* 26(2007): 2077-2081.
- [61] Zapata, F., Caballero, A., Espinosa, A., Tárraga, A., and Molina, P. Cation coordination induced modulation of the anion sensing properties of a ferrocene-imidazophenanthroline dyad: multichannel recognition from phosphate-related to chloride anions. *J. Org. Chem.* 73(2008): 4034-4044.
- [62] Zeng, Z., Torriero, A.A.J., Bond, A.M., and Spiccia, L. Fluorescent and electrochemical sensing of polyphosphate nucleotides by ferrocene functionalised with two  $\text{Zn}^{\text{II}}$ (TACN)(pyrene) complexes. *Chem. Eur. J.* 16(2010): 9154-9163.
- [63] Basurto, S., Riant, O., Moreno, D., Rojo, J., and Torroba, T. Colorimetric detection of  $\text{Cu}[\text{II}]$  cation and acetate, benzoate, and cyanide anions by cooperative receptor binding in new  $\alpha$ ,  $\alpha'$ -bis-substituted donor-acceptor ferrocene sensors. *J. Org. Chem.* 72(2007): 4673-4688.
- [64] Otón, F., and others. Mononuclear ferrocenophane structural motifs with two thiourea arms acting as a dual binding site for anions and cations. *Inorg. Chem.* 48(2009): 1566-1576.

- [65] Zhang, B.-g., Xu, J., Zhao, Y.-g., Duan, C.-y., Cao, X., and Meng, Q.-J. Host-guest complexation of a fluorescent and electrochemical chemsensor for fluoride anion. *Dalton Trans.* (2006): 1271-1276.
- [66] Tan, Q., and others. Study on anion electrochemical recognition based on a novel ferrocenyl compound with multiple binding sites. *J. Phys. Chem. B* 112(2008): 11171-11176.
- [67] Otón, F., Tárraga, A., and Molina, P. A Bis-guanidine-based multisignaling sensor molecule that displays redox-ratiometric behavior or fluorescence enhancement in the presence of anions and cations. *Org. Lett.* 8(2006): 2107-2110.
- [68] Zapata, F., Caballero, A., Tárraga, A., and Molina, P. Ferrocene-substituted nitrogen-rich ring systems as multichannel molecular chemosensors for anions in aqueous environment. *J. Org. Chem.* 75(2010): 162-169.
- [69] Gutsche, C.D., and Bauer, L.J., Calixarenes. 13. The conformational properties of calix[4]arenes, calix[6]arenes, calix[8]arene, and oxacalixarenes. *J. Am. Chem. Soc.* 107(1985): 6052-6059.
- [70] Alfonso, M., Tárraga, A., and Molina, P. Ferrocene-based heteroditopic receptors displaying high selectivity toward lead and mercury metal cations through different channels. *J. Org. Chem.* 76(2011): 939-947.
- [71] Miyaji, H., Collinson, S.R., Prokes, I., and Tucker, J.H.R. A ditopic ferrocene receptor for anions and cations that functions as a chromogenic molecular switch. *Chem. Commun.* (2003): 64-65.
- [72] Otón, F., Tárraga, A., Espinosa, A., Velasco, M. D., and Molina, P. Heteroditopic ferrocene-based ureas as receptors for anions and cations. *Dalton Trans.* (2006) : 3685-3692.
- [73] Suksai, C., and others. A new heteroditopic receptor and senso highly selective for bromide in the presence of a bound cation. *Tetrahedron Lett.* 46(2005): 2765-2769.



- [74] Suksai, C. *Supramolecular chemistry of ditopic anion sensors and amphiphilic molecules*. Ph.D.'s thesis, Department of Chemistry, Faculty of science, Chulalongkorn University, 2006.
- [75] Tomapatanaget, B., Tuntulani, T., and Chailapakul, O. Calix[4]arenes Containing ferrocene amide as carboxylate anion receptors and sensors. *Org. Lett.* 5(2003): 1539-1542.
- [76] Macomber, R.S. An introduction to NMR titration for studying rapid reversible complexation. *J. Chem. Educ.* 69(1992): 375-378.
- [77] Choi, J.K., Dim, S.H., Yoon, J., Lee, K.-H., Bartsch, R.A., and Kim, J.S. A PCT-Based, Pyrene-Armed Calix[4]crown Fluoroionophore. *J. Org. Chem.* 71(2006): 8011-8015.
- [78] Hynes, M.J. EQNMR: A computer program for the calculation of stability constants from nuclear magnetic resonance chemical shift data. *J. Chem. Soc. Dalton Tran.* (1993): 311-312.
- [79] Miler, S.R., Gustowski, D.A., Chen, Z.H., Gokel, G.W. Echegoyen, L. and Kaifer, A.E. Rationalization of the unusual electrochemical behavior observed in lariat ethers and other reducible macrocyclic systems. *Anal. Chem.* 60(1988): 2021-2024.
- [80] Beer, P.D., Graydon, A.R., Johnson, A.O.M., and Smith, D.K. Neutral ferrocenoyl receptors for the selective recognition and sensing of anionic guests. *Inorg. Chem.* 36(1997): 2112-2118.
- [81] Wopschall R.H. and Shain, I. Effects of adsorption of electroactive species in stationary electrode polarography. *Anal. Chem.* 39(1967): 1514-1527.
- [82] Mishra, A.K., Jacob, J. and Müllen, K, Synthesis of aminocarbazole anthraquinone fused dyes and polymers. *Dyes. Pigments.* 75(2007): 1-10.
- [83] Kaur, N. and Kumar, S. A diamide–diamine based Cu<sup>2+</sup> chromogenic sensor for highly selective visual and spectrophotometric detection. *Tetrahedron Lett.* 47(2006): 4109-4112.

- [84] Kaur, N. and Kumar, S. Colorimetric recognition of Cu(II) by (2-dimethylaminoethyl)amino appended anthracene-9,10-diones in aqueous solutions: deprotonation of aryl amine NH responsible for colour changes. *Dolton. Trans.* (2006) : 3766-3771.
- [85] Kim, H.J., Lee, S.J., Park, S.Y., Jung, J.H., and Kim, J.S. Detection of Cu<sup>II</sup> by a chemodosimeter-functionalized monolayer on mesoporous silica. *Adv. Mater.* 20(2008): 3229-3234.
- [86] Wu, S.-P., Du, K.-J. and Sung, Y.-M. Colorimetric sensing of Cu(II): Cu(II) induced deprotonation of an amide responsible for color changes. *Dolton. Trans.* 39(2010): 4363-4368.
- [87] Ranyuk, E., and others. Diaminoanthraquinone-linked polyazamacrocycles: efficient and simple colorimetric sensor for lead ion in aqueous solution. *Org. Lett.* 11(2009) : 987-990.
- [88] Zhang, Y.-J., He, X.-P., Hu, M., Li, Z., Shi, X.-X., and Chen, G.-R. Highly optically selective and electrochemically active chemosensor for copper (II) based on triazole-linked glucosyl anthraquinone. *Dyes. Pigments.* 88(2011): 391-395.
- [89] Kaur, N., and Kumar, S. Near-IR region absorbing 1,4-diaminoanthracene-9,10-dione motif based ratiometric chemosensors for Cu<sup>2+</sup>. *Tetrahedron* 64(2008): 3168-3175.
- [90] Kaur, N., and Kumar, S. Single molecular colorimetric probe for simultaneous estimation of Cu<sup>2+</sup> and Ni<sup>2+</sup>. *Chem. Commun.* (2007) : 3069-3070.
- [91] Kim, H.J., and others. ICT-based Cu(II)-sensing 9,10-anthraquinonecalix[4]crown. *Tetrahedron Lett.* 50(2009): 2782-2786.
- [92] Kim, S.H., Choi, H.S., Kim, J., Lee, S.J., Quang, D.T., and Kim, J.S. Novel Optical/Electrochemical Selective 1,2,3-Triazole Ring-Appended Chemosensor for the Al<sup>3+</sup> Ion. *Org. Lett.* 12(2010): 560-563.
- [93] Han, D.Y., and others. ESIPT-based anthraquinonylcalix[4]crown chemosensor for In<sup>3+</sup>. *Tetrahedron Lett.* 51(2010): 1947-1951.

- [94] Yang, H., Zhou, Z.-G., Xu, J., Li, F.-Y., Yi, T., and Huang, C.-H. A highly selective ratiometric chemosensor for  $\text{Hg}^{2+}$  based on the anthraquinone derivative with urea groups. *Tetrahedron* 63(2007): 6732-6736.
- [95] Peng, X., Wu, Y., Fan, J., Tian, M., and Han, K. Colorimetric and ratiometric fluorescence sensing of fluoride: tuning selectivity in proton transfer. *J. Org. Chem.* 70(2005): 10524-10531.
- [96] Kumar, S., Luxami, V., and Kumar, A. Chromofluorescent probes for selective detection of fluoride and acetate ions. *Org. Lett.* 10(2008): 5549-5552.
- [97] Batista, M.F., Olivira, E., Costa, S.P.G., Lodeiro, C., and Raposo, M.M.M. Synthesis and ion sensing properties of new colorimetric and fluorimetric chemosensors based on bithienyl-imidazo-anthraquinone chromophores. *Org. Lett.* 9(2007): 3201-3204.
- [98] Jiménez, D., Martínez-Máñez, R., Sancenón, F., and Soto, J. Selective fluoride sensing using colorimetric reagents containing anthraquinone and urea or thiourea binding sites. *Tetrahedron Lett.* 43(2002): 2823-2825.
- [99] Jose, D.A., Kumar, D.K., Ganguly, B., and Das, A. Efficient and simple colorimetric fluoride ion sensor based on receptors having urea and thiourea binding sites. *Org. Lett.* 6(2004): 3445-3448.
- [100] Wu, F.-Y., Hu, M.-H., Wu, Y.-M., Tan, X.-F., Zhao, Y.-Q., and Ji, Z.-J. Fluoride-selective colorimetric sensor based on thiourea binding site and anthraquinone reporter. *Spectrochim. Acta. A.* 65(2006): 633-637.
- [101] Jung, H.S., Kim, H.J., Vicens, J., and Kim, J.S. A new fluorescent chemosensor for  $\text{F}^-$  based on inhibition of excited-state intramolecular proton transfer. *Tetrahedron Lett.* 50(2009): 983-987.
- [102] González, F.J. Cyclic voltammetry of two analogue K-group vitamin compounds in dimethylsulfoxide. *Electroanal.* 10(1998): 638-642.

- [103] Ossowski, T., Pipka, P., Liwo, A., and Jeziorek, D. Electrochemical and UV-spectrophotometric study of oxygen and superoxide anion radical interaction with anthraquinone derivatives and their radical anions. *Electrochim. Acta.* 45(2000): 3581-3587.
- [104] Gupta, N., and Linschitz, H. Hydrogen-bonding and protonation effects in electrochemistry of quinones in aprotic solvents. *J. Am. Chem. Soc.* 119(1997): 6384-6391.
- [105] Gomóz, M., González, F.J., and González, I. Intra and intermolecular hydrogen bonding effects in the electrochemical reduction of  $\alpha$ -phenolic-naphthoquinones. *J. Electroanal. Chem.* 578(2005): 193-202.
- [106] Brooks, S.J., Birkin, P.R., and Gale, P.A. Electrochemical measurement of switchable hydrogen bonding in an anthraquinone-based anion receptor. *Electrochem. Commun.* 7(2005): 1351-1356.
- [107] Jaime, C., Mendoza, J., Prados, P., Nieto, P.M., and Sanchez, C.  $^{13}\text{C}$  NMR Chemical shifts. A single rule to determine the conformation of calix[4]arenes. *J. Org. Chem.* 56(1991): 3372-3376.
- [108] Kerdpaiboon, N., Tommapatanaget, B., Chailapakul, O., and Tuntulani, T. Calix[4]quinones derived from double calix[4]arenes: synthesis, complexation, and electrochemical properties toward alkali metal ions. *J. Org. Chem.*, 70(2005): 4797-4804.
- [109] Pulpoka, B., Baklouti, L., Kim, J.S., and Vicens, J. *Calixarenes in the nanoworld.*, Vicens, J. and Harrowfield, J. (ed.), pp.133-149. Springer 2007

## **Appendix**

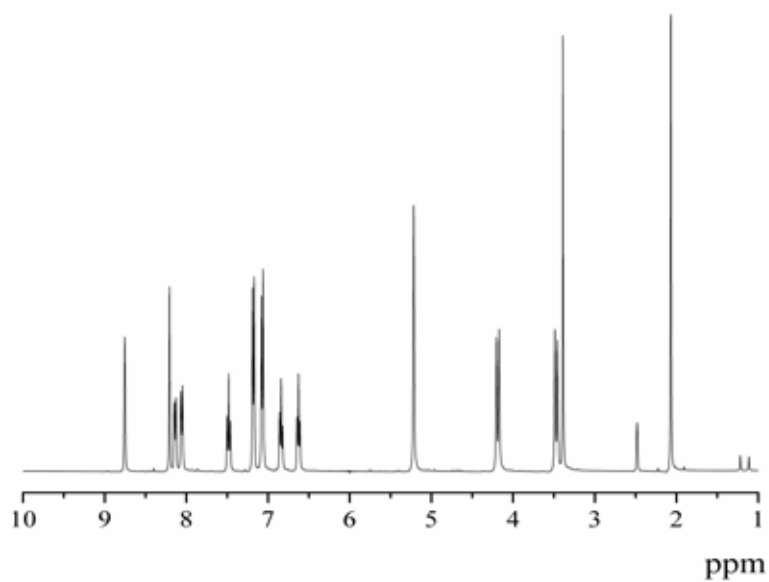


Fig. A1  $^1\text{H}$ -NMR spectrum of **1a** in DMSO

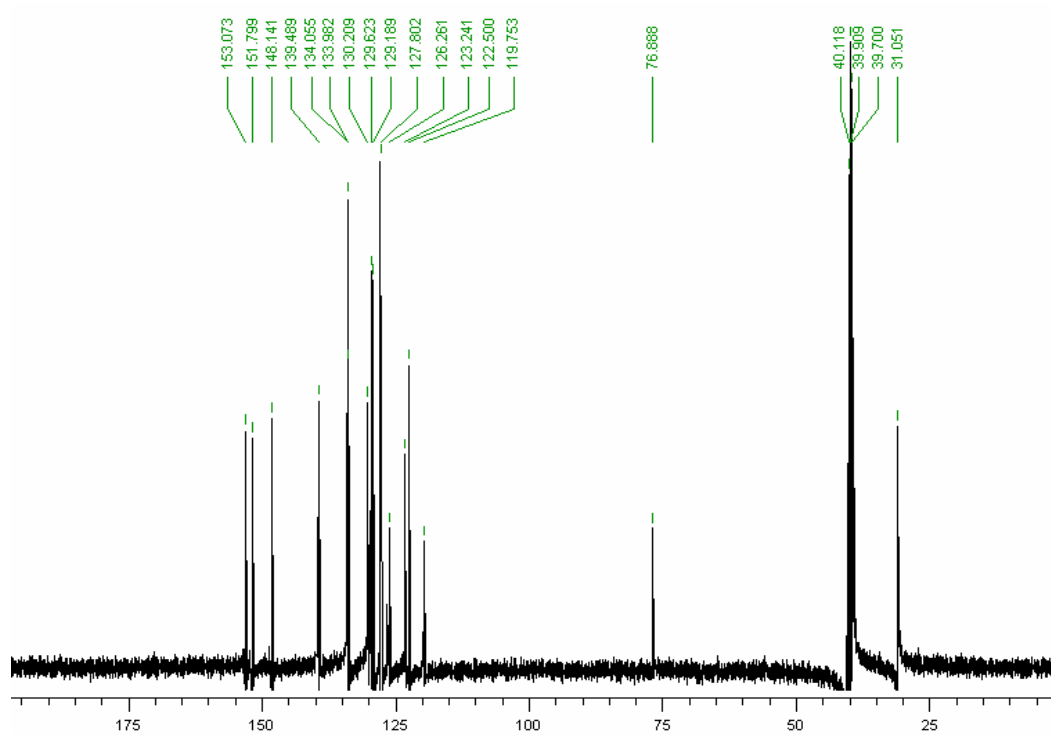
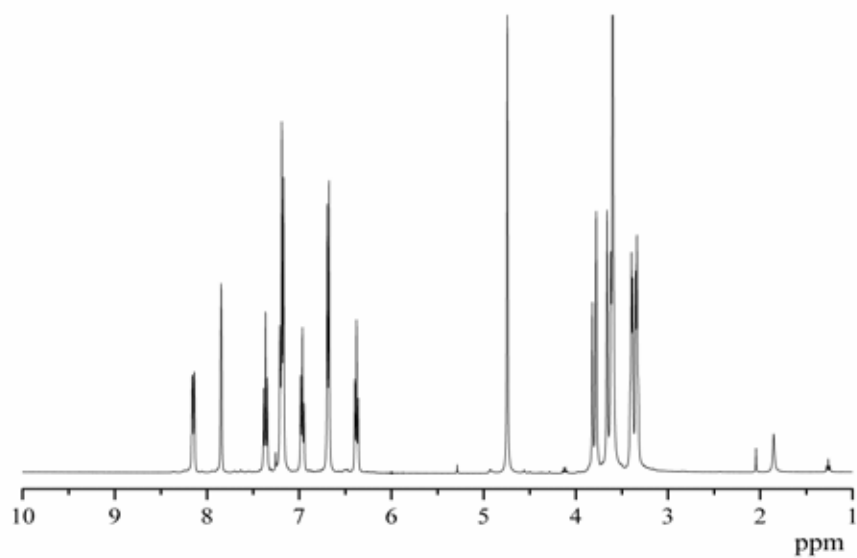
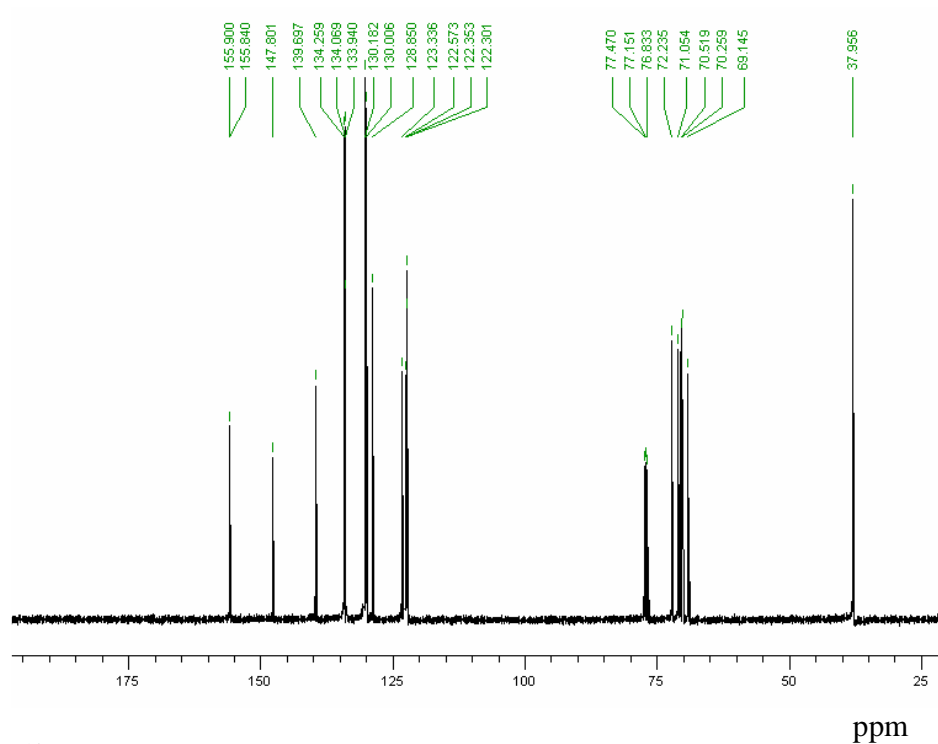


Fig. A2  $^{13}\text{C}$ -NMR spectrum of **1a** in DMSO

ppm



**Fig. A3**  $^1\text{H-NMR}$  spectrum of **1b** in  $\text{CDCl}_3$



**Fig. A4**  $^{13}\text{C-NMR}$  spectrum of **1b** in  $\text{CDCl}_3$

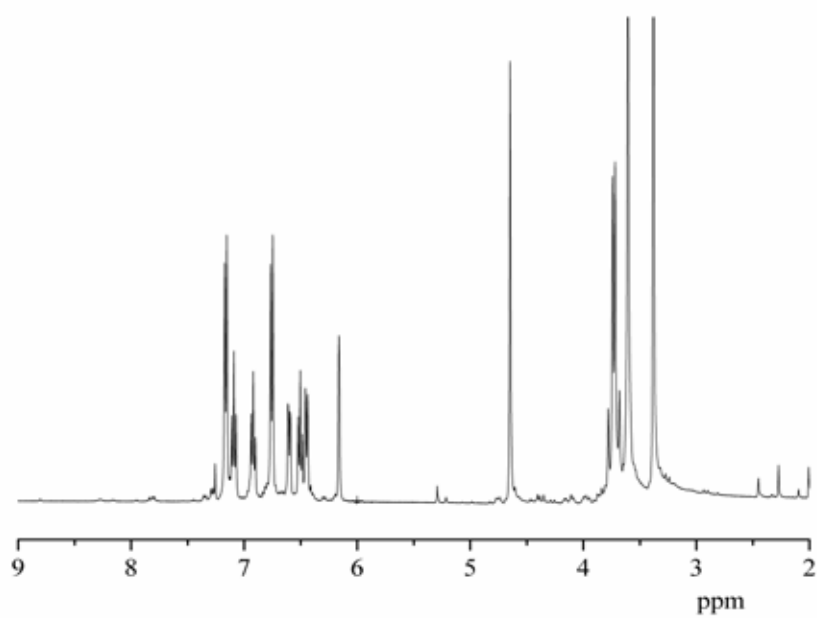


Fig. A5  $^1\text{H}$ -NMR spectrum of **1c** in  $\text{CDCl}_3$

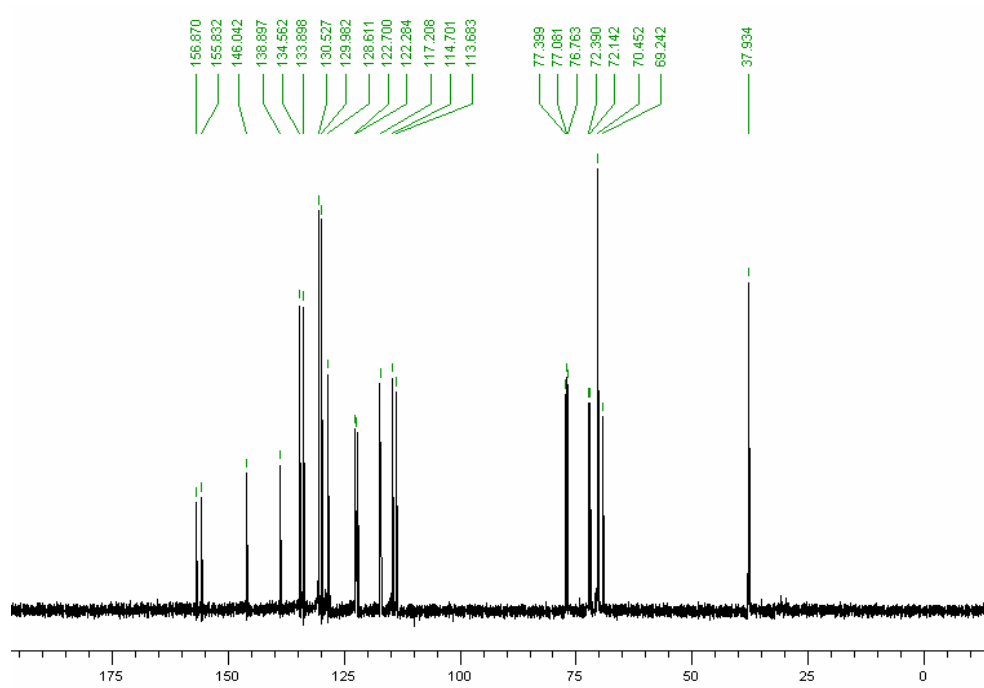


Fig. A6  $^{13}\text{C}$ -NMR spectrum of **1c** in  $\text{CDCl}_3$

ppm



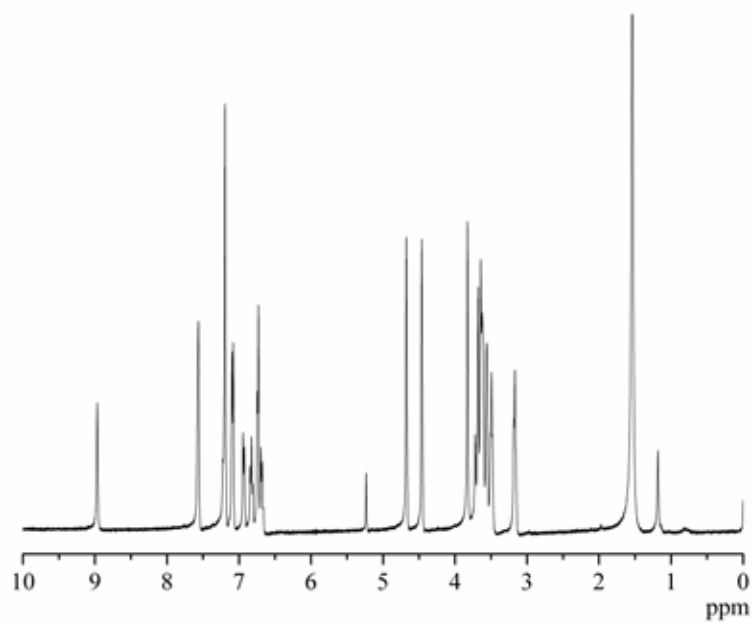


Fig. A7  $^1\text{H-NMR}$  spectrum of L1 in  $\text{CDCl}_3$

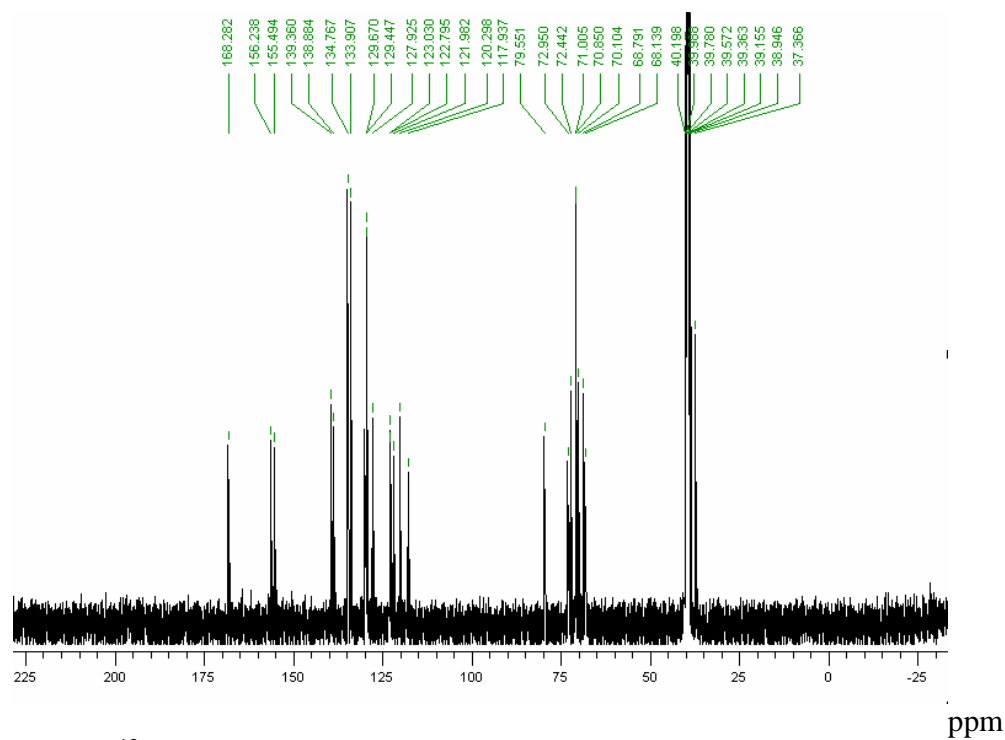
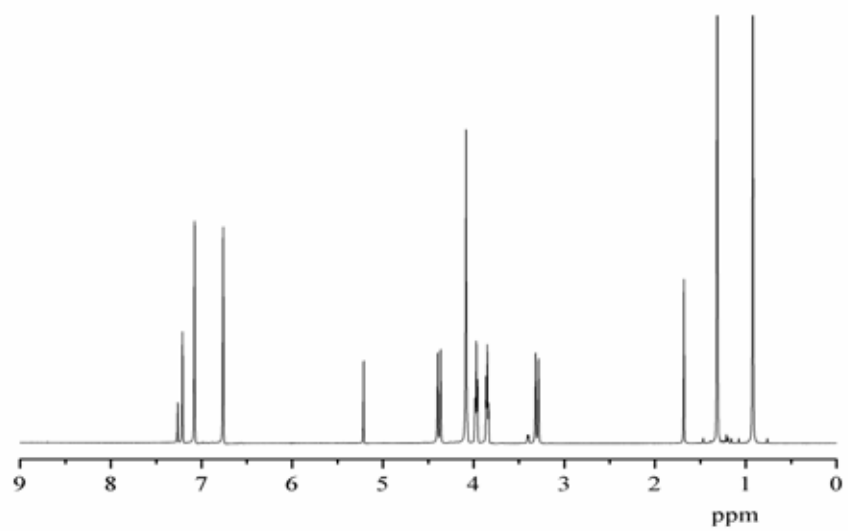
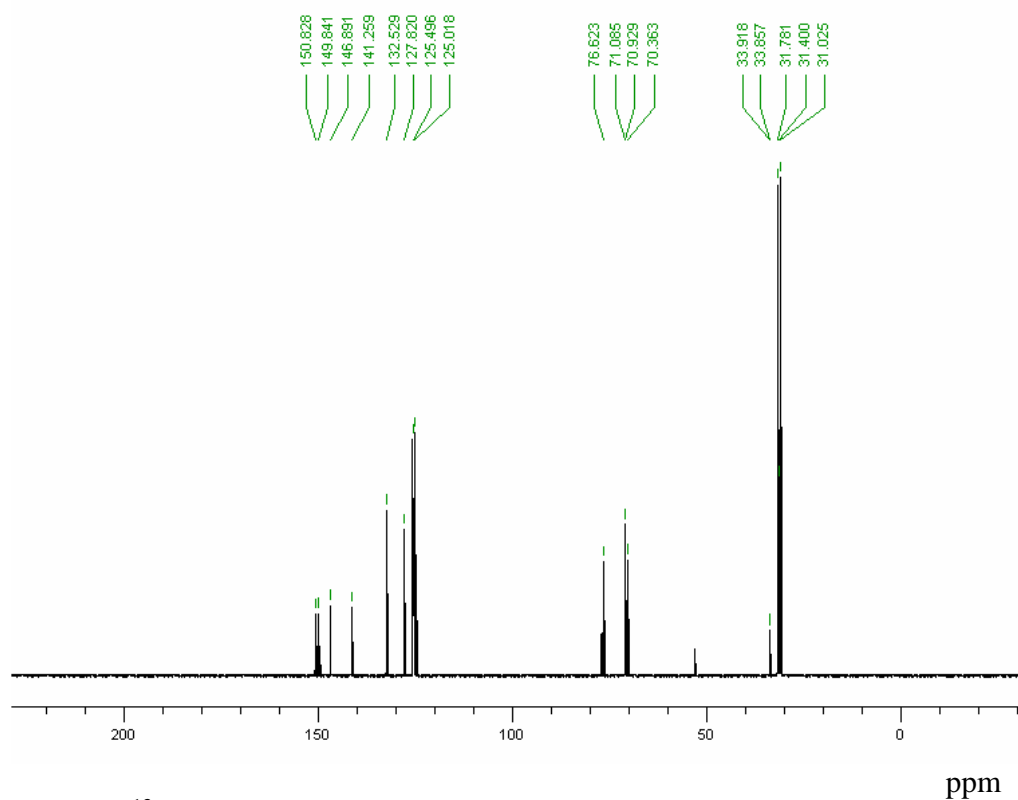


Fig. A8  $^{13}\text{C-NMR}$  spectrum of L1 in  $\text{CDCl}_3$



**Fig. A9**  $^1\text{H-NMR}$  spectrum of **3a** in  $\text{CDCl}_3$



**Fig. A10**  $^{13}\text{C-NMR}$  spectrum of **3a** in  $\text{CDCl}_3$

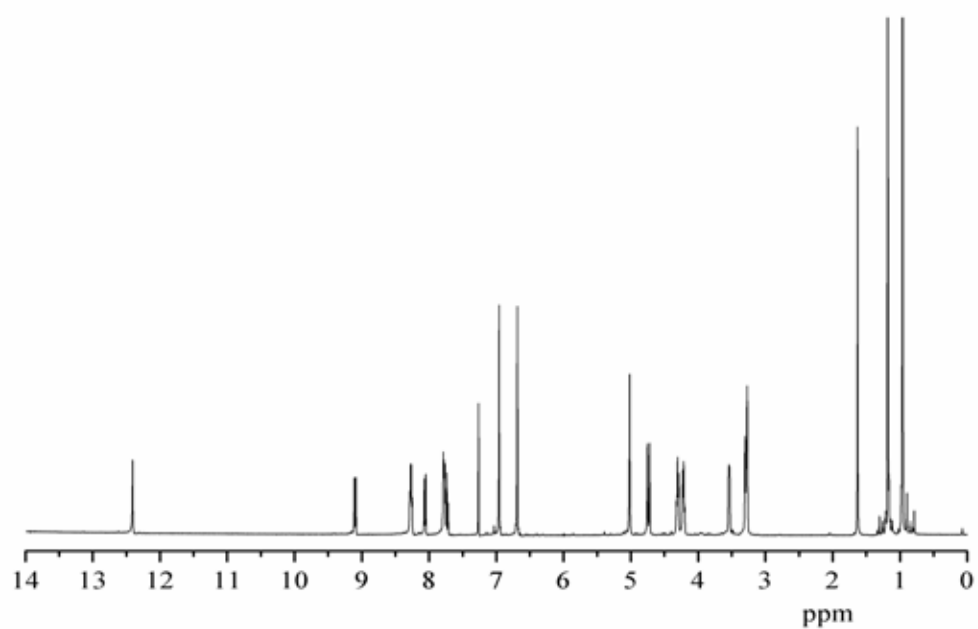


Fig. A11  $^1\text{H-NMR}$  spectrum of L3 in  $\text{CDCl}_3$

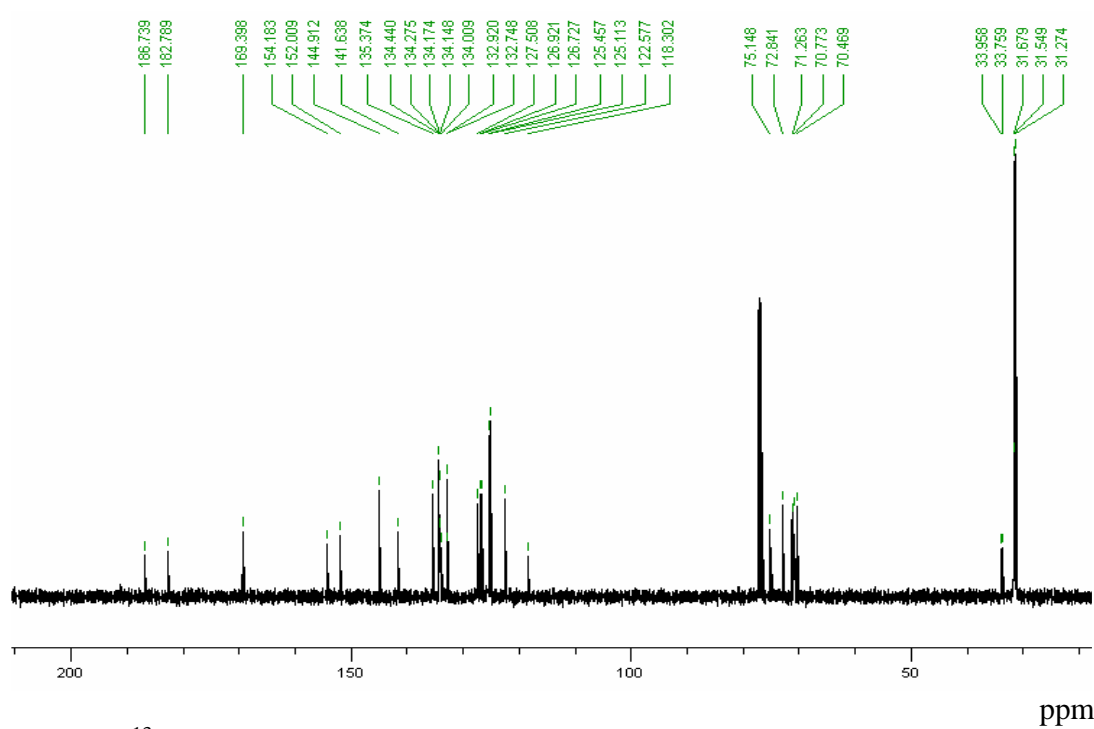


Fig. A12  $^{13}\text{C-NMR}$  spectrum of L3 in  $\text{CDCl}_3$

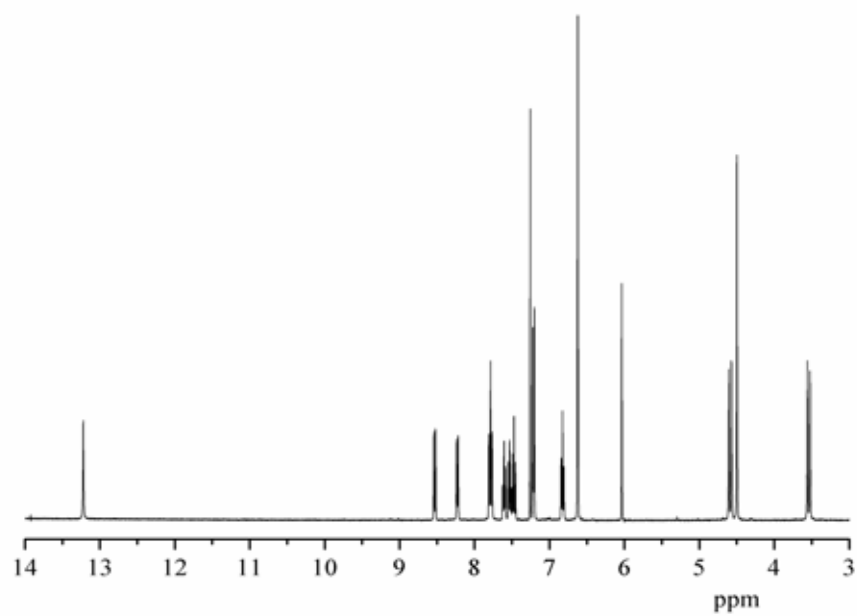


Fig. A13  $^1\text{H-NMR}$  spectrum of **4a** in  $\text{CDCl}_3$

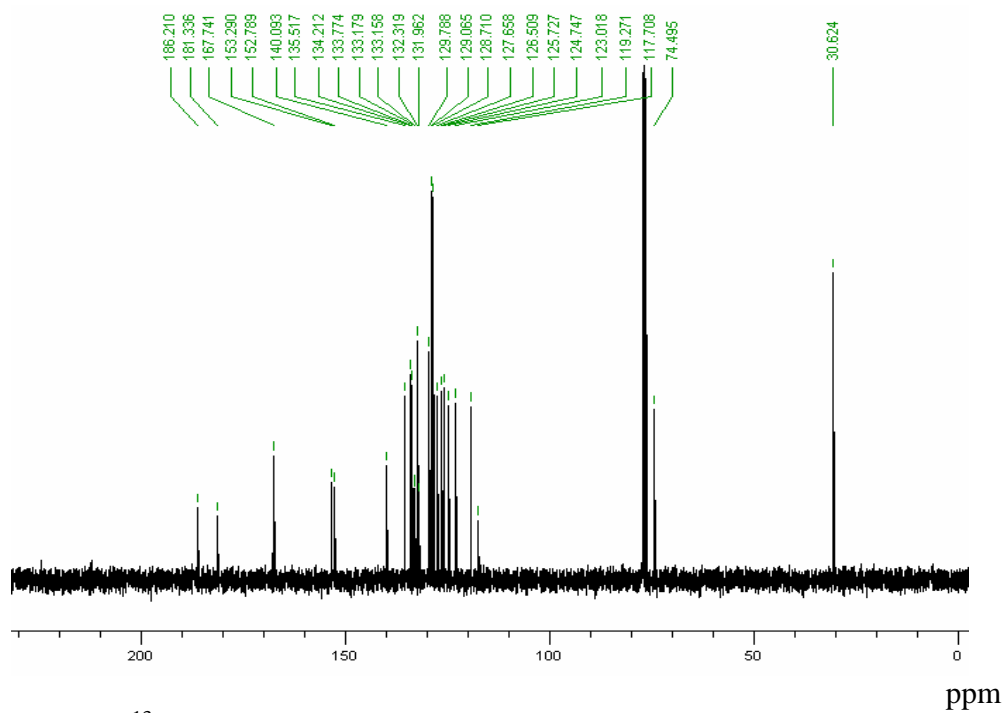


Fig. A14  $^{13}\text{C-NMR}$  spectrum of **4a** in  $\text{CDCl}_3$

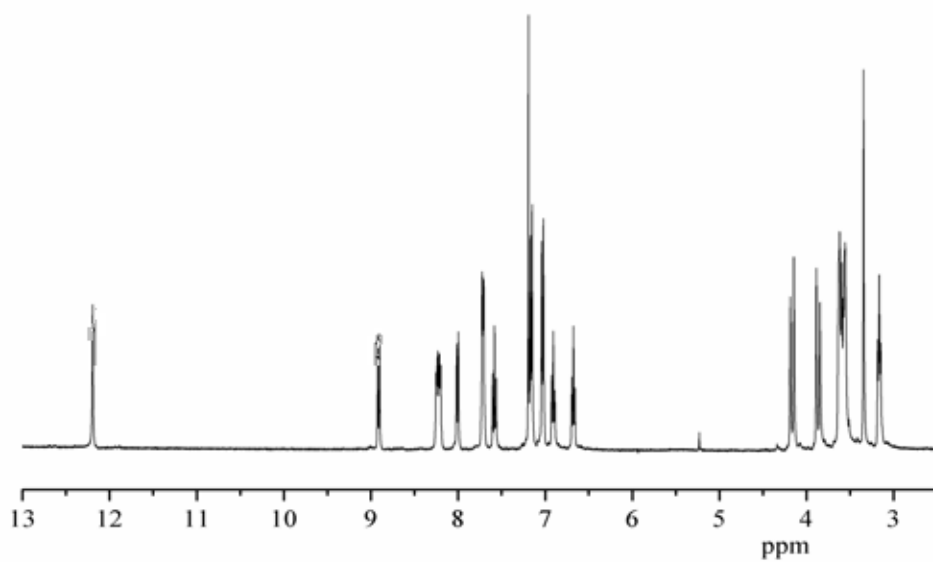


Fig. A15  $^1\text{H-NMR}$  spectrum of L4 in  $\text{CDCl}_3$

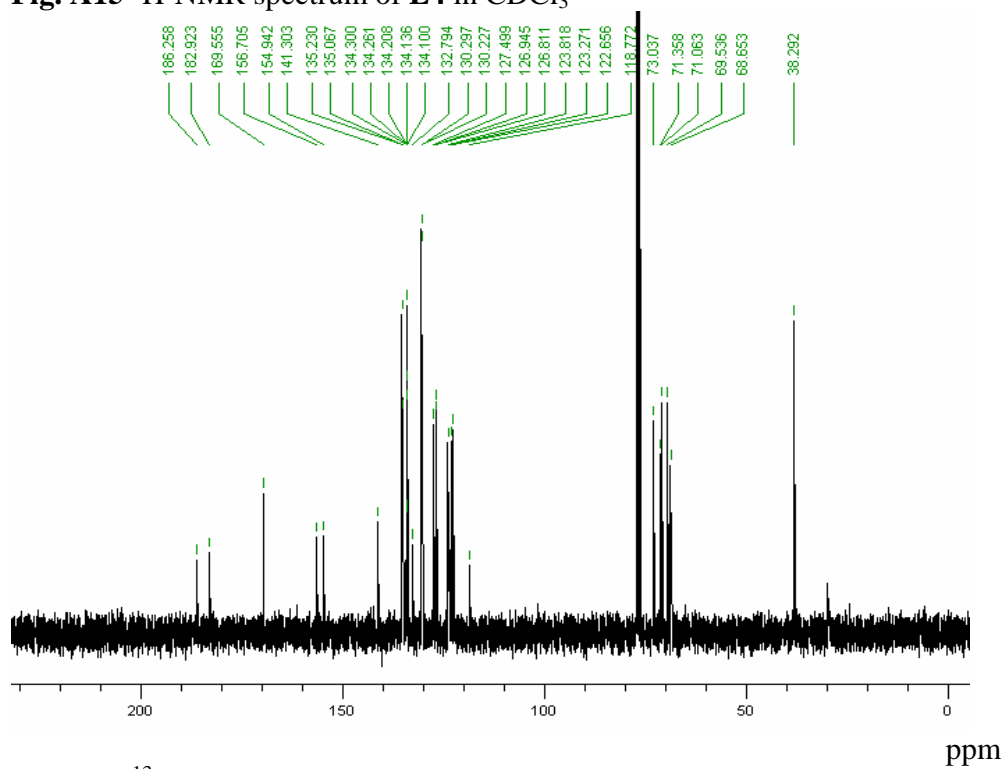


Fig. A16  $^{13}\text{C-NMR}$  spectrum of L4 in  $\text{CDCl}_3$

## VITAE

**Name:** Miss Benjamat Chailap

**Date of Birth:** January 27, 1984

### Education:

- 2011 (being pursued) Ph.D. Candidate in Inorganic Chemistry  
Chulalongkorn University, Bangkok, Thailand  
Dissertation: Electrochemical and Optical Anion  
Sensors Based on 1,3-Alternate Calix[4]arene crown  
ether  
Research Advisor: Prof. Dr. Thawatchai Tuntulani
- 2002 B.S. in Chemistry  
Prince of Songkla University, Songkla, Thailand

### Grants:

- 2002 – 2011 Development and Promotion of Science and Technology talents  
project (DPST)

### Presentations:

1. Heteroditopic electrochemical anion sensors containing amidoferrocene: structural and electrostatic effects toward anion binding abilities, **Oral presentation** in the 6<sup>th</sup> Pure and Applied Chemistry International Conference, 11-13 January 2012, The Empress Convention center, Chiang Mai.
2. Heteroditopic anion receptors containing amidoferrocene: structural and electrostatic effects toward anion binding abilities, **Poster presentation** in 14<sup>th</sup> Asian Chemical Congress 2011, 5-8 September 2011, Queen Sirikit National Convention Center, Bangkok.
3. Fluoride ion sensors containing calix[4]arene as a building block, **Oral presentation** in The Science Forum 2011, 10-11 March 2011, Chulalongkorn University, Bangkok.
4. Ditopic receptors and sensors containing calix[4]arene as a building block, **Oral presentation** in Pure and Applied Chemistry International Conference 2010, 21 – 23 January 2010, Sunee Grand Hotel and Convention Center Ubonratchathani, Ubonratchathani.

### Publications

1. Chailap, B., and Tuntulani, T. Optical and electrochemical properties of heteroditopic ion receptors derived from crown ether-based calix[4]arene with amido-anthraquinone pendants. *Org. Biomol. Chem.* 10(2012): 3617-3625.

2. Nerngchamnonng, N., Chailap, B., Leeladee, P., Chailapakul, O., Suksai, C., and Tuntulani, T. Topological and metal ion effects on the anion binding abilities of new heteroditopic receptors derived from p-tert-butylcalix[4]arene. *Tetrahedron Lett.* 52(2011): 2914-2917.